Partial Differential Equation and Noise

Ennio Fedrizzi

UNIVERSITÉ PARIS.DIDEROT (Paris 7)
ECOLE DOCTORALE 386 : SCIENCES MATHÉMATIQUES DE PARIS CENTRE
Laboratoire de Probabilité et Modèles Aléatoires

Doctorat en Mathématiques Appliquées

Ennio FEDRIZZI

Partial Differential Equations and Noise

Thèse dirigée par : Josselin GARNIER

Soutenue le 13/12/2012

JURY

Prof. Francis Comets	Université Paris 7
Prof. Josselin Garnier	Université Paris 7, Directeur
Prof. Massimiliano Gubinelli	Université Paris 9
Prof. Francesco Russo	ENSTA-ParisTech, Rapporteur
Prof. Knut Sølna	University of California Irvine
Prof. Lorenzo Zambotti	Université Paris 6

Acknowledgements

Looking back on these past few years, it is clear that this work owes a lot to many people, who have all contributed in one way or another to make it possible.

I was very fortunate to have the guidance of Prof. Josselin Garnier as my Ph.D supervisor. His encouragements, patience and good advice were essential in the completion of this work, and he was always there when I needed his council. I very much enjoyed working under his supervision, and hope this is just the beginning of an on-going collaboration.

I am also most grateful to the two referees, Prof. Lenya Ryzhik and Prof. Francesco Russo, who had the patience to carefully read my manuscript, and to professors Francis Comets, Massimiliano Gubinelli, Knut Sølna and Lorenzo Zambotti for granting me the honor of being in the jury of my doctoral defense.

I cannot give enough credit in particular to Prof. Franco Flandoli, whose support has never faltered over the years since I met him in my graduate studies in Pisa.

Also, this task could not have been completed without the friendly companionship of my fellow doctoral students, with whom I have shared the difficulties and the excitement of such an adventure. The administrative staff of the LPMA and doctoral school was always helpful in making our everyday lives as doctoral students easier.

I also wish to thank the Centre Interfacultaire Bernoulli and the École Polytechnique Fédérale de Lausanne for the invitation to the semester on stochastic analysis and applications 2012, during which part of this work was developed.

Finally, I would especially like to thank my family, who endured my work, and in particular my loving wife Mar, always so supportive and understanding.

Contents

1 Introduction **9**

1.1 Noise and solitons: nonlinear partial differential equations with random initial conditions . . . 10

1.2 Imaging with noise: a linear partial differential equation with random initial conditions . . . 11

1.3 The stochastic linear transport equation: regularization by noise. 12

2 Noise and solitons **15**

2.1 Rapidly oscillating random perturbations . . . 17

2.1.1 The Inverse Scattering Transform method . . . 18

2.1.2 Limit of rapidly oscillating processes . . . 22

2.2 Stability of solitons . . . 29

2.2.1 NLS solitons – deterministic background solution . . . 30

2.2.2 NLS solitons – small-intensity real noise . . . 32

2.2.3 NLS solitons – small-intensity complex noise . . . 37

2.2.4 KdV solitons – deterministic background solution . . . 37

2.2.5 KdV solitons – small-amplitude random perturbation with $q > 0$ . . . 39

2.2.6 KdV solitons – small-amplitude random perturbations with q=0 . . . 45

2.2.7 Perturbation of NLS and KdV solitons: similarities and differences . . 46

2.3 Examples . . . 47

2.3.1 Creation of solitons from a rapidly oscillating real noise . . . 48

2.3.2 Complex white noise: no soliton creation . . . 51

2.3.3 Complex noise of constant intensity: no soliton creation for fixed ξ . . 54

2.3.4 Complex telegraph noise: no soliton creation for fixed ξ . . . 58

2.3.5 Density of states – Ornstein-Uhlenbeck process . . . 59

2.3.6 Density of states – general case . . . 79

2.4 Appendix . . . 91

3 Imaging with noise **95**

3.1 Mathematical formulation . . . 97

3.1.1 The wave equation with random sources . . . 98
3.1.2 The background Green's function . . . 98
3.1.3 The scattering operator and the Born approximation . . . 99
3.1.4 The imaging problem . . . 102
3.1.5 The classical setting: multi-offset sources . . . 102
3.2 Stationary random sources . . . 103
3.3 Incoherence by blending . . . 107
3.4 High frequency analysis . . . 111
3.4.1 The imaging functional in a high frequency regime . . . 111
3.4.2 Expected contrast of the estimated perturbation . . . 113
3.4.3 Fluctuations and typical contrast . . . 116
3.4.4 Comments . . . 123
3.5 Applications and simulations . . . 124
3.5.1 Simultaneous source exploration . . . 124
3.5.2 Seismic forward simulations . . . 127
3.5.3 Numerical illustrations . . . 128
3.6 Appendices . . . 130
3.6.1 Appendix A: Statistical stability for a continuum of point sources . . . 130
3.6.2 Appendix B: Resolution analysis . . . 130

4 The stochastic transport equation 133
4.1 Introduction . . . 133
4.2 Convergence results . . . 135
4.3 Existence of weakly differentiable solutions . . . 140
4.4 Uniqueness of weakly differentiable solutions . . . 147
4.5 Appendix A: technical results . . . 151
4.6 Appendix B: Sobolev regularity of random fields . . . 157

Résumé

Dans ce travail, nous présentons quelques exemples des effets du bruit sur la solution d'une équation aux dérivées partielles (EDP) dans trois contextes différents. Nous examinons d'abord deux équations aux dérivées partielles non linéaires dispersives, l'équation de Schrödinger non linéaire et l'équation de Korteweg - de Vries. Nous allons analyser les effets d'une condition initiale aléatoire sur certaines solutions spéciales, les solitons. Le deuxième cas considéré est une EDP linéaire, l'équation d'onde, avec conditions initiales aléatoires. Nous allons montrer qu'avec des conditions initiales aléatoires particulières c'est possible de réduire considérablement les coûts de stockage des données et de calcul d'un algorithme pour résoudre un problème inverse basé sur les mesures de la solution de cette équation au bord du domaine. Enfin, le troisième exemple considéré est celui de l'équation de transport linéaire avec un terme de dérive singulière. Nous allons montrer que l'ajout d'un terme de bruit multiplicatif interdit l'explosion des solutions, et cela sous des hypothèses très faibles pour lesquelles dans le cas déterministe on peut avoir l'explosion de la solution à temps fini.

Abstract

In this work we present examples of the effects of noise on the solution of a partial differential equation (PDE) in three different settings. We will first consider random initial conditions for two nonlinear dispersive PDEs, the nonlinear Schrödinger equation and the Korteweg - de Vries equation, and analyze their effects on some special solutions, the soliton solutions. The second case considered is a linear PDE, the wave equation, with random initial conditions. We will show that special random initial conditions allow to substantially decrease the computational and data storage costs of an algorithm to solve the inverse problem based on the boundary measurements of the solution of this equation. Finally, the third example considered is that of the linear transport equation with a singular drift term, where we will show that the addition of a multiplicative noise term forbids the blow up of solutions, under very weak hypothesis for which we have finite-time blow up of solutions in the deterministic case.

Chapter 1

Partial differential equations and noise: introduction

This work examines some aspects regarding the effects of noise on partial differential equations (PDEs). This is an incredibly wide and extremely interesting field, where research is very active in numerous different directions.

One of the interesting points of this topic is that it allows to combine the tools from both classical and stochastic analysis.

The use of the word "noise" is inspired by the name of a widely used stochastic process, referred to as white noise. However, we shall not restrain the analysis to this single case, and we shall also consider examples of the effect of more general stochastic processes. With a slight abuse of notation, even when using general stochastic processes we will sometimes refer to them as noise. This is also justified by some applications, where the introduction of a random component is used to model chaotic or uncontrollable phenomena, which may be thought of as a form of "noise" in the data.

The word "noise" might convey a negative connotation, but we stress that in the contexts we consider its presence is not necessarily only a source of problems or difficulties. Indeed, we will have the opportunity to appreciate how in some applications, such as the imaging problem considered in chapter 3, the presence of noise may have some incredibly positive effects in terms of reduction of computational and data-storage costs for the algorithm. Also, from a more theoretical point of view, it may help stabilize some PDEs, in the sense that a stochastic partial differential equation (SPDE) can be well posed under more general hypotheses than its deterministic counterpart. This is the very interesting phenomenon known as regularization by noise, and we shall present an example of this in the last chapter.

A first consideration to make is that noise can be introduced in a PDE in two different ways. First, it is possible to consider a deterministic PDE, but with some random initial conditions. From the point of view of applications, this can serve to model the elaboration of data in which some uncontrolled and unavoidable errors are present. However, in certain cases the initial data can be intentionally chosen to contain some random perturbations, as under specific assumptions this can improve the efficiency of an algorithm based on the solution of the equation.

The second way to introduce noise in a PDE is to change the equation itself by the addition of a random term, called noise term. This turns the PDE into a SPDE. Two main classes of SPDEs can be distinguished, according to the nature of the noise term: SPDEs with either additive or multiplicative noise. For additive SPDEs the noise term does not

depend on the unknown function, while the unknown does appear in the noise term in the case of a multiplicative noise.

In this work we present examples of the effects of noise on the solution of a PDE in three different settings. We will first consider random initial conditions for two nonlinear dispersive PDEs, the nonlinear Schrödinger equation and the Korteweg - de Vries equation, and analyze their effects on some special solutions, the soliton solutions. The second case considered is a linear PDE, the wave equation, with random initial conditions. We will show that special random initial conditions allow to substantially decrease the computational and data storage costs of an algorithm to solve the inverse problem based on the boundary measurements of the solution of this equation. Finally, the third example considered is that of the linear transport equation with a singular drift term, where we will show that the addition of a multiplicative noise term forbids the blow up of solutions, under very weak hypothesis for which we have finite-time blow up of solutions in the deterministic case.

1.1 Noise and solitons: nonlinear partial differential equations with random initial conditions

In chapter 2, we consider the problem of wave propagation, which is modeled by nonlinear dispersive equations, with noisy initial conditions. As observed, noise can also be introduced directly into the equation, studying the propagation of waves according to stochastic nonlinear dispersive equations. But we will not detail this approach, and only briefly mention some important analytical and numerical results in the introduction of the chapter.

Solutions of certain nonlinear dispersive equations present a remarkable behavior: they can be decomposed in a radiative component and a soliton component. The amplitude of the radiative component decays in time polynomially: this is due to the dispersive effect. The soliton component instead is the effect of a delicate balance between the nonlinear and dispersive effects, which generates one or more stable waves, called solitons. These waves maintain a constant shape while propagating, and have constant amplitude and velocity. In other words, they characterize the long time behavior of the solution. Even from such a short introduction, the importance of solitons in applications should be clear. We shall focus on the effects of noise on this special class of solutions, studying in particular their stability with respect to noise perturbations of the initial condition and the possibility of creating solitons from random initial conditions. This is done for two important equations, which are analyzed and compared: the nonlinear Schrödinger (NLS) equation and the Korteweg - de Vries (KdV) equation. Both equations have a central role in literature for historical reasons and for their general character. Indeed, they are used in a wide range of very different physical models, mentioned in the introduction of chapter 2. Here we only observe that a main application of the nonlinear Schrödinger equation is the modelling of the propagation of short light pulses in optical fibers, and the Korteweg - de Vries equation is used for example to model the propagation of water waves in a channel, and is the first equation that has been used to study the dynamic of solitons.

A first general result (theorem 2.2) shows that the study of soliton emergence from a localized, bounded initial condition perturbed by a wide class of rapidly oscillating random processes can be reduced to the study of a canonical system of stochastic differential equations (SDEs), formally corresponding to the white noise perturbation of the initial condition. It should be stressed that the actual use of a white noise initial condition, sometimes present in the physical literature, not only has little physical significance, but is also mathematically incorrect if the approach is based on the inverse scattering transform method, which is often

the case. We therefore had to address the problem using an initial condition with rapid, but non infinitely rapid, oscillations, which has more physical relevance and for which a rigorous mathematical approach is possible. Moreover, when the random perturbation is small it is possible to use the above result combined with a perturbative approach to obtain quantitative information on the stability of solitons with respect to random perturbations of the initial condition. Perturbed solitons are characterized and described in different settings, according to the kind of noise (real or complex) and the presence or not of a deterministic background initial condition. All these results are contained in the preprint [Fe12a].

The chapter also includes a section of examples, where different interesting special cases of random initial conditions are considered for the NLS equation, and no small-noise assumption is made. Two main questions are addressed in this section. First, the question of the possibility to create solitons from a purely random initial condition with compact support is addressed. A positive result is obtained in the limit case of a real (or complex, but with constant phase) white noise, and negative results are provided for different kinds of complex noises, such as the symmetric complex white noise, a general complex jump process, and even a constant-intensity complex noise. All these examples, as well as some of the proofs, seem to hint to the fact that for the NLS equation with random initial condition, the changes of phase of the noise destroy the possibility of creating (with positive probability) solitons with a given speed. The proof of this intriguing fact remains however an open problem. The second question concerns the probability distribution of the parameters of created solitons (amplitude and speed) for random initial conditions with very long support $[0, R]$, $R \to \infty$. Using a perturbative approach we show that for rapidly oscillating random initial conditions this distribution is near to the distribution of the formal limit case of a white noise initial condition. We will explain a method with which it is possible to obtain the probability distribution. Explicit computations in the case of a rapidly oscillating Ornstein-Uhlenbeck process show that the first order correction term is zero, and provide the second order correction term. Curiously, this correction term only affects the distribution of the amplitude of created solitons. This method is then applied to random initial conditions given by more general Markov processes, to show that also in this case the first order correction term is zero. It is also possible to observe that if the process is not Gaussian, the second order term does modify also the distribution of the speed of created solitons.

1.2 Imaging with noise: a linear partial differential equation with random initial conditions

In chapter 3 we analyze solutions of the wave equation with random initial conditions. This problem arises from a practical application, an imaging problem, and provides the example mentioned above of an application for which the presence of noise has a beneficial effect.

The imaging problem aims at locating localized perturbations in the propagation speed of a medium (to which one typically has not direct access) from the measurements of waves at the boundary of the medium. A typical sensor array imaging experiment consists in two steps. The first step is the experimental data acquisition: a point source emits a wave into the medium, the wave is reflected by the singularities in the propagation speed of the medium and is recorded by an array of receivers. The second step is a numerical processing of the recorded data: the recorded signals are time reversed and resent in a numerical simulation into a model medium to locate the singularities in the propagation speed. From a mathematical point of view, the first step is modeled by an operator $\mathcal{F}$ mapping the perturbations to the recorded scattered waves. The second step is an inverse

problem, consisting in inverting the operator $\mathcal{F}$ to find the perturbations from the recorded data.

The classical approach to the imaging problem consists in performing a large number of experiments sounding each time a different source. For each experiment, the signal recorded at each receiver is stored and time reversed. This produces the data matrix. For each experiment, the time reversed data are reemitted (numerically) into the model medium in a new simulation, and the images obtained by each simulation are stacked. While this method provides a very good "image" of the medium, it involves gathering, storing and processing huge amounts of data. The approach in which all the sources are sounded simultaneously in a single experiment is an alternative strategy, but to obtain an image of good quality special care must be taken to ensure that cross-talk terms remain small. Various blending type methods have been investigated in order to be able to exploit this simultaneous sources approach, in particular in the context of seismic imaging. For example, in the case of classic vibratory sources one can seek to design a family of relatively long signals encoded such that the responses of each one of them can be identified at the receivers end and separated (deblending step) before the numerical processing of the data.

In this chapter we present another approach, based on the use of simultaneous random sources, which does not require the introduction of a deblending step. Two kinds of random sources are analyzed, emitting either stationary random signals or randomly delayed pulses. We describe the imaging functional to be used in the two cases and detail the scaling assumptions needed to ensure the stability of the method and a good quality of the image obtained.

We also present a detailed analysis of the behavior of the two imaging functionals when trying to locate singular perturbations in the velocity of propagation and in the high frequency regime. Three different kinds of perturbations (points, lines and surfaces) are considered to prove that the typical contrast seen in the image strongly depends on the type of perturbation. We perform a detailed resolution and stability analysis. Quantitative results show that point singularities are easily seen, and surface singularities are the hardest to locate.

Finally, some possible applications of our approach with simultaneous random sources are investigated and we elaborate on the fascinating fact that imaging with simultaneous sources of the two types we have described gives a resolution that corresponds to the one obtained in the classical setting, where the recordings of the responses at all of the receivers are available for each experiment (corresponding each time to a new source emitting the signal). Simple numerical results are shown to support this fact.

The results concerning the high frequency analysis of the imaging functional are contained in the preprint [Fe12b]. The remaining sections, namely the description of the imaging algorithm using the simultaneous random sources described, its statistical stability and the results contained in the final section on applications and simulations are taken from the joint work [DFGS12] with M. De Hoop, J. Garnier and K. Sølna published in Contemporary Mathematics.

1.3 The stochastic linear transport equation: regularization by noise.

The possibility that noise may prevent the emergence of singularities is an intriguing phenomenon that is under investigation for several systems. A number of equations have been studied with respect to this question, providing both positive and negative examples. In

general, regularization effects are more easily achieved with a multiplicative noise term, so that we shall restrict our analysis to this case.

In chapter 4 we provide a positive example showing that for the linear transport equation under very weak assumptions on the drift coefficient (we only require some degree of integrability) and in the presence of a multiplicative noise term, some degree of regularity of the initial condition is maintained. In particular, discontinuities cannot appear. This fact follows from a representation formula which expresses the solution in terms of the initial condition composed with a stochastic flow. In previous works [FF11, FF12a] we had analyzed the solution of the stochastic differential equation (SDE) that generates this flow and proved some important regularity properties. In particular, the flow is α-Hölder continuous for every $\alpha \in (0, 1)$, with probability one, and is differentiable in some weak sense. It follows that the solution starting from a regular initial condition remains at least Hölder continuous, so that no discontinuity can appear.

The description of the class of functions in which we look for solutions of the stochastic transport equation is quite technical, and is given by definition 4.6. We call a solution in this class a weakly differentiable solution. Existence of a weakly differentiable solution under our weak integrability assumptions on the drift coefficient is proved in theorem 4.10 by showing that the representation formula described above provides a solution. And by theorem 4.11 this fairly regular solution is also unique.

The results presented in this chapter are mainly contained in the preprint [FF12b], which is a joint work with F. Flandoli. Some necessary technical results from the previous joint works [FF11, FF12a] are also presented in appendix A.

Chapter 2

Noise and solitons

A solution of a nonlinear dispersive equation modelling the propagation of waves may show two components with a very distinct behavior. The radiation component is the one whose amplitude decays in time as a power law due to dispersive effects, which refers to the fact that the speed of the waves can vary according to frequency. For many nonlinear systems, a delicate balance between the dispersive and nonlinear effects may occur, producing stable waves. They are referred to as the soliton component of the solution (solitons, in short). Solitons are stable, solitary waves with elastic interactions (the only effect of a collision between two solitons is a phase shift). Stable refers to the fact that they propagate over arbitrarily large distances with constant velocity and profile. The identification of the soliton components is therefore essential to characterize the long-time behavior of the solution of the PDE. Examples of exactly solvable models which can produce solitons are the Korteweg - de Vries (KdV) equation, the nonlinear Schrödinger (NLS) equation and the sine-Gordon equation, the Kadomtsev-Petviashvili equation, the Toda lattice equation, the Ishimori equation, the Dym equation, etc.

Historically, solitons were first observed by John Scott Russell during the first half of the 19^{th} century [Ru1], [Ru2]. His observations dealt with stable water waves in a narrow channel. A lot of research followed, until Diederik Korteweg and Gustav de Vries proposed in 1895 what is now known as the KdV equation to model the propagation of waves in shallow waters [KV1]. This model also explains mathematically the existence of stable solitary waves. But it was only much later, in 1967, that a new technique allowing to find analytical solutions of the KdV equation was discovered by Gardner, Greene, Kruskal and Miura [GG67]. It is the inverse scattering transform (IST), which thanks to the successive work of Lax [La68] allows to treat analytically many soliton-generating systems, including the NLS equation.

Today, solitons still attract a lot of research which has potentially substantial applications in many fields. For example, in a fiber optic system one can exploit the solitons' inherent stability to improve long-distance transmission and increase the performance of optical telecommunications. Another broad domain in which soliton solutions appear is in water waves propagation, for both surface and internal waves.

One important field of research regards the effects of noise on solitons. Noise can be introduced in different ways, to account for different physical effects. For example, one can add an additive or multiplicative noise term in the equation to model some random forcing or external potential. Soliton dynamics for the KdV equation under random forcing, modeled by the addition of an additive noise term in the equation, has been analyzed in [dBD07]

while the case of solitons of the KdV equation with a potential given by a multiplicative noise term is studied in [dBD09]. Numerical results for these two kinds of random perturbations are presented in [SRC98] and [DP99]. Corresponding numerical and analytical results for the random NLS equation are presented in [FKLT01, DdM02b].

Another way to introduce random perturbations using a deterministic equation is to use random initial conditions. In this chapter we shall consider this approach and study how the introduction of noise in the initial condition affects solitons. We focus on two examples of nonlinear PDEs, the NLS and the KdV equations. They are completely integrable systems, widely employed in different fields to model nonlinear and dispersive effects in wave propagation. The (one - dimensional) NLS equation

$$\frac{\partial U}{\partial t} + \frac{i}{2}\frac{\partial^2 U}{\partial x^2} + i|U|^2 U = 0 \tag{2.0.1}$$

models in particular short pulse propagation in single - mode optical fibers (then, t is a propagation distance and x is a time) [MN]. The electromagnetic wave propagating in the fiber is the solution $U(t, x)$, which is a complex function. The NLS equation is also used to model the profile of the amplitude of wave groups for surface water waves: envelope solitons in deep waters approximately solve this equation [Za68]. The NLS equation is also used in the context of Bose - Einstein condensate theory, as the general time dependent Gross - Pitaevskii equation producing the wavefunction of a single particle immersed in the Bose - Einstein condensate reduces to the NLS equation is the absence of an external potential [PS].

The KdV equation

$$\frac{\partial U}{\partial t} + 6\,U\,\frac{\partial U}{\partial x} + \frac{\partial^3 U}{\partial x^3} = 0 \tag{2.0.2}$$

has been used since 1895 to model shallow water waves propagation [Wh], and recently it has also found applications in many other physical contexts, such as plasma physics [ZK65], internal waves (both in water and air) [AS], [Mi79], and many others [AC].

An effective method to deal with both equations is the Inverse Scattering Transform (IST), a powerful tool to study solutions of completely integrable nonlinear equations, see [APT]. In this framework, the problem is transformed into a linear system of differential equations where the initial condition enters as a potential and soliton components correspond to discrete eigenvalues. Our approach to both examples relies on this machinery.

The first result we obtain is that for the NLS and KdV equations the study of soliton emergence from a localized, bounded initial condition perturbed by a wide class of rapidly oscillating random processes can be reduced to the study of a canonical system of stochastic differential equations (SDEs), formally corresponding to the white noise perturbation of the initial condition [Fe12a]. The integrated covariance is the only parameter of the perturbation process that influences the limit system of SDEs. This is the main result of section 2.1.

In section 2.2 we study this limit system to obtain quantitative information on the stability of solitons with respect to small random perturbations in different settings: one can consider real or complex random perturbations (for NLS), with or without a background deterministic initial condition (for KdV).

Finally, in the last section we collect a few examples of different random initial conditions for the nonlinear Schrödinger equation and present the different techniques needed to treat them. We can describe different effects on the soliton generation according to the nature of the random process used as initial condition. For rapidly oscillating real processes we study the threshold of the length of the support of the initial condition needed to create the first soliton and show that it is almost surely finite. For other examples with complex initial

conditions we can show that the probability of creating solitons with any given velocity is zero. We then turn our attention to the density of the distribution of the velocity and amplitude of solitons created by complex random initial conditions. A formula for the limit case of rapid oscillations has been recently obtained [KM08]; we will explicit the computation needed to obtain this formula and the correction terms for fast, but not infinitely rapid, oscillations, in the practical example of a Ornstein-Uhlenbeck process and detail the scheme to apply for a general class of rapidly oscillating Markov processes.

Notation

We introduce some general notation used throughout the chapter. Further specific notation used only in a single passage are introduced when needed.

If $z \in \mathbb{C}$ is a complex number, we denote $\Re[z]$ its real part and $\Im[z]$ its imaginary part. z^* denotes the complex conjugate of z. In particular, ζ is used to denote the complex number which will be associated to each soliton; we shall write it as $\zeta = \xi + i\eta$.

For a vector $x \in \mathbb{R}^d$ or $x \in \mathbb{C}^d$, we will write x^T to denote the transposed vector and $x = (x_1, x_2, ...)$ to indicate its coordinates. The vectors $e_1 = (1, 0, ...)$, $e_2 = (0, 1, ...)$ always refer to the elements of the canonical basis of $\mathbb{R}^d$ (or $\mathbb{C}^d$). We will use $B_r(x)$ to denote the ball of radius r centered in x. We will use $|\cdot|$ to denote either the absolute value or the norm in $\mathbb{R}^d$ or $\mathbb{C}^d$. For norms defined on other spaces, and in particular on functional spaces, we will use $\|\cdot\|$.

We will use subscripts to denote the dependence of constants on the parameters of the problem, as in C_R.

For functional spaces, we use the notation $X(A; B)$, where X denotes the regularity of the functions, A indicates the domain and B the space in which the functions take values. For example, $\mathcal{C}^0$ denotes a space of continuous functions, $\mathcal{C}^1$ a space of continuously differentiable functions, L^p the space of p-integrable functions and $W^{l,k}$ is used to denote Sobolev spaces. Finally, $f \star g$ denotes the convolution product between f and g.

2.1 Rapidly oscillating random perturbations

We consider in this section the case of initial conditions perturbed with a rapidly oscillating random process. We prove that for both the NLS and KdV equations the behavior of the soliton components of the solution actually shows very little dependence on the kind of perturbation, the limit behavior being controlled by a canonical system of SDEs where the only parameter of the original perturbation playing a role is its integrated covariance.

Explicit computations are presented in the case of a square (box-like) initial condition perturbed with a zero mean, stationary, rapidly oscillating process $\nu_\varepsilon(x) := \nu(x/\varepsilon^2)$:

$$U_0(x) = \left(q + \frac{\sigma}{\varepsilon}\nu_\varepsilon\right) \mathbb{1}_{[0,R]}(x) \ , \tag{2.1.1}$$

but they can be extended to the case of perturbation of a more general initial condition defined by a bounded, compactly supported function $q(x)$. The rapidly oscillating fluctuations of the initial condition can model the high-frequency additive noise of the light source generating the pulse in nonlinear fiber optics, for instance.

We will show in subsection 2.1.2 that for rapidly oscillating processes (small values of ε) the limit system governing the stability of the soliton components reads as a set of SDEs

and it is formally equivalent to the system where the initial condition contains a white noise ($\dot{W}$) perturbation

$$U_0(x) = \left(q + \sqrt{2\alpha}\,\sigma \dot{W}_x\right) \mathbb{1}_{[0,R]}(x) \ , \tag{2.1.2}$$

where α is the integrated covariance of the process ν. This shows that to study the soliton components in the limit of rapid oscillations, the only required parameter of the statistics of ν is its integrated covariance. Notice however that we cannot directly use a white noise to perturb the initial condition, as the IST requires some integrability conditions on the initial condition (for example, $U_0 \in L^1$ for NLS), which are not satisfied by a white noise.

2.1.1 The Inverse Scattering Transform method

The essential technical instrument we will use to deal with the two nonlinear evolution equations we analyze is the inverse scattering transform. This method is a non-linear analogue of the Fourier transform, which can be used to solve many linear partial differential equations. The basic principle is the same, and with both methods the calculation of the solution of the initial value problem proceeds in three steps, as follows:

1. *the forward problem*: the initial conditions in the original "physical" variables are transformed into some spectral coefficients. For the Fourier transform they are simply the Fourier coefficients, while for the IST they are called scattering data. These scattering data characterize a spectral problem in which the initial conditions play the role of a potential. The Jost coefficients (a, b) together with the set of the discrete eigenvalues (ζ_n) of the spectral problem and the associated norming constants ρ_n compose the set of scattering data.

2. *time dependence*: the Fourier coefficients or the scattering data evolve according to simple, explicitly solvable ordinary differential equations. It is easy to obtain their value at any future time.

3. *the inverse problem*: the evolved solution in the original variables is recovered from the evolved solution in the transformed variables. This is done using the inverse Fourier transform or solving the Gelfand-Levitan-Marchenko equation (for the IST).

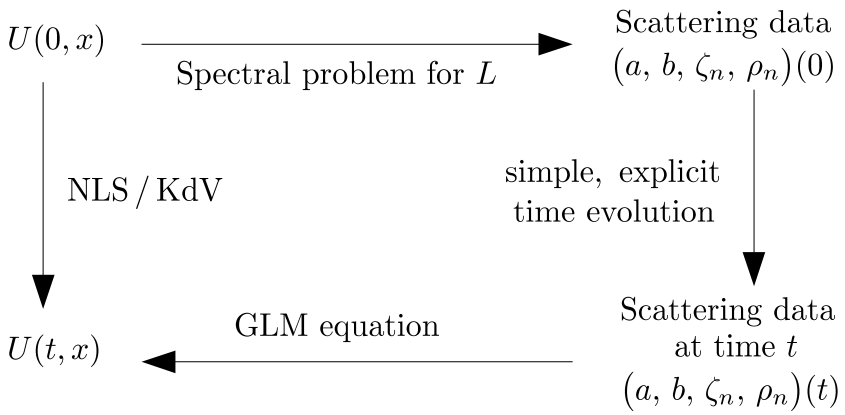

Figure 2.1: The IST method.

The direct transform (direct scattering problem) consists in the analysis of the spectrum of an associated operator L, where the initial condition U_0 enters as a potential. The explicit form of the operator $L(U_0)$ for NLS and KdV together with its domain are given below. L is known as the first operator of the Lax pair. From the eigenvalues and corresponding eigenfuctions of the operator L one can construct the Jost coefficients $a(\zeta, t)$ and $b(\zeta, t)$ at $t = 0$. The essential point is that the scattering data, which is to say the Jost coefficients together with the discrete spectrum and the norming constants associated to each discrete eigenvalue, contain enough information to completely characterize the function U. Moreover, the evolution of the Jost coefficients is very simple: it is governed by the second operator of the Lax pair, M, which is a linear differential operator. Finally, the inverse transform consist in the reconstruction of the solution $U(t, x)$ from the scattering data at time t. This is done by solving an integro-differential equation known as the Gelfand-Levitan-Marchenko equation. The principle of this method is schematically illustrated in figure 2.1.

The IST is a very efficient method to solve the initial value problem for many nonlinear evolution equations, but it can be used for other purposes too. For example, one can construct special solutions by posing an elementary solution in the transformed variables and applying the inverse transformed to obtain the corresponding solution in the original variables. Or, and this is how we will use it, one can study the Jost coefficients to see if a special solution, namely a soliton, will appear from a given initial condition. This approach is particularly convenient as solitons have very easy representations in terms of the scattering data: they correspond the discrete eigenvalues, which can be found as the zeros of the function a in the upper complex half-plane. The continuous spectrum, which for KdV and NLS is the real line, corresponds instead to the radiative component of the solution.

IST for NLS

Let us now apply the IST machinery to our first example, the NLS equation. To obtain the scattering data, the Zakharov-Shabat spectral problem (ZSSP) is introduced

$$\begin{cases} \frac{\partial \psi_1}{\partial x} = i\, U_0(x)\, \psi_2 - i\zeta\, \psi_1 \\ \frac{\partial \psi_2}{\partial x} = i\, U_0^*(x)\, \psi_1 + i\zeta\, \psi_2 \end{cases} , \tag{2.1.3}$$

where ψ_n are the components of a vector eigenfunction Ψ and $\zeta \in \mathbb{C}$ is the spectral parameter. This system is given by the operator

$$L(U_0) = i \begin{pmatrix} 1 & 0 \\ 0 & -1 \end{pmatrix} \partial_x + \begin{pmatrix} 0 & U_0 \\ -U_0^* & 0 \end{pmatrix}$$

acting on $\mathbb{H}^1(\mathbb{R}) = \{\Psi \,|\, \psi_i \in L^2(\mathbb{R}),\, \partial_x \psi_i \in L^2(\mathbb{R}),\, i = 1, 2\}$. When $U_0 = 0$, it is easy to see that the continuous part of the spectrum is composed by the whole real line. The eigenspace associated to the eigenvalue $\zeta \in \mathbb{R}$ has dimension 2 and the functions

$$\Psi \sim \begin{pmatrix} 1 \\ 0 \end{pmatrix} e^{-i\zeta x} , \qquad \Phi \sim \begin{pmatrix} 0 \\ 1 \end{pmatrix} e^{i\zeta x}$$

define a basis of this space. In this case, the discrete spectrum of $L(0)$ is empty, because the nontrivial solutions of $\partial_x f = i\zeta f$ are not in $L^2(\mathbb{R})$.

For any localized initial condition U_0, the continuous spectrum remains unchanged, and

for $\zeta \in \mathbb{R}$ the solutions Ψ, $\widetilde{\Psi}$, Φ, $\widetilde{\Phi}$ defined by the boundary conditions

$$\Psi \sim \begin{pmatrix} 1 \\ 0 \end{pmatrix} e^{-i\zeta x} \qquad \widetilde{\Psi} \sim \begin{pmatrix} 0 \\ 1 \end{pmatrix} e^{i\zeta x}\,, \qquad x \to -\infty \tag{2.1.4}$$

$$\Phi \sim \begin{pmatrix} 0 \\ 1 \end{pmatrix} e^{i\zeta x} \qquad \widetilde{\Phi} \sim \begin{pmatrix} 1 \\ 0 \end{pmatrix} e^{-i\zeta x}, \qquad x \to +\infty \tag{2.1.5}$$

produce two sets $\{\Psi, \widetilde{\Psi}\}$ and $\{\Phi, \widetilde{\Phi}\}$ of linearly independent solutions. These functions are related through the system

$$\begin{pmatrix} \Psi \\ \widetilde{\Psi} \end{pmatrix} = \begin{pmatrix} b(\zeta) & a(\zeta) \\ \widetilde{a}(\zeta) & \widetilde{b}(\zeta) \end{pmatrix} \begin{pmatrix} \Phi \\ \widetilde{\Phi} \end{pmatrix}\,, \tag{2.1.6}$$

where $\zeta \in \mathbb{R}$ and $a(\zeta)$, $b(\zeta)$ are the Jost coefficients (at time zero). They satisfy $|a|^2+|b|^2 = 1$. The functions Ψ and Φ are called Jost functions. If $U_0 \in L^1(\mathbb{R})$, the function $a(\zeta)$ can be continuously extended to the upper complex half-plane in a unique way, and the extended function is analytical for $\Im[\zeta] > 0$ (this extension is analytical if we require some additional fast-decay conditions on the initial condition, such as exponential decay), see [APT, Lemma 2.1]. Then, one can show that the extension of the Jost coefficient $a(\zeta)$ to the upper complex half-plane can only have a finite number of simple zeros. If ζ_n is a zero of a, then Ψ and Φ are linearly dependent, so that there exists a coefficient ρ_n for which $\Psi = \rho_n \Phi$. The eigenfunction corresponding to this spectral value is bounded and decays exponentially, so that ζ_n turns out to be an element of the discrete spectrum.

The scattering data evolve according to very easy and uncoupled equations:

$$\partial_t a(\zeta,t) = 0\,, \qquad \partial_t b(\zeta,t) = -4i\zeta^2 b(\zeta,t)\,, \qquad \partial_t \rho_n(t) = -4i\zeta_n^2 \rho_n(t)\,,$$

and the discrete spectrum $(\zeta_n)_{n=1\dots N}$ does not evolve.

The NLS equation presents an infinite number of quantities that are conserved (as soon as they are well defined) during the evolution [MNPZ]. We shall present here two of them which are of special physical interest.

Mass: The mass of a wave is defined as $N = \int_{\mathbb{R}} |U|^2 \,\mathrm{d}x$. It can be obtained from the scattering data using the formula

$$N = \sum_n 4\eta_n - \frac{1}{\pi}\int_{\mathbb{R}} \ln\left(|a(\zeta)|^2\right) \mathrm{d}\zeta\,,$$

where η_n is the imaginary part of a discrete eigenvalue ζ_n. From this expression one sees how the total mass easily decomposes into the sum of two contributions, one coming from the soliton components of the solution, $N_s = \sum_n 4\eta_n$, the other (the integral over the continuous spectrum, N_r) carried by the radiative part of the solution.

Energy: The energy (which is also twice the Hamiltonian) of a wave is given by the formula $E = \int_{\mathbb{R}} |\partial_x U|^2 - |U|^4 \,\mathrm{d}x$. It can be obtained from the scattering data as follows:

$$E = \sum_n \frac{8i}{3}\left[(\zeta_n^*)^3 - (\zeta_n)^3\right] - \frac{4}{\pi}\int_{\mathbb{R}} \zeta^2 \ln\left(|a(\zeta)|^2\right) \mathrm{d}\zeta\,.$$

Also the total energy decomposes into the sum of two contributions. Each soliton contributes with an energy of $(8i)/3 * \left[(\zeta_n^*)^3 - (\zeta_n)^3\right] = 16\eta_n(\xi_n^2 - \eta_n^2/3)$. The radiative

part of the solution provides an energy of $-4/\pi \int_{\mathbb{R}} \zeta^2 \ln\big(|a(\zeta)|^2\big)\,\mathrm{d}\zeta$.

Each discrete eigenvalue $\zeta = \xi + i\eta$, $\eta > 0$ corresponds to a soliton component of the solution. A pure soliton solution of the NLS equation has the form

$$U(t,x) = 2i\eta \frac{\exp\Big(-2i\xi(x-x_0) - 4i(\xi^2-\eta^2)t\Big)}{\cosh\Big(2\eta(x-x_0+4\xi t)\Big)}\ . \tag{2.1.7}$$

The amplitude of the soliton only depends on the imaginary part of the discrete eigenvalue associated, and is given by 2η. The mass of the soliton is 4η, according to the above definition. The speed of the soliton is determined by the real part of the eigenvalue, and is given by 4ξ. The energy of the soliton depends on both the real and imaginary part of the eigenvalue:

$$E_s = 16\eta\Big(\xi^2 - \frac{1}{3}\eta^2\Big)\,.$$

The pure soliton solution (2.1.7) is associated to the eigenvalue $\xi + i\eta$ and the scattering data

$$a(\zeta,t) = \frac{\zeta-\zeta_n}{\zeta-\zeta_n^*}\ , \qquad b(\zeta,t) = 0\ ,$$
$$\rho(t) = \frac{\eta}{\xi+i\eta}\,\exp\big[-2i(\xi+i\eta+\pi/4) - 4i(\xi+i\eta)^2 t\big]\,.$$

IST for KdV

Let us now consider the KdV equation. If we assume some integrability of the initial condition, namely

$$U_0 \in P_1 := \Big\{ f:\mathbb{R}\to\mathbb{R}\ \Big|\ \int_{-\infty}^{\infty} \big(1+|x|\big)\big|f(x)\big|\,\mathrm{d}x < \infty \Big\}, \tag{2.1.8}$$

it is possible to introduce a direct scattering problem associated to the KdV equation [AC], which is given by the first operator of the Lax pair acting on $H^2(\mathbb{R}) = \big\{ f \in L^2(\mathbb{R}) \,|\, \partial_x^2 f \in L^2(\mathbb{R})\big\}$, and reads

$$\frac{\partial^2\varphi}{\partial x^2} + (U_0+\zeta^2)\varphi = 0\,. \tag{2.1.9}$$

The continuous part of the spectrum of equation (2.1.9) is again the real axis. For $\zeta \in \mathbb{R}$, there are two convenient complete sets of bounded functions associated to equation (2.1.9), defined by their asymptotic behavior:

$$\begin{aligned} &\phi \sim e^{-i\zeta x} \qquad \widetilde{\phi} \sim e^{i\zeta x}\,, && \text{for } x\to-\infty \\ &\psi \sim e^{i\zeta x} \qquad \widetilde{\psi} \sim e^{-i\zeta x}\,, && \text{for } x\to+\infty\,. \end{aligned}$$

It follows from the above definitions that

$$\phi(x,\zeta) = \widetilde{\phi}(x,-\zeta)\,, \qquad \psi(x,\zeta) = \widetilde{\psi}(x,-\zeta)$$

and

$$\begin{pmatrix}\phi\\ \widetilde{\phi}\end{pmatrix} = \begin{pmatrix} b(\zeta) & a(\zeta)\\ \widetilde{a}(\zeta) & \widetilde{b}(\zeta)\end{pmatrix}\begin{pmatrix}\psi\\ \widetilde{\psi}\end{pmatrix}\,,$$

where $\zeta \in \mathbb{R}$ and $a(\zeta)$, $b(\zeta)$ are the Jost coefficients (at time zero). They satisfy $|a|^2 - |b|^2 = 1$. The function a can be continuously extended to an analytical (for $\Im[\zeta > 0]$) function in the upper complex half-plane, where it has only a finite number of simple zeros located on the imaginary axis $\zeta = i\eta$, see [AC, Lemma 2.2.2]. Just as for the NLS equation, these zeros turn out to be the eigenvalues of the discrete spectrum, which correspond to the soliton components of the solution. The scattering data evolve according to the uncoupled system

$$\partial_t a(\zeta, t) = 0\,, \qquad \partial_t b(\zeta, t) = 8i\zeta^3 b(\zeta, t)\,, \qquad \partial_t \rho_n(t) = 8i\zeta_n^3 \rho_n(t)\,,$$

and the discrete spectrum $(\zeta_n = i\eta_n)_{n=1\dots N}$ does not evolve.

Also the KdV equation has an infinite number of conserved quantities. The first two of them are called the mass and energy of the solution and are defined below, [Ga01].

Mass: The mass of a wave is defined as $N = \int_{\mathbb{R}} U \,\mathrm{d}x$. It can be obtained from the scattering data using the formula

$$N = \sum_n 4\eta_n - \frac{1}{\pi} \int_{\mathbb{R}} \ln\left(|a(\zeta)|^2\right) \mathrm{d}\zeta\,,$$

where η_n is the imaginary part of a discrete eigenvalue ζ_n. Each soliton component of the solution contributes with a mass of $4\eta_n$, while the term given by the integral over the continuous spectrum in the above equation represents the contribution to the total mass due to the radiative part of the solution.

Energy: The energy is given by $E = \int_{\mathbb{R}} U^2 \,\mathrm{d}x$, and it can be obtained from the scattering data using the formula

$$E = \sum_n \frac{16}{3}\eta_n^3 + \frac{4}{\pi} \int_{\mathbb{R}} \zeta^2 \ln\left(|a(\zeta)|^2\right) \mathrm{d}\zeta\,.$$

The total energy decomposes into the sum of two terms, one taking into account the contribution of each soliton component $(16\eta_n^3/3)$, the other accounting for the energy of the radiative part of the solution (the integral over the continuous spectrum).

Each discrete eigenvalue $\zeta = i\eta$, $\eta > 0$, corresponds to a soliton component of the solution. A pure soliton solution is given by

$$U(t, x) = 2\eta^2 \operatorname{sech}^2\big(\eta(x - x(t))\big)\,, \tag{2.1.10}$$

where $x(t) = x_0 + 4\eta^2 t$ is the center of the soliton. As one can see from this equation, the amplitude $2\eta^2$ and speed $4\eta^2$ of the solitons of the KdV equation are linked. The mass of a soliton is $N = 4\eta$ and its energy $E = 16\eta^3/3$. The soliton solution (2.1.10) is associated to the eigenvalue $i\eta_n$ and the scattering data

$$a(\zeta, t) = \frac{\zeta - i\eta}{\zeta + i\eta}\,, \qquad b(\zeta, t) = 0\,, \qquad \rho(t) = 2\eta e^{2\eta x_0} e^{8\eta^3 t}\,.$$

2.1.2 Limit of rapidly oscillating processes

This subsection contains a rigorous justification for the use of the IST. We have already remarked that to be able to apply the IST the initial condition U_0 needs to satisfy some integrability condition, L^1 for NLS and (2.1.8) for KdV. These hypotheses are satisfied by initial conditions of the form (2.1.1) for any $\varepsilon > 0$ if ν is bounded. Our objective is to show that the IST applied to these random initial conditions gives a problem that reads as a

canonical system of SDEs in the limit $\varepsilon \to 0$. Thanks to the convergence result of Theorem 2.2 below, this limit system can be used to study the behavior of rapidly oscillating initial conditions ($0 < \varepsilon \ll 1$), as we shall do in the following sections. We stress that our interest is in the study of rapidly oscillating initial conditions, which are physically more relevant than the limit case of infinitely rapid oscillations and for which the IST can be applied in a rigorous way. We make the following assumptions (standard in the diffusion approximation theory, [FGPS]) on the process ν:

Hypothesis 2.1. Let $\nu(x)$ be a real, homogeneous, ergodic, centered, bounded, Markov stochastic process, with finite integrated covariance $\int_0^\infty \mathbb{E}[\nu(0)\nu(x)]\,\mathrm{d}x = \alpha < \infty$ and with generator $\mathcal{L}_\nu$ satisfying the Freedholm alternative.

Set

$$U_0^\varepsilon(x) := \big(q + \frac{\sigma}{\varepsilon}\,\nu(x/\varepsilon^2)\big)\,\mathbb{1}_{[0,R]}(x) \tag{2.1.11}$$

and remark that for $x \in [0, R]$

$$\int_0^x U_0^\varepsilon(y)\,\mathrm{d}y \overset{\varepsilon\to 0}{\longrightarrow} \int_0^x U_0(y)\,\mathrm{d}y = qx + \sqrt{2\alpha}\,\sigma W_x$$

in the space of continuous functions $\mathcal{C}^0\big([0,R];\mathbb{R}\big)$, in distribution, see [FGPS]. For every $\varepsilon > 0$, we apply the first step of the IST to the NLS and KdV equations with the initial condition U_0^ε, to obtain the associated spectral problem. Then we will investigate the passage to the limit of this problem. We point out that this passage to the limit is quite delicate: if it is relatively easy to obtain a pointwise (in ζ) convergence of the spectral data, to obtain fine results for the limit case and for situations near the limit case ($0 < \varepsilon \ll 1$), a much stronger convergence will be needed.

NLS: pointwise convergence

We consider the ZSSP system associated to the NLS equation: our goal is to identify the points of the upper complex half-plane, $\zeta \in \mathbb{C}^+$, for which there exists a solution Ψ of the first order system (2.1.3) for $x \in [0, R]$, satisfying the boundary conditions

$$\Psi(0) = \begin{pmatrix} 1 \\ 0 \end{pmatrix} \qquad \text{and} \qquad \psi_1(R) = 0$$

derived from the exponential decay conditions (2.1.4). These particular values of ζ are the discrete eigenvalues of the ZSSP and correspond to the soliton components of the solution. The strategy employed is to consider the flow $\Psi(x,\zeta)$, $x \in [0,R]$, $\zeta \in \mathbb{C}^+$, solution of (2.1.3) with initial condition

$$\Psi(0) = \begin{pmatrix} 1 \\ 0 \end{pmatrix}, \tag{2.1.12}$$

and look for the values of ζ for which the final condition is satisfied.

For a fixed value of ζ, we consider the solution Ψ^ε of the ZSSP obtained from the application of the first step of the IST method:

$$\begin{cases} \frac{\partial \psi_1^\varepsilon}{\partial x} = -i\zeta\,\psi_1^\varepsilon + i\,U_0^\varepsilon(x)\,\psi_2^\varepsilon \\ \frac{\partial \psi_2^\varepsilon}{\partial x} = i\,\big(U_0^\varepsilon(x)\big)^*\,\psi_1^\varepsilon + i\zeta\,\psi_2^\varepsilon \end{cases}, \tag{2.1.13}$$

with initial condition

$$\Psi^\varepsilon(0) = \begin{pmatrix} 1 \\ 0 \end{pmatrix}.$$

Now, [FGPS, Theorem 6.1] states that the process Ψ^ε converges in distribution in $\mathcal{C}^0([0,R];\mathbb{C}^2)$ to the process Ψ solution of

$$\begin{cases} \mathrm{d}\psi_1 = \left[(-i\zeta - \alpha\sigma^2)\,\psi_1 + iq\,\psi_2\right]\mathrm{d}x + i\sqrt{2\alpha}\,\sigma\psi_2\,\mathrm{d}W_x \\ \mathrm{d}\psi_2 = \left[i\,q\,\psi_1 + (i\zeta - \alpha\sigma^2)\,\psi_2\right]\mathrm{d}x + i\sqrt{2\alpha}\,\sigma\psi_1\,\mathrm{d}W_x \end{cases} \tag{2.1.14}$$

with initial condition (2.1.12), which can be rewritten in Stratonovich form as

$$\mathrm{d}\Psi = i\begin{pmatrix} -\zeta & q \\ q & \zeta \end{pmatrix}\Psi\,\mathrm{d}x + i\sqrt{2\alpha}\,\sigma\begin{pmatrix} 0 & 1 \\ 1 & 0 \end{pmatrix}\Psi \circ \mathrm{d}W_x\,. \tag{2.1.15}$$

For NLS we can also consider perturbations produced by a complex process: let ν_1, ν_2 be two independent copies of the process ν and set $\widetilde{\nu} := \nu_1 + i\nu_2$. One can define U_0^ε using $\widetilde{\nu}$ instead of ν; proceeding as above, from the IST one obtains again the system (2.1.13), and from [FGPS, Theorem 6.1] one gets that in this case the limit process is the solution of

$$\mathrm{d}\Psi = i\begin{pmatrix} -\zeta & q \\ q & \zeta \end{pmatrix}\Psi\,\mathrm{d}x + i\sqrt{2\alpha}\,\sigma\begin{pmatrix} 0 & 1 \\ 1 & 0 \end{pmatrix}\Psi \circ \mathrm{d}W_x^{(1)} - \sqrt{2\alpha}\,\sigma\begin{pmatrix} 0 & 1 \\ -1 & 0 \end{pmatrix}\Psi \circ \mathrm{d}W_x^{(2)}, \tag{2.1.16}$$

where the $W^{(i)}$ are two independent Wiener processes, with the same initial condition (2.1.12).

KdV: pointwise convergence

We apply the same strategy to the KdV equation: the goal is to obtain the values of $\zeta \in \mathbb{C}^+$ for which there exists a solution φ of

$$\varphi^\varepsilon_{xx} + (U_0^\varepsilon + \zeta^2)\varphi^\varepsilon = 0 \tag{2.1.17}$$

with the boundary conditions

$$\varphi^\varepsilon(0) = 1\,, \qquad \varphi^\varepsilon_x(0) = -i\zeta\,, \qquad \varphi^\varepsilon_x(R) - i\zeta\varphi^\varepsilon(R) = 0\,.$$

These conditions correspond to imposing exponential decay of the solution at infinity. Setting $\Phi := (\varphi, \varphi_x)^T$ this equation can be transformed into

$$\mathrm{d}\Phi^\varepsilon = \begin{pmatrix} 0 & 1 \\ -U_0^\varepsilon - \zeta^2 & 0 \end{pmatrix}\Phi^\varepsilon \mathrm{d}x \tag{2.1.18}$$

with boundary conditions

$$\Phi^\varepsilon(0) = \begin{pmatrix} 1 \\ -i\zeta \end{pmatrix}\,, \quad \phi_2^\varepsilon(R) - i\zeta\phi_1^\varepsilon(R) = 0\,.$$

We consider the flow $\Phi^\varepsilon(x,\zeta)$, $x \in [0,R]$, $\zeta \in \mathbb{C}^+$, defined by the above equation with only the initial condition, and look for the values of ζ such that the final condition is satisfied.

Again by [FGPS, Theorem 6.1], Φ^ε converges in distribution to the solution of

$$\mathrm{d}\Phi = \begin{pmatrix} 0 & 1 \\ -q-\zeta^2 & 0 \end{pmatrix} \Phi \,\mathrm{d}x + \sqrt{2\alpha}\,\sigma \begin{pmatrix} 0 & 0 \\ 1 & 0 \end{pmatrix} \Phi \,\mathrm{d}W_x \tag{2.1.19}$$

which, in terms of the function φ, can be rewritten as

$$\mathrm{d}\varphi_x = -(q+\zeta^2)\,\varphi \,\mathrm{d}x + \sqrt{2\alpha}\,\sigma\varphi \,\mathrm{d}W_x\,. \tag{2.1.20}$$

The initial condition is

$$\Phi(0) = \begin{pmatrix} 1 \\ -i\zeta \end{pmatrix}, \qquad \text{or equivalently} \qquad \varphi(0) = 1\,, \quad \varphi_x(0) = -i\zeta\,. \tag{2.1.21}$$

Remark that in the last two differential equations above the Stratonovich and Itô stochastic integrals coincide.

Convergence as $\mathcal{C}^1$ functions

The convergence obtained above is only for a (finite number of) fixed ζ and σ, but we can do much better. Indeed, in the next section we will need to differentiate the limit process with respect to the parameters (ζ, σ), so that we look for a convergence in $\mathcal{C}^0\big([0,R];\mathcal{C}^1(\mathbb{R}^3)\big)$. This is the main result of this section; the exact formulation is given in the following theorem. We will focus on the problem of finding the values of ζ for which the limit flows Ψ and Φ match the final conditions in section 2.2.

Theorem 2.2. *Assume hypothesis 2.1 and define U_0^ε as in (2.1.11). Let $\Psi^\varepsilon := (\psi_1^\varepsilon, \psi_2^\varepsilon)^T$ be the solution of (2.1.13) with initial condition (2.1.12) and Ψ the solution of (2.1.15) with the same initial condition. Let also φ^ε be the solution of (2.1.17) with initial condition (2.1.21) and φ be the solution of (2.1.20) with the same initial condition. Considering these as functions of the space variable x and the parameters ξ, η, σ, we have in the limit of $\varepsilon \to 0$ that $\Psi^\varepsilon(x,\xi,\eta,\sigma) \to \Psi(x,\xi,\eta,\sigma)$ weakly in $\mathcal{C}^0\big([0,R];\mathcal{C}^1(\mathbb{R}^3;\mathbb{C}^2)\big)$ and $\varphi^\varepsilon(x,\xi,\eta,\sigma) \to \varphi(x,\xi,\eta,\sigma)$ weakly in $\mathcal{C}^0\big([0,R];\mathcal{C}^1(\mathbb{R}^3;\mathbb{R})\big)$.*

To prove this theorem we need a standard tightness criteria, provided by the two following lemmas [Me]. We will use $\mathcal{D}\big([0,R];E\big)$ to denote the space of CadLag processes defined for $x \in [0,R]$ and with values in the space E. The first lemma is due to Aldous, [Al78].

Lemma 2.3. *Let (E,d) be a metric space, and X^ε a process with paths in $\mathcal{D}\big([0,R];E\big)$. If for every x in a dense subset of $[0,R]$ the family $\big(X^\varepsilon(x)\big)_{\varepsilon\in(0,1]}$ is tight in E and X^ε satisfy the Aldous property:*

A *: For any $\kappa > 0, \lambda > 0$, there exists $\delta > 0$ such that*

$$\limsup_{\varepsilon\to 0} \sup_{\tau<R} \sup_{0<\theta<\delta\wedge(R-\tau)} \mathbb{P}\big(\|X^\varepsilon(\tau+\theta) - X^\varepsilon(\tau)\| > \lambda\big) < \kappa\,,$$

where τ is a stopping time;

then the family $\big(X^\varepsilon\big)_{\varepsilon\in(0,1]}$ is tight in $\mathcal{D}\big([0,R];E\big)$.

If $\mathcal{H}$ is a Hilbert space and $\mathcal{H}_n$ a subspace of $\mathcal{H}$, we shall use $\pi_{\mathcal{H}_n}$ to denote the projection of $\mathcal{H}$ onto $\mathcal{H}_n$. Also, $d_{\mathcal{H}}$ is used to denote the distance on $\mathcal{H}$ introduced by the inner product. The proof of this lemma can be found in [Me84].

Lemma 2.4. *Let $\mathcal{H}$ be a Hilbert space and $\mathcal{H}_n$ be an increasing sequence of finite-dimensional subspaces of $\mathcal{H}$ such that, for any $h \in \mathcal{H}$, $\lim_{n\to\infty} \pi_{\mathcal{H}_n} h = h$. Let $(Z^\varepsilon)_{\varepsilon\in(0,1]}$ be a family of $\mathcal{H}$-valued random variables. Then, the family $(Z^\varepsilon)_{\varepsilon\in(0,1]}$ is tight if and only if for any $\kappa > 0$ and $\lambda > 0$, there exist ρ_κ and a subspace $\mathcal{H}_{\kappa,\lambda}$ such that*

$$\sup_{\varepsilon\in(0,1]} \mathbb{P}\big(\|Z^\varepsilon\| \geq \rho_\kappa\big) \leq \kappa \qquad \textit{and} \qquad \sup_{\varepsilon\in(0,1]} \mathbb{P}\big(d_{\mathcal{H}}(Z^\varepsilon, \mathcal{H}_{\kappa,\lambda}) > \lambda\big) \leq \kappa\,. \tag{2.1.22}$$

Proof of Theorem 2.2. To unify notation, we shall use X^ε to denote both Ψ^ε and Φ^ε. Therefore, X^ε is the solution of what we shall call the approximated system, which is either system (2.1.13) or (2.1.18), with $\varepsilon > 0$.

Since propositions 2.14 and 2.21 ensure that the limit equations for Ψ and Φ have a unique solution which is $\mathcal{C}^0\big([0,R];\mathcal{C}^1(\mathbb{R}^3)\big)$, it suffices to prove convergence in the space of CadLag processes $\mathcal{D}\big([0,R];\mathcal{C}^1(\mathbb{R}^3)\big)$. We will do so in three steps.

Steps 1 contains a technical result needed for the application in step 2 of lemma 2.4, namely the proof of the bound (2.1.23).

In step 2, using lemma 2.4, we will show that for every fixed x the sequences $\big(\Psi^\varepsilon(x)\big)_\varepsilon$ and $\big(\Phi^\varepsilon(x)\big)_\varepsilon$, denoted $\big(X^\varepsilon(x)\big)_\varepsilon$ in the following, are tight in the Hilbert space $\mathcal{H} := W^{3,2}(G)$. Note that, by Sobolev imbedding, $\mathcal{H} \hookrightarrow \mathcal{C}^1(G)$. Here, G is an open, bounded subset of $\mathbb{R}^3$, the space of parameters. For simplicity we take $G = (-N, N)^3$ for some real positive constant N; a justification of the fact that it is not restrictive to assume that the set of parameters G is bounded is given below in the proof of proposition 2.14, where the convergences we are proving here will be used.

In the last step we will use lemma 2.3, where we take E to be the Hilbert space $\mathcal{H}$. This will provide the desired convergence of the family of processes $(X^\varepsilon)_{\varepsilon\in(0,1]}$ in $\mathcal{D}\big([0,R];\mathcal{C}^1(\mathbb{R}^3)\big)$.

Since X^ε is the solution of a linear differential equation with coefficients smooth in the parameters $\mu = (\xi, \eta, \sigma)$, from the explicit formula for the solution we get that $X^\varepsilon(x,\mu)$ is smooth in the parameters. We will soon use its derivatives in the parameters: the vector of X^ε and its first derivatives in μ still satisfy a linear system of ODEs whose coefficients depend linearly on the parameters and on the process $\nu(x/\varepsilon^2)$, and the same result holds adding higher order derivatives.

Step 1 (A preliminary estimate). The key point to show that $\big(X^\varepsilon(x,\mu)\big)_{\mu\in G}$ is tight in $\mathcal{H} = W^{3,2}(G)$ for every $x \in [0,R]$ is the proof of the bound

$$\limsup_{\varepsilon\to 0}\ \mathbb{E}\Big[\big\|X^\varepsilon(x,\cdot)\big\|_{W^{6,2}(G)}\Big] \leq C < \infty \tag{2.1.23}$$

uniformly in $x \in [0,R]$. This is the content of this step.

Define Y^ε as the vector process of X^ε and all of its derivatives in the parameters $\mu = (\xi,\eta,\sigma)$ up to order 6. As remarked above, this process is the solution of a linear system of ODEs with coefficients (the matrices M_1 and M_2) linear in the parameters:

$$\frac{\mathrm{d}}{\mathrm{d}x} Y^\varepsilon = M_1 Y^\varepsilon + \frac{1}{\varepsilon}\nu(x/\varepsilon^2) M_2 Y^\varepsilon\,.$$

Since G is bounded, we only need to check that the second moment of $Y^\varepsilon(x,\mu)$ is uniformly bounded with respect to $\varepsilon \in (0,1]$, $\mu \in G$ and $x \in [0,R]$. Actually, we aim at a stronger result, which we will need later. We are going to show that (recall that $Y_0 = Y_0^\varepsilon$ is deterministic since both $\Psi^\varepsilon(0)$, $\Phi^\varepsilon(0)$ and their derivatives in zero are defined by the equation

for $x \le 0$, which is deterministic, and the boundary condition at $x \to -\infty$)

$$\mathbb{E}\Big[\sup_{x\in[0,R]} \big|Y^\varepsilon(x)\big|^2\Big] \le C_R\Big(1 + \big|Y(0)\big|^2\Big) < \infty\,. \tag{2.1.24}$$

Following [FGPS, Section 6.3.5], we show this bound with the perturbed test function method. Let $\mathcal{L}^\varepsilon$ be the infinitesimal generator of the process Y^ε and $\mathcal{L}$ the infinitesimal generator of the process Y obtained from the process X solution of the limit system (2.1.15) or (2.1.19). Let $m \in N$ be such that $Y^\varepsilon(x) \in \mathbb{C}^m$ and let K be a compact subset of $\mathbb{R}$ containing the image of the bounded process ν. For every $y \in \mathbb{C}^m$ and $z \in K$, $\mathcal{L}^\varepsilon$ has the form

$$\mathcal{L}^\varepsilon g(y,z) = \frac{1}{\varepsilon^2}\mathcal{L}_\nu g(y,z) + \frac{z}{\varepsilon}\big(M_2 y\big)^T \nabla_y g(y,z) + \big(M_1 y\big)^T \nabla_y g(y,z)\,,$$

where $\mathcal{L}_\nu$ is the infinitesimal generator of the process ν, as defined in hypothesis 2.1. Let f be the identity function on $\mathbb{C}^m$ and $f^\varepsilon(y,z) = y + \varepsilon f_1(y,z)$ be the associated perturbed function, which is solution of the Poisson equation $\mathcal{L}_\nu f_1(y,z) = -z\big(M_2 y\big)^T \nabla_y f(y)$. In this equation, y plays the role of a frozen parameter, so that f_1 has linear growth in y, uniformly in z, and the same holds for

$$\mathcal{L}^\varepsilon f^\varepsilon(y,z) = z\big(M_2 y\big)^T \nabla_y f_1(y,z) + \varepsilon\big(M_1 y\big)^T \nabla_y f_1(y,z)\,.$$

Since

$$\begin{aligned} Y^\varepsilon(x) = Y^\varepsilon(0) &- \varepsilon\Big[f_1\big(Y^\varepsilon(x), \nu^\varepsilon(x)\big) - f_1\big(Y^\varepsilon(0), \nu^\varepsilon(0)\big)\Big] \\ &+ \int_0^x \mathcal{L}^\varepsilon f^\varepsilon\big(Y^\varepsilon(x'), \nu^\varepsilon(x')\big)\,\mathrm{d}x' + M_x^\varepsilon\,, \end{aligned}$$

where M_x^ε is a vector valued martingale, we get the bound

$$\begin{aligned} \sup_{x\in[0,R]} \big|Y^\varepsilon(x)\big| \le \big|Y^\varepsilon(0)\big| &+ \varepsilon C\Big[1 + \sup_{x\in[0,R]} \big|Y^\varepsilon(x)\big|\Big] \\ &+ C\int_0^R 1 + \sup_{x'\in[0,x]} \big|Y^\varepsilon(x')\big|\,\mathrm{d}x + C\sup_{x\in[0,R]} \big|M_x^\varepsilon\big|\,. \end{aligned}$$

For $\varepsilon \le \frac{1}{2C}$, applying Gronwall's inequality and renaming constants we get

$$\sup_{x\in[0,R]} \big|Y^\varepsilon(x)\big| \le C_R\Big(1 + \big|Y^\varepsilon(0)\big| + \sup_{x\in[0,R]} \big|M_x^\varepsilon\big|\Big)\,. \tag{2.1.25}$$

The quadratic variation of the martingale is given by

$$\langle M^\varepsilon\rangle_x = \int_0^x g^\varepsilon\big(Y^\varepsilon(x'), \nu^\varepsilon(x')\big)\,\mathrm{d}x'\,,$$

where

$$\begin{aligned} g^\varepsilon(y,z) = \big(\mathcal{L}^\varepsilon f^{\varepsilon 2} - 2f^\varepsilon \mathcal{L}^\varepsilon f^\varepsilon\big)(y,z) &= \big(\mathcal{L}_\nu f_1^2 - 2f_1\mathcal{L}_\nu f_1\big)(y,z) \\ &+ 2\varepsilon z\Big[\big(M_2 y\big)^T f_1(y,z) - \big(M_2 y\big)^T\big((\nabla_y f_1)^T f_1\big)(y,z)\Big] \\ &+ 2\varepsilon^2\Big[\big(M_1 y\big)^T f_1(y,z) - \big(M_1 y\big)^T\big((\nabla_y f_1)^T f_1\big)(y,z)\Big] \end{aligned}$$

has quadratic growth in y uniformly in $z \in K$. Therefore, by Doob's inequality,

$$\mathbb{E}\Big[\sup_{x\in[0,R]}\big|M_x^\varepsilon\big|^2\Big] \le C\,\mathbb{E}\Big[\big\langle M^\varepsilon\big\rangle_R\Big] \le C\int_0^R 1+\mathbb{E}\big[\big|Y^\varepsilon(x)\big|^2\big]\,\mathrm{d}x\,.$$

Substituting into the expected value of the square of (2.1.25) and using again Gronwall's inequality, we get (2.1.24), which gives (2.1.23).

Step 2 (Tightness of $X^\varepsilon(x)$). In this step we show how to obtain the tightness of the family $\big(X^\varepsilon(x,\mu)\big)_{\mu\in G}$ from (2.1.23) using lemma 2.4. Indeed, from this bound the first part of condition (2.1.22) follows by the Markov inequality if we take $\rho_\kappa = C/\kappa$. This bound also provides information on the regularity of $X^\varepsilon(x)$, which can be used to prove the second part of condition (2.1.22) as follows. By the Sobolev imbedding $W^{6,2}(G) \hookrightarrow \mathcal{C}^4(G)$ the bound (2.1.23) implies that $X^\varepsilon \in \mathcal{C}^4(G)$. An appropriate sequence of subspaces $(\mathcal{H}_n)_n$ is constructed in the appendix in lemma 2.48, and lemma 2.49 states that for any function $g \in \mathcal{C}^4(G)$ there exists an arbitrarily good approximation g_n belonging to some $\mathcal{H}_n$. The control on the distance between g and the subspace $\mathcal{H}_n$ only depends on the norm $\|g\|_{\mathcal{C}^4}$, so that by (2.1.23) the approximation is uniform in ε. This provides the second part of condition (2.1.22). Finally, corollary 2.50 provides the last hypothesis of lemma 2.4, namely that for the sequence of subspaces $\mathcal{H}_n$ constructed in lemma 2.48, for any $h \in \mathcal{H}$, $\lim_{n\to\infty} \pi_{\mathcal{H}_n} h = h$. Then, lemma 2.4 gives that for every x, the family $\big(X^\varepsilon(x,\mu)\big)_{\mu\in G}$ is tight in $\mathcal{H} = W^{3,2}(G)$.

Step 3 (Tightness of X^ε). Thanks to lemma 2.3, the tightness of the family of processes X^ε in $\mathcal{D}\big([0,R];\mathcal{H}\big)$ follows if we show that the Aldous property [**A**] holds. Since G is bounded, we can prove the Aldous property showing that

$$\lim_{\delta\to 0}\ \limsup_{\varepsilon\to 0}\ \sup_{\mu\in G}\ \sup_{\tau\le R}\ \sup_{0<\theta<\delta}\ \mathbb{E}\Big[\big|Y^\varepsilon(\tau+\theta,\mu)-Y^\varepsilon(\tau,\mu)\big|^2\Big] = 0\,, \tag{2.1.26}$$

where Y^ε is the vector process having as components X^ε and its derivatives in μ up to the third order only. We prove the above limit using again the perturbed test function method. With the notations introduced above, we have

$$\begin{aligned}
\big|Y^\varepsilon(\tau+\theta)-Y^\varepsilon(\tau)\big|^2 &\le C\Big|M^\varepsilon_{\tau+\theta}-M^\varepsilon_\tau\Big|^2 + C\int_\tau^{\tau+\theta}\Big|\mathcal{L}^\varepsilon f^\varepsilon\big(Y^\varepsilon(x),\nu^\varepsilon(x)\big)\Big|^2\mathrm{d}x\\
&\quad + C\varepsilon\Big(1+\sup_{x\in[\tau,\tau+\theta]}\big|Y^\varepsilon(x)\big|^2\Big)\\
&\le C\Big|M^\varepsilon_{\tau+\theta}-M^\varepsilon_\tau\Big|^2 + C\int_\tau^{\tau+\theta}\Big|\mathcal{L}^\varepsilon f^\varepsilon\big(Y^\varepsilon,\nu^\varepsilon\big)-\mathcal{L}f(Y^\varepsilon)\Big|^2\mathrm{d}x\\
&\quad + C\int_\tau^{\tau+\theta}\big|\mathcal{L}f(Y^\varepsilon)\big|^2\mathrm{d}x + C\varepsilon\Big(1+\sup_{x\in[\tau,\tau+\theta]}\big|Y^\varepsilon(x)\big|^2\Big)\,.
\end{aligned}$$

We have that

$$\mathbb{E}\Big[\big|M^\varepsilon_{\tau+\theta}-M^\varepsilon_\tau\big|^2\Big] = \mathbb{E}\Big[\big(M^\varepsilon_{\tau+\theta}\big)^2-\big(M^\varepsilon_\tau\big)^2\Big] = \mathbb{E}\Big[\int_\tau^{\tau+\theta}\mathrm{d}\langle M^\varepsilon\rangle_x\Big]\,.$$

Since $\big|\mathcal{L}^\varepsilon f^\varepsilon(y,z)-\mathcal{L}f(y)\big| \le \varepsilon C(1+|y|)$ and $|\mathcal{L}f(y)| \le C|y|$, for $\theta \le \delta$

$$\mathbb{E}\Big[\big|Y^\varepsilon(\tau+\theta)-Y^\varepsilon(\tau)\big|^2\Big] \le C_R\,(\delta+\varepsilon)\Big(1+\mathbb{E}\Big[\sup_{x\in[0,R]}\big|Y^\varepsilon(x)\big|^2\Big]\Big)\,.$$

The right-hand side is independent of τ and we can use estimate (2.1.24) to bound it uniformly in ε and μ. Therefore, (2.1.26) follows and the proof of Theorem 2.2 is complete. □

Remark 2.5. Using the notion of pseudo-generators, as introduced in [EK, Section 7.4], it is possible to relax the conditions imposed on the driving process $\nu(x)$ assuming that it is just a mixing process instead of Markov.

2.2 Stability of solitons

This section is devoted to the study of the stability of solitons with respect to rapidly oscillating random perturbations of the initial condition. Our results state that solitons of both the NLS and KdV equation are stable under perturbations of the initial condition. Moreover, for small-amplitude random perturbations, we provide an easy way to compute first order correction terms for the parameters characterizing the solitons. However, if for both equations solitons are stable, a few interesting differences must be pointed out. For example, for NLS there is a thresholding effect for the creation of solitons from noise, so that unless the integral of the deterministic initial condition exceeds a certain threshold, the addition of a small random perturbation cannot generate a soliton. On the other hand, for KdV even a very small random initial condition can produce a soliton. Moreover, we will see that in the presence of a random perturbation KdV solitons are perturbed in both amplitude and velocity, while unless the perturbation is complex the velocity of NLS solitons is not substantially affected.

Thanks to the results of the previous section, we know that for rapidly oscillating initial conditions both the NLS and KdV systems can be investigated using the limit equations (2.1.15) and (2.1.20), which formally correspond to a real or complex white noise perturbation on the initial condition.

For NLS we have seen that every soliton is identified by a complex number $\zeta = \xi + i\eta$ such that the flow $\Psi(x, \zeta)$ solution of (2.1.15) with initial condition (2.1.12) satisfies also a given final condition. The real and imaginary parts of ζ define the velocity and amplitude of the soliton, respectively. For KdV, solitons are identified by an imaginary number $\zeta = i\eta$, defining both the velocity and amplitude of the soliton, which are related.

We start analyzing the NLS equation, and leave KdV to the second part of this section. For each of the two equations we start by reporting, in subsections 2.2.1 and 2.2.4, some classical results on the background deterministic solution. Then we analyze how this solution is modified by the introduction of a real, small-amplitude, rapidly oscillating random perturbation of the initial condition. This is done in subsections 2.2.2 and 2.2.5. For NLS we can also consider the case of perturbations of the initial condition given by rapidly oscillating complex processes; the stability of solitons in this case is investigated in subsection 2.2.3. We deal with the limit cases of "quiescent" solitons for NLS and KdV in corollary 2.10, remark 2.18 and proposition 2.20. Finally, for KdV one can also consider the case of a perturbation of the zero initial condition: this is done in subsection 2.2.6.

For simplicity of exposition, in this section we choose the value of the integrated covariance of the process ν to be $\alpha = 1/2$.

2.2.1 NLS solitons – deterministic background solution

Let $U_0(x) = q\,\mathbb{1}_{[0,R]}(x)$. Burzlaff proved in [Bu88] that in this case the number of solitons generated is the integer part of $1/2+qR/\pi$ (see also the relevant discussion and generalization of [Ki89]). They remark how physical intuition suggests that the first soliton created when increasing R corresponds to $\zeta = 0$. This solution is obtained for $qR = \pi/2$ and contains a single "soliton" with zero amplitude that they called *quiescent soliton*. In this case, the velocity of this soliton is also zero. Remark that the quiescent soliton is not a physical soliton, since both its mass and energy are zero. But from a mathematical point of view it could be considered as a soliton, in the sense that it is a bounded solution of the spectral problem corresponding to a zero of the Jost coefficient a. We will also observe that this evanescent soliton is an interesting structure even from a physical point of view, since an infinitesimal random perturbation is sufficient to create (with positive probability) a "true" soliton with positive amplitude.

For values of qR just over the critical threshold of $1/2$, the created soliton has zero velocity and nonzero amplitude 2η which can be computed explicitly solving (2.1.3) for pure imaginary values of ζ.

In the first part of this subsection we report some computations relative to this case, as the results and explicit formulas will be used below. We then conclude providing the sketch of an analytical proof of the claimed fact that generated solitons correspond to purely imaginary values of ζ.

For purely imaginary values of $\zeta = i\eta$, from the decaying condition at $-\infty$ one obtains the initial condition

$$\Psi(0) = \begin{pmatrix} 1 \\ 0 \end{pmatrix} e^{\eta x}\Big|_{x=0} = \begin{pmatrix} 1 \\ 0 \end{pmatrix}. \tag{2.2.1}$$

The system (2.1.3) for $x \in [0, R]$ reads

$$\begin{cases} \frac{\partial \psi_1}{\partial x} = iq\,\psi_2 - i\zeta\,\psi_1 \\ \frac{\partial \psi_2}{\partial x} = iq\,\psi_1 + i\zeta\,\psi_2 \end{cases}$$

and $\Psi = (\psi_1, \psi_2)$ is a solution of the initial value problem for $\zeta \neq iq$ if (ζ is imaginary pure)

$$\begin{aligned} \psi_1(x) &= -\frac{i\zeta}{\sqrt{q^2+\zeta^2}} \sin\left(\sqrt{q^2+\zeta^2}\,x\right) + \cos\left(\sqrt{q^2+\zeta^2}\,x\right); \\ \psi_2(x) &= i\frac{q}{\sqrt{q^2+\zeta^2}} \sin\left(\sqrt{q^2+\zeta^2}\,x\right). \end{aligned} \tag{2.2.2}$$

To be a soliton solution, Ψ needs to satisfy also the decaying condition at $+\infty$, which is to say $\psi_1(R) = 0$. The condition can be rewritten for $\zeta \neq 0$ as

$$f(\zeta) = \tan(\sqrt{q^2+\zeta^2}R) + i\frac{\sqrt{q^2+\zeta^2}}{\zeta} = 0. \tag{2.2.3}$$

Since $a(\zeta) = \psi_1(R,\zeta)e^{i\zeta R}$, the function $f(\zeta)$ is linked to the first Jost coefficient $a(\zeta)$ by the relation

$$f(\zeta) = ia(\zeta)\,\frac{e^{-i\zeta R}}{\zeta}\,\frac{\sqrt{q^2+\zeta^2}}{\cos\left(\sqrt{q^2+\zeta^2}R\right)},$$

from which we see that the zeros of f coincide with those of a, except for $\zeta = iq$. However, for $\zeta = iq$ it is possible to compute explicitly the solution of (2.2.1) satisfying the initial

conditions, which is given by

$$\Psi(x) = \begin{pmatrix} 1+x \\ ix \end{pmatrix} .$$

Since this function cannot satisfy the final conditions, no soliton can be created for this particular value of ζ.

Now, plotting on the (ξ, η) - plane the level lines of the real and imaginary parts of f at level zero, one can already see that the first soliton component of the solution corresponds to an imaginary value of ζ. This fact can be proved in an analytic way as follows.

Proposition 2.6. *When increasing R or q, new solitons are created at the threshold $qR = (2n+1)\pi/2$, $n \in \mathbb{N}$ with zero velocity.*

Proof. We have seen that, except for $\zeta = iq$, the zeros of f coincide with those of a. We also know that the function $a(\xi, \eta, R)$ is analytic in the domain $\mathbb{R} \times (0, \infty) \times (0, \infty)$ and continuous in $\mathbb{R} \times [0, \infty) \times (0, \infty)$. We use the argument principle to study how the number of zeros in the upper half of the complex plane evolves when increasing R. For any fixed R we proceed as in [DP08], taking a loop C in the complex ζ-plane composed of the (lower) real axis C^- and the infinite semi-arc in the upper half plane. Then, the number of zeros of $a(\xi, \eta, R)$ in the domain defined by the boundary C is given by

$$N(R) = \frac{1}{2\pi} \int_C \frac{1}{a} \frac{\partial a}{\partial \zeta} \, \mathrm{d}\zeta \, .$$

Since for $|\zeta| \gg 1$ we have that $a(\zeta, R) = 1 + O(1/\zeta)$, the integral over the upper part of the loop is zero. With the change of variables $a(\zeta, R) = \rho(\zeta, R) \exp\big(i\alpha(\zeta, R)\big)$, the number of zeros can be rewritten as

$$N(R) = \frac{1}{2\pi} \int_{C^-} \frac{\partial \alpha}{\partial \zeta} \, \mathrm{d}\zeta \, . \tag{2.2.4}$$

If a new soliton is created at a given R, $N(R)$ must have a jump at that point. This is to say that

$$\partial_R \alpha(\zeta, R) = \big[\rho(\zeta, R)\big]^{-1} \Re\Big[b(\zeta, R) U_0(R) e^{2i\zeta R - i\alpha(\zeta R)}\Big] \tag{2.2.5}$$

must be singular. This expression for the derivative of α can be obtained using an invariant imbedding approach in the following way. In the invariant imbedding approach, the width R of the support of the initial condition is considered as a new dynamical variable. For an initial condition compactly supported on $[0, R]$, from the ZSSP system (2.1.3), the decay conditions (2.1.4) and (2.1.5), and the relation (2.1.6), one can obtain boundary conditions for Ψ at 0 and R, which are given by (2.2.1) and

$$\Psi(R) = a(\zeta, R) \begin{pmatrix} 1 \\ 0 \end{pmatrix} e^{-i\zeta R} + b(\zeta, R) \begin{pmatrix} 0 \\ 1 \end{pmatrix} e^{i\zeta R}.$$

From this equation one obtains a formula for $a(\zeta, R)$

$$a(\zeta, R) = \psi_1(R) e^{i\zeta R} \, ,$$

and a similar formula for b. Taking the derivative in R of this formula and using the relation $a = \rho e^{i\alpha}$, one gets (2.2.5).

We return to consider equation (2.2.5). Unless the function $\rho(\zeta, R)$ has at least one zero on the real axis, C^- can be analytically deformed into the real axis $\zeta = \xi$. Then the right

hand side of (2.2.5) becomes a continuous, finite function of ξ and the integral (2.2.4) is given by $[\alpha(\infty) - \alpha(-\infty)]$, which is zero due to the asymptotic behavior of a for large ζ and the normalization condition $|a|^2 + |b|^2 = 1$. This means that the necessary condition for the number of solitons to change at R is the existence of at least one real solution of the equation $a(\xi, 0, R) = 0$. It is easy to see that this condition is also sufficient.

We have obtained that the number $N(R)$ of zeros changes at R if and only if $a(\xi, 0, R) = 0$ admits a solution. But zeros of a and f coincide, and since in equation (2.2.3) for real values of $\zeta = \xi \neq 0$ the tangent is real and the second term is purely imaginary and non zero, solutions of $f(\xi, 0, R) = 0$ can only be found at $\xi = 0$.

Explicit computations easily show that $\zeta = 0$ corresponds to a soliton solution only for $R = (2n + 1)\pi/2q$, $n \in \mathbb{N}$. Computing explicitly the derivative of $a(\zeta)$ at $\zeta = 0$ we get

$$\begin{aligned}\partial_\zeta a(\zeta) = e^{i\zeta R}\Big[\Big(2\frac{\zeta R}{\sqrt{q^2+\zeta^2}} - i\frac{q^2}{\sqrt{q^2+\zeta^2}^3}\Big)\sin\big(\sqrt{q^2+\zeta^2}\,R\big) \\ + iR\frac{q^2}{q^2+\zeta^2}\cos\big(\sqrt{q^2+\zeta^2}\,R\big)\Big] \\ \partial_\zeta a(\zeta)\Big|_{\zeta=0} = -i\frac{1}{q}\sin(qR) + iR\cos(qR)\,,\end{aligned}$$

so that for $Rq = (2n + 1)\pi/2$ the derivative is equal to $(-1)^{n+1}i/q$ and is never zero. Therefore, when increasing R new solitons are generated one at a time and the eigenvalues ζ_n identifying them are immediately pushed towards the interior of the domain $\mathbb{C}^+$. [Ka79] showed that "$a(\zeta) = 0$ imply $a'(\zeta) \neq 0$" holds for all values of ζ; from this fact it follows that zeros in the interior of the domain are always simple. Considering the complex conjugate Ψ^*, which is a solution whenever Ψ is, one obtains that zeros not laying on the imaginary axis always come in pairs $\pm\xi + i\eta$. But since zeros move continuously (as R grows) in the upper complex plane, cannot coalesce and cannot leave the imaginary axis ($\xi = 0$) unless they form a pair, we get that they must remain on the imaginary axis. □

From the proof above we obtain a correspondence between zeros of the Jost coefficient $a(\zeta, R)$ in the complex upper half-plane and on the real line: as the support R of the initial condition grows, the appearance of a new zero of a on the real line corresponds to the creation or destruction of a zero in the complex upper half-plane. Since for a zero initial condition ($R = 0$) no soliton is created (there are no zeros in the complex upper half-plane), we can interpret this result as a correspondence between the presence of solitons in the solution of the NLS equation and zeros of the Jost coefficient a on the real line. More precisely,

Proposition 2.7. *For a fixed R, the presence of solitons in the solution of the NLS equation with initial condition U_0 having support on $[0, R]$ imply the presence of zeros of the function $a(\xi, x)$, $(\xi, x) \in \mathbb{R} \times [0, R]$. Also, the presence of one zero of $a(\xi, x)$ on $\mathbb{R} \times [0, R]$ implies the presence of one soliton.*

Remark 2.8. Remark that the correspondence result of proposition 2.7 also holds for non flat initial conditions, $U_0(x) = \nu(x)\,\mathbb{1}_{[0,R]}(x)$. In particular, ν can be taken to be a stochastic process.

2.2.2 NLS solitons – small-intensity real noise

In this subsection we consider the example of an initial condition composed of a square function perturbed with a small, real white noise ($\dot{W}$). First, we use a perturbative approach

to study the effects of the perturbation on solitons (proposition 2.9). Then, in the last part of this subsection, we study the effect of this perturbation on quiescent solitons (corollary 2.10).

We have here $U_0(x) = (q+\sigma\dot{W}_x)\,\mathbb{1}_{[0,R]}(x)$. The initial condition is (2.2.1) and the system (2.1.3) for $x \in [0,R]$ reads

$$\begin{cases} \mathrm{d}\psi_1 = i\big(q\,\psi_2 - \zeta\,\psi_1\big)\,\mathrm{d}x + i\sigma\,\psi_2 \circ \mathrm{d}W_x \\ \mathrm{d}\psi_2 = i\big(q\,\psi_1 + \zeta\,\psi_2\big)\,\mathrm{d}x + i\sigma\,\psi_1 \circ \mathrm{d}W_x \end{cases} . \tag{2.2.6}$$

Proposition 2.9. *For $qR > \frac{\pi}{2}$ and in the limit of a small real white noise type stochastic perturbation of the initial condition, the amplitude η of the soliton component of the solution is perturbed at first order by a small, zero-mean, Gaussian random variable. If the complex number identifying un unperturbed soliton (corresponding to $\sigma = 0$ in the initial condition) is $\zeta_0 = i\eta_0$, the perturbed soliton will correspond to a complex number $\zeta = i\eta$, where η can be written as $\eta = \eta_0 + \sigma\eta_1 + o(\sigma)$, with*

$$\eta_1 = \frac{q\sin(c_0R)\,W_R + \int_0^R 2\frac{\eta_0 q}{c_0}\sin\big(c_0(R-y)\big)\sin(c_0y)\mathrm{d}W_y}{2\Big[\frac{q^2}{c_0^2} + R\eta_0\Big]\sin\big(c_0R\big) - R\frac{\eta_0^2}{c_0}\cos\big(c_0R\big)}\,, \tag{2.2.7}$$

and $c_0 := \sqrt{q^2-\eta_0^2}$. The velocity of the soliton remains unchanged.

Corollary 2.10. *When $q = (2n+1)\pi/2R$ for some $n \in \mathbb{N}$, in the deterministic case we have the creation of what we called a quiescent soliton. Also in this case, the stochastic perturbation can modify, at first order, only the amplitude of the soliton. As a result, the quiescent soliton is destroyed with probability $1/2$ and a true soliton with positive amplitude $\eta > 0$ is created with probability $1/2$.*

Remark 2.11. With the same proofs, one can show that these results also hold for a purely imaginary (deterministic) initial condition perturbed by a purely imaginary, small white noise. And a simple phase shift [Ki89] allows to extend this result to any complex initial condition $U_0(x) = q * \mathbb{1}_{[0,R]}(x)$, $q \in \mathbb{C}$ perturbed with a white noise with the same constant phase of q.

Remark 2.12. With the same proofs, it is possible to show that solitons are stable with respect to small random perturbations under more general hypothesis. In particular, we only need the smallness assumption on the perturbing process, which does not need to be rapidly oscillating. For example, substituting the white noise with a general process Q_x in corollary 2.10 above one obtains the same result: $\partial_\sigma\eta = q\int_0^R Q_x\,\mathrm{d}x$, so that a true soliton is created whenever the integral is positive.

Indeed, another possible and equivalent approach for rapidly oscillating processes would be to work with the original process ν_ε for the IST and carry out the scaling limit only at this stage.

Remark 2.13. When creating a new soliton from a quiescent soliton, in the limit of a rapidly oscillating perturbation of the initial condition both the mass end energy conversion efficiency is very poor: the mass of the created soliton is $4\eta = 4\sigma q W_R$, while the input mass $\int_{\mathbb{R}} |U_0|^2\,\mathrm{d}x$ for the white noise is infinite; the energy captured by the created soliton is $E_s = -16\eta^3/3$, while the input energy is infinite.

On the contrary, when the (small) perturbation used is given by a smooth process, the mass conversion efficiency is very good, since the mass of the created soliton $4\eta =$

$4\sigma q \int_0^R Q_x \,\mathrm{d}x$ is of order σ, while the input mass is of order σ^2. For the energy, the conversion efficiency remains poor, since the energy of the created soliton $E_s = -16\eta^3/3$ is (negative and) of order σ^3, while the input energy $\int_0^R \sigma^2 q^2 |\partial_x Q| - \sigma^4 q^4 |Q|^4 \,\mathrm{d}x$ is (positive and) of order σ^2.

Recall however that the creation of a new soliton is not a sure event.

The following proposition provides results that we will need in the following on the uniqueness and regularity of solutions.

Proposition 2.14. *The system of SDEs (2.2.6) defines a stochastic flow $\Psi_x^{(\zeta,\sigma)} = (\psi_1, \psi_2)^T$ of $\mathcal{C}^1$-diffeomorphisms, which is $\mathcal{C}^1$ also in the parameters ξ, η, σ.*

Proof of Proposition 2.14. Write the SDE in Itô and vector form:

$$\mathrm{d}\Psi = i \begin{pmatrix} -\zeta + i\sigma^2 & q \\ q & \zeta + i\sigma^2 \end{pmatrix} \Psi \,\mathrm{d}x + i\sigma \begin{pmatrix} 0 & 1 \\ 1 & 0 \end{pmatrix} \Psi \,\mathrm{d}W_x \,. \tag{2.2.8}$$

The coefficients of the SDE are independent of x and Lipschitz continuous in Ψ for every ζ and σ. Therefore, the existence of a unique solution to the SDE, which defines a stochastic flow of homeomorphisms $\Psi^{(\zeta,\sigma)}(x)$, is a classical fact (see for example [Ku84]). Following the notation of [Ku], we define the local characteristic of the SDE as (α, β, x), where

$$\alpha(\zeta, \zeta', \sigma, \sigma', x) := -\sigma\sigma' \begin{pmatrix} 0 & 1 \\ 1 & 0 \end{pmatrix} ,$$
$$\beta(\zeta, \sigma, x) := \begin{pmatrix} -\zeta & q \\ q & \zeta \end{pmatrix} .$$

Fix any $n \in \mathbb{N}$, define the set $G_n := \{(\xi, \eta, \sigma) \;\big|\; |\xi| < n,\, 0 < \eta < n,\, 0 < \sigma < n\}$ and consider the SDE only with parameters in G_n. Then, both α and β are uniformly bounded and, together with their first derivatives, are Lipschitz continuous in the parameters. This means that the coefficients satisfy condition $(A.5)_{1,0}$ of [Ku, Chapter 4.6]. It follows from [Ku, Theorem 4.6.4] that $\Psi^{(\zeta,\sigma)}(x)$ is $\mathcal{C}^1$ in the parameters almost surely on G_n. Let Ω_n be the set of $\omega \in \Omega$ such that $\Psi^{(\zeta,\sigma)}(x) \in \mathcal{C}^1(G_n)$, which is a set of full measure. Since n is arbitrary, $\Psi^{(\zeta,\sigma)}(x)$ is actually $\mathcal{C}^1\big(\mathbb{R} \times \mathbb{R}_+ \times \mathbb{R}_+\big)$ for every $\omega \in \cap_n \Omega_n$, which is still a set of full measure. This proves the last statement of the proposition.

Since [Ku, Theorem 4.6.5] states that $\Psi^{(\zeta,\sigma)}(x)$ is actually a stochastic flow of $\mathcal{C}^1$-diffeomorphisms, the proof is complete. □

Proof of Proposition 2.9. Looking at the flow at point R we can define a complex-valued function of $\Psi(R)$ as $F(\xi, \eta, \sigma) := \psi_1^{(\zeta,\sigma)}(R)$. We look for the set of values of (ξ, η, σ) corresponding to zeros of the function F: they are the parameters $(\zeta = \xi + i\eta)$ defining the soliton components of the solution of the problem perturbed with a noise of amplitude σ. We claim that a small stochastic perturbation has only the effect of a small variation in the value of $\zeta = \xi + i\eta$ with respect to the value $\zeta_0 = i\eta_0$ of the corresponding soliton in the deterministic case. We will prove this using the implicit function theorem: for any fixed and sufficiently small σ, $F(\xi, \eta, \sigma)$ has a unique zero in some open set containing the point $(0, \eta_0, 0)$. The following lemma ensures that the most important hypothesis of the implicit function theorem is satisfied.

Lemma 2.15. *Let $F(\xi, \eta, \sigma)$ be the function defined above. Then, whenever $\zeta_0 = i\eta_0$ is the discrete eigenvalue corresponding to a soliton component of the solution of the deterministic*

problem, the determinant of the Jacobian matrix

$$J := \begin{pmatrix} \partial_\xi \Re(F) & \partial_\eta \Re(F) \\ \partial_\xi \Im(F) & \partial_\eta \Im(F) \end{pmatrix}$$

at point $(0, \eta_0, 0)$ *is not zero.*

Proof of Lemma 2.15. For $\sigma = 0$ the system (2.2.6) becomes deterministic and the solution is given by (2.2.2). Then, setting $c := \sqrt{q^2 - \zeta^2}$,

$$i\,\partial_\xi \psi_1(\xi, \eta, 0) = \partial_\eta \psi_1(\xi, \eta, 0) = \left[\frac{q^2}{c^3} - iR\frac{\zeta}{c}\right] \sin\big(cR\big) + R\frac{\zeta^2}{c^2}\cos\big(cR\big)$$

so that

$$i\,\partial_\xi F(0, \eta_0, 0) = \partial_\eta F(0, \eta_0, 0)\,.$$

We are left to verify that

$$\begin{aligned} 0 \neq \det J\ (0, \eta_0, 0) &= \Big[\partial_\xi \Re(F)\partial_\eta \Im(F) - \partial_\eta \Re(F)\partial_\xi \Im(F)\Big](0, \eta_0, 0) \\ &= \Big[\Re\big(\partial_\xi F\big)\Im\big(\partial_\eta F\big) - \Re\big(\partial_\eta F\big)\Im\big(\partial_\xi F\big)\Big](0, \eta_0, 0) \\ &= \Big[\Big(\Re(\partial_\xi F)\Big)^2 + \Big(\Im(\partial_\xi F)\Big)^2\Big](0, \eta_0, 0) \end{aligned}$$

or equivalently

$$\partial_\xi F\,(0, \eta_0, 0) = -i\left[\frac{q^2}{c_0^3} + R\frac{\eta_0}{c_0}\right] \sin\big(c_0 R\big) + iR\frac{\eta_0^2}{c_0^2}\cos\big(c_0 R\big) \neq 0\,, \tag{2.2.9}$$

where $c_0 = \sqrt{q^2 - \eta_0^2}$. Observe that condition (2.2.3) implies that $\eta_0 \leq q$; c_0 is therefore real. Indeed, for $\eta_0 > q$, c_0 would be imaginary pure and the function f of equation (2.2.3) would become the sum of two imaginary pure terms of the same sign, so that it cannot be zero. In equation (2.2.9) the coefficient of the sinus is the sum of two non zero terms of the same sign, so that to ensure the condition we need to check that

$$\tan(c_0 R) = \frac{R\eta_0^2 c_0}{q + R\eta_0 c_0^2} \tag{2.2.10}$$

does *not* holds for η_0 solution of (2.2.3). The compatibility condition between (2.2.3) and (2.2.10) is

$$-\frac{c_0}{\eta_0} = \frac{R\eta_0^2 c_0}{q + R\eta_0 c_0^2}$$

or equivalently

$$\Big(q + R\eta_0 c_0^2 + R\eta_0^3\Big)c_0 = 0\,,$$

which cannot be verified (recall that $\eta_0 \neq q$, so that $c_0 \neq 0$). The lemma is proved. □

We return to the proof of proposition 2.9. Since the previous lemma guarantees that the Jacobian matrix J of the derivatives of F with respect to ξ and η is invertible, we can apply the implicit function theorem at point $(\xi, \eta, \sigma) = (0, \eta_0, 0)$. Fix $\zeta = i\eta_0$. By proposition

2.14, the flow defined by the system (2.2.6) is $\mathcal{C}^1$ in the parameters, so that its derivative in σ coincides with the first term of the Taylor expansion, which we will denote $\Psi^{(1)}$. It is a solution of

$$\mathrm{d}\Psi^{(1)} = \begin{pmatrix} \eta_0 & iq \\ iq & -\eta_0 \end{pmatrix} \Psi^{(1)}\,\mathrm{d}x + i \begin{pmatrix} 0 & 1 \\ 1 & 0 \end{pmatrix} \Psi^{(0)}\,\mathrm{d}W_x\,. \tag{2.2.11}$$

Here, $\Psi^{(0)}$ denotes the solution of the deterministic problem ($\sigma = 0$). Let M be the matrix appearing in the drift term of the above equation; the solution can be computed explicitly, and it is given by

$$\Psi^{(1)}(x) = i \int_0^x \exp\big(M(x-y)\big) \begin{pmatrix} 0 & 1 \\ 1 & 0 \end{pmatrix} \Psi^{(0)}(y)\,\mathrm{d}W_y\,,$$

where

$$\begin{aligned} \Big[\exp\big(M(x-y)\big)\Psi^{(0)}(y)\Big]_1 &= i\frac{q}{c_0}\cos\big(c_0(x-y)\big)\sin(c_0 y) + 2i\frac{\eta_0 q}{c_0^2}\sin\big(c_0(x-y)\big)\sin(c_0 y) \\ &\quad + i\frac{q}{c_0}\sin\big(c_0(x-y)\big)\cos(c_0 y) \\ &= i\frac{q}{c_0}\sin(c_0 x) + 2i\frac{\eta_0 q}{c_0^2}\sin\big(c_0(x-y)\big)\sin(c_0 y)\,. \end{aligned}$$

It follows that

$$\partial_\sigma F(0,\eta_0,0) = i\int_0^R \Big[\exp\big(M(R-y)\big)\Psi_y^{(0)}\Big]_1 \mathrm{d}W_y\,.$$

Observe that $\partial_\xi F(0,\eta_0,0)$ is imaginary pure and, symmetrically, $\partial_\eta F(0,\eta_0,0)$ is real. Set

$$\alpha := \partial_\eta F(0,\eta_0,0) = \Big[\frac{q^2}{c_0^3} + R\frac{\eta_0}{c_0}\Big]\sin\big(c_0 R\big) - R\frac{\eta_0^2}{c_0^2}\cos\big(c_0 R\big)\,.$$

We can write

$$J^{-1} = \begin{pmatrix} 0 & -\frac{1}{\alpha} \\ \frac{1}{\alpha} & 0 \end{pmatrix}$$

and from the formula

$$v := \begin{pmatrix} \partial_\sigma \xi \\ \partial_\sigma \eta \end{pmatrix}(\sigma = 0) = -J^{-1} \begin{pmatrix} \Re\big(\partial_\sigma F\big) \\ \Im\big(\partial_\sigma F\big) \end{pmatrix}(0,\eta_0,0)$$

we get that $\partial_\sigma \eta$ is given by (2.2.7) and $\partial_\sigma \xi = 0$. □

Proof of Corollary 2.10. In the case of a quiescent soliton lemma 2.15 still holds. Indeed we have now $c_0 = q$ and $qR = (2n+1)\pi/2$, so that equation (2.2.9) becomes

$$\partial_\xi F\,(0,0,0) = -i\Big[\frac{q^2}{c_0^3} + R\frac{\zeta_0}{c_0}\Big]\sin\big(c_0 R\big) + iR\frac{\zeta_0^2}{c_0^2}\cos\big(c_0 R\big) = \mp i\frac{1}{q} \neq 0$$

and the determinant of the Jacobian is not zero. One has then $\alpha = \pm 1/q$ and

$$\partial_\sigma F(0,0,0) = -\int_0^R \sin(qR)\,\mathrm{d}W_y = \mp W_R\,,$$

which is real. Therefore,

$$v := \begin{pmatrix} \partial_\sigma \xi \\ \partial_\sigma \eta \end{pmatrix} (\sigma = 0) = - \begin{pmatrix} 0 & \mp q \\ \pm q & 0 \end{pmatrix} \begin{pmatrix} \mp W_R \\ 0 \end{pmatrix} = \begin{pmatrix} 0 \\ q W_R \end{pmatrix} .$$

A true soliton is created whenever $W_R > 0$. □

2.2.3 NLS solitons – small-intensity complex noise

The limit case of a small-amplitude complex white noise is very similar to the case of the real white noise treated above. Take $U_0(x) = (q + \sigma \dot{W}_x)\, \mathbb{1}_{[0,R]}(x)$ where $W_x = W_x^{(1)} + i W_x^{(2)}$ is a complex Wiener process. We have

Proposition 2.16. *For $qR > \frac{\pi}{2}$ and in the limit of a small complex white noise type stochastic perturbation of the initial condition, the parameters ξ, η defining the velocity and amplitude of each soliton are perturbed at first order by small, zero-mean, independent Gaussian random variables, which are given by*

$$\partial_\sigma \xi = - \frac{q \sin(c_0 R)\, W_R^{(2)} + \int_0^R 2 \frac{\eta_0 q}{c_0^2} \sin\big(c_0(R-y)\big) \sin(c_0 y) \mathrm{d}W_y^{(2)}}{2\Big[\frac{q^2}{c_0^2} + R\eta_0\Big] \sin\big(c_0 R\big) - R \frac{\eta_0^2}{c_0} \cos\big(c_0 R\big)} ,$$

$$\partial_\sigma \eta = \frac{q \sin(c_0 R)\, W_R^{(1)} + \int_0^R 2 \frac{\eta_0 q}{c_0^2} \sin\big(c_0(R-y)\big) \sin(c_0 y) \mathrm{d}W_y^{(1)}}{2\Big[\frac{q^2}{c_0^2} + R\eta_0\Big] \sin\big(c_0 R\big) - R \frac{\eta_0^2}{c_0} \cos\big(c_0 R\big)} ,$$

where $c_0 := \sqrt{q^2 - \eta_0^2}$, and η_0 is the parameter defining the amplitude of the soliton of the unperturbed system.

Proof. This proof is similar to the one of proposition 2.9. An analogous of proposition 2.14 holds in this setting, and lemma 2.15 remains unchanged (note that in lemma 2.15 we work on the deterministic equation). From equation (2.2.11) onward one has just to remember that W is now complex. □

Remark 2.17. In this case, since we used a noise with a symmetric law, the first order perturbations of the velocity and amplitude of the soliton have the same law and are independent. We could have taken a non symmetric complex noise to perturb the initial condition: $\widetilde{\nu} = \nu_1 + i\nu_2$, where ν_1 and ν_2 have different distributions. In this case, the perturbations of the velocity and amplitude of the soliton would still be independent, but not sharing the same law.

Remark 2.18. Quiescent solitons are perturbed in both amplitude and speed, leading to the possible creation of true solitons with nonzero velocity. The same result holds when perturbing the initial data with more general complex processes.

2.2.4 KdV solitons – deterministic background solution

In [Mu78], Murray obtained a $\mathcal{C}^\infty$ solution for the KdV equation with a deterministic "box-shaped" initial condition $U_0 = q * \mathbb{1}_{[-R,R]}(x)$. He showed that in this case the Jost coefficient a extends to an analytic function in the upper part of the ζ-plane. Only in the case of positive values of q, the Jost coefficient a has a finite number of zeros on the imaginary axis $\zeta = i\eta$ for $0 < \eta \leq \sqrt{q}$.

We report some explicit computations on our similar deterministic case, as these results will be used below, and study some properties of the soliton components of the solution. First, let us construct explicitly the solution of the deterministic equation, which we call φ_0. We assume that the initial condition of the NLS equation is given by $U_0 = q * \mathbb{1}_{[0,R]}(x)$ for some $q > 0$. Due to [AC, Lemma 2.2.2], we can assume that $\zeta = i\eta$; we need to solve

$$\varphi_{xx} = \begin{cases} \eta^2\varphi & x < 0, x > R \\ (-q+\eta^2)\varphi & x \in [0,R] \end{cases} . \tag{2.2.12}$$

For $\eta = 0$ the only integrable solution is $\varphi \equiv 0$. Soliton components corresponding to $\eta > 0$ must satisfy

$$\varphi = c_1 e^{\eta x} \qquad x < 0\,, \tag{2.2.13}$$

$$\varphi = c_2 e^{-\eta x} \qquad x > R\,. \tag{2.2.14}$$

For $x \in [0,R]$ one can rewrite the problem as

$$\begin{cases} \partial_x\varphi = \widetilde{\varphi} \\ \partial_x\widetilde{\varphi} = (-q+\eta^2)\varphi \end{cases} .$$

Note that for $\eta \geq \sqrt{q}$ the solution of (2.2.12) is monotone, so that it cannot be a Jost function corresponding to a soliton (which has to be integrable). We therefore look for solutions corresponding to $0 < \eta < \sqrt{q}$. Set $c = \sqrt{q-\eta^2}$. Due to (2.2.13) and (2.2.14), we only need to solve (2.2.12) for $x \in [0,R]$. From (2.2.12) and the initial conditions

$$\varphi_0(0) = c_1\,, \qquad\qquad \partial_x\,\varphi_0(0) = \eta c_1$$

derived from (2.2.13), we get

$$\varphi_0(x) = \alpha e^{icx} + \beta e^{-icx}\,, \qquad\qquad \alpha = \frac{c_1}{2}\big(1 - i\frac{\eta}{c}\big), \qquad \beta = \frac{c_1}{2}\big(1 + i\frac{\eta}{c}\big)\,,$$

which is to say

$$\varphi_0(x) = c_1\cosh(icx) - ic_1\frac{\eta}{c}\sinh(icx) = c_1\Big[\cos(cx) + \frac{\eta}{c}\sin(cx)\Big]\,. \tag{2.2.15}$$

We can set the global constant c_1 equal to 1. Matching this solution with the final condition (2.2.14)

$$\begin{cases} \varphi(R) = \cos(cR) + \frac{\eta}{c}\sin(cR) & = c_2 e^{-\eta R} \\ \partial_x\varphi(R) = -c\sin(cR) + \eta\cos(cR) & = -\eta c_2 e^{-\eta R} \end{cases} ,$$

we obtain an equation for η:

$$\begin{cases} q\,\sin(R\sqrt{q-\eta^2}) = 2c_2\eta\sqrt{q-\eta^2}e^{-R\eta} \\ q\,\cos(R\sqrt{q-\eta^2}) = c_2(q-2\eta^2)e^{-R\eta} \end{cases} .$$

For $\eta = \sqrt{q/2}$, the only possible solution is such that $R\sqrt{q-\eta^2} = \pi/2 + k\pi$, which means that

$$\sqrt{q}\,R = (2k+1)\pi/\sqrt{2}\,. \tag{2.2.16}$$

All other solutions can be found solving

$$f(\eta) := \tan(R\sqrt{q-\eta^2}) - \frac{2\eta\sqrt{q-\eta^2}}{q-2\eta^2} = 0 \tag{2.2.17}$$

for $\eta \in [0, \sqrt{q}) \backslash \{\sqrt{q/2}\}$. The existence and the number of solutions for the above equation depend on the quantity $R\sqrt{q}$. Consider some fixed value of R. As it is shown below, for small values of q a first soliton is created with $\eta^{(1)} \sim 0$. As q increases, the value of $\eta^{(1)}$ increases too and tends to $\sqrt{q/2}$ as q tends to $\pi^2/(2R^2)$. We have already found the solution for this specific value of q ($k = 0$ in equation (2.2.16)). For q larger than $\pi^2/(2R^2)$, $\eta^{(1)}$ continues to grow. A second solution appears ($\eta^{(2)} = 0$) when $q = \pi^2/R^2$. A third solution appears at $q = (2\pi/R)^2$; the values of $\eta^{(i)}$ (corresponding to the i^{th} soliton created) continuously increase as q grows, but remain ordered: $\eta^{(i)} < \eta^{(j)}$ for $i > j$. Therefore, the number of solitons created is $N = \lfloor R\sqrt{q}/\pi \rfloor + 1$, where $\lfloor \cdot \rfloor$ denotes the integer part.

A few examples of $f(\eta)$ are plotted in figure 2.2. We have taken $R = 1$ and different values of q. The first critical points (when new solitons are created) correspond here to $q^{(2)} = \pi^2 \sim 9.87$, $q^{(3)} = 4\pi^2 \sim 39.48$, $q^{(4)} = 9\pi^2 \sim 88.83$, $q^{(5)} = 16\pi^2$. The almost-vertical line appearing near $\eta = \sqrt{q/2}$ for $q = 44$ reflects the fact that we are near the critical points of (2.2.16): from (2.2.16) for $k = 1$ we have $q = 9\pi^2/2 \sim 44.41$.

Let us take a closer look at the case $q \to 0$. We assume $q = q_0\,\varepsilon$ and look for the first terms of the expansion of η in ε: $\eta = \eta_0 + \eta_1\varepsilon + \eta_2\varepsilon^2 + O(\varepsilon^3)$. For finite values of R, by the above considerations on the threshold effect, the first term of the expansion must be zero. Indeed, if we consider the expansion in ε of the function f defined by (2.2.17) we obtain

$$\text{(ord. 0)} \qquad f(\eta) = \tan(R\sqrt{-\eta_0^2}) + \frac{\sqrt{-\eta_0^2}}{\eta_0} + O(\varepsilon)\,,$$

and the order-zero term cannot be made equal to zero. We have therefore: $\eta = \eta_1\varepsilon + O(\varepsilon^2)$. Looking at equation (2.2.17) at first order

$$\text{(ord. 1)} \qquad f(\eta) = \left(R\,q_0 - 2\eta_1\right)\frac{\sqrt{\varepsilon}}{\sqrt{q_0}} + O(\varepsilon^{3/2}) = 0$$

we obtain $\eta_1 = \frac{R\,q_0}{2}$. Pushing the expansion further, one can obtain the following order coefficients. At order two we have:

$$\text{(ord. 2)} \qquad f(\eta) = -\left(\frac{4}{24}R^3\,q_0^2 + 2\eta_2\right)\frac{\varepsilon^{3/2}}{\sqrt{q_0}} + O(\varepsilon^{5/2})\,.$$

One has then

$$\eta = \frac{R\,q_0}{2}\varepsilon - \frac{R^3\,q_0^2}{12}\varepsilon^2 + O(\varepsilon^3)\,, \tag{2.2.18}$$

showing that in the limit $\varepsilon \to 0$, η is of the same order of q.

2.2.5 KdV solitons – small-amplitude random perturbation with $q > 0$

We now add some random perturbation to this "box-shaped" initial profile. Let $U_0 = (q + \sigma\dot{W}_x)\,\mathbb{1}_{[0,R]}(x)$ be the initial condition of the KdV equation, where W is a standard

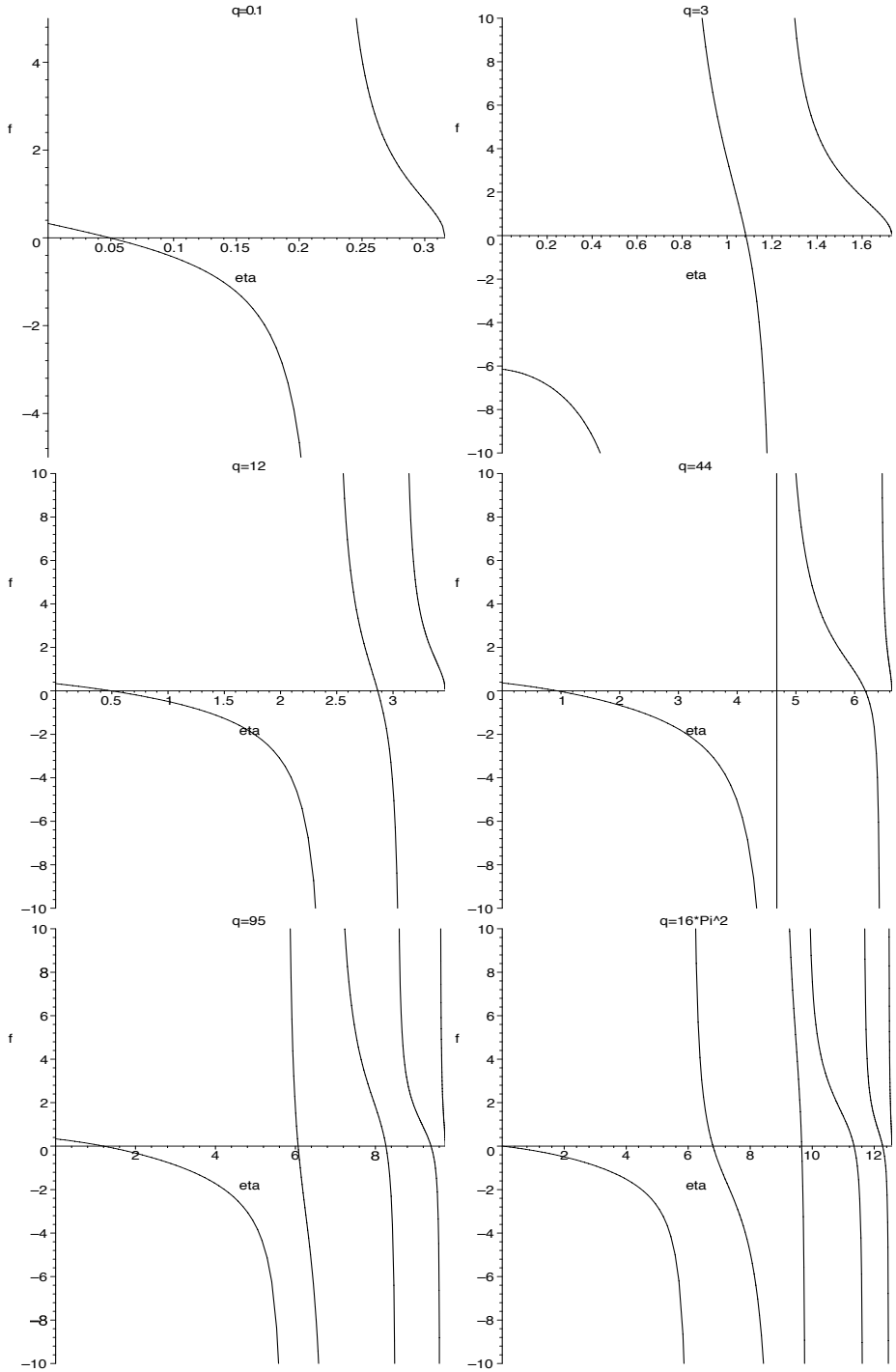

Figure 2.2: Plot of the function $f(\eta)$ for different values of the amplitude q of the initial condition. Each zero of $f(\eta)$ correspond to a soliton component of the solution identified by the complex number $i\eta$.

Wiener process and $\dot{W}$ is a white noise. Since solitons correspond to zeros of the complex extension of a, which in turn must be located on the imaginary axis, we look for bounded solutions of equation (2.1.9) for $\zeta = i\eta, \eta \in \mathbb{R}$. The first main result is contained in the following proposition.

Proposition 2.19. *In the limit of a small white noise type stochastic perturbation of the initial condition, the parameter η defining the velocity and amplitude of a generated soliton is perturbed at first order by a small, zero mean, Gaussian random variable. If η_0 is the parameter corresponding to the unperturbed soliton, we can write the parameter identifying the perturbed soliton as $\eta = \eta_0 + \sigma\eta_1 + o(\sigma)$, where*

$$\eta_1 = \frac{\int_0^R \varphi_0(R-x)\varphi_0(x)\,\mathrm{d}W_x}{\cos(c_0R)\left[2+\eta_0 R - \frac{\eta_0^3 R}{c_0^2}\right] + \sin(c_0R)\left[\frac{3\eta_0+2\eta_0^2 R}{c_0} + \frac{\eta_0^3}{c_0^3}\right]} \,. \tag{2.2.19}$$

Here, φ_0 is the deterministic solution of (2.2.12), given by

$$\varphi_0(x) = \cos(c_0 x) + \frac{\eta_0}{c_0}\sin(c_0 x)$$

for $c_0 := \sqrt{q^2 - \eta_0^2}$.

In certain cases, the stochastic perturbation can result in the creation of a new soliton. As for the NLS equation, since we are considering the limit of very small perturbations, this happens only for specific "critical" values of q (and R). The result is presented in the next proposition, which deals with the case of perturbations of a deterministic quiescent soliton.

Proposition 2.20. *If we are at a critical point, which is to say $\sqrt{q}\,R = n\pi$ for $n \in \mathbb{N}$, $n > 0$, a small amplitude white noise type stochastic perturbation of the potential* **may** *create a new small-amplitude soliton. The condition for the creation of a new soliton is that the zero-mean, Gaussian random variable given by the last term of equation (2.2.24) below is positive.*

Before we start the proof of the above propositions, we shall remark that an analog of proposition 2.14 holds in this setting, and it provides the uniqueness and regularity results for the solution. The result reads

Proposition 2.21. *The stochastic differential equation (2.2.20) below defines a stochastic flow $\Phi^{(\eta,\sigma)}(x) = \big(\varphi(x), \widetilde{\varphi}(x)\big)^T$ of $\mathcal{C}^1$-diffeomorphisms, which is $\mathcal{C}^1$ also in the parameters η, σ.*

Proof of Proposition 2.19. We need to solve

$$\begin{cases} \mathrm{d}\varphi = \widetilde{\varphi}\,\mathrm{d}x \\ \mathrm{d}\widetilde{\varphi} = (-q+\eta^2)\varphi\,\mathrm{d}x + \sigma\varphi \circ \mathrm{d}W_x \end{cases} \tag{2.2.20}$$

for $x \in [0, R]$ with initial conditions $\varphi(0) = 1$, $\widetilde{\varphi}(0) = \eta$. As we did for the NLS equation, we look at the flow provided by proposition 2.21 and define a function of the flow at the point $x = R$ as $F(\eta, \sigma) := \widetilde{\varphi}(R) + \eta\varphi(R)$. F remains a function of the two parameters (η, σ). To prove proposition 2.19 we use the implicit function theorem to show that $F(\eta, \sigma)$ has a unique zero in some open set containing $(\eta_0, 0)$, the point corresponding to the deterministic solution. The following lemma ensures that the hypothesis of the implicit function theorem are satisfied.

Lemma 2.22. *Let $F(\eta,\sigma)$ be the function defined above. Then, for all η_0 corresponding to a soliton component of the solution of the deterministic problem, $\partial_\eta F(\eta_0,0)\neq 0$.*

Proof of Lemma 2.22. For $\eta=\eta_0$ and $\sigma=0$ we have that $\varphi=\varphi_0$ and (recall that $c_0=\sqrt{q-\eta_0^2}$)

$$\partial_\eta\varphi\,(R)=\sin(c_0R)\Big[\frac{1+\eta_0R}{c_0}+\frac{\eta_0^2}{c_0^3}\Big]-\frac{R\eta_0^2}{c_0^2}\cos(c_0R)\,,$$
$$\partial_\eta\widetilde{\varphi}\,(R)=\cos(c_0R)\big[1+R\eta_0\big]+\frac{\eta_0}{c_0}\sin(c_0R)\big[1+\eta_0R\big]=\big[1+\eta_0R\big]\varphi_0(R)\,.$$

Since

$$\partial_\eta F=\partial_\eta\widetilde{\varphi}+\varphi+\eta\partial_\eta\varphi\,,$$

$$\partial_\eta F(\eta_0,0)=\cos(c_0R)\Big[2+\eta_0R-\frac{\eta_0^3R}{c_0^2}\Big]+\sin(c_0R)\Big[\frac{3\eta_0+2\eta_0^2R}{c_0}+\frac{\eta_0^3}{c_0^3}\Big]\,.$$

The coefficient of the sinus is strictly positive (the coefficient of the cosinus has instead at least one zero for $\eta_0\in[0,\sqrt{q}]$, since it is positive for $\eta_0=0$ and negative for $\eta_0\to\sqrt{q}$). Therefore, we only need to verify that the following equation

$$g(R,q,\eta_0):=\tan(c_0R)+\frac{2+\eta_0R-\frac{\eta_0^3R}{c_0^2}}{\frac{3\eta_0+2\eta_0^2R}{c_0}+\frac{\eta_0^3}{c_0^3}}=0 \tag{2.2.21}$$

is *not* satisfied, knowing that η_0 is a value corresponding to a soliton solution of the deterministic equation. As we have seen, we can either have $\eta_0=\sqrt{q/2}$ if condition (2.2.16) is satisfied, or else η_0 is given as the solution of equation (2.2.17) in $(0,\sqrt{q})\backslash\{\sqrt{q/2}\}$.
In the first case we have that $c_0=\sqrt{q/2}$, so that condition (2.2.16) implies that $\cos(c_0R)=0$ and $\sin(c_0R)=\pm1$. Therefore, $\partial_\eta F\neq 0$.
Consider now the second case. We look for points $\eta\in(0,\sqrt{q})\backslash\{\sqrt{q/2}\}$ such that $f(\eta)=g(\eta)=0$. If such a point exists, then

$$\frac{2\eta c}{q-2\eta^2}=-\frac{2+\eta R-\frac{\eta^3R}{c^2}}{\frac{3\eta+2\eta^2R}{c}+\frac{\eta^3}{c^3}}\,,$$

which also reads

$$\frac{2\eta}{q-2\eta^2}=-\frac{(2+\eta R)c^2-\eta^3R}{(3\eta+2\eta^2R)c^2+\eta^3}$$

or equivalently

$$\frac{(2\eta^2+2\eta^3R)(q-\eta^2)+2\eta^4(1+\eta R)+(2+\eta R)(q-\eta^2)q-\eta^3Rq}{(q-2\eta^2)[(3\eta+2\eta^2R)(q-\eta^2)+\eta^3]}=0\,. \tag{2.2.22}$$

For $\eta<\sqrt{q/2}$ the denominator is positive and the numerator

$$(2\eta^2+2\eta^3R)(q-\eta^2)+2\eta^4(1+\eta R)+(2+\eta R)(q-\eta^2)q-\eta^3Rq>\eta R(q-\eta^2)-\eta^3Rq>0\,,$$

so that the fraction on the left hand side of (2.2.22) is positive and cannot be zero. For

$\sqrt{q/2} < \eta < \sqrt{q}$ the denominator is negative and the numerator is larger than $2\eta^5 R - \eta^3 Rq = \eta^3 R(\eta^2 - q) > 0$, so that the fraction (2.2.22) is negative and cannot be zero. The lemma is proved. □

We return to the proof of proposition 2.19. Since the above lemma guarantees that $\partial_\eta F(\eta_0, 0) \neq 0$, we can apply the implicit function theorem. We have (at η_0)

$$\begin{cases} \mathrm{d}\partial_\sigma\varphi = \partial_\sigma\widetilde{\varphi}\,\mathrm{d}x \\ \mathrm{d}\partial_\sigma\widetilde{\varphi} = (-q+\eta_0^2)\partial_\sigma\varphi\,\mathrm{d}x - \big(\varphi + \sigma\partial_\sigma\varphi\big)\circ \mathrm{d}W_x \end{cases}.$$

By proposition 2.21 the flow $\Phi_x^{(\eta,\sigma)}$ is $\mathcal{C}^1$ in the parameters, so that its derivative in σ at $\sigma = 0$ coincide with the first term of the Taylor expansion, which is the solution of

$$\begin{cases} \mathrm{d}\partial_\sigma\varphi = \partial_\sigma\widetilde{\varphi}\,\mathrm{d}x \\ \mathrm{d}\partial_\sigma\widetilde{\varphi} = (-q+\eta_0^2)\partial_\sigma\varphi\,\mathrm{d}x - \varphi_0\,\mathrm{d}W_x \end{cases}.$$

In matricial notation,

$$\mathrm{d}\begin{pmatrix}\partial_\sigma\varphi \\ \partial_\sigma\widetilde{\varphi}\end{pmatrix} = \mathrm{d}\Phi = \begin{bmatrix} 0 & 1 \\ -c^2 & 0\end{bmatrix}\Phi\,\mathrm{d}x - \begin{pmatrix}0 \\ \varphi_0\,\mathrm{d}W_x\end{pmatrix},$$

with

$$M = \begin{bmatrix} 0 & 1 \\ -c^2 & 0\end{bmatrix}, \qquad e^{Mx} = \begin{bmatrix} \cos(cx) & \frac{1}{c}\sin(cx) \\ -c\,\sin(cx) & \cos(cx)\end{bmatrix}.$$

The solution is given by

$$\Phi(x) = \Phi(0) - \int_0^x e^{M(x-y)}\begin{pmatrix}0 \\ \varphi_0(y)\,\mathrm{d}W_y\end{pmatrix}.$$

We have

$$\begin{aligned}\partial_\sigma\varphi(x) &= -\frac{1}{c}\int_0^x \sin\big(c(x-y)\big)\Big[\cos(cy) + \frac{\eta}{c}\sin(cy)\Big]\,\mathrm{d}W_y\,, \\ \partial_\sigma\widetilde{\varphi}(x) &= -\int_0^x \cos\big(c(x-y)\big)\Big[\cos(cy) + \frac{\eta}{c}\sin(cy)\Big]\,\mathrm{d}W_y\,.\end{aligned}$$

Therefore,

$$\partial_\sigma F(\eta_0, 0) = \partial_\sigma\widetilde{\varphi}(R) + \eta_0\,\partial_\sigma\varphi(R) = -\int_0^R \varphi_0(R-x)\varphi_0(x)\,\mathrm{d}W_x$$

and we obtain, at first order, the perturbation of the value of the parameter η defining the velocity and amplitude of the soliton: for every (q, R, η_0),

$$\begin{aligned}\partial_\sigma\eta(\sigma) &= -\frac{\partial_\sigma F}{\partial_\eta F}(\eta_0, 0) \\ &= \frac{\int_0^R \Big[\cos\big(c_0(R-x)\big) + \frac{\eta_0}{c_0}\sin\big(c_0(R-x)\big)\Big]\Big[\cos(c_0x) + \frac{\eta_0}{c_0}\sin(c_0x)\Big]\,\mathrm{d}W_x}{\cos(c_0R)\Big[2 + \eta_0 R - \frac{\eta_0^3 R}{c_0^2}\Big] + \sin(c_0R)\Big[\frac{3\eta_0 + 2\eta_0^2 R}{c_0} + \frac{\eta_0^3}{c_0^3}\Big]}\,.\end{aligned}$$

The proposition is proved. □

We now turn to the case of quiescent solitons, where a small random perturbation of the initial condition may result in the creation of a new soliton. The result was stated in proposition 2.20, which we shall now prove.

Proof of Proposition 2.20. The deterministic background solution is ($c = \sqrt{q - \eta^2}$)

$$\varphi_0 = \cos(cx) + \frac{\eta}{c}\sin(cx)\,. \tag{2.2.23}$$

We have $U_0 = q + \sigma\dot{W}_x$; we want to apply the implicit function theorem to the function $F(\eta, \sigma)$ defined above, at the point $(0, 0)$. At this point

$$\begin{aligned}\partial_\eta\varphi(R) &= \frac{1}{\sqrt{q}}\sin(\sqrt{q}\,R) = 0\,,\\ \partial_\eta\widetilde{\varphi}(R) &= \cos(\sqrt{q}\,R) = \pm 1\,.\end{aligned}$$

Therefore

$$\partial_\eta F(0,0) = \partial_\eta\widetilde{\varphi} + \varphi + \eta\,\partial_\eta\varphi = 2\cos(\sqrt{q}\,R) = \pm 2\,,$$

and the implicit function theorem is applicable. We also have (again at $\eta = 0$)

$$\begin{cases} \mathrm{d}\partial_\sigma\varphi = \partial_\sigma\widetilde{\varphi}\,\mathrm{d}x \\ \mathrm{d}\partial_\sigma\widetilde{\varphi} = -q\,\partial_\sigma\varphi\,\mathrm{d}x - \big(\varphi + \sigma\partial_\sigma\varphi\big)\circ\mathrm{d}W_x \end{cases}.$$

As seen above, the solution of the above system coincides at $\sigma = 0$ with the solution of

$$\begin{cases} \mathrm{d}\partial_\sigma\varphi = \partial_\sigma\widetilde{\varphi}\,\mathrm{d}x \\ \mathrm{d}\partial_\sigma\widetilde{\varphi} = -q\,\partial_\sigma\varphi\,\mathrm{d}x - \varphi_0\,\mathrm{d}W_x \end{cases},$$

which is given by (here, $c = \sqrt{q}$)

$$\begin{aligned}\partial_\sigma\varphi(x) &= -\frac{1}{\sqrt{q}}\int_0^x \sin\big(\sqrt{q}(x-y)\big)\cos(\sqrt{q}\,y)\,\mathrm{d}W_y\,,\\ \partial_\sigma\widetilde{\varphi}(x) &= -\int_0^x \cos\big(\sqrt{q}(x-y)\big)\cos(\sqrt{q}\,y)\,\mathrm{d}W_y\,.\end{aligned}$$

We have therefore

$$\partial_\sigma F(0,0) = -\int_0^R \cos\big(\sqrt{q}\,(R-x)\big)\cos(\sqrt{q}\,x)\,\mathrm{d}W_x\,,$$

and since $\cos(\sqrt{q}\,R) = \pm 1$

$$\begin{aligned} v := \partial_\sigma\eta(\sigma) = -\frac{\partial_\sigma F}{\partial_\eta F}(0,0) &= \frac{\int_0^R \cos\big(\sqrt{q}\,(R-y)\big)\cos(\sqrt{q}\,y)\,\mathrm{d}W_y}{2\cos(\sqrt{q}\,R)} \\ &= \frac{1}{2}\int_0^R \cos^2(\sqrt{q}x)\,\mathrm{d}W_x\,. \end{aligned} \tag{2.2.24}$$

In this case, a new small-amplitude soliton, corresponding to $\eta = \sigma v$, is created whenever $v > 0$. □

2.2.6 KdV solitons – small-amplitude random perturbations with q=0

We analyze now the case in which the initial condition is the pure stochastic perturbation: contrarily to the NLS equation, even this small initial condition can generate a soliton. In this setting there is no (non trivial) solution in the deterministic case. This case is obtained at the critical point $\sqrt{q}\,R = 0$, where the first quiescent soliton is created. We consider in the next proposition the limit case of a rapidly oscillating perturbation. The case of a more general, smooth perturbation is discussed in remark 2.24. Remark 2.25 below discuss the energy and mass conversion efficiency for the creation of a new soliton using a random perturbation.

Proposition 2.23. *For $q = 0$, a small-amplitude ($\sigma \ll 1$) stochastic perturbation of the potential* **may** *create a new small-amplitude soliton. For a white noise type perturbation $\sigma\dot{W}_x$, a new soliton is created if $W_R > 0$ (which is an event of probability $1/2$). The created soliton corresponds to the value $\eta = \sigma W_R$.*

Proof. Retain the notation introduced in the previous subsection, namely $\widetilde{\varphi} = \partial_x\varphi$. We want to use again the implicit function theorem. Taking the limit of the deterministic solution (2.2.23) as $q \to 0$ we get

$$\varphi = 1\,, \qquad \text{and} \qquad \widetilde{\varphi} = 0\,.$$

We have

$$\partial_\eta F(0,0) = \partial_\eta\widetilde{\varphi} + \varphi + \eta\,\partial_\eta\varphi = 1$$

and ($\eta = 0$)

$$\begin{cases} \mathrm{d}\varphi = \widetilde{\varphi}\,\mathrm{d}x \\ \mathrm{d}\widetilde{\varphi} = -\sigma\,\varphi \circ \mathrm{d}W_x \end{cases},$$

$$\begin{cases} \mathrm{d}\partial_\sigma\varphi = \partial_\sigma\widetilde{\varphi}\,\mathrm{d}x \\ \mathrm{d}\partial_\sigma\widetilde{\varphi} = -\big(\varphi + \sigma\partial_\sigma\varphi\big) \circ \mathrm{d}W_x \end{cases}.$$

Therefore,

$$\partial_\sigma F(0,0) = \partial_\sigma\widetilde{\varphi} + \eta\,\partial_\sigma\varphi = -\int_0^R \varphi\,\mathrm{d}W_x = -W_R\,.$$

It follows that

$$\partial_\sigma\eta(\sigma) = -\frac{\partial_\sigma F}{\partial_\eta F}(0,0) = W_R\,,$$

and a single soliton corresponding to $\eta = \sigma W_R$ is generated whenever $W_R > 0$, which means with probability $1/2$. □

Remark 2.24. The result of proposition 2.23 holds with more general processes: if, instead of a white noise, we take $U_0(x) = \sigma\, Q_x$ in (2.2.12), where Q_x is a generic stochastic process, we have (at $\eta = 0$)

$$\begin{cases} \mathrm{d}\partial_\sigma\varphi = \partial_\sigma\widetilde{\varphi}\,\mathrm{d}x \\ \mathrm{d}\partial_\sigma\widetilde{\varphi} = -Q_x\big(\varphi + \sigma\,\partial_\sigma\varphi\big)\,\mathrm{d}x \end{cases},$$

$$\partial_\sigma F(0,0) = \partial_\sigma\widetilde{\varphi} + \eta\,\partial_\sigma\varphi = -\int_0^R Q_x\,\mathrm{d}x$$

and

$$\partial_\sigma\eta(\sigma) = -\frac{\partial_\sigma F}{\partial_\eta F}(0,0) = \int_0^R Q_x\,\mathrm{d}x\,.$$

In this case, a single soliton is created whenever the noise introduced has positive mean, and it corresponds to $\eta = \sigma\int_0^R Q_x\,\mathrm{d}x$.

Remark 2.25. Recall that the mass of a soliton of the KdV equation is $N_\eta = 4\eta$. Here, we have introduced a perturbation of mass $N_{U_0} = \sigma\int_{\mathbb{R}} Q_x\,\mathrm{d}x = \eta$. We see therefore that the soliton created has a larger mass that the initial perturbation, implying that the radiative part (going in the direction opposite to the one of the soliton) has absorbed a total mass of 3η.

The energy conversion efficiency from a small noise source to a soliton is very poor, since the input energy is of order σ^2 ($E_{U_0} = \sigma^2\int_{\mathbb{R}} Q_x^2\,\mathrm{d}x$), while the energy of the created soliton is only $E_\eta = \frac{16}{3}\eta^3 \sim \sigma^3$, for a smooth source. For a white noise source, the input energy is infinite, while the energy of the created soliton is finite.

2.2.7 Perturbation of NLS and KdV solitons: similarities and differences

We have shown that for both NLS and KdV, solitons are stable with respect to small random perturbations of the initial condition. We have also seen how small random perturbations affect solitons, and here a few differences between the two models appear. For NLS there is a thresholding effect for the creation of solitons, so that a pure random initial condition of very small amplitude cannot produce solitons. Studying the perturbation of a real box-like initial condition whose integral is sufficiently large to create at least one soliton, we showed how the effect strongly depends on the nature of the perturbation: if the random perturbation is aligned (has the same phase) to the deterministic initial condition (in the case studied this means that the random perturbation is real), the amplitude of solitons is indeed modified, but their velocity remains unaffected. On the contrary, for a complex random perturbation both the amplitude and velocity of solitons are modified.

KdV is a real equation, so that only real random perturbations can be used. However, unlike for NLS solitons, the amplitude and velocity of solitons are related, and both of them are affected by random perturbations. For KdV we can also consider the case of a purely random initial condition of small amplitude. In this case, and for very general random initial conditions, there is a positive and explicitly computable probability, which depends on the kind of noise used, to create a new soliton.

The mass conversion efficiency is also different. For NLS, using a real white noise perturbation of a "critical" initial condition, it is possible to transform a quiescent soliton into a real soliton with finite mass, but the mass introduced with the perturbation is infinite. For

KdV, the mass of the created soliton is 4 times the mass introduced by the perturbation (which is finite).

2.3 Examples

In this section we present some explicit examples of the influence of random initial conditions on soliton components of the solution of the NLS equation. We first consider the question of the probability of creating a soliton from noises with a compact support $[0, R]$. The picture is not simple, as the answer strongly depends on the kind of noise used. For example, for real initial conditions and in the limit of rapid oscillations, the threshold $\bar{R}$ of the length of the support of the initial condition necessary to create the first quiescent soliton with zero speed is almost surely finite (the quiescent soliton was defined at the beginning of subsection 2.2.1). A characterization of the distribution of this random threshold in given in proposition 2.26. The same result holds for complex initial conditions with a constant phase. For random initial conditions with varying phase the answer is different. We will show that for a symmetric, complex initial condition, and in the limit of rapid oscillations, no soliton can be generated. This suggests that a constant phase of the initial condition is a crucial element to obtain a positive probability of creating a soliton with a given velocity. The proof of this remains an open problem, but we present a somewhat complementary case to the fix phase initial condition to support this claim: in the third example we study we take a complex random initial condition with constant amplitude. Here, only the phase changes, and still the probability of creating a soliton with any given speed is zero. Another negative example follows, where the initial condition is given by a complex jump process.

From all these negative examples one may get the impression that using random initial conditions it is actually very difficult to create new solitons, but this is not the case. Even if for some complex random initial conditions the probability of creating a soliton with a given speed is zero, this does not imply that no soliton can be created since the distribution of the speed and amplitude of created solitons can have an absolutely continuous part with respect to the Lebesgue measure. This leads us to our second topic: the analysis of the continuous part of the distribution of the speed and amplitude of created solitons in the presence of random initial conditions. In the limit of a random initial condition with a very long support, $R \to \infty$, the density of this distribution, called density of states (DOS), can be computed explicitly in the limit of rapidly oscillating processes, as it was done, formally, in [KM08]. To find the DOS they use the Lyapunov exponent of the ZSSP and apply a generalized Thouless formula. One of the reasons why this result is only formal is that for a white noise initial condition the IST, which is the preliminary step for all successive manipulations, cannot be applied. To solve this problem, and because in applications one is often faced with such initial conditions, we shall consider processes that are rapidly, but not infinitely rapidly, oscillating, and express the DOS using a power series expansion around the limit case. We will show how to obtain the DOS for the limit case of infinitely rapid oscillations in a rigorous way (the expression we obtain is in accordance with the formal result cited above), and provide the following order correction term for fast oscillations. We investigate this problem performing explicit computations in the case of an initial condition given by a fast oscillating, complex Ornstein-Uhlenbeck process and detail the scheme to use for a wide class of rapidly oscillating bounded Markov processes. We will show that in both cases the first order term of the expansion is zero, and obtain an explicit expression for the second order correction for the Ornstein-Uhlenbeck process. In the general case of a

bounded Markov process the explicit formula for the second order term of the DOS is very complicated, but we will discuss and present qualitatively the result in a few special settings where simplifications occur.

2.3.1 Creation of solitons from a rapidly oscillating real noise

We analyze here the case of a purely random, real initial condition for the NLS equation. Given the random process providing the initial condition, the presence of a soliton component in the solution depends on the length R of the support of the process. We show how to obtain the threshold for the creation of the first soliton with zero speed, in the case of a rapidly oscillating initial condition. The precise result is stated in the following proposition.

Proposition 2.26. *Let the initial condition $\nu(x)$ of the NLS equation be given by a real, rapidly oscillating process, with support on $[0, R]$ and satisfying hypothesis 2.1. Then, the distribution of the threshold $\bar{R}$ at which the first (quiescent) soliton with zero initial velocity appears is given by the distribution of the hitting time for a one-dimensional Bessel process starting from zero, of the threshold $\pi/2$.*

Remark 2.27. With the same proof, one can show that this result also holds for an initial condition given by a purely imaginary, rapidly oscillating process. And a simple phase shift [Ki89] allows to extend this result to any complex, rapidly oscillating initial condition, with constant phase.

The case of a real, positive (deterministic) box-like initial condition has been first studied in [Ma73] and has been extended to the case of a general, real, positive initial condition in [Bu88]. Some of these results (the threshold effect for the creation of new solitons, the identification of the number of created solitons, etc.) have been discussed and illustrated in subsection 2.2.1. The extension to real, positive, stochastic potentials is also discussed in [DP08].

The first preliminary step of the proof of proposition 2.26 will be used also in the discussion of the following examples. We shall therefore present it in the more general framework of a possibly complex initial condition in the next paragraph. This step relies on the result of proposition 2.7, providing a correspondence between the existence of solitons and zeros of the function $a(\xi, x)$, $(\xi, x) \in \mathbb{R} \times [0, R]$. The function $a(\xi, x)$ is the Jost coefficient $a(\zeta)$ of a ZSSP problem with the same potential, but supported only on $[0, x]$, instead than on $[0, R]$, and evaluated on the real line $\zeta = \xi$.

The actual core of the proof of the proposition is left to the last part of this subsection.

Limit equations for rapidly oscillating initial conditions

As shown in subsection 2.1.2, to obtain information on the behavior of the soliton component of the solution for rapidly oscillating initial conditions we just have to study the canonical system (2.1.16)

$$\begin{cases} \mathrm{d}\psi_1 = -i\zeta\psi_1 \mathrm{d}x + iD\psi_2 \circ \mathrm{d}W_x \\ \mathrm{d}\psi_2 = i\zeta\psi_2 \mathrm{d}x + iD\psi_1 \circ \mathrm{d}W_x^* \end{cases} . \tag{2.3.1}$$

Here, $D = \sqrt{2}\alpha$ is a constant depending on the integrated covariance α of the process $\nu(x)$. For real values of the spectral parameter ζ, there are two sets of linearly independent solutions defined by the asymptotic behaviors given by (2.1.4 - 2.1.5) and related through the system (2.1.6). Recall that the initial condition was supposed to have compact support

contained in the interval $x \in [0, R]$; we therefore obtain the boundary conditions

$$\psi_1(0) = 1\,, \qquad \psi_2(0) = 0$$

and

$$\Psi(R) = a(\zeta)\widetilde{\Phi}(R) + b(\zeta)\Phi(R) = a(\zeta)\begin{pmatrix}1\\0\end{pmatrix}e^{i\zeta R} + b(\zeta)\begin{pmatrix}0\\1\end{pmatrix}e^{-i\zeta R}\,.$$

To look for the threshold $\bar{R}$ we have to consider the length R of the support of the initial condition ν as a new dynamical variable, which means that we shall use again the invariant imbedding approach introduced in the proof of proposition 2.6. As we have seen in the previous sections, the analysis of the Jost coefficients a, b, the discrete spectrum $(\zeta_n)_{n=1\ldots N}$ and some norming constants $(\rho_n)_{n=1\ldots N}$, provides exhaustive information about spectral properties of the Zakharov-Shabat eigenvalue problem (ZSSP) and therefore on the presence of solitons. However, it turns out that a lot of information can be obtained in an easier way by the analysis of the dynamics of a single complex variable, the reflection coefficient $r_R(\zeta)$ given by the ratio $b(\zeta)/a(\zeta)$ on the real axis $\zeta = \xi$. This can be understood in the following way. Consider the function $r(x) = \psi_2(x)/\psi_1(x)$. From the ZSSP system (2.3.1) we obtain the evolution equation for $r(x)$:

$$\mathrm{d}r(x) = 2i\xi r(x)\,\mathrm{d}x - iDr^2(x) \circ \mathrm{d}W_x + iD \circ \mathrm{d}W_x^*\,. \tag{2.3.2}$$

From the boundary conditions for Ψ we obtain boundary conditions for r, namely $r(0) = 0$ and $r(R) = r_R e^{2i\xi R}$. Then, we see that the reflection coefficient can be obtained from the solution of the complex Riccati equation (2.3.2) with initial condition $r(0) = 0$, evaluated at $x = R$. From the proof of proposition 2.6 we also obtain that the condition for the generation of the first soliton when the length of the support of the initial condition is $\bar{R}$ is that the Jost coefficient a must have a zero on the real line, $a(\xi, 0, \bar{R}) = 0$, which corresponds to a singularity (blow up) of the solution $r(x)$ at $x = \bar{R}$. The value of ξ for which $r(\bar{R})$ blows up provides the speed of the soliton created at the threshold $\bar{R}$. From this, one can obtain the distribution of the (random) threshold $\bar{R}$ for the creation of the first soliton. Moreover, the absence of singularities in $[0, R]$ implies the absence of soliton components in the solution of the NLS equation.

To better understand the evolution of the solution of (2.3.2) we introduce the change of variables $r(x) = \mathrm{cotg}\big(\theta(x)/2\big)e^{i\varphi(x)}$. With some algebraic manipulations

$$\begin{aligned}
\mathrm{d}r(x) &= 2i\xi r(x)\,\mathrm{d}x - iDr^2(x) \circ \mathrm{d}W_x + iD \circ \mathrm{d}W_x^* \\
&= -\frac{\mathrm{d}\theta(x)}{2\sin^2\big(\theta(x)/2\big)}e^{i\varphi(x)} + i\,\mathrm{cotg}\big(\theta(x)/2\big)e^{i\varphi(x)}\,\mathrm{d}\varphi(x)\,, \\
\frac{\mathrm{d}r(x)}{r(x)} &= 2i\xi\,\mathrm{d}x - iD\,r(x) \circ \mathrm{d}W_x + i\frac{D}{r(x)} \circ \mathrm{d}W_x^* \\
&= -\frac{\mathrm{d}\theta(x)}{2\sin\big(\theta(x)/2\big)\cos\big(\theta(x)/2\big)} + i\,\mathrm{d}\varphi(x)\,,
\end{aligned}$$

we get to the system of SDEs

$$\begin{cases}
\mathrm{d}\theta(x) = -2D\,\Im\left[e^{i\varphi(x)} \circ \mathrm{d}W_x\right] \\
\mathrm{d}\varphi(x) = 2\xi\,\mathrm{d}x - 2D\mathrm{cotg}\big(\theta(x)\big)\,\Re\left[e^{i\varphi(x)} \circ \mathrm{d}W_x\right]
\end{cases}, \tag{2.3.3}$$

for $\theta \in [0, \pi]$ and $\varphi \in \mathbb{R}$. One always starts from $\theta = \pi$, corresponding to $r = 0$. $\theta = 0$

corresponds to a singularity for r and therefore to the creation of a soliton.

Real white noise: threshold for a still soliton creation

We shall now work in the setting presented in the previous paragraph and prove proposition 2.26.

Proof of Proposition 2.26. From the proof of proposition 2.6 we see that the new soliton created at the threshold $\bar{R}$ is a quiescent soliton, which was defined in subsection 2.2.1. We can therefore set $\zeta = 0$ in equation (2.3.1), and obtain

$$\begin{cases} \mathrm{d}\psi_1 = i\psi_2 \circ \mathrm{d}W_x \\ \mathrm{d}\psi_2 = i\psi_1 \circ \mathrm{d}W_x \end{cases} .$$

The evolution equation for the variable $r(x) := \psi_2(x)/\psi_1(x)$ now reads

$$\mathrm{d}r(x) = i\big[-r^2(x) + 1\big] \circ \mathrm{d}W_x \,.$$

Using again the change of variables $r(x) = \operatorname{cotg}\big(\theta(x/2)\big)e^{i\varphi(x)}$ we get

$$\begin{cases} \mathrm{d}\theta(x) = \ -2\,\sin\big(\varphi(x)\big) \circ \mathrm{d}W_x \\ \mathrm{d}\varphi(x) = -2\operatorname{cotg}\big(\theta(x)\big)\,\cos\big(\varphi(x)\big) \circ \mathrm{d}W_x \end{cases} , \tag{2.3.4}$$

for $\theta \in [0, \pi]$ and $\varphi \in [0, 2\pi]$. We can look at the above system as governing the motion (if x plays the role of a time variable) of a "particle" on a finite box. The initial condition ($\psi_1(0) = 1$, $\psi_2(0) = 0$) is $r(0) = 0$, corresponding to $\theta(0) = \pi$, and the only finite solutions adhering to this initial condition have phase $\varphi = \pm\pi/2$. The value of $\varphi(0)$ must be chosen such that $\theta \leq \pi$, which formally means that $\mathrm{d}\theta(0) < 0$. The phase retains its value for $\theta \in (0, \pi)$, and may change its value every time the "particle" is reflected at $\theta = 0$ or $\theta = \pi$: each time the new value of φ must be chose such that $0 \leq \theta \leq \pi$. The boundary conditions in φ are periodic. The process $\gamma(x) = \big(\pi - \theta(x)\big)$ is therefore a reflected Wiener process, $\gamma = 2|W|$, starting from 0. We are interested in the hitting time for γ of the threshold π, which corresponds to $\theta = 0$. In turn, this corresponds to the threshold $\bar{R}$ of the length of the support of the initial condition of the NLS equation necessary to create the first still, quiescent soliton. Since almost surely the one-dimensional Wiener process W reaches the points $\pm\pi/2$ in a finite time, $\bar{R}$ is almost surely finite, and the distribution of the creation time $\bar{R}$ can then be obtained as the hitting time of the threshold $\pi/2$ for the Bessel process γ. □

Remark 2.28. When the initial condition $U(x)$ is real, and only when it is real, it is possible to obtain an explicit formula for the solution Ψ of the ZSSP system for $\zeta = 0$. This is given by [Ki89]

$$\begin{aligned} \psi_1(x) &= e^{iS(x)}\left[i\int_0^x U(y)e^{2iS(y)}\mathrm{d}y + 1\right] \\ \psi_2(x) &= e^{iS(x)} - \psi_1 \,, \end{aligned}$$

where

$$S(x) = \int_0^x U(y)\,\mathrm{d}y \,.$$

The solution Ψ defined above satisfies the initial condition (2.1.12) and for $S(R) = \pm\pi/2$ it also matches the final condition $\psi_1(R) = 0$, which means that a new quiescent soliton is created. This confirms the result of proposition 2.26. Unfortunately, when U is complex-valued it is not possible to find a closed form expression for the solution Ψ and then the strategy used in the proof of proposition 2.26 is the only possible one.

2.3.2 Complex white noise: no soliton creation

We study here the case where the initial condition is give by a complex process, in the limit of rapid oscillations. As proved in section 2.1, what we have to study is the ZSSP system with the potential given by a complex white noise. We will show that in this limit almost surely no soliton is created. The precise result is the following.

Proposition 2.29. *Let the initial condition $U_0(x)$ of the NLS equation be given by a complex, rapidly oscillating process, with support on $[0, R]$, of the form $U_0(x) = \nu_1(x) + i\nu_2(x)$, where ν_n, $n = 1, 2$ are two independent and identically distributed real processes satisfying hypothesis 2.1. Then, for any fixed $R > 0$ and in the limit of fast oscillations, the probability that the solution of the NLS equation contains a soliton component is zero.*

We shall use the approach presented in the previous subsection, and prove the following equivalent reformulation of proposition 2.29.

Proposition 2.30. *For any $R > 0$, consider the discrete spectrum of the ZSSP system (2.3.1) with a complex symmetric white noise as potential. Then, almost surely the discrete spectrum is empty.*

Proof. We start our analysis from the system (2.3.3), where now $W_x = W_x^{(1)} + iW_x^{(2)}$ is a complex Wiener process. We will work on the first equation of this system to show that $\theta(x) > 0$ for every $x \in [0, R]$ almost surely. This fact implies that the function r solution of the Riccati equation (2.3.2) does not blow up, the function $a(\xi, 0, x)$ is never zero for $(\xi, x) \in \mathbb{R} \times [0, R]$, and the Jost function $a(\zeta)$ cannot have a zero in the upper half of the complex plane. Therefore, the discrete spectrum of the ZSSP system is empty and no soliton is generated.

The difficult part is to show that $\theta(x) > 0$ for every $x \in [0, R]$ almost surely. The idea of the proof relies on the fact that the behavior of $\theta(x)$ is similar to the behavior of a Bessel process of dimension 2 (which almost surely never reaches zero), at least near zero. This is because the first equation in (2.3.3) is very similar to a Bessel equation since

$$\widetilde{W}_x := \int_0^x \cos\big(\varphi(x)\big)\,\mathrm{d}W_x^{(1)} + \int_0^x \sin\big(\varphi(x)\big)\,\mathrm{d}W_x^{(2)} \tag{2.3.5}$$

is still a Wiener process by Lévy characterization theorem, and near zero $\operatorname{cotg}(x) \sim x^{-1}$. With this notation, and rewriting (2.3.3) in Itô form, we have

$$\mathrm{d}\theta(x) = \mathrm{d}\widetilde{W}_x + \frac{1}{2}\operatorname{cotg}\big(\theta(x)\big)\,\mathrm{d}x\,. \tag{2.3.6}$$

Some preliminary steps are needed before we can obtain the announced Bessel equation. We shall start by showing that strong uniqueness holds for equation (2.3.6). To do so, define the new process $Y(x) := \cos\big(\theta(x)\big)$, which is a solution of

$$\mathrm{d}Y(x) = -\cos\big(\theta(x)\big)\,\mathrm{d}x - \sin\big(\theta(x)\big)\,\mathrm{d}\widetilde{W}_x = -Y(x)\,\mathrm{d}x - \sqrt{1 - Y_x^2}\,\mathrm{d}\widetilde{W}_x. \tag{2.3.7}$$

Since $\theta \in [0,\pi]$, uniqueness for $Y(x)$ implies uniqueness for $\theta(x)$. The drift of the above equation is Lipschitz continuous. As for the diffusion coefficient, that we will now call σ, we have that

$$\left|\sigma(x)-\sigma(y)\right|^2 = \left|\sqrt{1-x^2}-\sqrt{1-y^2}\right|^2 \leq 2-y^2-x^2 \leq \left|y^2-x^2\right| \leq 2|y-x|$$

for all x, y such that $|x|, |y| \leq 1$ (observe that $Y(x) \in [-1,1]$). Then, strong uniqueness for equation (2.3.7) follows from [RY, theorem 3.5, chapter IX].

Return now to consider the formulation of equation (2.3.6); we have to prove that for every fixed $\xi \in \mathbb{R}$ and $R > 0$, almost surely $\theta(x) > 0$ for all $x \in [0,R]$, which we do by showing that $P(\tau_0(\theta) \leq R) = 0$, where

$$\tau_0(\theta) = \inf\{x \geq 0 \big| \, \theta(x) = 0\}\,.$$

More generally, we set

$$\tau_y(\theta) = \inf\{x \geq 0 \big| \, \theta(x) = y\}\,.$$

Remark that $\tau_0(\theta) > R$ implies the non-explosion of $r(x)$ and therefore that no soliton can be created with speed ξ almost surely.

Recall that the initial condition for the process $\theta(x)$ was $\theta(0) = \pi$. Therefore, $\theta(x)$ must reach $\pi/2$ before reaching zero. Using the strong Markov property we get

$$P\big(\tau_0(\theta) \leq R \,\big|\, \theta(0) = \pi\big) \leq P\big(\tau_0(\theta) \leq R \,\big|\, \theta(0) = \pi/2\big)\,.$$

Remark also that the density of the process θ is symmetric with respect to $\pi/2$, so that

$$\begin{aligned} P\big(\tau_0(\theta) \leq R \,\big|\, \theta(0) = \pi/2\big) &\leq P\Big(\big\{\tau_0(\theta) \leq R\big\} \cup \big\{\tau_\pi(\theta) \leq R\big\} \,\Big|\, \theta(0) = \pi/2\Big) \\ &= P\big(\tau_0(\widetilde{\theta}) \leq R \,\big|\, \theta(0) = \pi/2\big) \\ &\leq P\big(\tau_0(\widetilde{\theta}) \leq R \,\big|\, \theta(0) = \pi/4\big)\,, \end{aligned}$$

where $\widetilde{\theta}$ is a solution of (2.3.6) reflected in $\pi/2$ and taking values in the interval $[0,\pi/2]$. We have to show that

$$P\big(\tau_0(\widetilde{\theta}) \leq R \,\big|\, \theta(0) = \pi/4\big) = 0\,. \tag{2.3.8}$$

From now on, we will work with this reflected process. Therefore, to ease notation, we will drop the conditioning on $\theta(0) = \pi/4$. This restriction to a process with values in $[0,\pi/2]$ is very useful because the function

$$f(x) = \frac{1}{2}\Big[\frac{1}{x} - \operatorname{cotg}(x)\Big]$$

is bounded on $(0,\pi/2]$. Since $\lim_{x\to 0} f(x) = 0$, we can extend this function to the domain $[0,\pi/2]$ by continuity. We have $f' \geq 0$ and $f(\pi/2) = 1/\pi$, from which we obtain that f takes values in $[0,1/\pi]$. It follows that for every fixed R,

$$\exp\Big(\frac{1}{2}\int_0^R f^2\big(\widetilde{\theta}(x)\big)\,\mathrm{d}x\Big) \leq \exp\Big(\frac{R}{2\pi^2}\Big) < \infty\,,$$

which is the Novikov condition implying that the process

$$Z(x) = \exp\Big(\int_0^x f\big(\widetilde{\theta}(y)\big)\,\mathrm{d}\widetilde{W}_y - \frac{1}{2}\int_0^x f^2\big(\widetilde{\theta}(y)\big)\,\mathrm{d}y\Big)$$

is a martingale on $[0, R]$. Girsanov theorem states that $B_x = \widetilde{W}_x - \int_0^x f\big(\widetilde{\theta}(y)\big)\,\mathrm{d}y$ is a Wiener process under a new probability measure Q absolutely continue with respect to the restriction of P to the natural filtration of the original Wiener process $\mathcal{F}_x^W$. Before we proceed and apply Girsanov theorem, we must introduce some additional stopping times. We stress that they all refer to the reflected process $\widetilde{\theta}$ starting from $\pi/4$. For $n \geq 1$ set

$$\begin{aligned}\sigma_1 &= \inf\{x > 0 \,|\, \widetilde{\theta} = \pi/2\}\,;\\ \sigma_{2n} &= \inf\{x > \sigma_{2n-1} \,|\, \widetilde{\theta} = \pi/4\}\,;\\ \sigma_{2n+1} &= \inf\{x > \sigma_{2n} \,|\, \widetilde{\theta} = \pi/2\}\,.\end{aligned}$$

Thanks to the strong Markov property of the process θ, we can work on each random interval $[\sigma_k, \sigma_{k+1}]$ independently. To fix the ideas, we shall consider the interval $[0, \sigma_1]$; on any other interval $[\sigma_{2n}, \sigma_{2n+1}]$ we may proceed in the same way. Restricted to this interval, the process $\widetilde{\theta}$ solves (2.3.6), and does not feel the effect of the reflection imposed in $\pi/2$. On this interval, it is also solution of the Bessel equation

$$\mathrm{d}\gamma = \frac{1}{2\gamma}\,\mathrm{d}x + \mathrm{d}B_x \tag{2.3.9}$$

under the probability measure Q introduced above. This solution is a two dimensional Bessel process, which never reaches the origin. This means that $Q(\gamma = 0) = 0$, or equivalently $Q(\tau_0(\gamma) < R) = 0$. However, $\widetilde{\theta}$ is a solution of the Bessel equation only on the interval $[0, \sigma_1]$, and only on this interval we can apply Girsanov theorem. Therefore, we can only use that Q is absolutely continues with respect to P on $\mathcal{F}_{\sigma_1}^W$. But this is enough to obtain

$$P\big(\tau_0(\widetilde{\theta}) < \sigma_1\big) = \mathcal{Q}\big(\tau_0(\gamma) < \sigma_1\big) = 0\,.$$

This means that almost surely the process $\widetilde{\theta}$ starting from $\pi/4$ reaches $\pi/2$ before 0. But then it must pass again through $\pi/4$ before getting to zero: by definition $\widetilde{\theta}$ cannot reach zero on the interval $[\sigma_1, \sigma_2]$, so that we have also

$$P\big(\tau_0(\widetilde{\theta}) < \sigma_2\big) = 0\,.$$

Repeating this construction using the strong Markov property and the Girsanov theorem on each interval $[\sigma_{2n}, \sigma_{2n+1}]$ we finally get to

$$\forall n\,, \quad P\big(\tau_0(\widetilde{\theta}) < \sigma_n\big) = 0\,.$$

We only have to show that there exists an n such that

$$P\big(\sigma_n > R\big) = 1\,. \tag{2.3.10}$$

Clearly, $P(\sigma_1 > 0) > 0$, which is to say that there exists an $\varepsilon > 0$ such that $P(\sigma_1 > \varepsilon) > \varepsilon$. Using the independence of the increments $(\sigma_{n+1} - \sigma_n)$, we get that

$$P\Big(\sum_{n=0}^{R/\varepsilon} \big(\sigma_{n+1} - \sigma_n\big) > R\Big) \geq \prod_{n=0}^{R/\varepsilon} P\Big(\sigma_{n+1} - \sigma_n > \varepsilon\Big) = \varepsilon^{R/\varepsilon} > 0$$

and

$$P\Big(\sum_{n=0}^{K}\big(\sigma_{n+1}-\sigma_n\big)<\varepsilon\Big)=\prod_{n=0}^{K}P\Big(\sigma_{n+1}-\sigma_n<\varepsilon\Big)=(1-\varepsilon)^K\overset{K\to\infty}{\longrightarrow}0\,.$$

Combining this two results we get (2.3.10), which completes the proof. □

2.3.3 Complex noise of constant intensity: no soliton creation for fixed ξ

We have studied above the behavior of a real (or complex, but with constant phase) initial condition. We consider now the somewhat complementary case of an initial condition given by a complex stochastic process with constant intensity.

Let the initial condition of the NLS equation be given by $U_0(x)=q\,e^{i\nu(x)}\mathbb{1}_{[0,R]}(x)$ for some real, continuous martingale $\nu(x)$ with bounded quadratic variation ($\langle\nu\rangle\le C$) and independent increments. We shall assume for simplicity that $|U_0(x)|=q=1$. Remark that this process is in L^1; the IST machinery can therefore be applied to obtain the ZSSP (2.1.3). With this initial condition we have

Proposition 2.31. *Consider the NLS equation with the initial condition U_0 described above. Then, for any fixed ξ, the probability of creating a soliton with the prescribed speed (ξ) is zero.*

Proof. We shall use the approach presented in the first paragraph of subsection 2.3.1. For real values of $\zeta=\xi$, define the function $r(x)=\psi_2(x)/\psi_1(x)$, which solves for $x\in[0,R]$

$$\mathrm{d}r(x)=2i\xi r(x)-iU_0(x)r^2(x)+iU_0^*(x)=2i\xi r(x)-ie^{i\nu(x)}r^2(x)+ie^{-i\nu(x)}\,.$$

Using again the change of variables $r(x)=\operatorname{cotg}\big(\theta(x)/2\big)e^{i\varphi(x)}$, the system of SDEs (2.3.3) becomes

$$\begin{cases}\dfrac{\mathrm{d}\theta(x)}{\mathrm{d}x}=-2\Im\Big[e^{i\left[\nu(x)+\varphi(x)\right]}\Big]=-2\sin\big(\nu(x)+\varphi(x)\big)\\[2ex]\dfrac{\mathrm{d}\varphi(x)}{\mathrm{d}x}=2\xi-2\operatorname{cotg}\big(\theta(x)\big)\Re\Big[e^{i\left[\nu(x)+\varphi(x)\right]}\Big]=2\xi-2\operatorname{cotg}\big(\theta(x)\big)\cos\big(\nu(x)+\varphi(x)\big)\end{cases}.\tag{2.3.11}$$

To simplify notation, we will use $\mathrm{d}\theta(x)/\mathrm{d}x=\dot\theta(x)$. From Itô formula we obtain

$$\begin{aligned}\mathrm{d}\dot\theta(x)&=-2\,\cos\big(\nu(x)+\varphi(x)\big)\,\mathrm{d}\nu(x)-4\,\xi\,\cos\big(\nu(x)+\varphi(x)\big)\,\mathrm{d}x\\&\quad+4\operatorname{cotg}\big(\theta(x)\big)\Big[1-\sin^2\big(\nu(x)+\varphi(x)\big)\Big]\mathrm{d}x\\&=-2\,\cos\big(\nu(x)+\varphi(x)\big)\,\mathrm{d}\nu(x)-4\,\xi\,\cos\big(\nu(x)+\varphi(x)\big)\,\mathrm{d}x\\&\quad+4\operatorname{cotg}\big(\theta(x)\big)\,\mathrm{d}x-\operatorname{cotg}\big(\theta(x)\big)\dot\theta(x)\,\mathrm{d}x\,,\end{aligned}$$

and multiplying by $\theta(x)$

$$\begin{aligned}\theta(x)\,\mathrm{d}\dot\theta(x)+\dot\theta^2(x)&=4\,\mathrm{d}x-2\,\theta(x)\cos\big(\nu(x)+\varphi(x)\big)\,\mathrm{d}\nu(x)-4\,\xi\,\theta(x)\,\cos\big(\nu(x)+\varphi(x)\big)\,\mathrm{d}x\\&\quad-\theta(x)\Big[\frac{1}{\theta(x)}-\operatorname{cotg}\big(\theta(x)\big)\Big]\big[4-\dot\theta^2(x)\big]\,\mathrm{d}x\,.\end{aligned}$$

Rename the last term above $-R(x)\,\mathrm{d}x$ and integrate twice:

$$\theta(x)\,\dot\theta(x) = \theta(0)\,\dot\theta(0) + 4x - 2\int_0^x \theta(y)\,\cos\big(\nu(y)+\varphi(y)\big)\,\mathrm{d}\nu(y) \\ - 4\,\xi\int_0^x \theta(y)\,\cos\big(\nu(y)+\varphi(y)\big)\,\mathrm{d}y - \int_0^x R(y)\,\mathrm{d}y\,,$$

$$\theta^2(x) = \theta^2(0) + 2x\,\theta(0)\,\dot\theta(0) + 4x^2 - 4\int_0^x\int_0^y \theta(z)\,\cos\big(\nu(z)+\varphi(z)\big)\,\mathrm{d}\nu(z)\,\mathrm{d}y \\ - 8\xi\int_0^x\int_0^y \theta(z)\,\cos\big(\nu(z)+\varphi(z)\big)\,\mathrm{d}z\,\mathrm{d}y - 2\int_0^x\int_0^y R(z)\,\mathrm{d}z\,\mathrm{d}y\,.$$

We claim that almost surely $\theta(x) > 0$, $\forall x \in [0,R]$. Proving this claim completes the proof of the proposition. We prove below an equivalent statement. □

Claim 2.32. *The event* $A = \big\{\omega \,|\, \exists x \in [0,R], \theta(x) = 0\big\}$ *is negligible.*

Proof. Recall that $\theta(0) = \pi$. We will show that, for ε small enough, if θ ever reaches the level ε, it experiences a positive acceleration so strong that it is rejected far from the origin before reaching zero.

For any $\varepsilon > 0$, define the stopping time

$$\tau_0 := \inf\Big\{x \ge 0 \;\Big|\; \theta(x) = \varepsilon\,, \dot\theta(x) \le 0\Big\}\,.$$

Set $\varepsilon^{1/4} = \delta$ and define a second stopping time as

$$\tau_1 := \sigma_1 \wedge \sigma_2\,, \tag{2.3.12}$$

where

$$\sigma_1 = \inf\Big\{x \ge \tau_0 \;\Big|\; \theta(x) > 2^4\delta^4\Big\}\,,$$
$$\sigma_2 = \inf\Big\{x \ge \tau_0 \;\Big|\; \Big|\int_{\tau_0}^x \theta(y)\cos\big(\nu(y)+\varphi(y)\big)\,\mathrm{d}\nu(y)\Big| > \delta^5\Big\}\,.$$

Note that for $x \in [\tau_0, \tau_1 \wedge R]$

$$-4\int_{\tau_0}^x\int_{\tau_0}^y \theta(z)\,\cos\big(\nu(z)+\varphi(z)\big)\,\mathrm{d}\nu(z)\,\mathrm{d}y \ge -4\delta^5 x\,; \\ -8\,\xi\int_{\tau_0}^x\int_{\tau_0}^y \theta(z)\,\cos(\nu(z)+\varphi(z))\,\mathrm{d}z\,\mathrm{d}y \ge -2^6\delta^4\,\xi\,x^2.$$

Also, for $\theta \le \pi/4$, $\big(1/\theta - \mathrm{cotg}(\theta)\big) \le 4/\pi - 1 \le 1/2$. Therefore, if

$$\varepsilon \le \pi/2^6 \tag{2.3.13}$$

for $x \in [\tau_0, \tau_1 \wedge R]$ we have that $\theta(x) \leq \pi/4$ and

$$-2\int_{\tau_0}^{x}\int_{\tau_0}^{y} R(z)\,\mathrm{d}z\,\mathrm{d}y = -2\int_{\tau_0}^{x}\int_{\tau_0}^{y} \theta(z)\left[\frac{1}{\theta(z)} - \operatorname{cotg}\big(\theta(z)\big)\right]\left[4 - \dot\theta(z)^2\right]\,\mathrm{d}z\,\mathrm{d}y$$
$$\geq -2\cdot 2^4\varepsilon\cdot\frac{1}{2}\cdot 4\cdot\frac{x^2}{2} = -2^5\delta^4\,x^2.$$

Summing up all these results, we have obtained that if $\varepsilon \leq \pi/2^6$

$$\theta^2(x) \geq \delta^8 + 2x\,\delta^4\,\dot\theta(\tau_0) + 4x^2 - 4\delta^5 x - 2^6\delta^4\,\xi\,x^2 - 2^5\delta^4\,x^2\,. \tag{2.3.14}$$

We look at the right hand side above as an equation of degree 2 in x: $ax^2 + bx + c$. The coefficients are:

$$a = 4 - 2^5\delta^4\big(2\xi + 1\big)\,, \qquad b = 2\delta^4\dot\theta(\tau_0) - 4\delta^5\,, \qquad c = \delta^8\,.$$

We would like to show that on an almost sure event

$$\begin{aligned} a &> 0\,;\\ \Delta = b^2 - 4ac &< 0\,;\\ \tau_1 &\geq \tau_0 - b/a\,. \end{aligned} \tag{2.3.15}$$

The first two inequalities prove that the right hand side of (2.3.14) is strictly positive. The bound (2.3.14) then implies that $\theta(x) > 0$ for $x \in [\tau_0, \tau_1 \wedge R]$. We will see below that $a > 3$, and since $b < -4\delta^5$ the last inequality can also be used to ensure that we only have to repeat the present construction (find a new $\tau_0' > \tau_1$ and so on) a finite number of time to account for the behavior of $\theta(x)$ over the entire range $[0, R]$. If for every iteration (2.3.15) hold on a set of full measure, the intersection of such events is still of full measure and is contained in the complement of A.

Unfortunately, the above set of inequalities do not hold on an almost sure event. However, on the "dangerous" event where they do not hold, we are able to perform some explicit estimates on θ using directly the evolution equation (2.3.11). These estimates show that also on this event θ cannot reach zero almost surely, which proves that A is negligible.

Remark that, unlike the set A, the above inequalities as well as the stopping times depend on δ. We are therefore free to chose a convenient value of δ. Let us start by assuming that $\delta < 2\xi^{-1}$ and $\delta < 2^{-2}$ (which is a slightly stronger condition than (2.3.13)). It is then easy to see that $a > 0$. Actually, what one obtains is that $a > 4 - 3/8 > 3$. We turn now to the last inequality of (2.3.15). We have that

$$-b = 2\delta^4\big|\dot\theta(\tau_0)\big| + 4\delta^5 \leq 4\delta^4(1+\delta) < 5\delta^4$$

and

$$\frac{-b}{a} \leq 2\delta^4 =: \bar x\,. \tag{2.3.16}$$

The probability that the last inequality of (2.3.15) holds can be computed as follows.

$$P\left(\tau_1 < \tau_0 - \frac{b}{a}\right) \le P\left(\tau_1 < \tau_0 + \bar{x}\right) \le P\left(\sup_{x\in[\tau_0,\tau_0+\bar{x}]} \left|\int_{\tau_0}^{x} \theta(y)\cos\big(\nu(y)+\varphi(y)\big)\,\mathrm{d}\nu(y)\right| > \delta^5\right) + P\left(\sup_{x\in[\tau_0,\tau_0+\bar{x}]} \theta(x) > 2^4\delta^4\right).$$

Let us first find an estimate for the second term on the right hand side. Since by the first equation in (2.3.11) we have that $\left|\dot\theta(x)\right| \le 2$,

$$\sup_{x\in[\tau_0,\tau_0+\bar{x}]} \theta(x) \le \theta(\tau_0) + 2\bar{x} = 5\delta^4. \tag{2.3.17}$$

We can now use this bound and Doob's inequality to get

$$P\left(\sup_{x\in[\tau_0,\tau_0+\bar{x}]} \left|\int_{\tau_0}^{x} \theta(y)\cos\big(\nu(y)+\varphi(y)\big)\,\mathrm{d}\nu(y)\right| > \delta^5\right) \le \frac{1}{\delta^{10}}\int_{\tau_0}^{\tau_0+\bar{x}} \theta^2(y)\;\mathrm{d}\langle\nu\rangle_y \le \frac{5^2\delta^8\,\bar{x}\,C}{\delta^{10}} = 50C\delta^2, \tag{2.3.18}$$

where the constant C is the bound on the quadratic variation $\langle\nu\rangle$ of the process ν assumed in the hypothesis stated at the beginning of this subsection. Therefore,

$$P\left(\tau_1 \ge \tau_0 - \frac{b}{a}\right) \ge 1 - 50C\delta^2 \;\stackrel{\delta\to 0}{\longrightarrow}\; 1\,. \tag{2.3.19}$$

We still have to work on the second inequality of (2.3.15). We have

$$\Delta/4\delta^8 = \dot\theta^2(\tau_0) + 4\delta^2 - 4\delta\dot\theta(\tau_0) - 4 + 2^5\delta^4(2\xi+1)\,. \tag{2.3.20}$$

This is not negative in general. Therefore, we consider the right hand side of (2.3.20) as an equation of degree 2 in the variable $t = \dot\theta(\tau_0)$. Recall that by definition $\dot\theta(\tau_0) \le 0$, so that we are interested only in the behavior of this equation for $t \le 0$. Since for $t = 0$ (2.3.20) is negative, we look for the smaller of the two zeros of the equation, $\bar t$, which can be found solving this new equation of degree 2 as follows.

$$\begin{aligned} \Delta/4 &= 4\delta^2 - 4\delta^2 + 4 - 2^5\delta^4(2\xi+1)\,; \\ \bar t &= 2\delta - \sqrt{4 - 2^5\delta^4(2\xi+1)}\,. \end{aligned} \tag{2.3.21}$$

If $\dot\theta(\tau_0) \in (\bar t, 0]$, then (2.3.20) is negative and we have obtained the second inequality in (2.3.15). We are left with one last case to study, $\dot\theta(\tau_0) \in [-2, \bar t]$, in particular as δ goes to zero.

Observe that $\bar t$ is increasing as a function of δ and converges to -2 as $\delta \to 0$. From the explicit formula (2.3.21) we get that the amplitude of the interval of "dangerous" initial velocities, $[-2, \bar t\,(\delta)]$, is of order δ. From the first equation of (2.3.11) we see that this corresponds to $\sin\big(\nu(x)+\varphi(x)\big)$ taking values in an interval of the same order around $+1$, so that the length of the corresponding interval of "dangerous" values of $\big(\nu(x)+\varphi(x)\big)$ is of order $\delta^{\frac12}$:

$$\nu(x) + \varphi(x) = \frac{\pi}{2} + O(\delta^{\frac12})\,. \tag{2.3.22}$$

From (2.3.16) we obtain that we are working on an interval of x of order δ^4. Assuming that the process ν varies on a scale of order 1, on the interval of interest its variation is of order δ^4. Also, $\cos\big(\nu(x)+\varphi(x)\big) = O(\delta^{\frac{1}{2}})$, $\operatorname{cotg}(\theta) \sim \theta^{-1}$ for $\theta \to 0$ and $\theta = \delta^4$, so that

$$\operatorname{cotg}\big(\theta(x)\big)\cos\big(\nu(x)+\varphi(x)\big) \sim O(\delta^{-\frac{7}{2}})\,.$$

It follows that the variation of φ is of order $\delta^{\frac{1}{2}}$. Therefore, on a sufficiently small scale $\delta \ll 1$, we can consider the process ν as approximately constant, the variation of φ being of a lower order.

Let us now look at the evolution of these quantities. Remark that since $\dot\theta < 0$, as x grows θ decreases, at least a small interval. Then, setting the new starting point just after τ_0, δ decreases.

Let as assume by contradiction that θ does reach zero with positive probability. Consider any fixed δ. We place ourselves at $x = \tau_0(\delta)$. The only possibility is that $\dot\theta$ always remains in the "dangerous" interval $[-2, \bar t(\delta)]$. We have already observed that this interval of dangerous velocities shrinks to -2 as $\delta \to 0$, and this will provide the contradiction. We shall consider two cases.

If $\dot\theta(\tau_0) > -2$ then necessarily $\nu + \varphi \neq \pi/2$. If $\nu + \varphi > \pi/2$ the cosinus is negative and by the equations (2.3.11) we get that $\dot\varphi > 0$. If δ is small enough, this implies that $\nu + \varphi$ is increasing, the sinus is decreasing and $\dot\theta$ is increasing. Symmetrically, if $\nu + \varphi < \pi/2$ for δ small enough, $\dot\varphi < 0$ and again $\dot\theta$ is increasing. But since we must have $\dot\theta(\tau_0) < \bar t \to -2$ as $\delta \to 0$, we have a contradiction.

The only possibility left is therefore that there exists a positive value δ_0 such that for all choices of initial levels $\delta \le \delta_0$, one finds that $\dot\theta(\tau_0) = -2$. But this means that on such an interval $\nu + \varphi \equiv \pi/2$ must be constant, so that necessarily $\nu = \pi/2 - \varphi$ and

$$\mathrm{d}\nu(x) = -2\xi\,. \tag{2.3.23}$$

At $\tau_0(\delta_0)$ we have $\theta = \delta_0^4$, and $\dot\theta = -2$ must remain fix until θ reaches zero. Therefore, equation (2.3.23) must hold on the interval $x \in [\tau_0(\delta_0), \tau_0(\delta_0) + \delta_0^4/2]$. But the event of ν having constant derivative on an interval of positive length is negligible due to the assumption of independent increments.

The contradiction found proves that for δ sufficiently small, even if the initial velocity $\dot\theta(\tau_0)$ is in the "dangerous" interval $[-2, \bar t(\delta)]$, θ does not reach zero almost surely. If $\dot\theta(\tau_0)$ is not in this interval, then we have proved that the three inequalities (2.3.15) hold, which proves that also in this case θ does not reach zero. Combining these two results, we finally get that the event A is negligible. □

2.3.4 Complex telegraph noise: no soliton creation for fixed ξ

We consider now the case where the initial condition $U_0(x)$ of the NLS equation is given by a jump process on the complex plane. We will show that the probability of creating a soliton with any prescribed velocity is zero.

Proposition 2.33. *Let the initial condition $U_0(x)$ of the NLS equation be given by a jump process supported on $[0, R]$, whose jumping times have a Poisson distribution of parameter λ. We assume that the amplitudes of the jumps are independent and identically distributed random variables admitting a density law on $\mathbb{C}$. Then, for any $R > 0$ and $\xi \in \mathbb{R}$, almost surely no soliton is created with speed ξ.*

Proof. Let $\{\tau_n\}_{n\geq 1}$ be the sequence of jump points of $U_0(x)$ and set $\tau_0 = 0$; it is sufficient to prove the result on any fixed interval $I_n := [\tau_n, \tau_{n+1} \wedge R]$, $n \geq 0$.

Note that on I_n, $U_0(x) = \rho_n\, e^{i\gamma_n}$ is constant. We will first deal with the case of still solitons, $\xi = 0$. We shall use again the approach described in the first paragraph of subsection 2.3.1. In our setting, the equivalent of equation (2.3.3) reads

$$\begin{cases} \dfrac{\mathrm{d}\theta(x)}{\mathrm{d}x} = -2\rho_n \sin\big(\varphi(x) + \gamma_n\big) \\ \dfrac{\mathrm{d}\varphi(x)}{\mathrm{d}x} = -2\rho_n \mathrm{cotg}\big(\theta(x)\big) \cos\big(\varphi(x) + \gamma_n\big) \end{cases} . \tag{2.3.24}$$

We have that

$$\begin{aligned} \frac{\mathrm{d}}{\mathrm{d}x} \sin\big(\theta(x)\big) \cos\big(\varphi(x) + \gamma_n\big) = &- 2\rho_n \cos\big(\theta(x)\big) \sin\big(\varphi(x) + \gamma_n\big) \cos\big(\varphi(x) + \gamma_n\big) \\ &+ 2\rho_n \sin\big(\theta(x)\big) \sin\big(\varphi(x) + \gamma_n\big) \mathrm{cotg}\big(\theta(x)\big) \cos\big(\varphi(x) + \gamma_n\big) \end{aligned}$$

is identically zero. Therefore, $\sin\big(\theta(x)\big) \cos\big(\varphi(x) + \gamma_n\big)$ is constant on I_n. This implies that $\theta(x)$ can reach zero only if $\varphi(\tau_n) + \gamma_n = \frac{\pi}{2}$. But this is a negligible event due to the density assumption on the law of the jumps of $\nu(x)$, so that the proposition is proved in the case $\xi = 0$.

Assume now that ξ is fixed and different form zero. Equation (2.3.3) becomes

$$\begin{cases} \dfrac{\mathrm{d}\theta(x)}{\mathrm{d}x} = -2\rho_n \sin\big(\varphi(x) + \gamma_n\big) \\ \dfrac{\mathrm{d}\varphi(x)}{\mathrm{d}x} = 2\xi - 2\rho_n \mathrm{cotg}\big(\theta(x)\big) \cos\big(\varphi(x) + \gamma_n\big) \end{cases}$$

and we have that

$$\frac{\mathrm{d}}{\mathrm{d}x} \sin\big(\theta(x)\big) \cos\big(\varphi(x) + \gamma_n\big) = -2\xi\rho_n \sin\big(\theta(x)\big) \sin\big(\varphi(x) + \gamma_n\big) = -2\xi \frac{\mathrm{d}}{\mathrm{d}x} \Big[\cos\big(\theta(x)\big) \Big] .$$

Therefore,

$$\sin\big(\theta(x)\big) \cos\big(\varphi(x) + \gamma_n\big) + 2\zeta \cos\big(\theta(x) = \sin\big(\theta(\tau_n)\big) \cos\big(\varphi(\tau_n) + \gamma_n\big) + 2\xi \cos\big(\theta(\tau_n)\big)$$

and $\theta(x)$ can reach zero only if

$$2\xi = \frac{\sin\big(\theta(\tau_n)\big)}{1 - \cos\big(\theta(\tau_n)\big)} \cos\big(\varphi(\tau_n) + \gamma_n\big) ,$$

which is to say

$$\xi = \frac{\mathrm{cotg}\big(\theta(\tau_n/2)\big)}{2} \cos\big(\varphi(\tau_n) + \gamma_n\big) . \tag{2.3.25}$$

But this is again a negligible event due to the density assumption on the law of the jumps of $U_0(x)$. The proof is complete. □

2.3.5 Density of states – Ornstein-Uhlenbeck process

In this subsection we study of the density of the distribution (density of states, or DOS) $\rho(\eta, \xi)$ on the upper complex half-plane $\zeta = \xi + i\eta$, $\eta \geq 0$ of the eigenvalues for the ZSSP with

a rapidly oscillating random potential. This corresponds to the distribution of the velocity and amplitude of solitons of the NLS equation with random initial conditions. Given an initial condition with support on $[0, R]$, the DOS is defined as the average density of the eigenvalues of the ZSSP system par unit length of R. It is given by the limit

$$\rho(\zeta) = \lim_{R\to\infty} \frac{1}{R}\mathbb{E}\Big[\sum_{n=1}^{N} \delta\big(\zeta - \zeta_n(R)\big)\Big]\,,$$

where $\big(\zeta_n(R)\big)_{n=1\dots N}$ are the discrete eigenvalues of the ZSSP system when the initial condition is supported on $[0, R]$ and δ is the Dirac delta function. Remark that in this case we have to work with initial conditions which in the limit have support on the half-line $\mathbb{R}_+ = \{x \in \mathbb{R} \,|\, x \geq 0\}$. This is an essential difference with respect to the examples considered above, since now we first take the limit in R, and only then we take the limit in ε to account for rapidly oscillating initial conditions.

Explicit computations are developed for an initial condition given by a (rescaled and time accelerated) complex Ornstein-Uhlenbeck (OU) process, which can be seen as an approximation of a complex white noise. The case of an initial condition given by more general rapidly oscillating random process is considered in the next subsection. The main result is given by the following theorem. Recall that the hyperbolic cotangent function is given by $\coth(x) = 1/\tanh(x)$ and the hyperbolic cosecant by $\operatorname{csch}(x) = 1/\sinh(x)$.

Theorem 2.34. *When the initial condition is given by a rapidly oscillating Ornstein-Uhlenbeck process, the DOS $\rho(\eta, \xi)$ of the ZSSP associated to the NLS equation is smooth, and can be written as a power series expansion around the limit case of infinitely rapid oscillations. If ε is the parameter controlling the rapidity of oscillations, we have*

$$\rho(\eta, \xi) = \rho_0(\eta) + \varepsilon^2\rho_2(\eta) + o(\varepsilon^2)\,,$$

where

$$\rho_0(\eta) = \frac{1}{4\pi}\,\frac{\eta\,\coth\big(\eta/2\big) - 2}{\sinh^2\big(\eta/2\big)} \tag{2.3.26}$$

is the DOS corresponding to the limit case, the first order term is zero, and the second order term is given by

$$\rho_2(\eta) = \frac{1}{4\pi^2}\Big[\frac{\eta^2+8}{\eta^2}\operatorname{csch}^2\big(\eta/2\big) - \frac{\eta^2-8}{2\eta}\operatorname{csch}^2\big(\eta/2\big)\coth\big(\eta/2\big) + \frac{16}{\eta^3}\big[\coth\big(\eta/2\big) - 1\big]\Big]. \tag{2.3.27}$$

Remark 2.35. Using the formula presented in subsection 2.1.1 it is possible to compute the order of magnitude of the mass and energy introduced by the rapidly oscillating initial condition $U(x/\varepsilon^2)/\varepsilon$. For any fixed R, the input mass is of order ε^{-2}

$$N = \frac{1}{\varepsilon^2}\int_0^R \big|U(x/\varepsilon^2)\big|^2\,\mathrm{d}x \simeq R\varepsilon^{-2}$$

and the input energy is of order ε^{-6}

$$E = \int_0^R \frac{1}{\varepsilon^2}\big|\partial_x U(x/\varepsilon^2)\big|^2 - \frac{1}{\varepsilon^4}\big|U(x/\varepsilon^2)\big|^4\,\mathrm{d}x \simeq R\varepsilon^{-6}\,.$$

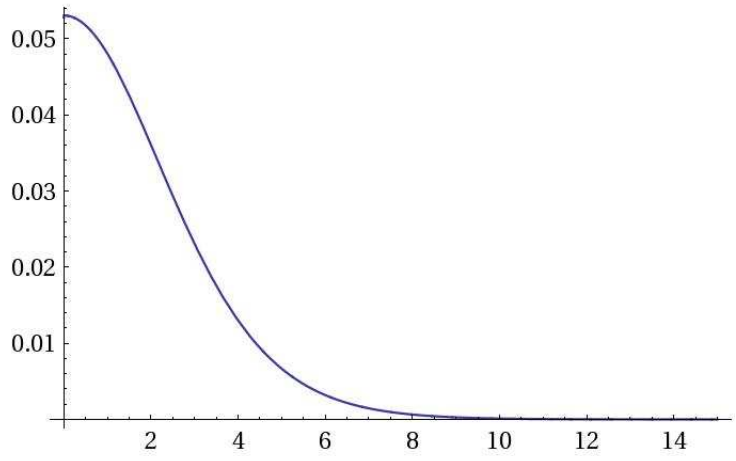

Figure 2.3: Plot of the DOS $\rho_0(\eta)$ at order zero (limit case of infinitely fast oscillations).

Remark 2.36. Using a rapidly oscillating complex OU process as initial condition for the NLS equation, the distribution of created solitons is uniform with respect to their speed (both in the limit case, and considering second order corrections). This result should not appear too surprising, since we can see from remark 2.35 that the input energy is much larger than the input mass.

Remark 2.37. In figure 2.4 is plotted the second order term $\rho_2(\eta)$ of the DOS. From the picture one can easily see that this second order term gives small-amplitude solitons a higher probability of being generated. This means that, comparing different fast-oscillating OU initial conditions, the slower the oscillations are, the easier it is to create solitons with very small amplitudes.

The proof of theorem 2.34 fills the rest of this subsection, and is divided into several steps. First, we present the general technique, for which we need the ergodicity result provided by propositions 2.38. Using this results we can obtain the DOS through the study of the Lyapunov exponent of the ZSSP system (recall that the initial condition has an infinite support) and a generalized Thouless formula. This is shown in lemma 2.41. Then, what is needed to complete the computations is just the invariant probability of some the variables $(U, \vec{\gamma})$, which will be introduced below. This invariant probability is obtained by solving a Fokker-Planck equation. However, the solution of the Fokker-Planck equation requires extensive computations, so that before performing them we shall present and explain the general scheme we want to apply.

The initial condition we consider for the example presented in this subsection is given by a (rescaled and time accelerated) complex Ornstein-Uhlenbeck (OU) process: $U_0 = U_1 + iU_2$. Here, U_1, U_2 are two independent real Ornstein-Uhlenbeck processes:

$$U_i(x) = U_i(0)e^{-x} + \sqrt{2}e^{-x}\int_0^x e^y \,\mathrm{d}W_y^{(i)}\,.$$

We will need to use the infinitesimal operator of the OU process, which is given by

$$\mathcal{L}_U = -u_1\partial_{u_1} - u_2\partial_{u_2} + \partial_{u_1}^2 + \partial_{u_2}^2\,.$$

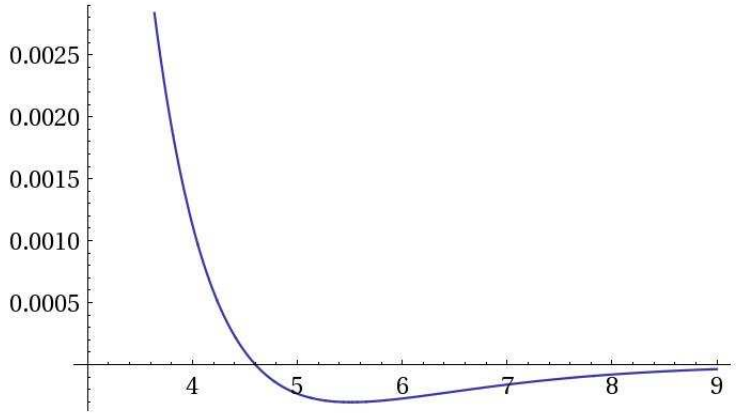

Figure 2.4: Plot of the second order correction term $\rho_2(\eta)$ of the DOS.

Its adjoint is

$$\mathcal{L}_U^* f = \partial_{u_1}\big(u_1 f\big) + \partial_{u_2}\big(u_2 f\big) + \big(\partial_{u_1}^2 + \partial_{u_2}^2\big) f\,. \tag{2.3.28}$$

To ease notation, in the sequel we will drop the subscript for the initial condition U_0.

An ergodicity result

To prove the next proposition we need to reformulate the ZSSP using linear algebra notations, and using $\mathbb{R}$ as base field. For the next few pages we will therefore use the embedding $\mathbb{C} \hookrightarrow \mathbb{R}^2$ for all complex variables. This means for example that we will consider Ψ as a vector of $\mathbb{R}^4$ instead of $\mathbb{C}^2$, transforming $\psi_1 = \Re_1 + i\Im_1$ into the vector $(\Re_1, \Im_1)$ and $\psi_2 = \Re_2 + i\Im_2$ into the vector $(\Re_2, \Im_2)$. With this notation, the ZSSP system can then be rewritten as

$$\partial_x \Psi = A(U)\Psi\,,$$

where

$$A(U) = i \begin{pmatrix} \eta & \xi & -U_2 & -U_1 \\ \xi & \eta & U_1 & -U_2 \\ U_2 & -U_1 & -\eta & \xi \\ U_1 & U_2 & \xi & -\eta \end{pmatrix}.$$

We shall also introduce polar coordinates in $\mathbb{R}^4$ to rewrite $\Psi = \rho\ \vec{\gamma}$, where $\rho = |\Psi| = \big(|\psi_1|^2 + |\psi_2|^2\big)^{1/2} \in \mathbb{R}$ and

$$\vec{\gamma} = \begin{pmatrix} \Re_1/|\Psi| \\ \Im_1/|\Psi| \\ \Re_2/|\Psi| \\ \Im_2/|\Psi| \end{pmatrix}$$

is a unitary vector in $\mathbb{R}^4$. We can now prove the following proposition

Proposition 2.38. *With the notation introduced above, the vector* $\big(U, \vec{\gamma}\,\big)$ *is ergodic.*

Proof. To prove the ergodicity of the vector $\big(\,\vec{\gamma}, U\,\big)$ we shall proceed as in [KA83], where ergodicity of linear systems of the kind of the ZSSP systems is studied in detail. By (2.1.3)

we obtain the evolution equations for ρ

$$\rho(x) = \rho(0) \exp\left(\int_0^x q\Big(U(y), \overrightarrow{\gamma}\ (y)\Big)\, \mathrm{d}y \right)$$

and for $\overrightarrow{\gamma}$

$$\partial_x\ \overrightarrow{\gamma} = h\Big(U(x), \overrightarrow{\gamma}\ (x)\Big)\,, \tag{2.3.29}$$

where, using matricial notations, $q : \mathbb{R}^2 \times \mathbb{R}^4 \to \mathbb{R}$ is defined by

$$q\big(U, \overrightarrow{\gamma}\ \big) = \overrightarrow{\gamma}^{\ T} A(U)\ \overrightarrow{\gamma} \tag{2.3.30}$$

and $h : \mathbb{R}^2 \times \mathbb{R}^4 \to \mathbb{R}^4$ is defined by

$$h\big(U, \overrightarrow{\gamma}\ \big) = \Big(A(U) - q\big(U, \overrightarrow{\gamma}\ \big) Id\Big)\ \overrightarrow{\gamma}\ .$$

Here, $\overrightarrow{\gamma}^{\ T}$ denotes the transposed of the vector $\overrightarrow{\gamma}$. By identifying $\overrightarrow{\gamma}$ and $-\overrightarrow{\gamma}$, the evolution equation (2.3.29) can be viewed as an equation on the projective space $\mathbb{P} = \mathbb{P}^3(\mathbb{R})$. Remark that this evolution equation is independent of ρ. We have that the infinitesimal operator of the OU process $\mathcal{L}_U$ is elliptic, U is an ergodic process and the matrix function $A(\cdot)$ is analytical. The couple $(U, \overrightarrow{\gamma})$ is a degenerate diffusion process with generator

$$\mathcal{L} = \mathcal{L}_U + h\, \partial_{\overrightarrow{\gamma}}\,.$$

To prove the ergodicity of $(U, \overrightarrow{\gamma})$ we have to show that the Lie algebra generated by the operator $\big(h(u,\cdot),\, u \in \mathbb{R}^2\big)(s)$, $s \in \mathbb{P}$ has dimension 3. In other words, we have to show that, starting from any point $s_0 \in \mathbb{P}$ and using suitable values $u^{(n)}$, $n = 1...N$, of the variable $u \in \mathbb{R}^2$, it is possible to reach any point $s_1 \in \mathbb{P}$ following the evolution prescribed by $s \mapsto h(u^{(n)}, s)$ in a finite number N of steps.

Remark that for any fixed $u \in \mathbb{R}^2$, $h(u,\cdot)$ is a vector field on $\mathbb{P}$, namely the projection of the linear vector field $A(u)x$, $x \in \mathbb{R}^4 \backslash \{0\}$ onto $\mathbb{P}$. We see that it is enough to show that the Lie algebra generated by $A(u)$, $u \in \mathbb{R}^2$ has dimension 4. To do so, we shall decompose $A(u)$ into a sum four matrices Σ_k, $k = 1...4$. Recall that we have $u = (u_1, u_2) \in \mathbb{R}^2$, and since we are using the embedding $\mathbb{C} \hookrightarrow \mathbb{R}^2$, $\zeta = (\xi, \eta) \in \mathbb{R}^2$.

$$A(u) = \Big\{ u_1\Sigma_1 + u_2\Sigma_2 + \eta\Sigma_3 + \xi\Sigma_4 \Big\}\,,$$

where

$$\Sigma_1 = \begin{pmatrix} 0 & 0 & 0 & -1 \\ 0 & 0 & 1 & 0 \\ 0 & -1 & 0 & 0 \\ 1 & 0 & 0 & 0 \end{pmatrix}, \quad \Sigma_2 = \begin{pmatrix} 0 & 0 & -1 & 0 \\ 0 & 0 & 0 & -1 \\ 1 & 0 & 0 & 0 \\ 0 & 1 & 0 & 0 \end{pmatrix},$$

$$\Sigma_3 = \begin{pmatrix} 1 & 0 & 0 & 0 \\ 0 & 1 & 0 & 0 \\ 0 & 0 & -1 & 0 \\ 0 & 0 & 0 & -1 \end{pmatrix}, \quad \Sigma_4 = \begin{pmatrix} 0 & 1 & 0 & 0 \\ -1 & 0 & 0 & 0 \\ 0 & 0 & 0 & -1 \\ 0 & 0 & 1 & 0 \end{pmatrix}.$$

The idea of this decomposition comes from the analysis of this problem on the complex field $\mathbb{C}$, which however cannot be implemented rigorously since we have to introduce the

projective space $\mathbb{P}$. The above matrices are obtained from the Pauli matrices σ_j, $j = 1...3$, using the matrix notation for complex numbers

$$i = \begin{pmatrix} 0 & -1 \\ 1 & 0 \end{pmatrix}$$

and the correspondences $\Sigma_1 = i\sigma_1$, $\Sigma_2 = -i\sigma_2$, $\Sigma_3 = \sigma_3$ and $\Sigma_4 = -i\sigma_3$. The computations presented from now on could be performed using this notation from linear algebra on the complex field $\mathbb{C}$, but we prefer to show them using the same notation used in the first part of the proof, namely working on the real field $\mathbb{R}$.

Remark that changing u our direct action is only on the first two matrices Σ_1 and Σ_2. If we take $u^{(1)}$ such that $u_1^{(1)} \gg 1$ and $u_2^{(1)} = 0$, we have that $A(u^{(1)}) \simeq \Sigma_1$. If instead we take $u^{(2)}$ such that $u_1^{(2)} = 0$ and $u_2^{(2)} \gg 1$, we get $A(u^{(2)}) \simeq \Sigma_2$. Also, explicit an computation shows that $A(u^{(1)})A(u^{(2)}) \simeq \Sigma_1\Sigma_2 = -\Sigma_4$ and $\left(\Sigma^4\right)^2 = -\mathbb{I}$, where $\mathbb{I}$ is the identity matrix in $\mathbb{R}^{4\times4}$. This shows that by choosing suitable values of u we can get arbitrarily good approximations of the four matrices Σ_1, Σ_2, $-\Sigma_4$ and $-\mathbb{I}$, which are linearly independent and generate a subspace of $\mathbb{R}^{4\times4}$ of dimension 4. Then, the projection on $\mathbb{P}$ produces a vector field $h(u,\cdot)$ generating a Lie algebra of dimension 3, which proves that the vector $(U, \vec{\gamma})$ is ergodic, [KA83]. □

Corollary 2.39. *By Hörmander's theorem, the operator $\mathcal{L}$ is hypoelliptic, so that the invariant probability measure associated to the vector $\left(U, \vec{\gamma}\ \right)$ admits a smooth density with respect to the Lebesgue measure.*

In view of this result, in the following we will allow ourselves to confound the invariant probability measure of $(U, \vec{\gamma})$ with its density, calling both of them $P(u,s)$, where $u \in \mathbb{R}^2$ and $s \in \mathbb{R}^4$ is a unitary vector.

Computing the DOS

Given the ergodicity of the couple $\left(U, \vec{\gamma}\ \right)$, we can use [KA83, theorem 4.1] to obtain the following result

Proposition 2.40. *The Lyapunov exponent of the ZSSP system is given by*

$$\kappa(\eta,\xi) = \int q(u,s)\,\mathrm{d}P(u,s)\,, \tag{2.3.31}$$

where $u \in \mathbb{R}^2$, $s \in \mathbb{R}^4$ is a unitary vector, $q(u,s) = s^T A(u)s$ is defined by (2.3.30) and $P(u,s)$ is the invariant probability measure of the couple $\left(U, \vec{\gamma}\ \right)$.

Once the Lyapunov exponent $\kappa(\eta,\xi)$ is known, one can recover the DOS through a generalized Thouless formula, as shown in [KM08].

Lemma 2.41. *The density $\rho(\eta,\xi)$ of the distribution of the eigenvalues of the ZSSP system with potential given by a complex Ornstein-Uhlenbeck process is given by*

$$\rho(\eta,\xi) = \frac{1}{2\pi}\left(\frac{\partial^2}{\partial\eta^2} + \frac{\partial^2}{\partial\xi^2}\right)\kappa(\eta,\xi)\,. \tag{2.3.32}$$

Combining the results of proposition 2.40 and lemma 2.41 we obtain an easy way to compute the DOS. The only missing element is the invariant probability P, whose density can be found solving

$$\mathcal{L}^* P(U,\gamma) = 0\,, \tag{2.3.33}$$

where

$$\mathcal{L}^* P = \mathcal{L}_U^* P - \partial_{\vec{\gamma}}\big(hP\big)\,.$$

It turns out that the computations to solve equation (2.3.31) are somewhat easier if we introduce some new variables. To do so, we shall momentarily leave the "real" notation introduced in the previous paragraph for the proof of proposition 2.38 and return to use the notation of complex variables $\Psi \in \mathbb{C}^2$, $U \in \mathbb{C}$. We shall also consider $\vec{\gamma} \in \mathbb{C}^2$ to be a unitary vector, which we will write as $\vec{\gamma} = (\gamma_1, \gamma_2)$. We can now define the two real variables $w \in (-\infty, \infty)$, $\varphi \in [0, 2\pi)$ as

$$\psi_1/\psi_2 = e^{w+i\varphi}\,.$$

We also set $v = \tanh(w)$, so that $v \in (-1, 1)$, and define $\theta \in [0, 2\pi)$ to be the argument of ψ_1/ψ_2^*.

The change of variables $\gamma \leftrightarrow (v, \varphi, \theta)$ can be described as follows. Remark that for any γ such that $\gamma_1 \neq 0$ and $\gamma_2 \neq 0$, one can find a unique corresponding vector (w, φ, θ) from the relations $\gamma_1/\gamma_2 = e^{w+i\varphi}$ and $\gamma_1/\gamma_2^* = e^{w+i\theta}$. The converse also holds, since

$$|\gamma_1| = \frac{|\psi_1|}{|\Psi|} = \frac{|\psi_1|/|\psi_2|}{\big(1 + |\psi_1|^2/|\psi_2|^2\big)^{1/2}} = \frac{e^w}{\big(1 + e^{2w}\big)^{1/2}}$$

and a similar expression can be found for $|\gamma_2|$. Moreover,

$$\theta - \varphi = \arg\big(\psi_2/\psi_2^*\big) = 2\arg(\gamma_2)\,,$$

which, together with the definition of θ, provides also $\arg(\gamma_1) = (\theta + \varphi)/2$.

In the new variables (v, φ, θ), the function q defined by (2.3.30) has a very simple form, which we shall now describe. To do so, we shall return to the real-variables notation introduced before the proof of proposition 2.38. We have that

$$A(U)\gamma = \frac{1}{|\Psi|}\partial_x \Psi = \frac{1}{|\Psi|}\partial_x \begin{pmatrix} \Re_1 \\ \Im_1 \\ \Re_2 \\ \Im_2 \end{pmatrix}$$

and (recall that V^T denotes the transposed of the vector V)

$$q(U,\gamma) = \gamma^T A(U)\gamma = \frac{1}{|\Psi|^2}\Psi^T \cdot \partial_x \Psi = \frac{1}{2|\Psi|^2}\,\partial_x |\Psi|^2 = \frac{1}{2}\partial_x \ln\big(|\Psi|^2\big)\,.$$

Rewriting this using the new variables (w, φ, θ) and using the relations given by the ZSSP system we get

$$q(U,\gamma) = \frac{1}{2}\partial_x \ln\big(|\Psi|^2\big) = \eta \tanh(w) = \eta\, v\,.$$

Therefore, the Lyapunov exponent can be rewritten in the new variables as

$$\kappa(\eta, \xi) = \eta \int v \,\mathrm{d}P(v, \varphi, \theta, U)\,. \tag{2.3.34}$$

We now have to find the form of the density of the invariant probability P, written in the new variables. This is done by finding the Fokker-Planck equation for $P(v, \varphi, \theta, U)$. The procedure to obtain the Fokker-Planck equation from the evolution equations for the new variables is detailed in the next two paragraphs. There, we will also introduce the rapidly oscillating initial conditions and finally describe the equation satisfied by the density of the stationary probability $P(v, \varphi, \theta, U)$ when U is a complex, rapidly oscillating OU process.

The Fokker-Planck equation

We return to use the complex-variable notation. When there is no risk of confusion, we will also omit to write the dependence on x. To obtain the evolution equations for the new variables (v, φ, θ) from the ZSSP system we shall introduce one more complex variable: $r(x) = \psi_1(x)/\psi_2(x) = e^{w(x)+i\varphi(x)}$. Remark that the function r defined here is the reciprocal of the function r introduced in the previous subsections. Moreover, r also depends on the spectral parameter ζ (through the Jost functions ψ_1 and ψ_2), for which we do not restrict to consider only real values $\zeta = \xi \in \mathbb{R}$, but rather work with any spectral parameter on the complex upper half-plane $\zeta = \xi + i\eta$, $\eta \geq 0$. Using this new variable, the ZSSP system (2.1.3) can be rewritten as

$$\frac{\mathrm{d}}{\mathrm{d}x} r(x) = iU - 2i\zeta r - iU^* r^2.$$

Since $\mathrm{d}r = r(\mathrm{d}w + i\mathrm{d}\varphi)$, we obtain the system governing the evolution of the variables w and φ

$$\begin{cases} \partial_x w(x) = 2\eta + \Im\Big[U^* e^{w+i\varphi} - U e^{-w-i\varphi}\Big] \\ \partial_x \varphi(x) = -2\xi - \Re\Big[U^* e^{w+i\varphi} - U e^{-w-i\varphi}\Big] \end{cases}.$$

With some easy algebraic manipulations this system can be rewritten as

$$\begin{cases} \partial_x w(x) = 2\eta + 2\Im\Big[U^* e^{i\varphi}\Big] \cosh(w) \\ \partial_x \varphi(x) = -2\xi - 2\Re\Big[U^* e^{i\varphi}\Big] \sinh(w) \end{cases}. \tag{2.3.35}$$

From the ZSSP system rewritten in the form (2.3.35) and using the adjoint of the generator of the OU process given by (2.3.28) we obtain the following Fokker-Planck equation for the density function of the joint probability $P(w, \varphi, u)$ of $\big(w(x), \varphi(x), U(x)\big)$

$$\begin{aligned} \partial_x P = &- 2\eta\, \partial_w P - 2\Im\big[u^* e^{i\varphi}\big] \partial_w \Big[\cosh(w)\, P\Big] \\ &+ 2\xi\, \partial_\varphi P + 2\sinh(w)\, \partial_\varphi \Big[\Re\big[u^* e^{i\varphi}\big] P\Big] \\ &+ \partial_{u_1}\big(u_1 P\big) + \partial_{u_2}\big(u_2 P\big) + \big(\partial^2_{u_1} + \partial^2_{u_2}\big) P\,. \end{aligned} \tag{2.3.36}$$

Remark that the vector (w, φ, U) already forms a Markov process. Therefore, considering the joint probability $P(w, \varphi, \theta, u)$ would produce a Fokker-Planck equation with an additional independent term, which we can disregard because θ does not appear explicitly in (2.3.34). Changing variables $v = \tanh(w)$ we can transform this equation into a Fokker-

Planck equation for the density of joint probability $P(v,\varphi,u)$ of $\big(v(x),\varphi(x),U(x)\big)$:

$$\begin{aligned}\partial_x P(v,\varphi,u) =& -2\eta\,\partial_v\Big[(1-v^2)P\Big] - 2\Im\big[u^* e^{i\varphi}\big]\partial_v\Big[\sqrt{1-v^2}P\Big]\\ &+ 2\xi\,\partial_\varphi P + 2\frac{v}{\sqrt{1-v^2}}\,\partial_\varphi\Big[\Re\big[u^* e^{i\varphi}\big]P\Big]\\ &+ \partial_{u_1}\big(u_1 P\big) + \partial_{u_2}\big(u_2 P\big) + \big(\partial_{u_1}^2+\partial_{u_2}^2\big)P\,.\end{aligned} \tag{2.3.37}$$

Rapidly oscillating initial conditions

Recall that the aim of this example is to obtain the distribution of the eigenvalues of the ZSSP for rapidly oscillating initial conditions. We therefore need to seep up time for the OU process $U_\varepsilon(t) = U(t/\varepsilon^2)$ and rescale it accordingly. The initial condition we will be working with is therefore $U_0 = \frac{1}{\varepsilon}U_\varepsilon$. By the result of corollary 2.39, the invariant probability P^ε of the couple $\big(U_\varepsilon/\varepsilon, \overrightarrow{\gamma}\,\big)$ has a density, which we also denote P^ε, solution of $\mathcal{L}_\varepsilon^* P^\varepsilon = 0$. The operator $\mathcal{L}_\varepsilon^*$ has a finite expansion in ε:

$$\mathcal{L}_\varepsilon^* = \frac{1}{\varepsilon^2}\mathcal{L}_U^* + \frac{1}{\varepsilon}\mathcal{L}_1^* + \mathcal{L}_2^*\,, \tag{2.3.38}$$

where

$$\begin{aligned}\mathcal{L}_U^* P^\varepsilon &= \partial_{u_1}\big(u_1 P^\varepsilon\big) + \partial_{u_2}\big(u_2 P^\varepsilon\big) + \big(\partial_{u_1}^2+\partial_{u_2}^2\big)P^\varepsilon\,,\\ \mathcal{L}_1^* P^\varepsilon &= -2\Im\left[u_\varepsilon^* e^{i\varphi_\varepsilon}\right]\partial_{v_\varepsilon}\left[\sqrt{1-v_\varepsilon^2}P^\varepsilon\right] + 2\frac{v_\varepsilon}{\sqrt{1-v_\varepsilon^2}}\,\partial_{\varphi_\varepsilon}\left[\Re\left[u_\varepsilon^*\, e^{i\varphi_\varepsilon}\right]P^\varepsilon\right]\\ &= -2\Im\left[u_\varepsilon^* e^{i\varphi_\varepsilon}\right]\sqrt{1-v_\varepsilon^2}\,\partial_{v_\varepsilon}P^\varepsilon + 2\frac{v_\varepsilon}{\sqrt{1-v_\varepsilon^2}}\Re\left[u_\varepsilon^*\, e^{i\varphi_\varepsilon}\right]\partial_{\varphi_\varepsilon}P^\varepsilon\,,\\ \mathcal{L}_2^* P^\varepsilon &= -2\eta\,\partial_{v_\varepsilon}\Big[(1-v_\varepsilon^2)P^\varepsilon\Big] + 2\xi\,\partial_{\varphi_\varepsilon}P^\varepsilon\,.\end{aligned}$$

The terms of this expansion can be found as follows. Using the rapidly oscillating initial condition described above, the system (2.3.35) becomes

$$\begin{cases}\partial_x w_\varepsilon = 2\eta + 2\cosh(w_\varepsilon)\Im\left[\frac{1}{\varepsilon}U_\varepsilon^*\, e^{i\varphi_\varepsilon}\right]\\ \partial_x\varphi_\varepsilon = -2\xi - 2\sinh(w_\varepsilon)\Re\left[\frac{1}{\varepsilon}U_\varepsilon^*\, e^{i\varphi_\varepsilon}\right]\end{cases} \tag{2.3.39}$$

and the Fokker-Planck equation

$$\partial_x P^\varepsilon = \frac{1}{\varepsilon^2}\mathcal{L}_U^* P^\varepsilon + \frac{1}{\varepsilon}\mathcal{L}_1^* P^\varepsilon + \mathcal{L}_2^* P^\varepsilon\,. \tag{2.3.40}$$

For the invariant probability measure, $\partial_x P^\varepsilon = 0$, and $\mathcal{L}_\varepsilon^* P^\varepsilon$ is given by the right hand side of (2.3.40).

We shall proceed as in [APW86] and assume that the density of the invariant probability P^ε solution of $\mathcal{L}_\varepsilon^* P^\varepsilon = 0$ can be formally rewritten using a power series expansion in ε around the limit case of infinitely rapid oscillations:

$$P^\varepsilon(v,\varphi,u) = \sum_{n\geq 0}\varepsilon^n P_n\,. \tag{2.3.41}$$

The first term of this expansion, P_0, is the invariant probability corresponding to the limit problem for infinitely rapid oscillations. It formally corresponds to a white noise initial

condition for the NLS equation (recall that with a white noise as initial condition one is not allowed to apply the IST and therefore one cannot obtain the ZSSP system). The DOS for the NLS equation with a white noise initial condition has been obtained in [KM08] working directly on the stochastic process v without introducing the process $\big(U, \vec{\gamma}\ \big)$, and (formally) assuming that (v, U) is ergodic. Their strategy is based on the use of the Thouless formula of lemma 2.41, the representation of the Lyapunov exponent given by (2.3.34) and the Fokker-Planck equation (2.3.37).

Our approach consist in taking an initial condition U_0 with fast, but not infinitely fast, oscillations and to express the invariant probability $P^\varepsilon(v, \varphi, u)$ as a power series development around the limit case, (2.3.41). This in turn will provide an expression for the DOS given by a power series. The first term we find, ρ_0, is therefore in accordance with the result of [KM08]. But we are also interested in finding the correction terms P_1 and P_2 for the invariant probability and the corresponding correction terms ρ_1 and ρ_2 for the DOS.

Looking at (2.3.34) one remarks that the full joint probability measure P^ε is not really necessary: what is needed is actually only $\bar{P}^\varepsilon(v) = \int_{\mathbb{R}^2} \int_0^{2\pi} P^\varepsilon(v, \varphi, u)\, \mathrm{d}\varphi\, \mathrm{d}u$.

The general scheme to find the invariant probability P^ε

Since the computations needed to find the correction terms are somewhat cumbersome, we sketch here the general strategy we will use. Further details on the perturbation approach and the solution of the Fokker-Planck equation can be found for example in [FGPS]. To ease notation we will drop the superscript ε.

Applying the operator $\mathcal{L}_\varepsilon^*$ defined by (2.3.38) to the power series representation of P (2.3.41) and separating scales according to the power of ε, we obtain an infinite system of coupled equations. Setting $P_n = 0$ for $n < 0$, the equation at order n for $n \geq -2$ reads

$$\varepsilon^n \Big[\mathcal{L}_2^* P_n + \mathcal{L}_1^* P_{n+1} + \mathcal{L}_U^* P_{n+2} \Big] = 0\,. \tag{2.3.42}$$

We set $g = \mathcal{L}_2^* P_n + \mathcal{L}_1^* P_{n+1}$. Due to the form of the operator $\mathcal{L}_U$ and of its adjoint, which can be rewritten as

$$\begin{aligned} \mathcal{L}_U f &= \frac{1}{2} e^{\frac{u_1^2}{2}} \partial_{u_1} e^{\frac{-u_1^2}{2}} \partial_{u_1} f + \frac{1}{2} e^{\frac{u_2^2}{2}} \partial_{u_2} e^{\frac{-u_2^2}{2}} \partial_{u_2} f\,, \\ \mathcal{L}_U^* f &= \frac{1}{2} \partial_{u_1} e^{\frac{-u_1^2}{2}} \partial_{u_1} e^{\frac{u_1^2}{2}} f + \frac{1}{2} \partial_{u_2} e^{\frac{-u_2^2}{2}} \partial_{u_2} e^{\frac{u_2^2}{2}} f\,, \end{aligned}$$

the equation $\mathcal{L}_U^* P_{n+2} = -g$ is equivalent to

$$\mathcal{L}_U \widetilde{P}_{n+2} = -\widetilde{g}\,, \tag{2.3.43}$$

where $\widetilde{P}_{n+2} = e^{|u|^2/2} P_{n+2}$ and $\widetilde{g} = e^{|u|^2/2} g$. This is a Poisson equation in the u variable, and its solvability condition is that $\widetilde{g}$ must be centered with respect to the invariant measure of U, [FGPS], which is to say that for every (v, φ) we must have

$$\mathbb{E}\big[\,\widetilde{g}\,\big] = \frac{1}{2\pi} \int_{\mathbb{R}^2} \Big[e^{\frac{|u|^2}{2}}\, g \Big]\, e^{-\frac{|u|^2}{2}}\ \mathrm{d}u = \frac{1}{2\pi} \int_{\mathbb{R}^2} \mathcal{L}_2^* P_n + \mathcal{L}_1^* P_{n+1}\ \mathrm{d}u = 0\,. \tag{2.3.44}$$

In the explicit computations of the following paragraphs we will drop the constant factor $1/2\pi$ of the above equation, and still call it the solvability condition for the Poisson problem. Once we have proved that the solvability condition (2.3.44) is verified, we can use the

following formula to solve the Poisson equation (2.3.43)

$$\widetilde{P}_{n+2}(u) = \frac{1}{2\pi} f_{n+2} + \int_0^\infty \mathbb{E}\Big[\widetilde{g}\big(U(x)\big) \,\Big|\, U(0) = u\Big]\, \mathrm{d}x\,.$$

Here, f_{n+2} is a function of (v, φ), but is constant in u. This equation provides information on P_{n+2} which will be used later: together with information from equations obtained at lower orders, the compatibility condition at order n allows to completely determine P_n.

Explicit computations: order -2

We have seen how the general procedure works. We shall now apply it to explicit the computations for our example. The first equation we need to solve is

$$0 = \mathcal{L}_U^* P_0\,,$$

which ensures that in (2.3.40) there is no term diverging as ε^{-2}. The solution is found to be

$$P_0(v, \varphi, u) = \frac{1}{2\pi} e^{-\frac{|u|^2}{2}} f_0(v, \varphi)\,,$$

for some function f_0 which will be determined below by the solvability condition of the equation at order zero.

Explicit computations: order -1

The second equation is

$$0 = \mathcal{L}_U^* P_1 + \mathcal{L}_1^* P_0\,. \tag{2.3.45}$$

We set $g := \mathcal{L}_1^* P_0$, and transform (2.3.45) into the Poisson equation

$$\mathcal{L}_U \widetilde{P}_1 = -\widetilde{g}\,, \tag{2.3.46}$$

where $\widetilde{P}_1 = e^{\frac{|u|^2}{2}} P_1$ and $\widetilde{g} = e^{\frac{|u|^2}{2}} g$, as explained in the paragraph describing the general scheme. The solvability condition is

$$\int_{\mathbb{R}^2} \mathcal{L}_1^* P_0 \,\mathrm{d}u = 0\,. \tag{2.3.47}$$

Using the explicit form of $\mathcal{L}_1^* P_0$ we can easily see that it is always verified because, since

$$\mathcal{L}_1^* P_0 = \frac{1}{\pi} e^{-\frac{|u|^2}{2}} \left[-\Im\left[u^*\, e^{i\varphi}\right] \sqrt{1 - v^2}\, \partial_v f_0 + \frac{v}{\sqrt{1 - v^2}} \Re\left[u^*\, e^{i\varphi}\right] \partial_\varphi f_0 \right]$$

is an odd function of u_1 and u_2, the integral on $\mathbb{R}^2$ is zero. Condition (2.3.47) being verified, we can solve (2.3.46) to find a first expression for P_1:

$$P_1(v, \varphi, u) = \frac{1}{2\pi}\, e^{-\frac{|u|^2}{2}} \left[\int_0^\infty \mathbb{E}\Big[\mathcal{L}_1^*\big(U(x)\big) f_0 \,\Big|\, U(0) = u\Big] \mathrm{d}x + f_1 \right]. \tag{2.3.48}$$

Explicit computations: order 0

We now need to solve the "order zero" equation, which reads

$$0 = \mathcal{L}_U^* P_2 + \mathcal{L}_1^* P_1 + \mathcal{L}_2^* P_0 \,. \tag{2.3.49}$$

We look first at the solvability condition for this equation, which is

$$\int_{\mathbb{R}^2} \mathcal{L}_1^* P_1 + \mathcal{L}_2^* P_0 \, \mathrm{d}u = 0 \,. \tag{2.3.50}$$

We already know that

$$\mathcal{L}_2^* P_0 = \frac{1}{2\pi}\, e^{-u_1^2/2} e^{-u_2^2/2} \Big[-2\eta\, \partial_v \Big[(1-v^2) f \Big] + 2\xi\, \partial_\varphi f_0 \Big] = \frac{1}{2\pi}\, e^{-\frac{|u|^2}{2}}\, \mathcal{L}_2^* f_0$$

and

$$\begin{aligned}
\mathcal{L}_1^* P_1 &= \frac{1}{2\pi}\, \mathcal{L}_1^*(u)\, e^{-\frac{|u|^2}{2}} \Big[\int_0^\infty \mathbb{E}\Big[\mathcal{L}_1^*\big(U(x)\big) f_0 \,\Big|\, U(0) = u \Big] \mathrm{d}x + f_1 \Big] \\
&= \frac{1}{\pi} e^{-\frac{|u|^2}{2}} \Big[\int_0^\infty 2 \Big\{ -\Im[u^*\, e^{i\varphi}] \sqrt{1-v^2}\, \partial_v + \frac{v}{\sqrt{1-v^2}} \Re[u^*\, e^{i\varphi}]\, \partial_\varphi \Big\} \times \\
&\qquad \times \Big\{ -\Im\big[U^*(x)\, e^{i\varphi}\big] \sqrt{1-v^2}\, \partial_v + \frac{v}{\sqrt{1-v^2}} \Re\big[U^*(x)\, e^{i\varphi}\big]\, \partial_\varphi \Big\} \big(f_0\big)\, \mathrm{d}x \\
&\qquad + \Big\{ -\Im[u^*\, e^{i\varphi}] \sqrt{1-v^2}\, \partial_v + \frac{v}{\sqrt{1-v^2}} \Re[u^*\, e^{i\varphi}]\, \partial_\varphi \Big\} (f_1) \Big] \\
&= \frac{2}{\pi}\, e^{-\frac{|u|^2}{2}} \int_0^\infty \Big[\Im[u^*\, e^{i\varphi}] \Im\big[U^*(x)\, e^{i\varphi}\big] \Big(-v\, \partial_v f_0 + (1-v^2)\, \partial_v^2 f_0 \Big) \\
&\qquad - \Im[u^*\, e^{i\varphi}] \Re\big[U^*(x)\, e^{i\varphi}\big] \Big(\frac{1}{1-v^2}\, \partial_\varphi f_0 + v\, \partial_\varphi\, \partial_v f_0 \Big) \\
&\qquad - \Re[u^*\, e^{i\varphi}] \Im\big[U^*(x)\, e^{i\varphi}\big] \Big(v\, \partial_\varphi\, \partial_v f_0 + \frac{v^2}{1-v^2}\, \partial_\varphi f_0 \Big) \\
&\qquad - \Re[u^*\, e^{i\varphi}] \Re\big[U^*(x)\, e^{i\varphi}\big] \Big(v\, \partial_v f_0 - \frac{v^2}{1-v^2}\, \partial_\varphi^2 f_0 \Big) \Big]\, \mathrm{d}x \\
&\quad + \frac{1}{\pi} e^{-\frac{|u|^2}{2}} \Big\{ -\Im[u^*\, e^{i\varphi}] \sqrt{1-v^2}\, \partial_v f_1 + \frac{v}{\sqrt{1-v^2}} \Re[u^*\, e^{i\varphi}]\, \partial_\varphi f_1 \Big\} \,.
\end{aligned} \tag{2.3.51}$$

We try to simplify the above equation. To ease notation, we shall drop the dependence on x in U. Note that

$$\begin{aligned}
\Im[u^*\, e^{i\varphi}] \Im[U^*\, e^{i\varphi}] &= u_1 U_1 \sin^2(\varphi) + u_2 U_2 \cos^2(\varphi) - \Big(u_1 U_2 + u_2 U_1 \Big) \sin(\varphi) \cos(\varphi) \,; \\
\Im[u^*\, e^{i\varphi}] \Re[U^*\, e^{i\varphi}] &= u_1 U_2 \sin^2(\varphi) - u_2 U_1 \cos^2(\varphi) + \Big(u_1 U_1 - u_2 U_2 \Big) \sin(\varphi) \cos(\varphi) \,; \\
\Re[u^*\, e^{i\varphi}] \Im[U^*\, e^{i\varphi}] &= u_2 U_1 \sin^2(\varphi) - u_1 U_2 \cos^2(\varphi) + \Big(u_1 U_1 - u_2 U_2 \Big) \sin(\varphi) \cos(\varphi) \,; \\
\Re[u^*\, e^{i\varphi}] \Re[U^*\, e^{i\varphi}] &= u_2 U_2 \sin^2(\varphi) + u_1 U_1 \cos^2(\varphi) + \Big(u_1 U_2 + u_2 U_1 \Big) \sin(\varphi) \cos(\varphi) \,.
\end{aligned}$$

When $i \neq j$, u_i and U_j are independent, so that $\mathbb{E}\big[u_i U_j\big] = 0$. Also, $\mathbb{E}\big[u_i U_i\big] = e^{-x}$ and $\mathbb{E}\Big[\int_0^\infty \mathbb{E}\big[U(0)U(x)\big|U(0)=u\big]\mathrm{d}x\Big] = 1$. Therefore,

$$\begin{aligned}\mathbb{E}\Big[\mathcal{L}_1^*(u)\int_0^\infty \mathbb{E}\Big[\mathcal{L}_1^*\big(U(x)\big)f_0\,\Big|\,U(0)=u\Big]\mathrm{d}x\Big] &= \mathbb{E}\Big[\int_0^\infty \mathbb{E}\Big[\mathcal{L}_1^*\big(U(0)\big)\mathcal{L}_1^*\big(U(x)\big)f_0\,\Big|\,U(0)=u\Big]\mathrm{d}x\Big]\\ &= 4\Big[-2v\,\partial_v f_0 + (1-v^2)\,\partial_v^2 f_0 + \frac{v^2}{1-v^2}\,\partial_\varphi^2 f_0\Big]\\ &= 4\Big[\partial_v\Big((1-v^2)\,\partial_v f_0\Big) + \frac{v^2}{1-v^2}\,\partial_\varphi^2 f_0\Big]\,.\end{aligned}$$

With these results, the compatibility condition (2.3.50) can be rewritten as

$$0 = \mathbb{E}\Big[\mathcal{L}_2^* f_0 + \mathcal{L}_1^*(u)\int_0^\infty \mathbb{E}\Big[\mathcal{L}_1^*\big(U(x)\big)f_0\,\Big|\,U(0)=u\Big]\mathrm{d}x + \mathcal{L}_1^*(u) f_1\Big] = \mathscr{L} f_0\,, \tag{2.3.52}$$

where

$$\begin{aligned}\mathscr{L} f &= \mathbb{E}\Big[\mathcal{L}_2^* f + \int_0^\infty \mathcal{L}_1^*\big(U(0)\big)\mathcal{L}_1^*\big(U(y)\big) f\,\mathrm{d}y\Big]\\ &= -2\eta\,\partial_v\Big((1-v^2)f\Big) + 2\xi\,\partial_\varphi f + 4\,\partial_v\Big((1-v^2)\,\partial_v f\Big) + 4\frac{v^2}{1-v^2}\,\partial_\varphi^2 f\,.\end{aligned} \tag{2.3.53}$$

The term $\mathcal{L}_1^* f_1$ in the first line of (2.3.52) is an odd function of u, so that its expected value is zero. The solution can be found setting $f_0 = g_0(v)/2\pi$: since the function g_0 needs to satisfy $\int_{-1}^1 g_0(v)\,\mathrm{d}v = 1$ and

$$\partial_v\Big[\eta/2\,(1-v^2) f_0\Big] = \partial_v\Big[(1-v^2)\,\partial_v f_0\Big]\,,$$

we get $g_0(v) = k e^{cv}$ for $k = \frac{c}{2\sinh(c)}$ and $c = \eta/2$. Therefore

$$P_0(v,\varphi,u) = \frac{1}{4\pi^2} k\, e^{cv} e^{-\frac{u^2}{2}}\,. \tag{2.3.54}$$

Since f_0 only depends on v, we can simplify (2.3.48), the expression of P_1 we have found solving the "order -1" equation. We get

$$P_1 = \frac{1}{2\pi} e^{-\frac{u^2}{2}}\left\{ f_1 - 2c\sqrt{1-v^2} f_0 \int_0^\infty \mathbb{E}\Big[\Im\big[U^*(x)\,e^{i\varphi}\big]\,\Big|\,U(0)=u\Big]\mathrm{d}x\right\},$$

and we also obtain that $\bar{P}_1(v) = \int_{\mathbb{R}^2}\int_0^{2\pi} P_1\,\mathrm{d}\varphi\,\mathrm{d}u = \int_0^{2\pi} f_1\,\mathrm{d}\varphi$. We can now return to the order zero equation, (2.3.49). Looking at it as a Poisson equation in the u variable provides

the solution

$$\begin{aligned}P_2 =&\frac{1}{2\pi}e^{-\frac{|u|^2}{2}}\Bigg\{f_2+\int_0^\infty \mathbb{E}\Big[\mathcal{L}_2^* f_0+\mathcal{L}_1^*\big(V(y)\big)f_1\\ &\qquad+\mathcal{L}_1^*\big(V(y)\big)\int_0^\infty \mathbb{E}\Big[\mathcal{L}_1^*\big(U(x)\big)f_0\,\Big|\,U(0)=V(y)\Big]\mathrm{d}x\,\Big|\,V(0)=u\Big]\mathrm{d}y\Bigg\}\\ =&\frac{1}{2\pi}e^{-\frac{|u|^2}{2}}\Bigg\{f_2+\int_0^\infty \mathbb{E}\Big[\mathcal{L}_2^* f_0+\mathcal{L}_1^*\big(U(y)\big)f_1\\ &\qquad+\int_0^\infty\Big(\mathcal{L}_1^*\big(U(y)\big)\mathcal{L}_1^*\big(U(x+y)\big)f_0\Big)\mathrm{d}x\,\Big|\,U(0)=u\Big]\mathrm{d}y\Bigg\},\end{aligned}$$

where V is an independent copy of the complex OU process U. We remark that the above equation may at first sight seem to present some problems, as we are integrating in $\mathrm{d}y$ on an infinite domain the term $\mathcal{L}_2^* f_0$, which does not depend on y. However, it turns out that this term partially simplifies with the last one, leaving only a centered term. This follows from equation (2.3.52). We will show this in detail below, when solving the "order 2" equation.

Finding the density of states at order zero: ρ_0

Now that we have completely determined the first term of the expansion of the invariant probability, P_0, we can use lemma 2.41 to compute the first term of the development of the DOS.

Integrating over u and φ, we get

$$\bar{P}_0(v)=\int_0^{2\pi}\int_{\mathbb{R}^2} P_0(v,\varphi,u)\,\mathrm{d}u\,\mathrm{d}\varphi = g_0(v)=ke^{cv}.$$

Using (2.3.34) we obtain the Lyapunov exponent at order zero:

$$\kappa(\eta,\xi)=\eta\int_{-1}^{1} v\,\bar{P}_0(v)\,\mathrm{d}v=\eta\coth(\eta/2)-2\,.$$

Remark that for large $|\eta|$, $\kappa\sim|\eta|$ ($\coth\to\pm1$). From the Thouless formula (2.3.32) we get the density of eigenstates at order zero:

$$\rho_0(\eta,\xi)=\frac{1}{2\pi}\Big(\partial_\eta^2+\partial_\xi^2\Big)\kappa(\eta,\xi)=\frac{1}{2\pi}\,\frac{c\coth(c)-1}{\sinh^2(c)}\,. \tag{2.3.55}$$

This proves (2.3.26) of theorem 2.34 and is in accordance with the result obtained in [KM08]. Since $c=\eta/2$, at order zero the density is independent of ξ, which means that in the limit one finds the probability of creating a new soliton to be independent of its velocity, see remark 2.36 below.

Figure 2.3 above provides a plot of $\rho_0(\eta)$ (recall that $\eta\geq 0$).

Explicit computations: order 1 - $\rho_1=0$

Let us turn to the following order equation, which reads

$$0=\mathcal{L}_U^* P_3+\mathcal{L}_1^* P_2+\mathcal{L}_2^* P_1\,. \tag{2.3.56}$$

We first need to look at the solvability condition

$$\int_{\mathbb{R}^2} \mathcal{L}_1^* P_2 + \mathcal{L}_2^* P_1 \,\mathrm{d}u = 0\,, \tag{2.3.57}$$

using which we want to completely determine P_1. From the above results we have

$$\begin{aligned}
\mathcal{L}_2^* P_1 =& \frac{1}{2\pi} e^{-\frac{|u|^2}{2}} \left\{ \mathcal{L}_2^* f_1 + \mathcal{L}_2^* \int_0^\infty \mathbb{E}\Big[\mathcal{L}_1^*\big(U(x)\big) f_0 \,\Big|\, U(0) = u \Big] \mathrm{d}x \right\} \\
=& \frac{1}{2\pi} e^{-\frac{|u|^2}{2}} \left\{ \mathcal{L}_2^* f_1 + \mathcal{L}_2^* \Big[-2c\sqrt{1-v^2} f_0 \int_0^\infty \mathbb{E}\Big[\Im\big[U^*(x)\, e^{i\varphi}\big] \,\Big|\, U(0) = u \Big] \mathrm{d}x \right\}; \\
\mathcal{L}_1^* P_2 =& \frac{1}{2\pi} e^{-\frac{|u|^2}{2}} \left\{ \mathcal{L}_1^*(u) f_2 + \mathcal{L}_1^*(u) \int_0^\infty \mathbb{E}\Big[\mathcal{L}_2^* f_0 + \mathcal{L}_1^*\big(U(y)\big) f_1 \right. \\
& \left. + \int_0^\infty \Big(\mathcal{L}_1^*\big(U(y)\big) \mathcal{L}_1^*\big(U(x+y)\big) f_0 \Big) \mathrm{d}x \,\Big|\, U(0) = u \Big] \mathrm{d}y \right\}.
\end{aligned}$$

Since in the integral (2.3.57) all terms with a odd power of u do not contribute, we do not need to track them. Remark that $\mathcal{L}_1^*$ is linear in u and $\mathcal{L}_2^*$ is independent of u, so that for the solvability condition (2.3.57) we only need to consider the terms where $\mathcal{L}_1^*$ appears twice or does not appear at all. The solvability condition is therefore

$$\mathscr{L} f_1 = 0\,, \tag{2.3.58}$$

where the operator $\mathscr{L}$ is defined as in (2.3.53). This time we have the constraint

$$\int_{-1}^1 \int_0^{2\pi} f_1 \,\mathrm{d}\varphi \,\mathrm{d}v = 0\,,$$

which gives $f_1 = 0$. It follows that $\bar{P}_1(v) = 0$ and the first order correction term to the density of states is zero. We must look for the second order term. Solving the Poisson equation (2.3.56), we get

$$\begin{aligned}
P_3 =& \frac{1}{2\pi} e^{-\frac{|u|^2}{2}} \left\{ f_3 + \int_0^\infty \mathbb{E}\Big[\mathcal{L}_1^*\big(U(z)\big) f_2 + \int_0^\infty \mathcal{L}_2^* \mathcal{L}_1^*\big(U(x+z)\big) f_0 \,\mathrm{d}x \right. \\
& + \int_0^\infty \Big(\mathcal{L}_1^*\big(U(z)\big) \mathcal{L}_2^* f_0 \\
& \left. \left. + \int_0^\infty \mathcal{L}_1^*\big(U(z)\big) \mathcal{L}_1^*\big(U(y+z)\big) \mathcal{L}_1^*\big(U(x+y+z)\big) f_0 \,\mathrm{d}x \Big) \mathrm{d}y \,\Big|\, U(0) = u \Big] \mathrm{d}z \right\}.
\end{aligned}$$

Explicit computations: order 2

The "order 2" equation reads

$$0 = \mathcal{L}_U^* P_4 + \mathcal{L}_1^* P_3 + \mathcal{L}_2^* P_2\,. \tag{2.3.59}$$

Since we are only interested in finding the second order correction term for the DOS, we only need to find P_2. This means that we do not really have to solve this equation, we are

only interested in its solvability condition:

$$\int_{\mathbb{R}^2} \mathcal{L}_1^* P_3 + \mathcal{L}_2^* P_2 \, \mathrm{d}u = 0 \,, \tag{2.3.60}$$

where using the results of the previous steps we can write

$$\mathcal{L}_2^* P_2 = \frac{1}{2\pi} e^{-\frac{|u|^2}{2}} \Big\{ \mathcal{L}_2^* f_2 + \int_0^\infty \mathbb{E}\Big[\mathcal{L}_2^* \mathcal{L}_2^* f_0 + \int_0^\infty \mathcal{L}_2^* \mathcal{L}_1^*\big(U(y)\big) \mathcal{L}_1^*\big(U(x+y)\big) f_0 \mathrm{d}x \,\Big|\, U(0) = u \Big] \mathrm{d}y \Big\} \,;$$

$$\begin{aligned} \mathcal{L}_1^* P_3 = \frac{1}{2\pi} e^{-\frac{|u|^2}{2}} \Big\{ & \mathcal{L}_1^*(u) f_3 + \mathcal{L}_1^*(u) \int_0^\infty \mathbb{E}\Big[\mathcal{L}_1^*\big(U(z)\big) f_2 + \int_0^\infty \mathcal{L}_2^* \mathcal{L}_1^*\big(U(x+z)\big) f_0 \, \mathrm{d}x \\ & + \int_0^\infty \Big(\mathcal{L}_1^*\big(U(z)\big) \mathcal{L}_2^* f_0 \\ & + \int_0^\infty \mathcal{L}_1^*\big(U(z)\big) \mathcal{L}_1^*\big(U(y+z)\big) \mathcal{L}_1^*\big(U(x+y+z)\big) f_0 \, \mathrm{d}x \Big) \mathrm{d}y \,\Big|\, U(0) = u \Big] \mathrm{d}z \Big\} \,. \end{aligned}$$

Again, we can disregard the terms where $\mathcal{L}_1^*$ appears an odd number of times, since they do not contribute to the integral (2.3.60). Therefore the solvability condition becomes

$$\begin{aligned} 0 = \mathbb{E}\Big[& \mathcal{L}_2^* f_2 + \int_0^\infty \Big\{ \mathcal{L}_2^* \mathcal{L}_2^* f_0 + \int_0^\infty \mathcal{L}_2^* \mathcal{L}_1^*\big(U(z)\big) \mathcal{L}_1^*\big(U(x+z)\big) f_0 \, \mathrm{d}x \\ & + \mathcal{L}_1^*\big(U(0)\big) \mathcal{L}_1^*\big(U(z)\big) f_2 + \int_0^\infty \mathcal{L}_1^*\big(U(0)\big) \mathcal{L}_2^* \mathcal{L}_1^*\big(U(x+z)\big) f_0 \, \mathrm{d}x \\ & + \int_0^\infty \mathcal{L}_1^*\big(U(0)\big) \mathcal{L}_1^*\big(U(z)\big) \Big[\mathcal{L}_2^* f_0 + \int_0^\infty \mathcal{L}_1^*\big(U(y+z)\big) \mathcal{L}_1^*\big(U(x+y+z)\big) f_0 \mathrm{d}x \Big] \mathrm{d}y \Big\} \, \mathrm{d}z \Big] \,. \end{aligned}$$

The part of the above equation which contains f_2 is exactly (2.3.53). We analyze the parts containing f_0. Due to (2.3.52), the first two terms simplify. We are left with three terms to study, the last three on the right hand side:

$$\begin{aligned} \mathcal{I}_1 &= \iint_0^\infty \mathcal{L}_1^*\big(U(0)\big) \mathcal{L}_2^* \mathcal{L}_1^*\big(U(x+z)\big) f_0 \, \mathrm{d}x \, \mathrm{d}z \,. \\ \mathcal{I}_2 &= \iint_0^\infty \mathcal{L}_1^*\big(U(0)\big) \mathcal{L}_1^*\big(U(z)\big) \mathcal{L}_2^* f_0 \, \mathrm{d}y \, \mathrm{d}z \,. \\ \mathcal{I}_3 &= \iiint_0^\infty \mathcal{L}_1^*\big(U(0)\big) \mathcal{L}_1^*\big(U(z)\big) \mathcal{L}_1^*\big(U(y+z)\big) \mathcal{L}_1^*\big(U(x+y+z)\big) f_0 \, \mathrm{d}x \, \mathrm{d}y \, \mathrm{d}z \,. \end{aligned}$$

We can rewrite the solvability condition as

$$\mathscr{L} f_2 = -F \,, \tag{2.3.61}$$

where $F = \mathbb{E}\big[\mathcal{I}_1 + \mathcal{I}_2 + \mathcal{I}_3\big]$ and the operator $\mathscr{L}$ is defined by (2.3.53). We have to analyze the three terms $\mathcal{I}_n$, $n = 1, 2, 3$; we start from the first one. Since f_0 only depends on v,

$$\mathcal{L}_1^*\big(U(x+z)\big) f_0 = -2\Im\big[U^*(x+z)e^{i\varphi}\big]\sqrt{1-v^2}\,\partial_v f_0\,.$$

We shall introduce some more compact notation. All the terms like $\Re\big[U^*(x)e^{i\varphi}\big]$ will be denoted by $\Re_x$, and the same for the imaginary parts. We also have that $\partial_\varphi \Re_x = -\Im_x$ and $\partial_\varphi \Im_x = \Re_x$. Then,

$$\begin{aligned}
&\mathcal{L}_1^*\big(U(0)\big)\mathcal{L}_2^*\mathcal{L}_1^*\big(U(x+z)\big) f_0 \\
&= 4\mathcal{L}_1^*\big(U(0)\big)\Big\{\eta\,\Im_{x+z}\,\partial_v\Big[(1-v^2)^{3/2}\,\partial_v f_0\Big] - \xi\,\Re_{x+z}\sqrt{1-v^2}\,\partial_v f_0\Big\} \\
&= 8\Big\{ -\eta\,\Im_0\Im_{x+z}\sqrt{1-v^2}\,\partial_v^2\Big[(1-v^2)^{3/2}\,\partial_v f_0\Big] + \xi\,\Im_0\Re_{x+z}\sqrt{1-v^2}\,\partial_v\Big[\sqrt{1-v^2}\,\partial_v f_0\big)\Big] \\
&\qquad + \eta\,\Re_0\Re_{x+z}\frac{v}{\sqrt{1-v^2}}\,\partial_v\Big[(1-v^2)^{3/2}\partial_v f_0\Big] + \xi\,\Re_0\Im_{x+z} v\,\partial_v f_0\Big\}\,.
\end{aligned}$$

Proceeding as we did when dealing with the equation at order zero, we see that the terms containing $\Im\Re$ or $\Re\Im$ are centered, so that taking the expected value of $\mathcal{I}_1$ we are left with just

$$\begin{aligned}
\mathbb{E}\big[\mathcal{I}_1\big] &= 8\iint_0^\infty e^{-(x+z)}\,\mathrm{d}x\,\mathrm{d}z\,\Big\{ -\eta\sqrt{1-v^2}\,\partial_v^2\Big[(1-v^2)^{3/2}\,\partial_v f_0\Big] \\
&\qquad\qquad + \eta\frac{v}{\sqrt{1-v^2}}\,\partial_v\Big[(1-v^2)^{3/2}\,\partial_v f_0\Big]\Big\} \\
&= 16c\Big\{ -\sqrt{1-v^2}\,\partial_v^2\Big[(1-v^2)^{3/2}\,\partial_v f_0\Big] + \frac{v}{\sqrt{1-v^2}}\,\partial_v\Big[(1-v^2)^{3/2}\,\partial_v f_0\Big]\Big\}.
\end{aligned} \tag{2.3.62}$$

Let us consider $\mathcal{I}_2$. Since $\mathcal{L}_2^* f_0 = -2\eta\,\partial_v[(1-v^2)f_0]$ does not depend on φ, the integrand becomes

$$\begin{aligned}
\mathcal{L}_1^*\big(U(0)\big)\mathcal{L}_1^*\big(U(z)\big)\mathcal{L}_2^* f_0 &= 4\mathcal{L}_1^*\big(U(0)\big)\Big\{\eta\,\Im_z\sqrt{1-v^2}\,\partial_v^2\big[(1-v^2)f_0\big]\Big\} \\
&= 8\eta\Big\{ -\Im_0\Im_z\Big(\sqrt{1-v^2}\,\partial_v\Big)^2\Big(\partial_v\big[(1-v^2)f_0\big]\Big) + \Re_0\Re_z\, v\,\partial_v^2\big[(1-v^2)f_0\big]\Big\}\,.
\end{aligned}$$

Taking the expected value we get

$$\begin{aligned}
\mathbb{E}\big[\mathcal{I}_2\big] &= \int_0^\infty 8\eta\Big\{ v\,\partial_v^2\big[(1-v^2)f_0\big] - \Big(\sqrt{1-v^2}\,\partial_v\Big)^2\Big(\partial_v\big[(1-v^2)f_0\big]\Big)\Big\}\,\mathrm{d}y \\
&= -16\int_0^\infty \Big\{\partial_v\big[(1-v^2)\,\partial_v\big]\Big\}^2\big(f_0\big)\,\mathrm{d}y\,.
\end{aligned} \tag{2.3.63}$$

This term is clearly infinite, but recall that we still have to consider the third term, which will simplify the diverging part of $\mathcal{I}_2$.

We turn now to consider the last term, $\mathcal{I}_3$, which is more complicated. We have

$$\mathcal{L}_1^*\big(U(y+z)\big)\mathcal{L}_1^*\big(U(x+y+z)\big) f_0 = 4\Big\{\Im_{y+z}\Im_{x+y+z}\Big(\sqrt{1-v^2}\,\partial_v\Big)^2 f_0 - \Re_{y+z}\Re_{x+y+z}\, v\,\partial_v f_0\Big\}$$

and

$$\begin{aligned}
&\mathcal{L}_1^*\big(U(z)\big)\mathcal{L}_1^*\big(U(y+z)\big)\mathcal{L}_1^*\big(U(x+y+z)\big)f_0\\
&\quad= 8\Big\{ -\Im_z\Im_{y+z}\Im_{x+y+z}\Big(\sqrt{1-v^2}\,\partial_v\Big)^3 f_0 + \Re_z\,\partial_\varphi\Big(\Im_{y+z}\Im_{x+y+z}\Big)\,v\,\partial_v\big(\sqrt{1-v^2}\,\partial_v f_0\big)\\
&\qquad + \Im_z\Re_{y+z}\Re_{x+y+z}\,\sqrt{1-v^2}\,\partial_v\big(v\,\partial_v f_0\big) - \Re_z\,\partial_\varphi\Big(\Re_{y+z}\Re_{x+y+z}\Big)\,\frac{v^2}{\sqrt{1-v^2}}\,\partial_v f_0\Big\}.
\end{aligned}$$

We can use the relations $\partial_\varphi\Im\Im = (\Re\Im + \Im\Re) = -\partial_\varphi\Re\Re$ and

$$v\,\partial_v\big(\sqrt{1-v^2}\,\partial_v f_0\big) = -\frac{v^2}{\sqrt{1-v^2}}\,\partial_v f_0 + v\sqrt{1-v^2}\,\partial_v^2 f_0$$

to slightly simplify the above formula, which becomes

$$\begin{aligned}
&\mathcal{L}_1^*\big(U(z)\big)\mathcal{L}_1^*\big(U(y+z)\big)\mathcal{L}_1^*\big(U(x+y+z)\big)f_0\\
&\quad= 8\Big\{ -\Im_z\Im_{y+z}\Im_{x+y+z}\Big(\sqrt{1-v^2}\,\partial_v\Big)^3 f_0 + \Im_z\Re_{y+z}\Re_{x+y+z}\,\sqrt{1-v^2}\,\partial_v\big(v\,\partial_v f_0\big)\\
&\qquad + \Re_z\Big(\Re_{y+z}\Im_{x+y+z} + \Im_{y+z}\Re_{x+y+z}\Big)\,v\sqrt{1-v^2}\,\partial_v^2 f_0\Big\}.
\end{aligned}$$

We can finally get to the last step of the computations to obtain the integrand term of $\mathcal{I}_3$. We have:

$$\begin{aligned}
&\mathcal{L}_1^*\big(U(0)\big)\mathcal{L}_1^*\big(U(z)\big)\mathcal{L}_1^*\big(U(y+z)\big)\mathcal{L}_1^*\big(U(x+y+z)\big)f_0\\
&\qquad= 16\Big\{\Im_0\Im_z\Im_{y+z}\Im_{x+y+z}\Big(\sqrt{1-v^2}\,\partial_v\Big)^4 f_0\\
&\qquad\quad - \Im_0\Re_z\Big(\Re_{y+z}\Im_{x+y+z} + \Im_{y+z}\Re_{x+y+z}\Big)\sqrt{1-v^2}\,\partial_v\Big(v\sqrt{1-v^2}\,\partial_v^2 f_0\Big)\\
&\qquad\quad - \Im_0\Im_z\Re_{y+z}\Re_{x+y+z}\Big(\sqrt{1-v^2}\,\partial_v\Big)^2\big(v\,\partial_v f_0\big)\\
&\qquad\quad - \Re_0\,\partial_\varphi\big(\Im_z\Im_{y+z}\Im_{x+y+z}\big)\,v\,\partial_v\Big(\sqrt{1-v^2}\,\partial_v\Big)^2 f_0\\
&\qquad\quad + \Re_0\,\partial_\varphi\Big[\Re_z\big(\Re_{y+z}\Im_{x+y+z} + \Im_{y+z}\Re_{x+y+z}\big)\Big]\,v^2\,\partial_v^2 f_0\\
&\qquad\quad + \Re_0\,\partial_\varphi\big(\Im_z\Re_{y+z}\Re_{x+y+z}\big)\big(v\,\partial_v\big)^2 f_0\Big\}.
\end{aligned}$$

We have to integrate and take the expected value of this. Taking the expected value first allows for some simplifications. Since $\mathbb{E}[U_i(0)U_j(z)U_h(y+z)U_k(x+y+z)] = 0$ whenever exactly 3 index are the same ($i,j,h,k \in \{1,2\}$), we do not track these terms. There are only four kinds of terms left to consider:

$$\begin{aligned}
A &= \mathbb{E}\big[U_i(0)U_i(z)U_i(y+z)U_i(x+y+z)\big] = e^{-(x+z)} + 2e^{-(x+2y+z)},\\
B &= \mathbb{E}\big[U_i(0)U_i(z)U_j(y+z)U_j(x+y+z)\big] = e^{-(x+z)},\\
C &= \mathbb{E}\big[U_i(0)U_j(z)U_i(y+z)U_j(x+y+z)\big] = e^{-(x+2y+z)},\\
A &= \mathbb{E}\big[U_i(0)U_j(z)U_j(y+z)U_i(x+y+z)\big] = e^{-(x+2y+z)} = C\,.
\end{aligned}$$

We set

$$\alpha = \int_0^\infty A\,\mathrm{d}x = e^{-z} + 2e^{-(z+2y)}, \qquad \beta = \int_0^\infty B\,\mathrm{d}x = e^{-z}, \qquad \gamma = \int_0^\infty C\,\mathrm{d}x = e^{-(z+2y)}$$

and remark that $A = B + 2B$ and $\alpha = \beta + 2\gamma$. We have that

$$\begin{aligned}
\Im_0\Im_z\Im_{y+z}\Im_{x+y+z} = \Re_0\Re_z\Re_{y+z}\Re_{x+y+z} &= A\Big(\sin^2(\varphi) + \cos^2(\varphi)\Big)^2 = A\,,\\
\Im_0\Im_z\Re_{y+z}\Re_{x+y+z} = \Re_0\Re_z\Im_{y+z}\Im_{x+y+z} &= B\Big(\sin^2(\varphi) + \cos^2(\varphi)\Big)^2 = B\,,\\
\Im_0\Re_z\Re_{y+z}\Im_{x+y+z} = \Re_0\Im_z\Im_{y+z}\Re_{x+y+z} &= \Im_0\Re_z\Im_{y+z}\Re_{x+y+z} = \Re_0\Im_z\Re_{y+z}\Im_{x+y+z}\\
&= C\Big(\sin^2(\varphi) + \cos^2(\varphi)\Big)^2 = C\,.
\end{aligned}$$

Putting everything together, we finally obtain

$$\begin{aligned}
&\int_0^\infty \mathbb{E}\Big[\mathcal{L}_1^*\big(U(0)\big)\mathcal{L}_1^*\big(U(z)\big)\mathcal{L}_1^*\big(U(y+z)\big)\mathcal{L}_1^*\big(U(x+y+z)\big)f_0\Big]\,\mathrm{d}x\\
&\quad=16\Big\{\alpha\Big(\sqrt{1-v^2}\,\partial_v\Big)^4 f_0 - 2\gamma\sqrt{1-v^2}\,\partial_v\Big(v\sqrt{1-v^2}\,\partial_v^2 f_0\Big)\\
&\qquad - \beta\Big(\sqrt{1-v^2}\,\partial_v\Big)^2\big(v\,\partial_v f_0\big) - \alpha\, v\,\partial_v\Big(\sqrt{1-v^2}\,\partial_v\Big)^2 f_0 + 2\gamma\, v^2\,\partial_v^2 f_0 + \beta\big(v\,\partial_v\big)^2 f_0\Big\}.
\end{aligned}$$

We have to integrate in $\mathrm{d}z$, then join this with (2.3.63) and integrate in $\mathrm{d}y$ to verify that the diverging terms simplify. We have

$$\int_0^\infty \alpha\,\mathrm{d}z = 1 + 2e^{-2y}\,, \qquad \int_0^\infty \beta\,\mathrm{d}z = 1\,, \qquad \int_0^\infty \gamma\,\mathrm{d}x = e^{-2y}\,,$$

which leads to

$$\begin{aligned}
\mathbb{E}\big[\mathcal{I}_3\big] = 16\int_0^\infty &\Big\{\Big(\sqrt{1-v^2}\,\partial_v\Big)^4 - \Big(\sqrt{1-v^2}\,\partial_v\Big)^2\big(v\,\partial_v\big)\\
&\qquad - v\,\partial_v\Big(\sqrt{1-v^2}\,\partial_v\Big)^2 + \big(v\,\partial_v\big)^2\Big\}\big(f_0\big)\\
&+2e^{-2y}\Big\{\Big(\sqrt{1-v^2}\,\partial_v\Big)^4 f_0 - \sqrt{1-v^2}\,\partial_v\Big(v\sqrt{1-v^2}\,\partial_v^2 f_0\Big)\\
&\qquad - v\,\partial_v\Big(\sqrt{1-v^2}\,\partial_v\Big)^2 f_0 + v^2\,\partial_v^2 f_0\Big\}\,\mathrm{d}y\,.
\end{aligned}$$

The first term on the right hand side can be rewritten as

$$\Big[\Big(\sqrt{1-v^2}\,\partial_v\Big)^2 - \big(v\,\partial_v\big)\Big]^2\big(f_0\big) = \Big\{\partial_v\big[(1-v^2)\,\partial_v\big]\Big\}^2\big(f_0\big)\,,$$

which cancels exactly with (2.3.63). Finally, using (2.3.62), we get

$$\begin{aligned} F &= \mathbb{E}\big[\mathcal{I}_1 + \mathcal{I}_2 + \mathcal{I}_3\big] \\ &= 16\Big\{ \Big(\sqrt{1-v^2}\,\partial_v\Big)^4 f_0 - \sqrt{1-v^2}\,\partial_v\Big(v\sqrt{1-v^2}\,\partial_v^2 f_0\Big) - v\,\partial_v\Big(\sqrt{1-v^2}\,\partial_v\Big)^2 f_0 \\ &\qquad + v^2\,\partial_v^2 f_0 - \sqrt{1-v^2}\,\partial_v^2\Big[(1-v^2)^{3/2}\,\partial_v^2 f_0\Big] + \frac{v}{\sqrt{1-v^2}}\,\partial_v\Big[(1-v^2)^{3/2}\partial_v^2 f_0\Big]\Big\}. \end{aligned}$$

Explicit computations give finally

$$F = 16c\big[2v + (4v^2-2)c - c^2 v(1-v^2)\big] f_0 = \frac{4c^2}{\pi \sinh(c)}\big[c^2v^3 + 4cv^2 + (2-c^2)v - 2c\big]e^{cv}.$$

We can return to the solvability condition (2.3.61), which we treat as we did above to find P_0. The equation can be rewritten as

$$-2\eta\,\partial_v\Big((1-v^2)f_2\Big) + 2\xi\,\partial_\varphi f_2 + 4\,\partial_v\Big((1-v^2)\,\partial_v f_2\Big) + 4\frac{v^2}{1-v^2}\,\partial_\varphi^2 f_2 + F(v) = 0$$

with the constraint $\int_0^{2\pi}\int_{-1}^1 f_2\,\mathrm{d}v\,\mathrm{d}\varphi = 0$. We can therefore assume f_2 to be independent of φ and a solution of

$$-2\eta\,\partial_v\Big((1-v^2)f_2\Big) + 4\,\partial_v\Big((1-v^2)\partial_v f_2\Big) = -F(v)\,.$$

Integrating, we get

$$-c(1-v^2)f_2 + (1-v^2)\partial_v f_2 = -\frac{1}{4}G(v) + \frac{G(0)}{4} - cf_2(0) + \partial_v f_2(0)\,,$$

where $G(v)$ is the antiderivative of $F(v)$:

$$G(v) = -16c(1+cv)(1-v^2)f_0\,.$$

We can choose $G(0)$ so that $G(0)/4 - cf_2(0) + \partial_v f_2(0) = 0$. Then

$$-cf_2 + \partial_v f_2 = -\frac{G(v)}{4(1-v^2)} = 4c(1+cv)f_0\,,$$

from which we can easily find the solution

$$f_2 = 2c(2v + cv^2)f_0 + C_0 f_0\,.$$

Note that $f_2(0) = C_0 k$ and $\partial_v f_2(v) = ck(C_0+4)$, so that the value of $G(0)$ we must take is $G(0) = -4ck = -c^2/(\pi\sinh(c))$. We still have to impose that

$$0 = \int_0^{2\pi}\int_{-1}^1 f_2(v)\,\mathrm{d}v\,\mathrm{d}\varphi = C_0 + 2c^2\,,$$

so that we obtain $C_0 = -2c^2$ and f_2 is completely determined:

$$f_2 = 2c(-2c + 2v + cv^2)f_0 = \frac{c^2}{2\pi\sinh(c)}(-2c + 2v + cv^2)e^{cv}.$$

Finding the second order term for the density of states: ρ_2

We can finally compute the second order correction for the DOS. We start by computing the (second order) correction term $\delta\kappa$ for the Lyapunov exponent. Recall that $c = \eta/2$.

$$\delta\kappa = \eta \int_{-1}^{1} v f_2(v)\,\mathrm{d}v = \frac{c^2-2}{c\,\pi}\big(1-\coth(c)\big)\,.$$

Observe that for $\eta \gg 1$, $\delta\kappa \sim 0$. From the Thouless formula (2.3.32) we get the second order correction ρ_2 for the density of the eigenstates. Since $\delta\kappa$ only depends on c, we can compute it as

$$\begin{aligned}\rho_2(\eta,\xi) &= \frac{1}{2\pi}\Big(\partial_\eta^2+\partial_\xi^2\Big)\delta\kappa(\eta,\xi) = \frac{1}{8\pi}\partial_c^2\delta\kappa(c)\\ &= \frac{1}{4\pi^2}\Big[\frac{c^2+2}{c^2}\mathrm{csch}^2(c) - \frac{c^2-2}{c}\mathrm{csch}^2(c)\coth(c) + \frac{2}{c^3}\big(\coth(c)-1\big)\Big]\,.\end{aligned}$$

This provides (2.3.27) and completes the proof of theorem 2.34. Plotting the correction, we see that we are also moving mass from the interval $[\alpha,+\infty]$ towards zero, see figure 2.4. The approximate value of α is $\alpha = 4.599$.

2.3.6 Density of states – general case

In this subsection we focus on the method for computing the density of eigenstates (DOS) of the ZSSP for a more general class of potentials (which corresponds to the initial condition of the NLS equation) with rapid (but not infinitely rapid) oscillations. The scheme of the computations is similar to the one presented above, where the initial condition was taken to be a rapidly oscillating Ornstein-Uhlenbeck process. We shall now take the initial condition of the form

$$U_0^\varepsilon(x) = \varepsilon^{-1}F\big(Q(x/\varepsilon^2)\big)\,, \tag{2.3.64}$$

where the process $Q(x)$ and the function F satisfy the following assumptions

Hypothesis 2.42. $Q = (Q_1, Q_2)$ is given by a couple of independent, identically distributed, ergodic Markov processes on a smooth, compact, connected Riemannian manifold M with invariant probability μ. The infinitesimal generator of Q, denoted by $\mathcal{L}_Q$, is a self-adjoint, elliptic diffusion operator on M, with zero an isolated, simple eigenvalue.

$F : M^2 \mapsto \mathbb{C}$ is a smooth non-constant function of the form $F(Q) = F_1(Q_1) + iF_2(Q_2)$, where $F_n : M \mapsto \mathbb{R}$, $n = 1, 2$, and that it satisfy the following centering condition

$$\mathbb{E}\Big[F\big(Q(x)\big)\Big] = \int_M F(q)\,\mathrm{d}\mu(q) = 0\,. \tag{2.3.65}$$

These are easy technical conditions which ensures that if we rewrite the ZSSP system using polar coordinates (ρ,γ) as we did in the previous subsection, the vector $\big(Q,\vec{\gamma}\,\big)$ is ergodic, [APW86]. Under hypothesis 2.42 we can therefore compute the DOS using the method explained in lemma 2.41, which relays on the computation of the Lyapunov exponent κ, (2.3.31), and the Thouless formula, (2.3.32). The explicit computations presented below are done in the new variables (v,φ,Q) and using equation (2.3.34) to obtain the Lyapunov exponent. We stress that the essential point for the application of this method is the ergodicity of the vector $\big(Q,\vec{\gamma}\,\big)$, so that the technical hypothesis on the process Q could

actually be considerably relaxed, see the following remarks. A detailed analysis of linear systems and different conditions ensuring ergodicity are contained in [AKO].

Remark 2.43. If we require the generator of the process Q to be self adjoint is because this considerably simplifies computations. However, in some cases it is possible to work also with processes not satisfying this assumption, as it was the case for the OU process considered in the previous subsection. Also the independence of the real and imaginary part of $F(Q)$ is only assumed in order to simplify computations.

Remark 2.44. An easy example of a process Q satisfying hypothesis 2.42 can be obtained taking Q a Wiener process on a torus.

Remark 2.45. Remark that since for the invariant measure $\mathcal{L}_Q^*\mu = 0$ and since constants are in the kernel of the generator ($\mathcal{L}_Q 1 = 0$), which is a one dimensional subspace, the invariant measure μ of the process Q must be constant [FGPS]. The constant μ can therefore be seen as the volume of the manifold M. In the following, we maintain the same notation for the (constant) invariant measure $\mathrm{d}\mu(q) = \mu\,\mathrm{d}q$ and the constant μ.

Our main result is the following.

Theorem 2.46. *Consider the NLS equation with initial condition given by a rapidly oscillating process Q satisfying hypothesis 2.42. The distribution of eigenstates $\rho(\eta,\xi)$ (DOS) of the corresponding ZSSP is smooth and can be written as a power series expansion around the limit case of infinitely rapid oscillations. If ε is the parameter controlling the rapidity of oscillations, we have*

$$\rho(\eta,\xi) = \rho_0(\eta) + O(\varepsilon^2)\,, \tag{2.3.66}$$

where

$$\rho_0(\eta) = \frac{1}{2\pi\,\bar\alpha}\frac{\eta\coth\big(\eta/\bar\alpha\big) - \bar\alpha}{\sinh^2\big(\eta/\bar\alpha\big)} \tag{2.3.67}$$

is the DOS corresponding to the limit case, and the first order term is zero. Here, $\bar\alpha$ is the integrated covariance of the process $U = F(Q)$, which is given by

$$\bar\alpha = \int_0^\infty \mathbb{E}\Big[F\big(Q(0)\big)F\big(Q(x)\big)\Big]\,\mathrm{d}x\,. \tag{2.3.68}$$

Remark 2.47. The second order term $\rho_2(\eta,\xi)$ of the expansion (2.3.66) is in general quite complicated. A discussion of a method that can be used to obtain it and of some special cases for which simplifications occur is provided at the end of this subsection.

The proof of theorem 2.46 and the discussion on the second order correction term ρ_2 of the DOS fill the rest of this subsection.

The Fokker-Planck equation

From now on we will use the notation $U_0(x) = F\big(Q(x)\big)$. We will also drop the subscript U_0 for the initial condition and, when there is no risk of confusion, also the dependence on x. Just as we did in the previous subsection, we introduce some new variables,

$$r(x) = \psi_1(x)/\psi_2(x) = e^{w(x)+i\varphi(x)}\,,$$

where $w \in (-\infty, \infty)$ and $\varphi \in [0, 2\pi)$. Using these variables we can rewrite the ZSSP system (2.1.3) as

$$\frac{\mathrm{d}}{\mathrm{d}x} r(x) = iU - 2i\zeta r - iU^* r^2$$

and since $\mathrm{d}r = r(\mathrm{d}w + i\mathrm{d}\varphi)$, we obtain the system governing the evolution of the variables w, φ

$$\begin{cases} \partial_x w = 2\eta + 2\cosh(w)\Im\left[U^* e^{i\varphi}\right] \\ \partial_x \varphi = -2\xi - 2\sinh(w)\Re\left[U^* e^{i\varphi}\right] \end{cases}.$$

With the change of variable $v = \tanh(w)$, we obtain to the Fokker-Planck equation

$$\partial_x P(v, \varphi, q) = \mathcal{L}_Q^* P + \mathcal{L}_1^* P + \mathcal{L}_2^* P\,, \tag{2.3.69}$$

where

$$\begin{aligned} \mathcal{L}_1^* f &= -2\eta\, \partial_v \Big[(1 - v^2) f\Big] + 2\xi\, \partial_\varphi f\,, \\ \mathcal{L}_2^* f &= -2\Im\left[U^* e^{i\varphi}\right]\, \partial_v \Big[\sqrt{1 - v^2} f\Big] + 2\frac{v}{\sqrt{1 - v^2}}\, \partial_\varphi \Big[\Re\left[U^* e^{i\varphi}\right] f\Big]\,. \end{aligned}$$

To obtain a rapidly oscillating initial condition we still have to speed up the process Q and rescale $U = F(Q)$ accordingly. The resulting rapidly oscillating potential used in the ZSSP is the process U^ε given by (2.3.64). In the following, we will always work with the fast oscillating process $Q^\varepsilon(x) = Q(x/\varepsilon^2)$. Let $P^\varepsilon(v, \varphi, Q^\varepsilon)$ be the invariant probability measure. Under hypothesis 2.42 the invariant probability P^ε admits a smooth density with respect to the Lebesgue measure, which is the solution of $\mathcal{L}_\varepsilon^* P^\varepsilon = 0$. In the following we shall therefore confound the invariant probability with its density. The operator $\mathcal{L}_\varepsilon^*$ has a finite expansion in ε:

$$\mathcal{L}_\varepsilon^* = \frac{1}{\varepsilon^2}\mathcal{L}_Q^* + \frac{1}{\varepsilon}\mathcal{L}_1^* + \mathcal{L}_2^*\,.$$

We assume that the density of the invariant probability P^ε solution of $\mathcal{L}_\varepsilon^* P^\varepsilon = 0$ can be formally rewritten using a power series expansion in ε around the limit case of infinitely rapid oscillations: $P^\varepsilon = P_0 + \varepsilon P_1 + \varepsilon^2 P_2 + \dots$, [APW86]. The first term of the expansion, P_0, is the invariant probability of the limit problem for infinitely rapid oscillations, which thanks to the results of section 2.1 can be found solving the formal problem of a white noise initial condition. We are interested here in finding the correction terms P_1 and P_2. To do so, we shall rewrite the equation $\mathcal{L}_\varepsilon^* P^\varepsilon = 0$ using the expansions of both $\mathcal{L}_\varepsilon^*$ and P^ε, divide scales according to the power of ε and study them separately, posing the term at each order equal to zero.

To ease notation, in the following computations we shall drop all the superscript ε.

Explicit computations: order -2

The first equation is the "order -2" equation, containing the only term scaling as ε^{-2}. This is simply

$$\mathcal{L}_Q\, P_0 = 0\,,$$

from which we get that $P_0 = \mu f_0(v, \varphi)$.

Explicit computations: order -1

The following equation is $\mathcal{L}_1^* P_0 + \mathcal{L}_Q P_1$. This can be seen as a Poisson equation in the q variable

$$\mathcal{L}_Q P_1 = g\,,$$

where $g = -\mathcal{L}_1^* P_0$. The solvability condition for the Poisson equation is that the function g must be centered with respect to the invariant measure of Q. Rewriting $\mathcal{L}_1^*(u) = \mathcal{L}_1^*\big(F(q)\big)$ we obtain the following equivalent formulation of the solvability condition:

$$0 = \int_{M^2} \mathcal{L}_1^* P_0 \,\mathrm{d}\mu = \int_{M^2} \mathcal{L}_1^*\big(F(q)\big) f_0 \;\mu^2 \,\mathrm{d}q\,. \tag{2.3.70}$$

Since $\mathcal{L}_1^*(u)$ is linear in u and μ is a constant, the condition becomes

$$\int_{K^2} F(q)\,\mu^2 \,\mathrm{d}q = \mu\,\mathbb{E}\Big[F\big(Q\big)\Big] = 0\,,$$

which is always verified thanks to the centering condition (2.3.65), and from (2.3.70) we obtain no additional information on f_0. However, we can now solve $\mathcal{L}_1^* P_0 + \mathcal{L}_Q P_1$ to get the following expression for P_1:

$$\begin{aligned} P_1(q) &= \mu f_1 + \int_0^\infty \mathbb{E}\Big[\mathcal{L}_1^*\big(U(x)\big)\, P_0\big(U(x)\big) \,\Big|\, U(0) = u = F(q)\Big]\,\mathrm{d}x \\ &= \mu f_1 + \int_0^\infty \mu\,\mathbb{E}\Big[\mathcal{L}_1^*\big(U(x)\big)\, f_0 \,\Big|\, U(0) = F(q)\Big]\,\mathrm{d}x\,, \end{aligned}$$

where f_1 is a function of (v, φ), but does not depend on q.

Explicit computations: order 0

The next order equation is

$$\mathcal{L}_2^* P_0 + \mathcal{L}_1^* P_1 + \mathcal{L}_Q P_2 = 0\,. \tag{2.3.71}$$

Again, we look at it as a Poisson equation in the q variable, and the solvability condition is

$$\int \mathcal{L}_2^* P_0 + \mathcal{L}_1^* P_1 \,\mathrm{d}\mu = 0\,. \tag{2.3.72}$$

We have

$$\mathcal{L}_2^* P_0 = \mu\Big(- 2\eta\,\partial_v\big[(1-v^2) f_0\big] + 2\xi\,\partial_\varphi f_0\Big)\,.$$

Introduce the compact notation $\Im_x = \Im\big[U(x)e^{i\varphi}\big]$ and $\Re_x = \Re\big[U(x)e^{i\varphi}\big]$, so that $\partial_\varphi \Re_x = -\Im_x$ and $\partial_\varphi \Im_x = \Re_x$. Then, we also have

$$\begin{aligned}
\mathcal{L}_1^*(q)P_1(q) &= \mu\mathcal{L}_1^*(q)f_1 + \int_0^\infty \mu\,\mathbb{E}\Big[\mathcal{L}_1^*\big(U(0)\big)\mathcal{L}_1^*\big(U(x)\big)\, f_0 \,\Big|\, U(0) = F(q)\Big]\,\mathrm{d}x \\
&= \mu\mathcal{L}_1^*(q)f_1 + 4\mu\int_0^\infty E\Big[\Im_0\Im_x\,\partial_v\Big[\sqrt{1-v^2}\,\partial_v\big(\sqrt{1-v^2}f_0\big)\Big] \\
&\qquad + \Im_0\Im_x\,\partial_v\big(vf_0\big) - \Im_0\Re_x\,\partial_v\big(v\,\partial_\varphi f_0\big) \\
&\qquad + \frac{v}{\sqrt{1-v^2}}\Big[\big(\Im_0\Im_x - \Re_0\Re_x\big)\,\partial_v\big(\sqrt{1-v^2}f_0\big) \\
&\qquad\qquad - \Re_0\Im_x\,\partial_v\big(\sqrt{1-v^2}\,\partial_\varphi f_0\big)\Big] \\
&\qquad + \frac{v^2}{1-v^2}\partial_\varphi\big(\Re_0\,\partial_\varphi(\Re_x f_0)\big)\,\Big|\, U(0) = F(q)\Big]\,\mathrm{d}x\,.
\end{aligned}$$

The integrated covariance $\bar\alpha$ of the process U defined by (2.3.68) plays an important role. However, to develop computations it is more convenient to introduce the quantity α defined by

$$\int_0^\infty \mathbb{E}\Big[U_i(0)U_j(x)\Big]\,\mathrm{d}x = \alpha\,\delta_{i,j}\,,$$

where $\delta_{i,j}$ is the Kronecker delta function. Remark that this is simply half of the integrated covariance: $\bar\alpha = 2\alpha$. Since $\mathcal{L}_1^*$ is linear in u, the expected value of the term $\mathcal{L}_1^* f_1$ is zero, and we have

$$\mathbb{E}\Big[\mathcal{L}_1^*(q)P_1(q)\Big] = 4\mu^2\alpha\Big\{\partial_v\big[(1-v^2)\,\partial_v f_0\big] + \frac{v^2}{1-v^2}\,\partial_\varphi^2 f_0\Big\}\,.$$

Since $\mathcal{L}_2^* P_0$ is constant in q, condition (2.3.72) becomes

$$\mathscr{L} f_0 = 0\,,$$

where

$$\begin{aligned}
\mathscr{L} f &= \mathbb{E}\Big[\mathcal{L}_2^* f - \int_0^\infty \mathcal{L}_1^*\big(U(0)\big)\mathcal{L}_1^*\big(U(x)\big) f\,\mathrm{d}x\Big] \\
&= -2\eta\,\partial_v\Big[(1-v^2)f\Big] + 2\xi\,\partial_\varphi f + 4\alpha\Big\{\partial_v\big[(1-v^2)\,\partial_v f\big] + \frac{v^2}{1-v^2}\,\partial_\varphi^2 f\Big\}\,. \qquad (2.3.73)
\end{aligned}$$

Setting $c := \eta/2\alpha$, the solution is given by

$$f_0(v,\varphi) = \frac{1}{2\pi}ke^{cv}, \qquad (2.3.74)$$

where k is a constant that has to be chosen so that $\int_0^{2\pi}\int_{-1}^1 f_0\,\mathrm{d}v\,\mathrm{d}\varphi = 1$. This gives $k = c/2\sinh(c)$. Therefore,

$$P_0(v,\varphi,q) = \frac{\mu c}{4\pi\sinh(c)}\,e^{cv}\,. \qquad (2.3.75)$$

With f_0 given by (2.3.74), the solvability condition (2.3.72) is satisfied and we can solve (2.3.71) to get the following expression for P_2:

$$P_2 = \mu f_2 + \mu \int_0^\infty E\Big[\mathcal{L}_2^* f_0 + \mathcal{L}_1^*\big(U(x)\big) f_1 + \int_0^\infty \mathcal{L}_1^*\big(U(x)\big)\mathcal{L}_1^*\big(U(x+y)\big) f_0 \,\mathrm{d}y \,\Big|\, U(0) = F(q)\Big]\mathrm{d}x\,.$$

Here, f_2 is a function of (v, φ), but is constant in q.

Finding the density of states at order zero: ρ_0

Using the explicit expression (2.3.75) for P_0 we obtain

$$\bar{P}_0(v) := \int_0^{2\pi} \int_{M^2} P_0(v, \varphi, q)\,\mathrm{d}\mu\,\mathrm{d}\varphi = k e^{cv},$$

from which we find that the Lyapunov exponent at order zero is

$$\kappa = \eta \int_{-1}^{1} v\,\bar{P}_0(v)\,\mathrm{d}v = \eta \coth(\eta/2\alpha) - 2\alpha\,.$$

From the Thouless formula we get that the density of eigenstates is, at order zero,

$$\rho_0(\eta, \xi) = \frac{1}{2\pi} \frac{c\coth(c) - 1}{\sinh^2(c)}\,.$$

We recall that $c = \eta/2\alpha = \eta/\bar{\alpha}$. We have obtained (2.3.67).

Explicit computations: order 1 - $\rho_1 = 0$

We now need to solve the next order equation, which is

$$\mathcal{L}_2^* P_1 + \mathcal{L}_1^* P_2 + \mathcal{L}_Q P_3 = 0\,, \tag{2.3.76}$$

where

$$\begin{aligned}
\mathcal{L}_2^* P_1 &= \mu \mathcal{L}_2^* f_1 + \mu \int_0^\infty \mathbb{E}\Big[\mathcal{L}_2^*\mathcal{L}_1^*\big(U(x)\big)\, f_0 \,\Big|\, U(0) = F(q)\Big]\,\mathrm{d}x\,,\\
\mathcal{L}_1^*(q) P_2 &= \mu \mathbb{E}\Big[\mathcal{L}_1^*\big(U(0)\big) f_2 + \int_0^\infty \mathcal{L}_1^*\big(U(0)\big)\mathcal{L}_2^* f_0 + \mathcal{L}_1^*\big(U(0)\big)\mathcal{L}_1^*\big(U(x)\big) f_1\\
&\qquad + \int_0^\infty \mathcal{L}_1^*\big(U(0)\big)\mathcal{L}_1^*\big(U(x)\big)\mathcal{L}_1^*\big(U(x+y)\big) f_0 \,\mathrm{d}y\;\mathrm{d}x \,\Big|\, U(0) = F(q)\Big].
\end{aligned}$$

Looking at (2.3.76) as a Poisson equation in the q variable and setting

$$\mathbb{E}\Big[\iint_0^\infty U_i(0) U_i(x) U_i(x+y)\,\mathrm{d}y\,\mathrm{d}x\Big] = \delta_{i,j}\delta_{j,k}\,\beta\,, \tag{2.3.77}$$

we find that the solvability condition is

$$0 = \mathcal{L}_2^* f_1 + \mathbb{E}\Big[\int_0^\infty \mathcal{L}_1^*\big(U(0)\big)\mathcal{L}_1^*\big(U(x)\big) f_1 + \int_0^\infty \mathcal{L}_1^*\big(U(0)\big)\mathcal{L}_1^*\big(U(x)\big)\mathcal{L}_1^*\big(U(x+y)\big) f_0 \,\mathrm{d}y\,\mathrm{d}x\Big],$$

which is to say

$$\mathscr{L} f_1 = -g,$$

where $\mathscr{L}$ is defined by (2.3.73) and the function g is given by

$$\begin{aligned} g = 8\mu\,\mathbb{E}\Bigg[& \Im_0\Im_x\Im_{x+y}\Big(\partial_v\sqrt{1-v^2}\,\cdot\Big)^3(f_0) - \Im_0\Im_x\,\partial_v\Big[\sqrt{1-v^2}\,\partial_v\Big[v\,\partial_\varphi\big(\Re_{x+y}f_0\big)\Big]\Big] \\ & - \Im_0\,\partial_v\Big[v\,\partial_\varphi\Big[\Re_x\Im_{x+y}\,\partial_v\big(\sqrt{1-v^2}f_0\big)\Big] - \frac{v^2}{\sqrt{1-v^2}}\,\partial_\varphi\Big[\Re_x\,\partial_\varphi\big(\Re_{x+y}f_0\big)\Big]\Big] \\ & - \frac{v}{\sqrt{1-v^2}}\,\partial_\varphi\Big[\Re_0\Im_x\Im_{x+y}\Big(\partial_v\sqrt{1-v^2}\,\cdot\Big)^2(f_0) - \Re_0\Im_x\,\partial_v\Big[v\,\partial_\varphi\big(\Re_{x+y}f_0\big)\Big]\Big] \\ & + \frac{v^2}{1-v^2}\,\partial_\varphi\Big[\Re_0\,\partial_\varphi\Big[\Re_x\Im_{x+y}\,\partial_v\big(\sqrt{1-v^2}f_0\big)\Big]\Big] \\ & - \frac{v^3}{(1-v^2)^{3/2}}\,\partial_\varphi\Big[\Re_0\,\partial_\varphi\Big(\Re_x\,\partial_\varphi\big(\Re_{x+y}f_0\big)\Big)\Big]\Bigg]. \end{aligned}$$

Developing the computations in the above equation one is left with

$$\begin{aligned} g = 8\mu\beta\Bigg\{ & \big(\cos^3(\varphi)+\sin^3(\varphi)\big)f_0\sqrt{1-v^2}\Big[c^3(1-v^2) - 3c^2v - c - \frac{2v^3}{(1-v^2)^2}\Big] \\ & - \big(\cos(\varphi)+\sin(\varphi)\big)f_0\sqrt{1-v^2}\Big[2vc^2 + 3c - \frac{2c}{1-v^2} - \frac{2v^3}{(1-v^2)^2}\Big]\Bigg\}. \end{aligned}$$

The solution of $\mathscr{L} f_1 = g$ must therefore be of the form

$$f_1(v,\varphi) = \cos(\varphi)f_{1,1}(v) + \sin(\varphi)f_{1,2}(v) + \cos^3(\varphi)f_{1,3}(v) + \sin^3(\varphi)f_{1,4}(v)\,,$$

so that $\bar{P}_1(v) = \int_0^{2\pi} f_1 \mathrm{d}\varphi = 0$ and we see that the first order term $\rho_1(\eta,\xi)$ of the development of the Lyapunov exponent is zero. This proves theorem 2.46.

For f_1 of the form given above, the solvability condition is satisfied and we can solve the Poisson equation to obtain

$$\begin{aligned} P_3 = & \mu f_3 + \mu\int_0^\infty \mathbb{E}\Bigg[\mathcal{L}_2^* f_1 + \int_0^\infty \mathcal{L}_2^*\mathcal{L}_1^*\big(U(x+z)\big)f_0\,\mathrm{d}x + \mathcal{L}_1^*\big(U(z)\big)f_2 \\ & + \int_0^\infty \mathcal{L}_1^*\big(U(z)\big)\mathcal{L}_2^* f_0 + \mathcal{L}_1^*\big(U(z)\big)\mathcal{L}_1^*\big(U(x+z)\big)f_1 \\ & + \int_0^\infty \mathcal{L}_1^*\big(U(z)\big)\mathcal{L}_1^*\big(U(z+x)\big)\mathcal{L}_1^*\big(U(x+y+z)\big)f_0\,\mathrm{d}y\;\mathrm{d}x\,\Big|U(0)=F(q)\Bigg]\mathrm{d}z\,. \end{aligned}$$

Explicit computations: order 2

To find the second order term of the Lyapunov exponent, and therefore for the DOS, we must push our analysis one step further. The next order equation we need to consider is

$$\mathcal{L}_2^* P_2 + \mathcal{L}_1^* P_3 + \mathcal{L}_Q P_4 = 0\,. \tag{2.3.78}$$

We have that

$$\mathcal{L}_2^* P_2 = \mu \mathcal{L}_2^* f_2 + \mu \int_0^\infty \mathbb{E}\Big[\mathcal{L}_2^*\mathcal{L}_2^* f_0 + \mathcal{L}_2^*\mathcal{L}_1^*\big(U(x)\big) f_1 + \int_0^\infty \mathcal{L}_2^*\mathcal{L}_1^*\big(U(x)\big)\mathcal{L}_1^*\big(U(x+y)\big) f_0 \,\mathrm{d}y \,\Big|\, U(0) = F(q)\Big]\,\mathrm{d}x\,,$$

so that, due to (2.3.73),

$$\mathbb{E}\Big[\mathcal{L}_2^* P_2\Big] = \mu \mathcal{L}_2^* f_2\,.$$

Also,

$$\begin{aligned}\mathcal{L}_1^*(q) P_3 = \mu \mathbb{E}\Big[\mathcal{L}_1^*\big(U(0)\big) f_3 + \int_0^\infty \Big\{\mathcal{L}_1^*\big(U(0)\big)\mathcal{L}_2^* f_1 + \int_0^\infty \mathcal{L}_1^*\big(U(0)\big)\mathcal{L}_2^*\mathcal{L}_1^*\big(U(x+z)\big) f_0 \,\mathrm{d}x \\ + \mathcal{L}_1^*\big(U(0)\big)\mathcal{L}_1^*\big(U(z)\big) f_2 \\ + \int_0^\infty \mathcal{L}_1^*\big(U(0)\big)\mathcal{L}_1^*\big(U(z)\big)\mathcal{L}_2^* f_0 + \mathcal{L}_1^*\big(U(0)\big)\mathcal{L}_1^*\big(U(z)\big)\mathcal{L}_1^*\big(U(x+z)\big) f_1 \\ + \int_0^\infty \mathcal{L}_1^*\big(U(0)\big)\mathcal{L}_1\big(U(z)\big)\mathcal{L}_1^*\big(U(x+z)\big)\mathcal{L}_1\big(U(x+y+z)\big) f_0 \,\mathrm{d}y\,\mathrm{d}x\Big\}\mathrm{d}z \,\Big|\, U(0) = F(q)\Big].\end{aligned}$$

The expected value of the first two terms on the right hand side of the above equation is zero, and the fourth one can be joined with the term $\mathbb{E}[\mathcal{L}_2^* f_2]$ to obtain $\mathscr{L} f_2$, with $\mathscr{L}$ is given by (2.3.73). Therefore, the solvability condition for (2.3.78) reduces to

$$\mathscr{L} f_2 = -F\,, \tag{2.3.79}$$

where $F = \mathbb{E}\big[\mathcal{I}_1 + \mathcal{I}_2 + \mathcal{I}_3 + \mathcal{I}_4\big]$ and

$$\begin{aligned}\mathcal{I}_1 &= \iint_0^\infty \mathcal{L}_1^*\big(U(0)\big)\mathcal{L}_2^*\mathcal{L}_1^*\big(U(x+z)\big) f_0 \,\mathrm{d}x\,\mathrm{d}z\,,\\ \mathcal{I}_2 &= \iint_0^\infty \mathcal{L}_1^*\big(U(0)\big)\mathcal{L}_1^*\big(U(z)\big)\mathcal{L}_2^* f_0 \,\mathrm{d}x\,\mathrm{d}z\,,\\ \mathcal{I}_3 &= \iint_0^\infty \mathcal{L}_1^*\big(U(0)\big)\mathcal{L}_1^*\big(U(z)\big)\mathcal{L}_1^*\big(U(x+z)\big) f_1 \,\mathrm{d}x\,\mathrm{d}z\,,\\ \mathcal{I}_4 &= \iiint_0^\infty \mathcal{L}_1^*\big(U(0)\big)\mathcal{L}_1\big(U(z)\big)\mathcal{L}_1^*\big(U(x+z)\big)\mathcal{L}_1\big(U(x+y+z)\big) f_0 \,\mathrm{d}x\,\mathrm{d}y\,\mathrm{d}z\,.\end{aligned}$$

We shall now analyze all these terms. Setting

$$\iint_0^\infty \mathbb{E}\Big[U_i(0) U_j(x+z)\Big]\,\mathrm{d}x\,\mathrm{d}z = \delta_{i,j}\,\gamma$$

we have

$$\begin{aligned}\mathbb{E}\big[\mathcal{I}_1\big] &= \iint_0^\infty \mathbb{E}\Big[\mathcal{L}_1^*\big(U(0)\big)\mathcal{L}_2^*\mathcal{L}_1^*\big(U(x+z)\big) f_0\Big]\,\mathrm{d}x\,\mathrm{d}z \\ &= -8\,\eta\gamma\,\partial_v\Big[\sqrt{1-v^2}\,\partial_v\Big[(1-v^2)\,\partial_v(\sqrt{1-v^2} f_0) + v\sqrt{1-v^2} f_0\Big]\Big]\,.\end{aligned} \tag{2.3.80}$$

Also,

$$\begin{aligned}\mathbb{E}\big[\mathcal{I}_3\big] &= \iint_0^\infty \mathbb{E}\Big[\mathcal{L}_1^*\big(U(0)\big)\mathcal{L}_1^*\big(U(z)\big)\mathcal{L}_1^*\big(U(x+z)\big)f_1\Big]\,\mathrm{d}x\,\mathrm{d}z \\ &= 8\beta\Big\{\big(\cos^3(\varphi)+\sin^3(\varphi)\big)f_1\sqrt{1-v^2}\Big[c^3(1-v^2)-3c^2v-c-\frac{2v^3}{(1-v^2)^2}\Big] \\ &\qquad -\big(\cos(\varphi)+\sin(\varphi)\big)f_1\sqrt{1-v^2}\Big[2vc^2+3c-\frac{2c}{1-v^2}-\frac{2v^3}{(1-v^2)^2}\Big]\Big\}.\end{aligned}$$

Two terms are left: one is

$$\begin{aligned}\mathbb{E}\big[\mathcal{I}_2\big] &= \iint_0^\infty \mathbb{E}\Big[\mathcal{L}_1^*\big(U(0)\big)\mathcal{L}_1^*\big(U(z)\big)\mathcal{L}_2^*f_0\Big]\,\mathrm{d}x\,\mathrm{d}z \\ &= -16c\int_0^\infty \alpha\,\mathrm{d}x\,\partial_v\Big[vf_0+\sqrt{1-v^2}\,\partial_v\Big[\sqrt{1-v^2}\,\partial_v\Big((1-v^2)f_0\Big)\Big]\Big],\end{aligned}$$

which is infinite, as in the OU case, but will simplify with part of the last term. The last term requires more computations, and we shall start by introducing some more notation. For $i,j\in\{1,2\}$, $i\neq j$ set

$$\begin{aligned}a &:= \iiint \mathbb{E}\Big[U_i(0)U_i(z)U_i(x+z)U_i(x+y+z)\Big]\,\mathrm{d}x\,\mathrm{d}y\,\mathrm{d}z\,,\\ b &:= \iiint \mathbb{E}\Big[U_i(0)U_i(z)\Big]\mathbb{E}\Big[U_j(x+z)U_j(x+y+z)\Big]\,\mathrm{d}x\,\mathrm{d}y\,\mathrm{d}z\,,\\ c &:= \iiint \mathbb{E}\Big[U_i(0)U_i(x+z)\Big]\mathbb{E}\Big[U_j(z)U_j(x+y+z)\Big]\,\mathrm{d}x\,\mathrm{d}y\,\mathrm{d}z\,,\\ d &:= \iiint \mathbb{E}\Big[U_i(0)U_i(x+y+z)\Big]\mathbb{E}\Big[U_j(z)U_j(x+z)\Big]\,\mathrm{d}x\,\mathrm{d}y\,\mathrm{d}z\,.\end{aligned}$$

Note that, by the stationarity of Q, $b=\int_0^\infty \alpha^2\,\mathrm{d}x$ and $c=\int_0^\infty \gamma(x)^2\,\mathrm{d}x$, where

$$\gamma(x) := \int_0^\infty \mathbb{E}\Big[U_i(0)U_i(x+z)\Big]\,\mathrm{d}z\,.$$

To ease notation, in the following series of four $\Im$ and $\Re$ we shall drop the subscript. However, the first symbol will always refer to $[U(0)e^{i\varphi}]$, the second to $[U(z)e^{i\varphi}]$, the third to $[U(x+z)e^{i\varphi}]$, and the last one to $[U(x+y+z)e^{i\varphi}]$. We will also use a compact notation $\Im^2$ for $\Im\Im$

etc. With all this notation we have

$$\begin{aligned}
\iiint_0^\infty \mathbb{E}\Big[\Im^4\Big]\,\mathrm{d}x\,\mathrm{d}y\,\mathrm{d}z = \iiint_0^\infty \mathbb{E}\Big[\Re^4\Big]\,\mathrm{d}x\,\mathrm{d}y\,\mathrm{d}z &= a\Big(\sin^4+\cos^4\Big)+2\sin^2\cos^2\big(b+c+d\big)\\
&= a+2\sin^2\cos^2\big(-a+b+c+d\big)\\
\iiint_0^\infty \mathbb{E}\Big[\Im^2\Re^2\Big]\mathrm{d}x\,\mathrm{d}y\,\mathrm{d}z = \iiint_0^\infty \mathbb{E}\Big[\Re^2\Im^2\Big]\mathrm{d}x\,\mathrm{d}y\,\mathrm{d}z &= b\Big(\sin^4+\cos^4\Big)+2\sin^2\cos^2\big(a-c-d\big)\\
&= b+2\sin^2\cos^2\big(a-b-c-d\big)\\
\iiint_0^\infty \mathbb{E}\Big[\Im\Re\Im\Re\Big]\mathrm{d}x\mathrm{d}y\mathrm{d}z = \iiint_0^\infty \mathbb{E}\Big[\Re\Im\Re\Im\Big]\mathrm{d}x\mathrm{d}y\mathrm{d}z &= c\Big(\sin^4+\cos^4\Big)+2\sin^2\cos^2\big(a-b-d\big)\\
&= c+2\sin^2\cos^2\big(a-b-c-d\big)\\
\iiint_0^\infty \mathbb{E}\Big[\Im\Re^2\Im\Big]\mathrm{d}x\mathrm{d}y\mathrm{d}z = \iiint_0^\infty \mathbb{E}\Big[\Re\Im^2\Re\Big]\mathrm{d}x\mathrm{d}y\mathrm{d}z &= d\Big(\sin^4+\cos^4\Big)+2\sin^2\cos^2\big(a-b-c\big)\\
&= d+2\sin^2\cos^2\big(a-b-c-d\big).
\end{aligned}$$

Setting $A := \big(-a+b+c+d\big)$, we finally get that

$$\begin{aligned}
\mathbb{E}\big[\mathcal{I}_4\big] &= 16\Big\{\Big[a+2A\sin^2\cos^2\Big]R_1(v)+\Big[\big(a-b\big)+4A\sin^2\cos^2\Big]R_2(v)\\
&\qquad+\Big[\big(a-c-d\big)+6A\sin^2\cos^2\Big]R_3(v)+\\
&\qquad\Big[\big(a-b-2c-2d\big)+12A\sin^2\cos^2\Big]R_4(v)+\Big[A+8A\sin^2\cos^2\Big]R_5(v)\Big\}\\
&= 16\Big\{A\Big(R_1+R_2+R_3+R_4+R_5\Big)+b\Big(R_1+R_3\Big)+(c+d)\Big(R_1+R_2-R_4\Big)\\
&\qquad+2A\,\sin^2\cos^2\Big(R_1+2R_2+3R_3+6R_4+4R_5\Big)\Big\},
\end{aligned}$$

where

$$\begin{aligned}
R_1(v) &= \Big(\partial_v\sqrt{1-v^2}\,\cdot\Big)^2\Big[\partial_v\big[(1-v^2)\,\partial_v f_0\big]\Big],\\
R_2(v) &= \partial_v\Big[\sqrt{1-v^2}\,\partial_v\Big[v\,\partial_v\big(\sqrt{1-v^2}f_0\big)+\frac{v^2}{\sqrt{1-v^2}}f_0\Big]\Big],\\
R_3(v) &= \big(\partial_v v\,\cdot\big)\Big[\partial_v\big[(1-v^2)\,\partial_v f_0\big]\Big],\\
R_4(v) &= \partial_v\Big[\frac{v^2}{\sqrt{1-v^2}}\,\partial_v\big(\sqrt{1-v^2}f_0\big)+\frac{v^3}{(1-v^2)}f_0\Big],\\
R_5(v) &= \Big\{\frac{v}{\sqrt{1-v^2}}\,\partial_v\Big[\sqrt{1-v^2}\,\partial_v\big[(1-v^2)\,\partial_v f_0\big]+2v\,\partial_v\big(\sqrt{1-v^2}f_0\big)+2\frac{v^2}{\sqrt{1-v^2}}f_0\\
&\qquad\qquad+3\sqrt{1-v^2}\,\partial_v\big(\sqrt{1-v^2}f_0\big)\Big]\\
&\qquad+6\frac{v^3}{(1-v^2)^{3/2}}\,\partial_v\big(\sqrt{1-v^2}f_0\big)+6\frac{v^4}{(1-v^2)^2}f_0+3\frac{v^2}{1-v^2}\,\partial_v\big(vf_0\big)\Big\}.
\end{aligned}$$

Finding the second order term of the density of states: ρ_2

One can now in principle compute $F(v,\varphi) = \mathbb{E}[\mathcal{I}_1+\mathcal{I}_2+\mathcal{I}_3+\mathcal{I}_4]$, and find f_2 by solving the compatibility equation (2.3.79). Then, one only needs to integrate to find $\bar{P}_2(v) = \int f_2 \,\mathrm{d}\varphi$, integrate again to find the correction term for the Lyapunov exponent $\kappa(\eta,\xi) = \eta \int v \,\mathrm{d}\bar{P}_2(v)$, and differentiate in η, ξ to find the second order term $\rho_2(\eta,\xi)$ of the DOS.

Computations in the general case are quite cumbersome, but important simplifications occur in some special cases. We shall discuss them now. First of all, we remark that

$$R_1 + R_3 = \Big\{\partial_v\big[(1-v^2)\,\partial_v\,\cdot\,\big]\Big\}^2\big(f_0\big)\,,$$

so that if the integrated covariance of the processes U_i is unitary ($\alpha = 1$), then proceeding as in the OU case one can show that $b = \int_0^\infty \alpha \,\mathrm{d}x$, and $\mathbb{E}[\mathcal{I}_2]$ is exactly $-\mathbb{E}[b(R_1+R_3)]$.

If we also have that U is Gaussian, then $A = 0$ and $\beta = 0$. This means that $\mathbb{E}[\mathcal{I}_3] = 0$ and the term deriving from $\mathcal{I}_4$ reduces to

$$\mathbb{E}\big[\mathcal{I}_4\big] = (c+d)\big(R_1 + R_2 - R_4\big)\,.$$

In this case, the dependence on φ of F disappears, f_2 is independent of φ, and the second order correction term to the density of states will be independent of ξ.

Remark that the dependence of f_1 on φ is only through odd powers of trigonometric functions. Then, in the case of a non-Gaussian process U, both $\mathbb{E}[\mathcal{I}_3]$ and $\mathbb{E}[\mathcal{I}_4]$ will show a dependence on φ only through even powers of trigonometric functions, and we expect the second order correction term of the DOS to have a non trivial dependence on ξ. We will show below that it is actually quite easy to construct a process with $\beta \neq 0$.

Example of a process for which $\beta \neq 0$.

Even though for many common examples the constant β defined in (2.3.77) is zero, this is not always the case. Indeed, there are examples of homogeneous Markov processes for which β does not vanish. We provide here an easy example of such a process.

Consider the continuous time process $A(t)$, $t \geq 0$ with a finite number of stated, $\{-1,0,1\}$. Let the transition rate matrix be given by

$$M = \begin{pmatrix} -3 & 2 & 1 \\ 2 & -2 & 0 \\ 1 & 0 & -1 \end{pmatrix}$$

Denote by $P_t(\cdot,\cdot)$ the probability of transition between states. In the following, we shall use italics lower case letters $a, b \in \{-1,0,1\}$ to denote the values of the process A, and boldface lower case letters $\mathbf{a}, \mathbf{b} \in \{e_1, e_2, e_3\}$ to denote the associated state vector. We shall represent state vectors using the standard basis $\{e_1, e_2, e_3\}$ of $\mathbb{R}^3$. In our notation, the same letter in italics and boldface character represents the same element so that, for example, we have the correspondence $e_1 = \mathbf{a} = a = -1$. When performing linear algebra operations, we will also use $\mathbf{a}^T$ to denote the transposed of the vector $\mathbf{a}$. When in need to denote the components of a vector $\mathbf{a}$, we will use $\mathbf{a} = (\mathbf{a}_1, \mathbf{a}_2, \mathbf{a}_3)$.

Using the Markov property and the definition of β given by (2.3.77) we have

$$\beta = \iint_0^\infty \mathbb{E}\Big[A(0)A(t)A(t+s)\Big]\,\mathrm{d}s\,\mathrm{d}t = \mathbb{E}\Big[A(0)\int_0^\infty \mathbb{E}\big[A(t)\big|A(0)\big]\int_0^\infty \mathbb{E}\big[A(s)\big|A(0)\big]\,\mathrm{d}s\,\mathrm{d}t\Big]$$
$$= \sum_a a\Big\{\int_0^\infty \sum_b \Big(P_t(a,b)\,b\Big)\,\mathrm{d}t\Big\}^2 = \sum_a a\Big\{\int_0^\infty \sum_b b\left(\mathbf{b}^T\,e^{Mt}\mathbf{a}\right)\mathrm{d}t\Big\}^2. \tag{2.3.81}$$

The eigenvalues for M are $\lambda_1 = 0, \lambda_2 = -3+\sqrt{3}$ and $\lambda_3 = -3-\sqrt{3}$, so that

$$e^{Mt} = M_1 + e^{\lambda_2 t}M_2 + e^{\lambda_3 t}M_3\,,$$

where the three matrices M_1, M_2, M_3 are given by

$$M_1 = \frac{1}{3}\begin{pmatrix} 1 & 1 & 1\\ 1 & 1 & 1\\ 1 & 1 & 1\end{pmatrix} \qquad M_2 = \frac{1}{6}\begin{pmatrix} 2-\sqrt{3} & -1+\sqrt{3} & -1\\ -1+\sqrt{3} & -2 & -1-\sqrt{3}\\ -1 & -1-\sqrt{3} & 1+\sqrt{3}\end{pmatrix}$$
$$M_3 = \frac{1}{6}\begin{pmatrix} 2+\sqrt{3} & -1-\sqrt{3} & -1\\ -1-\sqrt{3} & 2 & -1+\sqrt{3}\\ -1 & -1+\sqrt{3} & 1-\sqrt{3}\end{pmatrix}.$$

Let us compute the value of β. We start by analyzing the curly brackets $\{\cdot\}$ in the last term of equation (2.3.81). We have that

$$\sum_b b\left(\mathbf{b}\,M_1\mathbf{a}\right) = -1(\mathbf{a}_1+\mathbf{a}_2+\mathbf{a}_3) + 0 + 1(\mathbf{a}_1+\mathbf{a}_2+\mathbf{a}_3) = 0\,.$$

However, this sum is not zero for the other two terms, the ones containing M_2 and M_3. Setting

$$M_{23} = -\frac{1}{\lambda_2}M_2 - \frac{1}{\lambda_3}M_3 = \frac{1}{6}\begin{pmatrix} 1 & 0 & -1\\ 0 & 2 & -2\\ -1 & -2 & 2\end{pmatrix}$$

we have that

$$\int_0^\infty \sum_b b\left(\mathbf{b}\left(e^{\lambda_2 t}M_2 + e^{\lambda_3 t}M_3\right)\mathbf{a}\right)\mathrm{d}t = \sum_b b\left(\mathbf{b}\,M_{23}\mathbf{a}\right) = -(\mathbf{a}_1-\mathbf{a}_3) + (-\mathbf{a}_1-2\mathbf{a}_2-2\mathbf{a}_3)$$
$$= -2\mathbf{a}_1 - 2\mathbf{a}_2 + 3\mathbf{a}_3\,.$$

Inserting this into (2.3.81) we easily find that

$$\beta = -4+9 = 5 \neq 0\,.$$

2.4 Appendix

We collect here a few technical results needed for the proof of theorem 2.2. We shall retain the different notations introduced there.

Lemma 2.48. *We construct an explicit example of the subspaces $\mathcal{H}_n \subset \mathcal{H} = W^{3,2}(G)$ to be used in the proof of theorem 2.2 and lemma 2.49.*

Construction of $\mathcal{H}_n$. Divide $G = (-N, N)^3$ into cubes with sides of length $1/n$ and add one extra layer of cubes around it:

$$A_{i,j,k} := \big[i/n, (i+1)/n\big) \times \big[j/n, (j+1)/n\big) \times \big[k/n, (k+1)/n\big)\,,$$

for $i, j, k = -(nN+1), \dots, nN$. Define the piecewise (on every cube) polynomials of fourth degree as

$$\widetilde{h}(x) := \sum_{i,j,k=-(Nn+1)}^{Nn} \sum_{m=0}^{4} \frac{1}{m!} \langle a^{(m)}_{i,j,k} \,|\, x - y_{i,j,k} \rangle^{(m)} \; \mathbb{1}_{\{A_{i,j,k}\}}(x)\,, \tag{2.4.1}$$

where $y_{i,j,k}$ is the center of the cube $A_{i,j,k}$, $a^{(m)}_{i,j,k}$ are families of m-dimensional tensors and the brackets denote the relative tensor products (so that, for example, $\langle a^{(4)}_{i,j,k} \,|\, x - y_{i,j,k} \rangle^{(4)}$ denotes the product between the four-dimensional tensor $a^{(4)}_{i,j,k}$ and four copies of the vector $(x - y_{i,j,k})$). With these definitions $\widetilde{h}$ is a function defined on $[-N - \frac{1}{n}, N + \frac{1}{n})^3$, but its restriction to G does not belong to $\mathcal{H}$ in general since it may not even be continuous. Let Γ be a real, nonnegative, smooth function, with compact support contained in $[-1/2, 1/2]^3$ and such that $\int_{[-1/2,1/2]^3} \Gamma(y)\,\mathrm{d}y = 1$. Setting $\Gamma^n(y) := n^3\Gamma(ny)$ we can finally define $\mathcal{H}_n$ as the finite dimensional space of functions of the form $h(x) := (\widetilde{h} \star \Gamma^n)(x)$. Remark that $\widetilde{h}$ has been defined on a set larger than G, so that the convolution product is well defined for $x \in G$. □

Lemma 2.49. *For every $g \in \mathcal{C}^4(G)$, there exists a $g_n \in \mathcal{H}_n$ such that*

$$\big\|g - g_n\big\|_{\mathcal{H}} \le C\frac{1}{n}\big\|g\big\|_{\mathcal{C}^4(G)}\,.$$

Proof. Step 1 (Construction of g_n). For $i, j, k = -nN, \dots, nN - 1$ (which means that $y_{i,j,k} \in G$) set $a^{(m)}_{i,j,k} := D^m g(y_{i,j,k})$. For i, j, k such that $y_{i,j,k} \notin G$ set $a^{(m)}_{i,j,k} := D^m g(y')$, where y' is the nearest cube center; notice that the distance of these two points is at most the diameter of the cubes, which we call $2\delta := 2\sqrt{3}n^{-1}$. With the $a^{(m)}_{i,j,k}$ thus defined we construct the piecewise polynomial function $\widetilde{g}_n$ as in (2.4.1): on the cubes the centers of which are not in G, this function is just a copy of the function defined on the nearest cube with center in G. Finally, we define g_n as the convolution product $g_n := \Gamma^n \star \widetilde{g}_n$.

Step 2 (Estimates). For every multiindex $a \in \mathbb{N}^3$ such that $|a|_1 := a_1 + a_2 + a_3 \le 3$, we need to estimate

$$\int_G \Big|\partial^a(\Gamma^n \star \widetilde{g}_n)(x) - \partial^a g(x)\Big|^2 \mathrm{d}x\,.$$

To clarify the procedure to obtain an estimate for the above term we first give explicit computations for the case $a = e_1 = (1, 0, 0)$. Recall that, by definition,

$$\sum_{i,j,k} \int_{A_{i,j,,k}} \Gamma^n(x - y)\,\mathrm{d}y = \int_{[-(N+1/n),N+1/n)^3} \Gamma^n(x - y)\,\mathrm{d}y = 1\,.$$

For $a = (1, 0, 0)$, using twice the inequality $(a + b)^2 \leq 2(a^2 + b^2)$, we have

$$\begin{aligned}
\Big|\partial_1(\Gamma^n \star \widetilde{g}_n)(x) - \partial_1 g(x)\Big|^2 &= \Big|\sum_{i,j,k}\int_{A_{i,j,k}} -\partial_{y_1}\Gamma^n(x-y)\widetilde{g}_n(y)\mathrm{d}y \;-\; \partial_1 g(x)\Big|^2 \\
&\leq 2\Big\{\Big|\sum_{i,j,k}\int_{A_{i,j,k}} \Gamma^n(x-y)\partial_{y_1}\widetilde{g}_n(y)\mathrm{d}y - \partial_1 g(x)\Big|^2 \\
&\qquad + \Big|\sum_{i,j,k}\int_{\partial_1 A_{i,j,k}} \Gamma^n(x-y)\Big[\widetilde{g}_n(y_1^+, y_2, y_3) - \widetilde{g}_n(y_1^-, y_2, y_3)\Big]\mathrm{d}y_2\,\mathrm{d}y_3\Big|^2\Big\} \\
&\leq 4\Big\{\Big|\sum_{i,j,k}\int_{A_{i,j,k}} \Gamma^n(x-y)\big|\partial_{y_1}\widetilde{g}_n(y) - \partial_1\widetilde{g}_n(x)\big|\mathrm{d}y\Big|^2 + \Big|\partial_1\widetilde{g}_n(x) - \partial_1 g(x)\Big|^2 \\
&\qquad + \Big|\sum_{i,j,k}\int_{\partial_1 A_{i,j,k}} \Gamma^n(x-y)\Big[\widetilde{g}_n(y_1^+, y_2, y_3) - \widetilde{g}_n(y_1^-, y_2, y_3)\Big]\mathrm{d}y_2\,\mathrm{d}y_3\Big|^2\Big\} \\
&= 4\Big\{S_1 + S_2 + S_3\Big\}, \qquad (2.4.2)
\end{aligned}$$

where $\partial_1 A_{i,j,k}$ denotes the faces of the cubes orthogonal to the direction $e_1 := (1, 0, 0)$. Notice that the number of non zero terms in the sums over i, j, k of this proof is limited to 8 because the support of Γ^n can intersect at most 8 cubes. The term S_1 can be bounded by the square of

$$\Big(\sum_{i,j,k}\|\Gamma^n(x-\cdot)\|_{L^1(A_{i,j,k})}\Big)\big\|\partial_1\widetilde{g}_n(\cdot) - \partial_1\widetilde{g}_n(x)\big\|_{L^\infty(B_{1/(2n)}(x))},$$

where the second term is regarded as a function of y (x is fixed) and the L^∞-norm is taken on the ball $B_{1/2n}(x)$, which is the support of $\Gamma^n(x-y)$. The first term above is 1, and to estimate the second term the worst case is when y does not belong to the same cube as x: let us say that $y \in A^{(1)}$ and $x \in A^{(2)}$, where $y^{(1)}$ and $y^{(2)}$ are the centers of the cubes $A^{(1)}$ and $A^{(2)}$ respectively. We have therefore the bound

$$\begin{aligned}
&\big\|\partial_1\widetilde{g}_n(\cdot) - \partial_1\widetilde{g}_n(x)\big\|_{L^\infty(B_{1/(2n)}(x))} \\
&\qquad \leq \big\|\partial_1\widetilde{g}_n(\cdot) - \partial_{y_1}\widetilde{g}_n(y^{(1)})\big\|_{L^\infty} + \big|\partial_1 g(y^{(1)}) - \partial_1 g(y^{(2)})\big| + \big|\partial_{y_1}\widetilde{g}_n(y^{(2)}) - \partial_{y_1}\widetilde{g}_n(x)\big| \\
&\qquad \leq 4\delta\,\big\|D^2 g\big\|_{L^\infty(G)}.
\end{aligned}$$

This provides the bound for the term S_1. Similarly, for S_2 we have the bound

$$\begin{aligned}
\big|\partial_1\widetilde{g}_n(x) - \partial_1 g(x)\big| &\leq \big|\partial_1\widetilde{g}_n(x) - \partial_1 g(y^{(2)})\big| + \big|\partial_1 g(y^{(2)}) - \partial_1 g(x)\big| \\
&\leq 2\delta\|D^2 g\|_{L^\infty(G)}\,.
\end{aligned}$$

We still need to estimate S_3, which contains the boundary terms deriving from the discontinuities of $\widetilde{g}_n$ (and, in the general case, of its derivatives). This term requires more careful estimates. With $C_\Gamma := \sup_x \Gamma(x)$ and using the fact that $\|\Gamma^n(x-\cdot)\|_{L^1(\partial_1 A_{i,j,k})} \leq nC_\Gamma$, we

have

$$\begin{aligned}\sum_{i,j,k} &\|\Gamma^n(x-\cdot)\|_{L^1(\partial_1 A_{i,j,k})}\big\|\widetilde{g}_n(y_1^+,\cdot)-\widetilde{g}_n(y_1^-,\cdot)\big\|_{L^\infty(\partial_1 A_{i,j,k})}\\ &\le nC_\Gamma\sum_{i,j,k}\left\{\big\|\widetilde{g}_n(y_1^+,\cdot)-g(y_1,\cdot)\big\|_{L^\infty(\partial_1 A_{i,j,k})}+\big\|g(y_1,\cdot)-\widetilde{g}_n(y_1^-,\cdot)\big\|_{L^\infty(\partial_1 A_{i,j,k})}\right\}\\ &\le 8nC_\Gamma\delta^4\|D^4 g\|_{L^\infty(G)}=C\delta^3\|D^4 g\|_{L^\infty(G)}\,.\end{aligned}$$

The sums over i,j,k above are meant as sums over the faces $\partial_1 A_{i,j,k}$ intersecting the support of $\Gamma^n(x-\cdot)$, which are at most 4. Collecting all these results, we have the uniform bound

$$\Big|\partial_1(\Gamma^n\star\widetilde{g}_n)(x)-\partial_1 g(x)\Big|^2\le C\delta^2\Big(\|D^2 g\|^2_{L^\infty(G)}+\delta^4\|D^4 g\|^2_{L^\infty(G)}\Big)\,.$$

We proceed in the same way with higher order derivatives to get, for a generic derivative a of order $0\le|a|\le 3$, the estimate

$$\begin{aligned}\Big|\partial^a(\Gamma^n\star\widetilde{g}_n)(x)-\partial^a g(x)\Big|^2 \le& C\bigg\{\Big|\sum_{i,j,k}\int_{A_{i,j,k}}\Gamma^n(x-y)\big|\partial^a\widetilde{g}_n(y)-\partial^a\widetilde{g}_n(x)\big|\,\mathrm{d}y\Big|^2\\ &+\Big|\partial^a\widetilde{g}_n(x)-\partial^a g(x)\Big|^2+S_3^a\bigg\}\\ \le& C\Big(\|D^{|a|+1}g\|^2_{L^\infty(G)}\delta^2+S_3^a\Big)\,.\end{aligned}$$

For $a=0$, $S_3^a=0$, but in the general case the estimate of the term S_3^a is a little bit more delicate, since one gets more boundary terms. In particular, when integrating by parts, derivatives along different directions result in terms containing discontinuities of $\widetilde{g}_n$ and its derivatives along the faces (that we denote for brevity ∂A), edges (denoted $\partial^2 A$) or vertices (denoted $\partial^3 A$) of the cubes, while multiple derivatives along the same direction result in derivatives of Γ^n appearing. For example, for $a=(1,1,1)$ we get three kinds of terms:

$$\int_{\partial^3 A_{i,j,k}}\Gamma^n(x-y)\,\Delta\widetilde{g}_n(y)\,\mathrm{d}y\,,\qquad\int_{\partial^2 A_{i,j,k}}\Gamma^n(x-y)\,\Delta\partial\widetilde{g}_n(y)\,\mathrm{d}y\,,$$
$$\int_{\partial A_{i,j,k}}\Gamma^n(x-y)\,\Delta\partial^2\widetilde{g}_n(y)\,\mathrm{d}y\,,$$

where Δ denotes the jump of the function. For $a=(3,0,0)$ we also have terms like

$$\int_{\partial_1 A_{i,j,k}}\partial_1^2\Gamma^n(x-y)\,\Delta\widetilde{g}_n(y)\,\mathrm{d}y\,,\qquad\int_{\partial_1 A_{i,j,k}}\partial_1\Gamma^n(x-y)\,\Delta\partial_1\widetilde{g}_n(y)\,\mathrm{d}y\,,$$

and in the general case we find also terms like

$$\int_{\partial^2 A_{i,j,k}}\partial\Gamma^n(x-y)\,\Delta\widetilde{g}_n(y)\,\mathrm{d}y\,.$$

However, we can bound all this terms in the same way. We have that, for $m \in \mathbb{N}$ and $b, c \in \mathbb{N}^3$,

$$\int_{\partial^m A_{i,j,k}} \partial^b \Gamma^n(x) \mathrm{d}x \leq C_\Gamma \, n^{m+|b|} = C\delta^{-(m+|b|)} \,,$$
$$\left|\Delta \partial^c \widetilde{g}_n(y)\right| = \left|\partial^c \widetilde{g}_n(y^+) - \partial^c \widetilde{g}_n(y^-)\right| \leq 2\|D^4 g\|_{L^\infty(G)} \delta^{4-|c|} \,.$$

Therefore

$$S_3^a \leq C\|D^4 g\|^2_{L^\infty(G)} \delta^{2(4-|a|)} \,.$$

Remark that for all the terms composing S_3^a we always have $m+|b|+|c| = |a| \leq 3$. Summing up, we have obtained the bound

$$\begin{aligned} \left\|g - g_n\right\|^2_{\mathcal{H}} &= \sum_a \int_G \left|\partial^a (\Gamma^n \star \widetilde{g}_n)(x) - \partial^a g(x)\right|^2 \mathrm{d}x \\ &\leq C \sum_a \left(\|D^{|a|+1} g\|^2_{L^\infty(G)} \delta^2 + \|D^4 g\|^2_{L^\infty(G)} \delta^{2(4-|a|)} \right) \\ &\leq C \frac{1}{n^2} \|g\|^2_{\mathcal{C}^4(G)} \,. \end{aligned}$$

The lemma is proved. □

Corollary 2.50. *For any $h \in \mathcal{H}$, $\lim_{n\to\infty} \pi_{\mathcal{H}_n} h = h$.*

Proof. Fix any $\varepsilon > 0$. By density, there exist a $h_\varepsilon \in \mathcal{C}^4(G)$ such that $\|h - h_\varepsilon\|_{\mathcal{H}} \leq \varepsilon/2$. Also, by the continuity of the projection, $\|\pi_{\mathcal{H}_n} h - \pi_{\mathcal{H}_n} h_\varepsilon\|_{\mathcal{H}} \leq \|h - h_\varepsilon\|_{\mathcal{H}} \leq \varepsilon/2$. Since $\|\pi_{\mathcal{H}_n} h_\varepsilon - h_\varepsilon\|_{\mathcal{H}} \leq \|h_{\varepsilon,n} - h_\varepsilon\|_{\mathcal{H}}$, by the above lemma we get

$$\begin{aligned} \left\|\pi_{\mathcal{H}_n} h - h\right\|_{\mathcal{H}} &\leq \left\|\pi_{\mathcal{H}_n}(h - h_\varepsilon)\right\|_{\mathcal{H}} + \left\|\pi_{\mathcal{H}_n} h_\varepsilon - h_\varepsilon\right\|_{\mathcal{H}} + \left\|h_\varepsilon - h\right\|_{\mathcal{H}} \\ &\leq \varepsilon + C\frac{1}{n}\|h_\varepsilon\|_{\mathcal{C}^4(G)}. \end{aligned}$$

Therefore

$$\limsup_{n\to\infty} \left\|\pi_{\mathcal{H}_n} h - h\right\|_{\mathcal{H}} \leq \varepsilon \,,$$

and since ε is arbitrary, the corollary is proved. □

Chapter 3

Imaging with noise

An amazing fact in the analysis of imaging functionals, that has been recently pointed out and is currently under investigation, is that specific kinds of noise can improve the image quality or drastically reduce computational costs associated to the evaluation of the imaging functional. A strong motivation is the observation that time reversal refocusing is enhanced when the medium is randomly scattering. A time reversal experiment is based on the use of a special device called a time reversal mirror (TRM), which is an array of transducers that can be used as receivers and transmitters. A typical time reversal experiment consists in two steps. In a first step, a point source emits a short pulse that propagates through the medium and is recorded by the TRM used as an array of receivers. In a second step, the recorded signals are time reversed and reemitted by the TRM used as an array of transmitters. The waves then refocus on the original point source location. The striking observation is that refocusing is enhanced when the medium is randomly heterogeneous and scattering compared to the situation in which the medium is homogeneous [FCD00]. Moreover, the refocused pulse is statistically stable in the sense that it does not depend on the realization of the random medium, but only on the statistical distributions of its fluctuations [FGPS]. The technique has had some successful applications in the context where one can carry out physical time reversal, that is actually resend the signal physically into the medium to refocus the energy for kidney stone destruction for instance [FCD00].

In the context of sensor array imaging, a similar technique is employed. The typical experiment still consists in two steps. The first step is the experimental data acquisition: a point source emits a wave into the medium, the wave is reflected by the singularities in the propagation speed of the medium and is recorded by an array of receivers. The second step is a numerical processing of the recorded data: the recorded signals are time reversed and resent in a numerical simulation into a model medium to locate the singularities in the propagation speed. However, in contrast with physical time reversal, the fictitious medium employed in the imaging process cannot in general capture complex heterogeneities of the original medium. Therefore, research has focused on other approaches to improve the imaging process, such as the use of random sources [DFGS12, GP10, HSH08, SWH11, VB11, WNT12].

The classical approach to the imaging problem consists in performing a large number of experiments sounding each time a different source. For each experiment, the signal recorded at each receiver is stored and time reversed. This produces the data matrix. For each experiment, the time reversed data are reemitted (numerically) into the model medium in a new simulation, and the images obtained by each simulation are stacked. While this method provides a very good "image" of the medium, it involves gathering, storing and processing

huge amounts of data [Be09a, MDB11].

In the *noisy sources* approach we discuss in this chapter random sources are used and they are all sounded simultaneously (both in the case of probing and backpropagation) in a single experiment. In this case, the time reversed recorded signals from the physical experiment are stored in a data vector and resent simultaneously into the model medium in a single simulation. However, special care must be put in the choice of the noisy sources in order to ensure that the cross talk terms are very small and do not compromise image quality.

This approach with simultaneous sources means significant savings both in the data gathering, storing and processing stages. The analysis of this phenomenon in the imaging context is analogous to the analysis for time-reversal techniques [FGPS] and bears also similarities with techniques for passive imaging based on ambient noise sources [ABGW12, DeS09, GP09, GP11, YVD06]. The technique associated with ambient noise is another spectacular imaging situation that recently has received a lot of attention, in which one exploits the correlations in between recordings at different stations to infer some information about the medium. In this case as in the time-reversal case the presence of heterogeneities may improve the imaging result, here due to the enhanced phase space diversity that it produces.

Various blending type methods have been investigated in order to be able to exploit the simultaneous sources approach, in particular in the context of seismic imaging. In the case of classic vibratory source approaches one seeks to design a family of relatively long sources encoded such that the responses of each one of them can be identified in a preprocessing step, with oil companies often having their own patented approaches for the encoding [Ba10, Be09a]. More recently there has also been work on using simultaneous impulsive sources such as in the case of air guns that are fired with random time delays. The idea of "deblending" is to try to recover the full "single-survey" response [Be09a, HSH08]. In fact similar techniques can also be used in the context of blending at the receiver end [Be09b].

Applications of these different techniques are being investigated in different fields, from seismology [SCS06, LMD06, SCSR05, GSB08], to volcano monitoring [SRG06, BSC07, BSC08], to petroleum prospecting [CGS06] and medicine [FCD00].

Our point of view differs somewhat from the ones above in that we are not seeking deblending approaches. We will rather present a general theoretical framework that shows how, when data are viewed through the actual image, the cross-talk effect associated with simultaneity of sources may actually be effectively mitigated by the image formation algorithm: we do not need to deblend and to estimate the full single-survey response, because the appropriate imaging algorithm will actually produce the same image as if we had the full single-survey response. We articulate explicitly the crucial scaling assumptions that should be satisfied for this to happen. Our point of view is similar to that presented in [DaS09] where a least squares approach was used in the context of simultaneous sources for a particular data set and it was demonstrated how this could lead to surprisingly good results. The results obtained there are consistent with the analysis we set forth here with a probabilistic modeling of the sources.

This chapter is organized as follows. In section 3.1 we describe the mathematical setting and present the results about the classic experimental configuration in which the full multistatic response matrix can be recorded and used. We then present the *noisy sources* approach for two different kinds of random sources. In the cases of simultaneous sources emitting either stationary random signals or randomly delayed pulses we derive and discuss the main result regarding the normal operator and its stability in sections 3.2 and 3.3. In section 3.4 we use

high frequency analysis to obtain quantitative results on the image quality and statistical stability of this algorithm, when the goal is to image singular perturbations in the speed of propagation. We will see that the result strongly depends on the type of perturbation. The application of these results to a physical exploration problem is discussed in more detail in section 3.5 where we elaborate on the fascinating fact that imaging with simultaneous sources of the two types we have described gives a resolution that corresponds to the one obtained if the full multi-static response matrix was available, that is if we have the recordings of the responses at all of the receivers for all the surveys where only one source emits at a time. Simple numerical results are also presented to support this result.

The main mechanism that allows us to obtain this striking result is the separation of scales that is inherent in our formulation and that serves to eliminate cross-talk terms that otherwise could contaminate the image obtained using simultaneous sources.

Notation

We use italics characters to denote scalar variables and boldfaced characters to denote vectors: for example $x \in \mathbb{R}$, but $\boldsymbol{x} = (x, y, z) \in \mathbb{R}^3$. B_r will denote the ball of radius r in $\mathbb{R}^d$ for d equals 2 or 3: $B_r = \{\boldsymbol{x} \in \mathbb{R}^d | \, |\boldsymbol{x}| \leq r\}$. When the ball is not centered in the origin, we will use the notation $B_r(\boldsymbol{x})$ to specify its center $\boldsymbol{x}$. In section 3.4 we will also need some notation for the order of amplitude of some variables. There, we will use $A = O(\varepsilon)$ to indicate that the quantity A is *exactly* of order ε, which is to say that there exists constants $0 < c < C < \infty$ such that $c\varepsilon < A < C\varepsilon$. To say that A is of order ε or smaller we will write $A \leq O(\varepsilon)$.

The Fourier transform of a function $f(t)$ is defined by

$$\widehat{f}(\omega) = \int f(t) e^{i\omega t} \, \mathrm{d}t \, .$$

We will also have to work with complex numbers or functions: in this case, we will use a bar to denote the complex conjugate. We do so to avoid confusion with the Fourier transform of the conjugate complex functions: if $\overline{G}$ is the complex conjugate of G, then $\widehat{\overline{G}}$ is the Fourier transform of the complex conjugate of G, while $\overline{\widehat{G}}$ is the complex conjugate of the Fourier transform of G.

Given an operator $\mathcal{L}$, we will denote by $\mathcal{L}^*$ its adjoint.

3.1 Mathematical formulation and classical approach

This section is devoted to the description of the mathematical model lying behind the imaging algorithm. We will present the basic equation governing the propagation of waves in a medium, the classical wave equation, and the method to solve it through the use of the associated Green function. We will also present the Born approximation, which is by now part of the classical mathematical setting to treat imaging problems.

Given this mathematical setting, we introduce the operators modelling the direct and inverse problem in the case of individual or simultaneous sources. Finally, we illustrate the imaging process by detailing the classical approach to the imaging problem, where each source is sounded in a different experiment and the full multi-static response (MSR) matrix

is available. This will serve as a comparison for the following sections, where we will explain the approach using simultaneous random sources.

3.1.1 The wave equation with random sources

We consider the solution u of the wave equation in a three-dimensional inhomogeneous medium:

$$\frac{1}{c^2(\boldsymbol{x})}\frac{\partial^2 u}{\partial t^2} - \Delta_{\boldsymbol{x}} u = n(t,\boldsymbol{x})\,. \tag{3.1.1}$$

The term $n(t,\boldsymbol{x})$ models the point sources emitting deterministic or random signals. For instance, in the context of seismic exploration they could be point sources emitting well separated short pulses in a sequence of experiments. We discuss this classical configuration in subsection 3.1.5. They could be sources emitting simultaneously stationary random signals. We discuss this configuration in section 3.2. They could also be simultaneous blended (i.e. time-delayed impulsive) sources emitting from the surface. We discuss this configuration in section 3.3.

In the wave equation above, $c(\boldsymbol{x})$ denotes the velocity of propagation of waves at a point $\boldsymbol{x} = (x, y, z) \in \mathbb{R}^3$ in the medium. We shall rewrite the velocity in a more convenient form as

$$c^{-2}(\boldsymbol{x}) = c_0^{-2}(\boldsymbol{x}) + \delta c^{-2}(\boldsymbol{x})\ , \tag{3.1.2}$$

where $c_0(\boldsymbol{x})$ is the known **smooth** background velocity and $\delta c^{-2}(\boldsymbol{x})$ is the velocity perturbation that we want to estimate, whose spatial support is contained in some bounded domain $\Omega \subset \mathbb{R}^3$.

The direct and inverse problems can be formulated in terms of the background Green's function, the fundamental solution of the wave equation (3.1.1).

3.1.2 The background Green's function

The solution of the wave equation (3.1.1) with the background velocity $c_0(\boldsymbol{x})$ has the integral representation

$$u(t,\boldsymbol{x}) = \iint G(s,\boldsymbol{x},\boldsymbol{y})\, n(t-s,\boldsymbol{y})\,\mathrm{d}s\,\mathrm{d}\boldsymbol{y}\,, \tag{3.1.3}$$

where $G(t,\boldsymbol{x},\boldsymbol{y})$ is the time-dependent causal Green's function, which is to say the fundamental solution of the wave equation with a Dirac delta (in both space and time) source term

$$\frac{1}{c_0^2(\boldsymbol{x})}\frac{\partial^2 G}{\partial t^2} - \Delta_{\boldsymbol{x}} G = \delta(t)\delta(\boldsymbol{x}-\boldsymbol{y})\,, \tag{3.1.4}$$

starting from $G(0,\boldsymbol{x},\boldsymbol{y}) = \partial_t G(0,\boldsymbol{x},\boldsymbol{y}) = 0$, and continued on the negative time axis by $G(t,\boldsymbol{x},\boldsymbol{y}) = 0$, $\forall t \le 0$.

For a homogeneous background (constant c_0), the Green's function in the Fourier domain is given by

$$\widehat{G}(\omega,\boldsymbol{x},\boldsymbol{y}) = \frac{1}{4\pi|\boldsymbol{x}-\boldsymbol{y}|}\exp\Big(i\frac{\omega}{c_0}|\boldsymbol{x}-\boldsymbol{y}|\Big)\,. \tag{3.1.5}$$

For a general smoothly varying background, the high-frequency behavior of the Green's function is related to the travel time and it is given by the optical (or acoustical) geometric approximation [BCS]

$$\widehat{G}(\omega,\boldsymbol{x},\boldsymbol{y}) \simeq \mathcal{A}(\boldsymbol{x},\boldsymbol{y})\exp\big(i\omega\,\mathcal{T}(\boldsymbol{x},\boldsymbol{y})\big)\,, \tag{3.1.6}$$

which is valid when the frequency ω is much larger than the inverse of the travel time $\mathcal{T}(\boldsymbol{x},\boldsymbol{y})$. Here the coefficients $\mathcal{A}(\boldsymbol{x},\boldsymbol{y})$ and $\mathcal{T}(\boldsymbol{x},\boldsymbol{y})$ are smooth except at $\boldsymbol{x}=\boldsymbol{y}$. The amplitude $\mathcal{A}(\boldsymbol{x},\boldsymbol{y})$ satisfies a transport equation and the travel time $\mathcal{T}(\boldsymbol{x},\boldsymbol{y})$ satisfies the eikonal equation.

3.1.3 The scattering operator and the Born approximation

In this section we introduce the scattering operator, that is, the mapping from velocity perturbations to the data. We will show that the exact scattering operator is a nonlinear operator, which makes the treatment of the inverse problem (considered in the next subsection) very difficult, if not impossible. We then have to introduce the classical Born approximation, which results in a linearization of the scattering operator and opens the possibility to work on the inverse problem. At the end of this subsection, we will also detail the explicit form of the scattering operator in both the individual and simultaneous sources settings, in the Born approximation. Our analysis pertaining to imaging and inverse scattering is based on this operator.

The scattering operator

We assume that signals are observed at a passive sensor array $(\boldsymbol{x}_r)_{r=1,\dots,N_r}$ for some time interval $[-T/2,T/2]$. What is usually required is that the recording time T should be larger than the typical travel time for a round trip from the array to the search region, so as to guarantee that the backscattered signals are completely recorded. This is what is needed in the classical setting detailed in subsection 3.1.5. In the case of noise blended sources that is considered in section 3.3 we will also require that the recording time T be much larger than the typical time delays, while for stationary random sources (section 3.2) the additional condition is that it should be taken much larger that the inverse of the bandwidth of the noise sources (i.e. much larger than the decoherence time).

The recorded signals form the data set $\mathbf{D}$, which for each experiment is given by the vector of functions

$$\big(D(t,\boldsymbol{x}_r)\big)_{r=1,\dots,N_r,\, t\in[-T/2,T/2]}$$

representing the signal recorded by the sensor located at $\boldsymbol{x}_r$. These data are modeled by the scattering operator

$$\mathbf{F} : \big(\delta c^{-2}(\boldsymbol{x})\big)_{\boldsymbol{x}\in\Omega} \to \mathbf{D}\,.$$

We describe now how to obtain the scattering operator. Using the decomposition of the background velocity of propagation (3.1.2) we can write the solution of the wave equation

$$\Big(\frac{1}{c_0^{-2}(\boldsymbol{x})}+\frac{1}{\delta c^2(\boldsymbol{x})}\Big)\frac{\partial^2 u}{\partial t^2}-\Delta_{\boldsymbol{x}} u = n(t,\boldsymbol{x})\,. \tag{3.1.7}$$

as the sum of two terms

$$u(t,\boldsymbol{x}) = u_0(t,\boldsymbol{x}) + u_1(t,\boldsymbol{x})\,,$$

where u_0 is the solution of the wave equation with background velocity $c_0(\boldsymbol{x})$, which is to say the propagating wave if the perturbation were not present. In the Fourier domain u_0 is given by

$$\widehat{u}_0(\boldsymbol{x},\omega) = \int \widehat{\mathbf{G}}_0(\omega,\boldsymbol{x},\boldsymbol{y})\widehat{n}(\omega,\boldsymbol{y})\,\mathrm{d}\boldsymbol{y}\,, \tag{3.1.8}$$

where $\mathbf{G}_0$ is the Green function for the wave equation with background velocity of prop-

agation $c_0(\boldsymbol{x})$. Then, the wave equation (3.1.7) can be transformed into a wave equation for u_1 with background velocity of propagation c_0 and source term which is given by $\eta = -\delta c^{-2}(\boldsymbol{x})\,\partial_t^2 u$:

$$\frac{1}{c_0^2(\boldsymbol{x})}\frac{\partial^2 u_1}{\partial t^2} - \Delta_{\boldsymbol{x}} u_1 = -\delta c^{-2}(\boldsymbol{x})\frac{\partial^2 u}{\partial t^2}\,.$$

u_1 is the component of the propagating wave which is scattered by the perturbation: it is the wave recorded by the array of sensors to create the data set $\mathbf{D}$. In the Fourier domain u_1 is given by

$$\widehat{u}_1(\boldsymbol{x},\omega) = \omega^2 \int \widehat{\mathbf{G}}_0(\omega,\boldsymbol{x},\boldsymbol{y})\delta c^{-2}(\boldsymbol{y})\,\widehat{u}(\boldsymbol{y},\omega)\,\mathrm{d}\boldsymbol{y}\,. \tag{3.1.9}$$

This expression is exact, and it is known as the Lippmann-Schwinger equation. Using this formula one can express the action of the exact scattering operator in terms of some kernel $\mathbf{Q}$:

$$\mathbf{D} = \big(\mathbf{F}\delta c^{-2}\big)(t,\boldsymbol{x}_r) = \int \mathbf{Q}(t,\boldsymbol{x}_r,\boldsymbol{y})\delta c^{-2}(\boldsymbol{y})\,\mathrm{d}\boldsymbol{y}\,.$$

The Fourier representation of the kernel $\mathbf{Q}$ obtained from the Lippmann-Schwinger equation (3.1.9) is

$$\widehat{\mathbf{Q}}(\omega,\boldsymbol{x}_r,\cdot) = \omega^2\,\widehat{\mathbf{G}}_0(\omega,\boldsymbol{x}_r,\cdot)\,\widehat{u}(\cdot,\omega)\,. \tag{3.1.10}$$

The Born approximation

As we can see from (3.1.10), the kernel $\mathbf{Q}$ depends on the function $u = u_0 + u_1$. Inspecting (3.1.8), we see that the dependence of u_0 on δc^{-2} is quite easy. But the dependence of u_1 is much more complex. Indeed, the exact scattering operator $\mathbf{F}$ is a nonlinear operator. Inverting it, which is to say try to find the velocity perturbation from the recorded data (this is the aim of the imaging process, which is detailed in the next subsection), is therefore a highly nontrivial task. Indeed, considering the huge amounts of data one is usually confronted with in typical imaging problems, inverting the functional $\mathbf{F}$ can be considered from a practical point of view as impossible. Then, in order to be able to deal with the problem one is forced to introduce some approximations.

The Born approximation (or single-scattering approximation) consists in replacing $\widehat{u}$ on the right hand side of (3.1.9) with the field $\widehat{u}_0$, [BCS]. Using (3.1.8) this gives:

$$\widehat{u}_1(\boldsymbol{x},\omega) \simeq \omega^2 \iint \widehat{\mathbf{G}}_0(\omega,\boldsymbol{x},\boldsymbol{y})\delta c^{-2}(\boldsymbol{y})\,\widehat{\mathbf{G}}_0(\omega,\boldsymbol{y},\boldsymbol{z})\widehat{n}(\omega,\boldsymbol{z})\,\mathrm{d}\boldsymbol{z}\,\mathrm{d}\boldsymbol{y}\,.$$

This approximation is valid if the field u_1 scattered by the perturbation δc^{-2} is small compared to the incident field u_0. In the Born approximation, the kernel $\mathbf{Q}$ in the Fourier domain is given by

$$\widehat{\mathbf{Q}}(\omega,\boldsymbol{x}_r,\cdot) = \omega^2 \int_\Omega \widehat{\mathbf{G}}_0(\omega,\boldsymbol{x}_r,\cdot)\widehat{\mathbf{G}}_0(\omega,\cdot,\boldsymbol{z})\widehat{n}(\omega,\boldsymbol{z})\,\mathrm{d}\boldsymbol{z}\,.$$

Using this linearized approximation of the kernel $\mathbf{Q}$ results in substantial simplifications in the computation of the scattering operator, making the inversion process accessible. In the following, we will always work in the Born approximation.

The structure of recorded data set varies according to the kind of experiment performed, implying that different scattering operators must be introduced to model these data if we

use the classical scheme with a large number of experiment with a single source, or if we are performing a single experiment using simultaneous (random) sources. The two operators are described below.

Individual sources

In the case when it is possible to emit a short pulse $f(t)$ from each point source located at $\boldsymbol{y}_s$, $s = 1, \ldots, N_s$, the multi-offset data are given by the matrix of signals

$$\mathbf{d} = \big(d(t, \boldsymbol{x}_r, \boldsymbol{y}_s)\big)_{r=1,\ldots,N_r,\, s=1\ldots,N_s,\, t\in[-T/2,T/2]}$$

recorded by the sensor located at $\boldsymbol{x}_r$ when the source at $\boldsymbol{y}_s$ emits the short pulse at time 0. These data are modeled by the operator

$$\mathcal{F}_0 : \big(\delta c^{-2}(\boldsymbol{x})\big)_{\boldsymbol{x}\in\Omega} \to \big(d(t, \boldsymbol{x}_r, \boldsymbol{y}_s)\big)_{r=1,\ldots,N_r,\, s=1\ldots,N_s,\, t\in[-T/2,T/2]}\,.$$

Its action

$$\big(\mathcal{F}_0\delta c^{-2}\big)(t, \boldsymbol{x}_r, \boldsymbol{y}_s) = \int_\Omega Q_0(t, \boldsymbol{x}_r, \boldsymbol{y}_s, \boldsymbol{x})\delta c^{-2}(\boldsymbol{x})\,\mathrm{d}\boldsymbol{x}$$

is described by the kernel

$$Q_0(t, \boldsymbol{x}_r, \boldsymbol{y}_s, \boldsymbol{x}) = -\frac{\partial^2}{\partial t^2}\iint G(t_2, \boldsymbol{x}_r, \boldsymbol{x})G(t_1, \boldsymbol{x}, \boldsymbol{y}_s)\, f(t - t_1 - t_2)\,\mathrm{d}t_1\mathrm{d}t_2\,,$$

which in the Fourier domain is given by

$$\widehat{Q}_0(\omega, \boldsymbol{x}_r, \boldsymbol{y}_s, \boldsymbol{x}) = \omega^2\,\widehat{G}(\omega, \boldsymbol{x}_r, \boldsymbol{x})\widehat{G}(\omega, \boldsymbol{x}, \boldsymbol{y}_s)\,\widehat{f}(\omega)\,. \tag{3.1.11}$$

Simultaneous sources

In the situation in which all sources emit simultaneously, the data consist of the vector of signals

$$\boldsymbol{d} = \big(d(t, \boldsymbol{x}_r)\big)_{r=1,\ldots,N_r,\, t\in[-T/2,T/2]}$$

recorded by the sensor located at $\boldsymbol{x}_r$. The source term $n(t, \boldsymbol{x})$ of the wave equation is in this case spatially supported on the whole set of point sources. These data are modeled by the operator

$$\mathcal{F} : \big(\delta c^{-2}(\boldsymbol{x})\big)_{\boldsymbol{x}\in\Omega} \to \big(d(t, \boldsymbol{x}_r)\big)_{r=1,\ldots,N_r,\, t\in[-T/2,T/2]}$$

with

$$\big(\mathcal{F}\delta c^{-2}\big)(t, \boldsymbol{x}_r) = \int_\Omega Q(t, \boldsymbol{x}_r, \boldsymbol{x})\delta c^{-2}(\boldsymbol{x})\,\mathrm{d}\boldsymbol{x}\,, \tag{3.1.12}$$

where the kernel Q is

$$Q(t, \boldsymbol{x}_r, \boldsymbol{x}) = -\frac{\partial^2}{\partial t^2}\iiint G(t_1, \boldsymbol{x}_r, \boldsymbol{x})G(t_2, \boldsymbol{x}, \boldsymbol{y})\, n(t - t_1 - t_2, \boldsymbol{y})\,\mathrm{d}t_1\,\mathrm{d}t_2\,\mathrm{d}\boldsymbol{y}\,, \tag{3.1.13}$$

which in the Fourier domain reads as

$$\widehat{Q}(\omega, \boldsymbol{x}_r, \boldsymbol{x}) = \omega^2\int \widehat{G}(\omega, \boldsymbol{x}_r, \boldsymbol{x})\widehat{G}(\omega, \boldsymbol{x}, \boldsymbol{y})\,\widehat{n}(\omega, \boldsymbol{y})\,\mathrm{d}\boldsymbol{y}\,. \tag{3.1.14}$$

3.1.4 The imaging problem

The imaging problem (inverse problem) aims at inverting the mapping $\mathcal{F}_0$ or $\mathcal{F}$ in order to reconstruct the velocity perturbation $\delta c^{-2}(\boldsymbol{x})$ from the data set.

When the sources can be used separately and the full data set or multi-static response matrix $\mathbf{d} = \big(d(t, \boldsymbol{x}_r, \boldsymbol{y}_s)\big)_{r=1,\dots,N_r,\, s=1\dots,N_s,\, t\in[-T/2,T/2]}$ is available, then the usual (least-square) inversion process consists in applying the operator $(\mathcal{F}_0^*\mathcal{F}_0)^{-1}\mathcal{F}_0^*$ to the data set $\mathbf{d}$, where the adjoint of the scattering operator is

$$\big(\mathcal{F}_0^*\mathbf{d}\big)(\boldsymbol{x}) = \sum_{r=1}^{N_r}\sum_{s=1}^{N_s}\int_{-\frac{T}{2}}^{\frac{T}{2}} Q_0(t, \boldsymbol{x}_r, \boldsymbol{y}_s, \boldsymbol{x}) d(t, \boldsymbol{x}_r, \boldsymbol{y}_s)\,\mathrm{d}t\,.$$

When simultaneous sources are used and the data set consists of the vector of recorded signals $\boldsymbol{d} = \big(d(t, \boldsymbol{x}_r)\big)_{r=1,\dots,N_r,\, t\in[-T/2,T/2]}$, then the inversion process consists in applying the operator $(\mathcal{F}^*\mathcal{F})^{-1}\mathcal{F}^*$ to the data set $\boldsymbol{d}$, where the adjoint of the scattering operator is

$$\big(\mathcal{F}^*\boldsymbol{d}\big)(\boldsymbol{x}) = \sum_{r=1}^{N_r}\int_{-\frac{T}{2}}^{\frac{T}{2}} Q(t, \boldsymbol{x}_r, \boldsymbol{x}) d(t, \boldsymbol{x}_r)\,\mathrm{d}t\,.$$

Note that the kernel of the adjoint $\mathcal{F}^*$ depends on the background Green's function $G(t, \boldsymbol{x}, \boldsymbol{y})$ and on the source term $n(t, \boldsymbol{y})$. This means that we need to know the signals emitted by the sources in order to be able to apply the adjoint to the recorded data.

In both cases, the full least square inversion is in practice too complicated and the normal operator $\mathcal{F}_0^*\mathcal{F}_0$ or $\mathcal{F}^*\mathcal{F}$ is usually dropped in the inversion process. This procedure gives a reasonable estimate $\widetilde{\delta c^{-2}}(\boldsymbol{x})$ of the velocity perturbation $\delta c^{-2}(\boldsymbol{x})$ provided the normal operator is close to the identity operator. This is approximately true for $\mathcal{F}_0^*\mathcal{F}_0$ when the multi-static response matrix is available and we will recall this result in subsection 3.1.5. In [DFGS12] it is proved that this is also approximately true for $\mathcal{F}^*\mathcal{F}$ in the case of two special models of random sources. We will detail this result in the next sections. In particular, in sections 3.2 and 3.3 we will carry out a detailed statistical analysis of the kernel of the normal operator $\mathcal{F}^*\mathcal{F}$ in the two special cases mentioned. The kernel of the normal operator is given by

$$\mathcal{F}^*\mathcal{F}(\boldsymbol{x}, \boldsymbol{x}') = \sum_{r=1}^{N_r}\int_{-\frac{T}{2}}^{\frac{T}{2}} Q(t, \boldsymbol{x}_r, \boldsymbol{x}) Q(t, \boldsymbol{x}_r, \boldsymbol{x}')\,\mathrm{d}t\,; \tag{3.1.15}$$

we will show that this kernel is statistically stable (i.e. its fluctuations are smaller than its expectation) and that it is concentrated along the diagonal $\boldsymbol{x} \simeq \boldsymbol{x}'$.

Remark 3.1. The adjoint operator $\mathcal{F}^*$, and therefore the imaging functional $\big(\mathcal{F}^*\boldsymbol{d}\big)(\boldsymbol{x})$, can be computed solving only two wave equations. For the adjoint operator $\mathcal{F}_0^*$ the optimal scheme requires $2N_s$ calls to the numerical wave solver. The two methods are explained and discussed in subsection 3.5.1.

3.1.5 The classical setting: multi-offset sources

We assume in this section that multi-offset data can be recorded. The sources are localized at the points $(\boldsymbol{y}_s)_{s=1,\dots,N_s}$ and they emit short pulses $\big(f(t)\big)_{t\in\mathbb{R}}$. The data acquisition is achieved during a sequence of N_s experiments. In the s^{th} experiment, the source term in the wave equation (3.1.1) is

$$n(t, \boldsymbol{x}) = f(t)\delta(\boldsymbol{x} - \boldsymbol{y}_s)\,.$$

We stress that in the following proof it is important to assume that the duration of the pulse f is much smaller than the typical travel time.

The normal operator is

$$\big(\mathcal{F}_0^*\mathcal{F}_0\delta c^{-2}\big)(\boldsymbol{x}) = \int_\Omega \mathcal{F}_0^*\mathcal{F}_0(\boldsymbol{x},\boldsymbol{x}')\delta c^{-2}(\boldsymbol{x}')\,\mathrm{d}\boldsymbol{x}'\,, \tag{3.1.16}$$

with the kernel given by

$$\mathcal{F}_0^*\mathcal{F}_0(\boldsymbol{x},\boldsymbol{x}') = \sum_{r=1}^{N_r}\sum_{s=1}^{N_s}\int_{-\frac{T}{2}}^{\frac{T}{2}} Q_0(t,\boldsymbol{x}_r,\boldsymbol{y}_s,\boldsymbol{x})Q_0(t,\boldsymbol{x}_r,\boldsymbol{y}_s,\boldsymbol{x}')\,\mathrm{d}t\,. \tag{3.1.17}$$

We assume that T is large enough, so that the backscattered signals are completely recorded over $[-T/2,T/2]$. This means that T should be larger than the typical travel time for a round trip from the array to the search region. We can then replace the integral over $[-T/2,T/2]$ in (3.1.17) by the integral over $\mathbb{R}$. Using (3.1.11) and applying Parseval formula to express the quantities in the Fourier domain, we find the following expression for the kernel of the normal operator:

$$\begin{aligned}\mathcal{F}_0^*\mathcal{F}_0(\boldsymbol{x},\boldsymbol{x}') = \frac{1}{2\pi}\int \omega^4\big|\widehat{f}(\omega)\big|^2\Big[\sum_{s=1}^{N_s}\overline{\widehat{G}}(\omega,\boldsymbol{x},\boldsymbol{y}_s)\widehat{G}(\omega,\boldsymbol{x}',\boldsymbol{y}_s)\Big]\\ \times\Big[\sum_{r=1}^{N_r}\overline{\widehat{G}}(\omega,\boldsymbol{x}_r,\boldsymbol{x})\widehat{G}(\omega,\boldsymbol{x}_r,\boldsymbol{x}')\Big]\mathrm{d}\omega\,.\end{aligned} \tag{3.1.18}$$

When the duration of the pulse f is much smaller than the typical travel time (which is a usual assumption), it is possible to use the high-frequency approximation of the Green's function (3.1.6) and to perform a detailed resolution analysis which shows that the kernel $\mathcal{F}_0^*\mathcal{F}_0(\boldsymbol{x},\boldsymbol{x}')$ is concentrated along the diagonal band $\boldsymbol{x}\simeq\boldsymbol{x}'$. This comes from the fact that the two squares brackets in the expression in (3.1.18) behave like the kernel studied in appendix B which is concentrated along the diagonal band. The width of the diagonal band depends on the source and receiver array apertures. If the source and receiver arrays densely sample a domain on a two-dimensional surface whose diameter is (at least) of the order of the distance from the arrays to the points $\boldsymbol{x}$ and $\boldsymbol{x}'$, then the width of the diagonal band is of the order of the wavelength.

This proves that the normal operator $\mathcal{F}_0^*\mathcal{F}_0$ is close to the identity operator, and the error committed dropping it in the inversion process is small.

3.2 Stationary random sources

In this section we consider the situation with stationary random sources. This is our first example of random sources for which the use of a single experiment with simultaneous sources still produces a good quality image of the medium. We will describe the imaging functional to use in this setting and prove its statistical stability. The main result is that the algorithm is statistically stable if the recording time is sufficiently long, which is to say much longer than the decoherence time of the random sources used. But since from a practical point of

view it is not difficult today to create (or simulate) random or heterogeneous source signals whose characteristic time scale is small compared to the travel time to the probed region, this is not a very restrictive condition and the large recording time can actually be of the same order of the recording time needed in the classical setting described above.

We assume that the sources are localized at the points $(\boldsymbol{y}_s)_{s=1,\dots,N_s}$ and emit stationary random signals $\big(n_s(t)\big)_{t\in\mathbb{R}}$. The source term in the wave equation (3.1.1) has the form

$$n(t,\boldsymbol{x}) = \sum_{s=1}^{N_s} n_s(t)\,\delta(\boldsymbol{x}-\boldsymbol{y}_s)\,. \tag{3.2.1}$$

The random functions $\big(n_s(t)\big)_{t\in\mathbb{R}}$, $s=1,\dots,N_s$, are independent, zero-mean, stationary Gaussian processes with autocorrelation function

$$\big\langle n_s(t_1)n_{s'}(t_2)\big\rangle = \delta_{ss'}F(t_2-t_1)\,. \tag{3.2.2}$$

Here $\delta_{ss'}$ is the Kronecker symbol and $\langle\,\cdot\,\rangle$ stands for statistical average with respect to the distribution of the random sources. Note that we model here in terms of discrete sources at $\boldsymbol{y}_s$, $s=1,\dots,N_s$. However, as described in appendix A, our analysis also captures the main aspects in a situation with a continuum of sources.

In the proof it is important to assume that the decoherence time of the random sources is much smaller than typical travel times, i.e. that the width of the function F is much smaller than typical travel times. The Fourier transform $\widehat{F}$ of the time correlation function is a nonnegative, even, real-valued function, and by the Wiener-Khintchine theorem it is proportional to the power spectral density of the sources [Ri]. Note that we have

$$\big\langle \widehat{n}_s(\omega)\overline{\widehat{n}_{s'}}(\omega')\big\rangle = 2\pi\delta_{ss'}\widehat{F}(\omega)\delta(\omega-\omega')\,. \tag{3.2.3}$$

Using the stationarity of the noise sources, the expectation of the kernel of the normal operator (3.1.15) can be rewritten as

$$\big\langle \mathcal{F}^*\mathcal{F}(\boldsymbol{x},\boldsymbol{x}')\big\rangle = T\sum_{r=1}^{N_r}\big\langle Q(0,\boldsymbol{x}_r,\boldsymbol{x})Q(0,\boldsymbol{x}_r,\boldsymbol{x}')\big\rangle\,.$$

Substituting the Fourier representation (3.1.14) into this expression and using (3.2.3) we find that the expectation of the kernel of the normal operator is for any T

$$\begin{aligned}\big\langle \mathcal{F}^*\mathcal{F}(\boldsymbol{x},\boldsymbol{x}')\big\rangle = \frac{T}{2\pi}\int \omega^4\widehat{F}(\omega)\Big[\sum_{s=1}^{N_s}\overline{\widehat{G}}\big(\omega,\boldsymbol{x},\boldsymbol{y}_s\big)\widehat{G}\big(\omega,\boldsymbol{x}',\boldsymbol{y}_s\big)\Big]\\ \times\Big[\sum_{r=1}^{N_r}\overline{\widehat{G}}\big(\omega,\boldsymbol{x}_r,\boldsymbol{x}\big)\widehat{G}\big(\omega,\boldsymbol{x}_r,\boldsymbol{x}'\big)\Big]\mathrm{d}\omega\,.\end{aligned} \tag{3.2.4}$$

Note that the mean kernel has the same expression as the approximation obtained for the kernel of the normal operator (3.1.18) when the multi-static response matrix is available and the recording time T is larger than the typical travel time. Therefore it enjoys the same property, that is to say, it is localized on the diagonal band $\boldsymbol{x}\simeq\boldsymbol{x}'$. The important question is whether the normal operator $\mathcal{F}^*\mathcal{F}$ is statistical stable, in the sense that its typical behavior is similar to the one of its expectation. From known results about the cross correlation of

ambient noise signals [GP09] we anticipate that it is indeed the case when $T \to \infty$, but it is relevant to estimate carefully the fluctuations since the quantity T in typical applications cannot be taken arbitrarily large. The variance of the kernel of the normal operator is

$$\begin{aligned}\operatorname{Var}\big(\mathcal{F}^*\mathcal{F}(\boldsymbol{x},\boldsymbol{x}')\big) = \sum_{r,r'=1}^{N_r} \iint_{-\frac{T}{2}}^{\frac{T}{2}} \Big(&\big\langle Q(t,\boldsymbol{x}_r,\boldsymbol{x}) Q(t,\boldsymbol{x}_r,\boldsymbol{x}') Q(t',\boldsymbol{x}_{r'},\boldsymbol{x}) Q(t',\boldsymbol{x}_{r'},\boldsymbol{x}')\big\rangle \\ &- \big\langle Q(t,\boldsymbol{x}_r,\boldsymbol{x}) Q(t,\boldsymbol{x}_r,\boldsymbol{x}')\big\rangle \big\langle Q(t',\boldsymbol{x}_{r'},\boldsymbol{x}) Q(t',\boldsymbol{x}_{r'},\boldsymbol{x}')\big\rangle \Big) \mathrm{d}t \mathrm{d}t'. \quad (3.2.5)\end{aligned}$$

We can write Q in the form

$$Q(t,\boldsymbol{x}_r,\boldsymbol{x}) = \sum_{s=1}^{N_s} \int \mathcal{G}(v,\boldsymbol{x}_r,\boldsymbol{y}_s,\boldsymbol{x})\, n_s(t-v)\, \mathrm{d}v\,, \quad (3.2.6)$$

with

$$\mathcal{G}(v,\boldsymbol{x}_r,\boldsymbol{y}_s,\boldsymbol{x}) = -\int \partial_w^2\, G(w,\boldsymbol{x}_r,\boldsymbol{x}) G(v-w,\boldsymbol{x},\boldsymbol{y}_s)\, \mathrm{d}w\,. \quad (3.2.7)$$

Therefore the variance of the kernel of the normal operator can be written as

$$\begin{aligned}\operatorname{Var}\big(\mathcal{F}^*\mathcal{F}(\boldsymbol{x},\boldsymbol{x}')\big) = \sum_{r,r'=1}^{N_r} \sum_{s_1,s_2,s_1',s_2'=1}^{N_s} \iiint\!\!\int &\mathcal{G}(v,\boldsymbol{x}_r,\boldsymbol{y}_{s_1},\boldsymbol{x}) \mathcal{G}(u,\boldsymbol{x}_r,\boldsymbol{y}_{s_2},\boldsymbol{x}') \mathcal{G}(v',\boldsymbol{x}_{r'},\boldsymbol{y}_{s_1'},\boldsymbol{x}) \\ &\times \mathcal{G}(u',\boldsymbol{x}_{r'},\boldsymbol{y}_{s_2'},\boldsymbol{x}')\, \mathcal{S}_{T,s_1s_2s_1's_2'}(v,u,v',u')\, \mathrm{d}v\, \mathrm{d}u\, \mathrm{d}v' \mathrm{d}u', \quad (3.2.8)\end{aligned}$$

with

$$\begin{aligned}\mathcal{S}_{T,s_1s_2s_1's_2'}(v,u,v',u') = \iint_{-\frac{T}{2}}^{\frac{T}{2}} \Big(&\big\langle n_{s_1}(t-v) n_{s_2}(t-u) n_{s_1'}(t'-v') n_{s_2'}(t'-u')\big\rangle \\ &- \big\langle n_{s_1}(t-v) n_{s_2}(t-u)\big\rangle \big\langle n_{s_1'}(t'-v') n_{s_2'}(t'-u')\big\rangle \Big) \mathrm{d}t\, \mathrm{d}t'. \quad (3.2.9)\end{aligned}$$

The product of second-order moments of the random processes $n_s(t)$ is

$$\big\langle n_{s_1}(t-v)\, n_{s_2}(t-u)\big\rangle \big\langle n_{s_1'}(t'-v')\, n_{s_2'}(t'-u')\big\rangle = \delta_{s_1s_2}\delta_{s_1's_2'} F(v-u) F(v'-u')\,.$$

The fourth-order moment of the Gaussian random process n is

$$\begin{aligned}\big\langle n_{s_1}(t-v) n_{s_2}(t-u) n_{s_1'}(t'-v') n_{s_2'}(t'-u')\big\rangle = &\delta_{s_1s_2}\delta_{s_1's_2'} F(v-u) F(v'-u') \\ &+ \delta_{s_1s_1'}\delta_{s_2s_2'} F(t'-t-v'+v) F(t'-t-u'+u) \\ &+ \delta_{s_1s_2'}\delta_{s_2s_1'} F(t'-t-u'+v) F(t'-t-v'+u)\,.\end{aligned}$$

Consequently, we have that for any $T > 0$

$$\mathcal{S}_{T,s_1s_2s_1's_2'}(v,u,v',u') = \delta_{s_1s_1'}\delta_{s_2s_2'} S_T(v-v',u-u') + \delta_{s_1s_2'}\delta_{s_2s_1'} S_T(v-u',u-v')\,, \quad (3.2.10)$$

where

$$S_T(s,u) = \frac{T^2}{4\pi^2} \iint \widehat{F}(\omega)\widehat{F}(\omega') \operatorname{sinc}^2\Big(\frac{(\omega-\omega')\,T}{2}\Big)\, e^{i\omega s - i\omega' u}\, \mathrm{d}\omega\, \mathrm{d}\omega'. \quad (3.2.11)$$

The sinus cardinal function is defined as $\mathrm{sinc}(x) = \sin(x)/x$. When T is much larger than the inverse of the bandwidth of the noise sources (i.e. T is much larger than the decoherence time), we can use the approximation

$$T\ \mathrm{sinc}^2\Big(\frac{(\omega-\omega')\,T}{2}\Big) \simeq 2\pi\,\delta(\omega-\omega')$$

in (3.2.11), and therefore

$$S_T(s,u) \simeq \frac{T}{2\pi}\int \big[\widehat{F}(\omega)\big]^2\, e^{i\omega(s-u)}\,\mathrm{d}\omega\,. \tag{3.2.12}$$

Substituting (3.2.10) and (3.2.12) into (3.2.8), we obtain for all T larger than the decoherence time the following expression for the variance of the kernel $\mathcal{F}^*\mathcal{F}(\boldsymbol{x},\boldsymbol{x}')$:

$$\begin{aligned}\mathrm{Var}\big(\mathcal{F}^*\mathcal{F}(\boldsymbol{x},\boldsymbol{x}')\big) = \frac{T}{2\pi}\int \widehat{F}(\omega)^2\omega^8 \Big[\sum_{s=1}^{N_s}\big|\widehat{G}(\omega,\boldsymbol{x},\boldsymbol{y}_s)\big|^2\Big]\Big[\sum_{s=1}^{N_s}\big|\widehat{G}(\omega,\boldsymbol{x}',\boldsymbol{y}_s)\big|^2\Big]\\ \times\Big|\sum_{r=1}^{N_r}\overline{\widehat{G}}(\omega,\boldsymbol{x}_r,\boldsymbol{x})\widehat{G}(\omega,\boldsymbol{x}_r,\boldsymbol{x}')\Big|^2\mathrm{d}\omega\\ + \frac{T}{2\pi}\int \widehat{F}(\omega)^2\omega^8\Big[\sum_{s=1}^{N_s}\overline{\widehat{G}}(\omega,\boldsymbol{x},\boldsymbol{y}_s)\widehat{G}(\omega,\boldsymbol{x}',\boldsymbol{y}_s)\Big]^2\\ \times\Big[\sum_{r=1}^{N_r}\overline{\widehat{G}}(\omega,\boldsymbol{x}_r,\boldsymbol{x})\widehat{G}(\omega,\boldsymbol{x}_r,\boldsymbol{x}')\Big]^2\mathrm{d}\omega\,.\end{aligned} \tag{3.2.13}$$

Using the approximation (3.1.6), we have in particular in the high-frequency regime for $\boldsymbol{x}=\boldsymbol{x}'$

$$\frac{\mathrm{Var}\big(\mathcal{F}^*\mathcal{F}(\boldsymbol{x},\boldsymbol{x})\big)}{\big\langle\mathcal{F}^*\mathcal{F}(\boldsymbol{x},\boldsymbol{x})\big\rangle^2} = \frac{4\pi}{T}\frac{\int\omega^8\widehat{F}(\omega)^2\,\mathrm{d}\omega}{\big(\int\omega^4\widehat{F}(\omega)\,\mathrm{d}\omega\big)^2} \simeq \frac{4\pi}{BT}\ , \tag{3.2.14}$$

where B is the bandwidth of signals emitted by the random sources. This gives the order of magnitude of the signal-to-noise ratio. Note that the ratio (3.2.14) does not depend on the number of source and receiver points, but only on the bandwidth B and the recording time T. Only these two parameters control the fluctuations of the kernel $\mathcal{F}^*\mathcal{F}(\boldsymbol{x},\boldsymbol{x}')$ along the diagonal band $\boldsymbol{x}\simeq\boldsymbol{x}'$.

When $\boldsymbol{x}$ is different from $\boldsymbol{x}'$ the first term in the right-hand side of (3.2.13) is dominant (because of the absolute values). In particular, the decay of the variance as a function of the distance $|\boldsymbol{x}-\boldsymbol{x}'|$ is ensured only by the sum over the receiver points, while the sum over the source points does not contribute to the decay, contrarily to the expectation (3.2.4). Therefore the corresponding fluctuations of the kernel $\mathcal{F}^*\mathcal{F}(\boldsymbol{x},\boldsymbol{x}')$ become larger away from the diagonal band, but we always have

$$\frac{\mathrm{Var}\big(\mathcal{F}^*\mathcal{F}(\boldsymbol{x},\boldsymbol{x}')\big)}{\big\langle\mathcal{F}^*\mathcal{F}(\boldsymbol{x},\boldsymbol{x})\big\rangle\big\langle\mathcal{F}^*\mathcal{F}(\boldsymbol{x}',\boldsymbol{x}')\big\rangle} \le \frac{4\pi}{T}\frac{\int\omega^8\widehat{F}(\omega)^2\,\mathrm{d}\omega}{\big(\int\omega^4\widehat{F}(\omega)\,\mathrm{d}\omega\big)^2} \simeq \frac{4\pi}{BT}\ . \tag{3.2.15}$$

We remark that the important scaling constraint in order to ensure statistical stability is that the decoherence time of the random traces is much smaller than the recording time, that is T. Note that the total recording time, even without simultaneous sources, must be

at least of the order of $c_0 L$ where L is the propagation distance. Thus, the durations of the experiments may be of the same order in the simultaneous source case as in a more classic measurement configuration with a single source at a time as long as one can generate random or heterogeneous source signals whose characteristic time scale is small compared to the travel time to the probed region. The only, but major, difference is that one performs only one experiment in the simultaneous case, while one performs N_s experiments in the classical case, where N_s is the number of sources.

3.3 Incoherence by blending

We present here our second example of random sources enabling to perform a single experiment in the imaging process. The signal emitted is a (deterministic) short pulse, but randomly delayed in time. We describe the imaging functional and detail the scaling assumptions on the kind of emitted pulse and the distribution of the time delays necessary to guarantee the statistical stability of the method.

Consider the situation in which N_s point sources emit the same short pulse waveform, but at randomly delayed times. We refer to this situation as noise blending. It is modeled by the wave equation (3.1.1) with a source term of the form

$$n(t, \boldsymbol{x}) = \sum_{s=1}^{N_s} f(t - \tau_s)\delta(\boldsymbol{x} - \boldsymbol{y}_s)\,. \tag{3.3.1}$$

The pulse function $\big(f(t)\big)_{t\in\mathbb{R}}$ is deterministic. Call its carrier frequency ω_0 and its bandwidth B. The time delays $(\tau_s)_{s=1,\dots,N_s}$ are zero-mean independent and identically distributed random variables with the probability density function $p_\tau(t)$. We denote by $\sigma_\tau^2 = \langle \tau_s^2 \rangle = \int t^2 p_\tau(t)\,\mathrm{d}t$ the variance of the random time delays. Here $\langle\,\cdot\,\rangle$ stands for statistical average with respect to the distribution of the random time delays. Note that the source is not a Gaussian process, so the recorded signals are not Gaussian either, contrarily to the case addressed in the previous section, and the evaluations of second- and fourth-order moments require specific calculations which are different from the standard rules for moments of Gaussian processes.

The expectation of the kernel of the normal operator is

$$\big\langle \mathcal{F}^*\mathcal{F}(\boldsymbol{x}, \boldsymbol{x}')\big\rangle = \sum_{r=1}^{N_r}\sum_{s,s'=1}^{N_s} \iint \mathcal{G}(u, \boldsymbol{x}_r, \boldsymbol{y}_s, \boldsymbol{x})\mathcal{G}(u', \boldsymbol{x}_r, \boldsymbol{y}_{s'}, \boldsymbol{x}')\,\mathcal{I}_{T,ss'}(u, u')\,\mathrm{d}u\,\mathrm{d}u'\,,$$

where $\mathcal{G}$ is given by (3.2.7) and $\mathcal{I}_{T,ss'}$ is defined by

$$\mathcal{I}_{T,ss'}(u, u') = \int_{-\frac{T}{2}}^{\frac{T}{2}} \big\langle f(t - u - \tau_s) f(t - u' - \tau_{s'})\big\rangle\,\mathrm{d}t\,. \tag{3.3.2}$$

We assume that T is large enough, so that the backscattered signals are completely recorded over $[-T/2, T/2]$. This means that T should be larger than the typical travel time from the array to the search region and than the typical time delay σ_τ. We can then replace the

integral over $[-T/2, T/2]$ in (3.3.2) by the integral over $\mathbb{R}$ and we find

$$\mathcal{I}_{T,ss'}(u,u') = \frac{1}{2\pi}\int \big|\widehat{f}(\omega)\big|^2 e^{-i\omega(u-u')}\big\langle e^{-i\omega(\tau_s-\tau_{s'})}\big\rangle\,\mathrm{d}\omega\,.$$

If $s \neq s'$, then

$$\big\langle e^{-i\omega(\tau_s-\tau_{s'})}\big\rangle = \big|\big\langle e^{i\omega\tau_s}\big\rangle\big|^2 = \big|\widehat{p}_\tau(\omega)\big|^2\,.$$

Therefore, if $\sigma_\tau\omega_0 \gg 1$ then $\big|\widehat{p}_\tau(\omega)\big|^2 \simeq 0$ for all ω in the bandwidth and

$$\mathcal{I}_{T,ss'}(u,u') = \begin{cases} \frac{1}{2\pi}\int \big|\widehat{f}(\omega)\big|^2 e^{-i\omega(u-u')}\,\mathrm{d}\omega & \text{if } s = s', \\ 0 & \text{otherwise.} \end{cases}$$

This result shows that the expectation of the kernel of the normal operator is

$$\big\langle \mathcal{F}^*\mathcal{F}(\boldsymbol{x},\boldsymbol{x}')\big\rangle = \frac{1}{2\pi}\int \omega^4\big|\widehat{f}(\omega)\big|^2\Big[\sum_{s=1}^{N_s}\overline{\widehat{G}}(\omega,\boldsymbol{x},\boldsymbol{y}_s)\widehat{G}(\omega,\boldsymbol{x}',\boldsymbol{y}_s)\Big] \times\Big[\sum_{r=1}^{N_r}\overline{\widehat{G}}(\omega,\boldsymbol{x}_r,\boldsymbol{x})\widehat{G}(\omega,\boldsymbol{x}_r,\boldsymbol{x}')\Big]\mathrm{d}\omega\,, \tag{3.3.3}$$

which has the same form and the same properties (in terms of concentration along the diagonal $\boldsymbol{x} \simeq \boldsymbol{x}'$) as the expectation of the kernel of the normal operator (3.2.4) in the case of stationary random sources, or as the kernel of the normal operator (3.1.18) obtained when the full multi-static response matrix is available. The important issue to be clarified is the statistical stability of the normal operator $\mathcal{F}^*\mathcal{F}$.

The analysis of the variance of the kernel of the normal operator is based on the following basic result: for any $u, u', \tilde{u}, \tilde{u}' \in \mathbb{R}$ and $s, s', \tilde{s}, \tilde{s}' = 1, \ldots, N_s$, and again for T much larger than the typical travel time and time delay,

$$\begin{aligned}\mathcal{J} :=& \int_{-\frac{T}{2}}^{\frac{T}{2}}\int_{-\frac{T}{2}}^{\frac{T}{2}}\Big(\big\langle f(t-u-\tau_s)f(t-u'-\tau_{s'})f(\tilde{t}-\tilde{u}-\tau_{\tilde{s}})f(\tilde{t}-\tilde{u}'-\tau_{\tilde{s}'})\big\rangle \\ &\qquad - \big\langle f(t-u-\tau_s)f(t-u'-\tau_{s'})\big\rangle\big\langle f(\tilde{t}-\tilde{u}-\tau_{\tilde{s}})f(\tilde{t}-\tilde{u}'-\tau_{\tilde{s}'})\big\rangle\Big)\,\mathrm{d}t\,\mathrm{d}\tilde{t} \\ \simeq& \frac{1}{(2\pi)^2}\iint \big|\widehat{f}(\omega)\big|^2\big|\widehat{f}(\tilde{\omega})\big|^2 e^{-i\omega(u-u')}e^{-i\tilde{\omega}(\tilde{u}-\tilde{u}')} \\ &\qquad\times\big[\big\langle e^{-i\omega(\tau_s-\tau_{s'})}e^{-i\tilde{\omega}(\tau_{\tilde{s}}-\tau_{\tilde{s}'})}\big\rangle - \big\langle e^{-i\omega(\tau_s-\tau_{s'})}\big\rangle\big\langle e^{-i\tilde{\omega}(\tau_{\tilde{s}}-\tau_{\tilde{s}'})}\big\rangle\big]\,\mathrm{d}\omega\,\mathrm{d}\tilde{\omega}\,.\end{aligned}$$

If $\sigma_\tau\omega_0 \gg 1$, then

$$\begin{aligned}\mathcal{J} =& \delta_{s\tilde{s}}\delta_{s'\tilde{s}'}(1-\delta_{ss'})\frac{1}{(2\pi)^2}\iint \big|\widehat{f}(\omega)\big|^2\big|\widehat{f}(\tilde{\omega})\big|^2 e^{-i\omega(u-u')}e^{-i\tilde{\omega}(\tilde{u}-\tilde{u}')}\big|\widehat{p}_\tau(\omega+\tilde{\omega})\big|^2\mathrm{d}\omega\,\mathrm{d}\tilde{\omega} \\ &+ \delta_{s\tilde{s}'}\delta_{s'\tilde{s}}(1-\delta_{ss'})\frac{1}{(2\pi)^2}\iint \big|\widehat{f}(\omega)\big|^2\big|\widehat{f}(\tilde{\omega})\big|^2 e^{-i\omega(u-u')}e^{-i\tilde{\omega}(\tilde{u}-\tilde{u}')}\big|\widehat{p}_\tau(\omega-\tilde{\omega})\big|^2\mathrm{d}\omega\,\mathrm{d}\tilde{\omega}\,.\end{aligned}$$

Therefore the variance of the kernel $\mathcal{F}^*\mathcal{F}(\boldsymbol{x},\boldsymbol{x}')$ is:

$$\begin{aligned}
\mathrm{Var}\big(\mathcal{F}^*\mathcal{F}(\boldsymbol{x},\boldsymbol{x}')\big) &= \frac{1}{(2\pi)^2}\iint \mathrm{d}\omega\,\mathrm{d}\tilde\omega\ \big|\widehat f(\omega)\big|^2\omega^4\big|\widehat f(\tilde\omega)\big|^2\tilde\omega^4 \\
&\quad\times \sum_{r=1}^{N_r}\overline{\widehat G}(\omega,\boldsymbol{x}_r,\boldsymbol{x})\widehat G(\omega,\boldsymbol{x}_r,\boldsymbol{x}')\ \sum_{r=1}^{N_r}\overline{\widehat G}(\tilde\omega,\boldsymbol{x}_r,\boldsymbol{x})\widehat G(\tilde\omega,\boldsymbol{x}_r,\boldsymbol{x}') \\
&\quad\times\Big[\sum_{s,s'=1,s\neq s'}^{N_s}\overline{\widehat G}(\omega,\boldsymbol{x},\boldsymbol{y}_s)\overline{\widehat G}(\tilde\omega,\boldsymbol{x},\boldsymbol{y}_s)\widehat G(\omega,\boldsymbol{x}',\boldsymbol{y}_{s'})\widehat G(\tilde\omega,\boldsymbol{x}',\boldsymbol{y}_{s'})\big|\widehat p_\tau(\omega+\tilde\omega)\big|^2 \\
&\qquad+\sum_{s,s'=1,s\neq s'}^{N_s}\overline{\widehat G}(\omega,\boldsymbol{x},\boldsymbol{y}_s)\widehat G(\tilde\omega,\boldsymbol{x}',\boldsymbol{y}_s)\overline{\widehat G}(\tilde\omega,\boldsymbol{x},\boldsymbol{y}_{s'})\widehat G(\omega,\boldsymbol{x}',\boldsymbol{y}_{s'})\big|\widehat p_\tau(\omega-\tilde\omega)\big|^2\Big],
\end{aligned}$$

that we can also write as (after the change of variable $\tilde\omega\to-\tilde\omega$ in the first part of the right member)

$$\begin{aligned}
\mathrm{Var}\big(\mathcal{F}^*\mathcal{F}(\boldsymbol{x},\boldsymbol{x}')\big) &= \frac{1}{(2\pi)^2}\iint \mathrm{d}\omega\,\mathrm{d}\tilde\omega\big|\widehat f(\omega)\big|^2\omega^4\big|\widehat f(\tilde\omega)\big|^2\tilde\omega^4 \\
&\quad\times\Big[\sum_{r=1}^{N_r}\overline{\widehat G}(\omega,\boldsymbol{x}_r,\boldsymbol{x})\widehat G(\omega,\boldsymbol{x}_r,\boldsymbol{x}')\Big]\Big[\sum_{r=1}^{N_r}\widehat G(\tilde\omega,\boldsymbol{x}_r,\boldsymbol{x})\overline{\widehat G}(\tilde\omega,\boldsymbol{x}_r,\boldsymbol{x}')\Big] \\
&\quad\times\Big\{\Big[\sum_{s=1}^{N_s}\overline{\widehat G}(\omega,\boldsymbol{x},\boldsymbol{y}_s)\widehat G(\tilde\omega,\boldsymbol{x},\boldsymbol{y}_s)\Big]\Big[\sum_{s=1}^{N_s}\widehat G(\omega,\boldsymbol{x}',\boldsymbol{y}_s)\overline{\widehat G}(\tilde\omega,\boldsymbol{x}',\boldsymbol{y}_s)\Big] \\
&\qquad-\sum_{s=1}^{N_s}\overline{\widehat G}(\omega,\boldsymbol{x},\boldsymbol{y}_s)\widehat G(\tilde\omega,\boldsymbol{x},\boldsymbol{y}_s)\widehat G(\omega,\boldsymbol{x}',\boldsymbol{y}_s)\overline{\widehat G}(\tilde\omega,\boldsymbol{x}',\boldsymbol{y}_s)\Big\}\big|\widehat p_\tau(\omega-\tilde\omega)\big|^2 \\
&+\frac{1}{(2\pi)^2}\iint \mathrm{d}\omega\,\mathrm{d}\tilde\omega\big|\widehat f(\omega)\big|^2\omega^4\big|\widehat f(\tilde\omega)\big|^2\tilde\omega^4 \\
&\quad\times\Big[\sum_{r=1}^{N_r}\overline{\widehat G}(\omega,\boldsymbol{x}_r,\boldsymbol{x})\widehat G(\omega,\boldsymbol{x}_r,\boldsymbol{x}')\Big]\Big[\sum_{r=1}^{N_r}\overline{\widehat G}(\tilde\omega,\boldsymbol{x}_r,\boldsymbol{x})\widehat G(\tilde\omega,\boldsymbol{x}_r,\boldsymbol{x}')\Big] \\
&\quad\times\Big\{\Big[\sum_{s=1}^{N_s}\overline{\widehat G}(\omega,\boldsymbol{x},\boldsymbol{y}_s)\widehat G(\tilde\omega,\boldsymbol{x}',\boldsymbol{y}_s)\Big]\Big[\sum_{s=1}^{N_s}\overline{\widehat G}(\tilde\omega,\boldsymbol{x},\boldsymbol{y}_s)\widehat G(\omega,\boldsymbol{x}',\boldsymbol{y}_s)\Big] \\
&\qquad-\sum_{s=1}^{N_s}\overline{\widehat G}(\omega,\boldsymbol{x},\boldsymbol{y}_s)\widehat G(\tilde\omega,\boldsymbol{x}',\boldsymbol{y}_s)\overline{\widehat G}(\tilde\omega,\boldsymbol{x},\boldsymbol{y}_s)\widehat G(\omega,\boldsymbol{x}',\boldsymbol{y}_s)\Big\}\big|\widehat p_\tau(\omega-\tilde\omega)\big|^2. \quad (3.3.4)
\end{aligned}$$

The statistical stability follows from the fact that the variance of the kernel is small. In order to prove that the variance is small we first want to show that the integral in $(\omega,\tilde\omega)$ concentrates on a small band around the diagonal $\omega=\tilde\omega$. The double integral in $(\omega,\tilde\omega)$ can be written as a double integral in $\big((\omega+\tilde\omega)/2\,,\ \omega-\tilde\omega\big)$. The products of terms that depend on $\widehat G$ vary in $\omega-\tilde\omega$ on a scale of the order of the reciprocal of the typical travel time c_0/L (where L is the typical propagation distance). This can be seen from the high-frequency asymptotic expression (3.1.6) of the Green's function. Moreover, the terms depending on $\widehat f$ are varying in $\omega-\tilde\omega$ on a scale of the order B and the term $\big|\widehat p_\tau(\omega-\tilde\omega)\big|^2$ concentrates on a band of size $|\omega-\tilde\omega|<\sigma_\tau^{-1}$. Therefore, provided $\sigma_\tau^{-1}\ll\min(c_0/L,B)$, we can make the

approximation

$$\big|\widehat{p}_\tau(\omega-\tilde{\omega})\big|^2 \simeq \frac{2\pi}{T_\tau}\delta(\omega-\tilde{\omega})\,,$$

where

$$\frac{1}{T_\tau} = \int p_\tau^2(t)\,\mathrm{d}t\,.$$

To summarize, if $\sigma_\tau \gg L/c_0$ and $\sigma_\tau B \gg 1$, then the variance of the kernel $\mathcal{F}^*\mathcal{F}(\boldsymbol{x},\boldsymbol{x}')$ is given by

$$\begin{aligned}
\mathrm{Var}\big(\mathcal{F}^*\mathcal{F}(\boldsymbol{x},\boldsymbol{x}')\big) &= \frac{1}{2\pi T_\tau}\int \mathrm{d}\omega\,\big|\widehat{f}(\omega)\big|^4\omega^8\,\Big|\sum_{r=1}^{N_r}\overline{\widehat{G}}(\omega,\boldsymbol{x}_r,\boldsymbol{x})\widehat{G}(\omega,\boldsymbol{x}_r,\boldsymbol{x}')\Big|^2 \\
&\quad\times\Big\{\sum_{s=1}^{N_s}\big|\widehat{G}(\omega,\boldsymbol{x},\boldsymbol{y}_s)\big|^2\sum_{s=1}^{N_s}\big|\widehat{G}(\omega,\boldsymbol{x}',\boldsymbol{y}_s)\big|^2 - \sum_{s=1}^{N_s}\big|\widehat{G}(\omega,\boldsymbol{x},\boldsymbol{y}_s)\big|^2\big|\widehat{G}(\omega,\boldsymbol{x}',\boldsymbol{y}_s)\big|^2\Big\} \\
&\qquad + \frac{1}{2\pi T_\tau}\int \mathrm{d}\omega\big|\widehat{f}(\omega)\big|^4\omega^8\Big[\sum_{r=1}^{N_r}\overline{\widehat{G}}(\omega,\boldsymbol{x}_r,\boldsymbol{x})\widehat{G}(\omega,\boldsymbol{x}_r,\boldsymbol{x}')\Big]^2 \\
&\quad\times\Big\{\Big[\sum_{s=1}^{N_s}\overline{\widehat{G}}(\omega,\boldsymbol{x},\boldsymbol{y}_s)\widehat{G}(\omega,\boldsymbol{x}',\boldsymbol{y}_s)\Big]^2 - \sum_{s=1}^{N_s}\overline{\widehat{G}}(\omega,\boldsymbol{x},\boldsymbol{y}_s)^2\widehat{G}(\omega,\boldsymbol{x}',\boldsymbol{y}_s)^2\Big\}\,.
\end{aligned}$$

The hypothesis $\sigma_\tau B \gg 1$ is not restrictive and it was already required in the framework of the stationary random sources in section 3.2. The hypothesis $\sigma_\tau \gg L/c_0$ means that the random time delays, and therefore the recording time, must be larger than the typical travel time. We will see in the numerical illustrations of section 3.5 that it is enough to have random time shifts of the same order of typical travel time.

We have in particular for $\boldsymbol{x}=\boldsymbol{x}'$

$$\frac{\mathrm{Var}\big(\mathcal{F}^*\mathcal{F}(\boldsymbol{x},\boldsymbol{x})\big)}{\big\langle\mathcal{F}^*\mathcal{F}(\boldsymbol{x},\boldsymbol{x})\big\rangle^2} \simeq \frac{4\pi}{T_\tau}\Big(1-\frac{1}{N_s}\Big)\frac{\int\omega^8\big|\widehat{f}(\omega)\big|^4\,\mathrm{d}\omega}{\big(\int\omega^4\big|\widehat{f}(\omega)\big|^2\,\mathrm{d}\omega\big)^2} \simeq \frac{4\pi}{BT_\tau}\,. \tag{3.3.5}$$

This gives the order of magnitude of the signal-to-noise ratio. The quantity BT_τ controls the statistical stability. It should be large so that the kernel $\mathcal{F}^*\mathcal{F}(\boldsymbol{x},\boldsymbol{x}')$ is statistically stable. Using the method of Lagrange multipliers we get the two following results:

- The maximal value of T_τ amongst all probability density functions p_τ compactly supported in $[-\tau_{\max},\tau_{\max}]$ is $T_\tau = 2\tau_{\max}$ and it is obtained for a uniform density over $[-\tau_{\max},\tau_{\max}]$.

- The maximal value of T_τ amongst all probability density functions p_τ with variance σ_τ^2 is $T_\tau = \frac{5\sqrt{5}}{3}\sigma_\tau$ and it is obtained for a probability density function of the form

$$p_\tau(t) = \frac{3}{4\sqrt{5}\sigma_\tau}\Big(1-\frac{t^2}{5\sigma_\tau^2}\Big)\,\mathbb{1}_{\{[-\sqrt{5}\sigma_\tau,\sqrt{5}\sigma_\tau]\}}(t)\,.$$

3.4 High frequency analysis of the imaging functional

In this section we perform a detailed analysis of the imaging functional in the case of simultaneous sources, for the two kinds of random sources presented in sections 3.2 and 3.3, and in the high frequency regime. We use the imaging functional $\big(\mathcal{F}^*\boldsymbol{d}\big)(\boldsymbol{x})$ to locate singular perturbations in the velocity of propagation.

The contrast in the image obtained strongly depends on the type of perturbation. We therefore consider three types of perturbations, supported respectively on small balls, thin tubes and thin discs. With a slight abuse of notation we will refer to them as point, line and surface singularities, as they can be thought of as approximations of singular perturbations of the velocity of propagation supported on subspaces of lower dimension.

For each kind of perturbation we first analyze the expectation of the imaging functional, which gives the average image contrast seen between the center of the perturbation and a point far from it: this will provide an hint on the level of difficulty to correctly image these perturbations. This is done in subsection 3.4.2. An even more interesting result follows: in subsection 3.4.3 we perform a quantitative analysis of the statistical stability of the imaging functional with the two kinds of noisy sources presented in the previous sections. The statistical stability can be characterized by the standard deviation of the imaging functional. The calculations of the average and standard deviation of the imaging functional allow us to characterize the typical contrast seen for the three perturbations.

With a careful analysis of fluctuations produced by the random sources in this section we show that, in the high frequency regime, the typical contrast is actually much better than just of order $\sqrt{T}$ as one might have expected from the general results of the previous sections. However, the exact order of amplitude of the contrast depends on the shape of the perturbation: point singularities are easy to observe, while surface type perturbations are the hardest to locate.

3.4.1 The imaging functional in a high frequency regime

Geometry of the model

To be able to perform explicit computations, we shall simplify at most the geometry of the model. We will assume that the domain we are investigating is a ball $\Omega = B_R$ with radius R. We also assume to have N_s point sources located at points $(\boldsymbol{y}_s)_{s=1,\dots,N_s}$ lying on the surface of the ball ∂B_R and dense enough (ideally, closer than half of the central wavelength) so that a continuum approximation can be used. The sources can either emit independent stationary random signals, as in the case studied in section 3.2, or they emit (almost) simultaneously the same short pulse waveform, but randomly delayed in time, as described in section 3.3. We will refer to the first case as *stationary random* sources and to the second as (*noise*) *blended* sources.

Signals are observed at the passive sensor array $(\boldsymbol{x}_r)_{r=1,\dots,N_r}$ for some large time interval $[-T/2, T/2]$. Sensors are also assumed to densely sample the surface of the ball ∂B_R. Recall that for noise blended sources the recording time T should be much larger than the typical travel time, so as to guarantee that the backscattered signals are completely recorded. Similarly, for stationary random sources T must be taken much larger that the inverse of the bandwidth of the noise sources (i.e. much larger than the decoherence time).

Finally, we shall also take the background velocity of propagation $c_0(\boldsymbol{x})$, which is assumed to be known, to be constant, and assume that perturbations are located near the center of the ball. This means that the medium is homogeneous outside of a ball B_r of radius $r \ll R$.

The kernel of the imaging functional

We now turn our attention to the kernel $\mathcal{F}^*\mathcal{F}$, which as we have seen plays an essential role in the evaluation of the imaging functional, and analyze its behavior in the high frequency regime. Since in this model sources and receivers are located on the surface of the ball $\Sigma = \partial B_R$ and are sufficiently dense, we can rewrite the kernel (3.6.2) using the continuum approximation formula (3.6.3) of appendix B. When the surface density ρ of the receivers is constant, we obtain

$$\mathcal{K}_\omega(\boldsymbol{x},\boldsymbol{y}) := \sum_{r=1}^{N_r} \overline{\widehat{G}}(\omega,\boldsymbol{x}_r,\boldsymbol{x})\widehat{G}(\omega,\boldsymbol{x}_r,\boldsymbol{y}) \;\simeq \int_{\partial B_R} \rho\, \overline{\widehat{G}}(\omega,\boldsymbol{x}_r,\boldsymbol{x})\widehat{G}(\omega,\boldsymbol{x}_r,\boldsymbol{y})\,\mathrm{d}\sigma(\boldsymbol{x}_r)\,.$$

Since perturbations are located in a small area, far from the sources and sensors, we can use the approximate identity [GP09, Proposition 4.3]

$$\frac{2i\omega}{c_0}\int_{\partial B_R} \overline{\widehat{G}}(\omega,\boldsymbol{x}_r,\boldsymbol{x})\widehat{G}(\omega,\boldsymbol{x}_r,\boldsymbol{y})\,\mathrm{d}\sigma(\boldsymbol{x}_r) \;\simeq\; \widehat{G}(\omega,\boldsymbol{x},\boldsymbol{y}) - \overline{\widehat{G}}(\omega,\boldsymbol{x},\boldsymbol{y})\,,$$

which follows from Green's identity and the Sommerfeld radiation condition. This result can be viewed as a version of the Helmholtz-Kirchhoff integral theorem. Using the function $sinc(x) = sin(x)/x$, the right hand side of the above equation can be rewritten as

$$2i\,\Im\Big(\widehat{G}(\omega,\boldsymbol{x},\boldsymbol{y})\Big) = \frac{2i}{4\pi}\,\frac{\omega}{c_0}\,\mathrm{sinc}\Big(\frac{\omega}{c_0}|\boldsymbol{x}-\boldsymbol{y}|\Big)$$

and assuming that both receivers and sources have constant density on the surface ∂B_R we obtain

$$\mathcal{K}_\omega(\boldsymbol{x},\boldsymbol{y}) = \frac{1}{4\pi}\,\mathrm{sinc}\Big(\frac{\omega}{c_0}|\boldsymbol{x}-\boldsymbol{y}|\Big)\,. \tag{3.4.1}$$

Recall that for simultaneous sources the imaging functional is

$$\widetilde{\delta c}^{-2}(\boldsymbol{x}) = \big(\mathcal{F}^*\boldsymbol{d}\big)(\boldsymbol{x}) = \int_{B_R} \mathcal{F}^*\mathcal{F}(\boldsymbol{x},\boldsymbol{x}')\delta c^{-2}(\boldsymbol{x}')\,\mathrm{d}\boldsymbol{x}', \tag{3.4.2}$$

where δc^{-2} is the velocity perturbation and $\widetilde{\delta c}^{-2}(\boldsymbol{x})$ is the obtained estimation. Thanks to (3.4.1) and using the explicit formulas (3.3.3) and (3.2.4) we can rewrite the mean of the kernel $\mathcal{F}^*\mathcal{F}$ as

$$\begin{aligned}\langle\mathcal{F}^*\mathcal{F}\rangle(\boldsymbol{x},\boldsymbol{x}') &= \frac{1}{2\pi}\int \omega^4\,\big|\widehat{f}(\omega)\big|^2 \sum_{s=1}^{N_s} \overline{\widehat{G}}(\omega,\boldsymbol{x},\boldsymbol{y}_s)\widehat{G}(\omega,\boldsymbol{x}',\boldsymbol{y}_s) \sum_{r=1}^{N_r} \overline{\widehat{G}}(\omega,\boldsymbol{x}_r,\boldsymbol{x})\widehat{G}(\omega,\boldsymbol{x}_r,\boldsymbol{x}')\,\mathrm{d}\omega \\ &= \frac{1}{2^5\pi^3}\int \omega^4\,\big|\widehat{f}(\omega)\big|^2\,\mathrm{sinc}^2\Big(\frac{\omega}{c_0}|\boldsymbol{x}-\boldsymbol{x}'|\Big)\,\mathrm{d}\omega\end{aligned}$$

for noise blended sources, and as

$$\langle\mathcal{F}^*\mathcal{F}\rangle(\boldsymbol{x},\boldsymbol{x}') = \frac{T}{2^5\pi^3}\int \omega^4\,\widehat{F}(\omega)\,\mathrm{sinc}^2\Big(\frac{\omega}{c_0}|\boldsymbol{x}-\boldsymbol{x}'|\Big)\,\mathrm{d}\omega$$

for the stationary random sources.

We stress that the focus of this section is on the high frequency analysis of this functional.

We will analyze its performances in localizing singularities in the background velocity of propagation, in the high frequency regime $\eta \ll 1$, where

$$\frac{\omega_0}{c_0} = \frac{1}{\eta}\,.$$

Note that with this notation the wavelength is equal to $2\pi\eta$.

3.4.2 Expected contrast of the estimated perturbation

Even if the estimated perturbation $\widetilde{\delta c}^{-2}(\boldsymbol{x})$ provided by the imaging functional does not have the exact shape of the real perturbation, due to the different approximations used, it still shows a peak on the actual location of the velocity perturbation. We study in this section the expected (average in the statistical sense) contrast seen in the estimated velocity perturbation between the actual location of the perturbation and points far from it.

The expected estimated perturbation for noise blended sources is given by

$$\big\langle \widetilde{\delta c}^{-2}(\boldsymbol{x}) \big\rangle = \frac{1}{2^5\pi^3} \int \mathcal{I}_1(\boldsymbol{x},\omega)\omega^4 \big|\hat{f}(\omega)\big|^2 \mathrm{d}\omega\,,$$

with

$$\mathcal{I}_1(\boldsymbol{x},\omega) = \int_{B_R} \mathrm{sinc}^2\Big(\frac{\omega}{c_0}|\boldsymbol{x}-\boldsymbol{x}'|\Big)\delta c^{-2}(\boldsymbol{x}')\,\mathrm{d}\boldsymbol{x}'.$$

When the bandwidth of the source pulse is smaller than the central frequency, it is enough to study the behavior of the spatial integral $\mathcal{I}_1(\boldsymbol{x})$ at the central frequency. For simplicity of notation we drop the dependence on ω. It turns out that $T \cdot \mathcal{I}_1(\boldsymbol{x})$ is the quantity one has to study also in the case of stationary random sources. All the computations presented in the remaining part of this section are performed in the noise blended case; to obtain the different orders of amplitude provided by the imaging functional for stationary random sources it sufficess to multiply the results by T.

To simplify the presentation of some computations, we assume that the support of the perturbation is centered on the center of the ball B_R on the surface of which are located the sources and receivers, and choose this center as the origin of our system of coordinates.

We remark that for the purposes of this subsection it would not be necessary to distinguish between the scale of the wavelength of the signals (η) and that of the size of the perturbation (ε). However, this distinction turns out to be crucial in the analysis of fluctuations carried out in subsection 3.4.3.

We introduce now the different kinds of singularities and compute the relative order al amplitude of the average contrast shown by the imaging functional.

Point singularities

Let us start by considering a point singularity, that is to say, a singularity whose support has a very small diameter. We model it with a perturbation of the velocity of propagation that is supported on a ball of radius ε:

$$\delta c^{-2}(\boldsymbol{x}) = \alpha\, \mathbb{1}_{\{B_\varepsilon\}}(\boldsymbol{x})\,. \tag{3.4.3}$$

To simplify computations, we can take α to be constant. Indeed, it only enters formulas as a multiplicative constant (squared in subsection 3.4.3): since it is of no relevance to our

scopes, we set it equal to 1, also for the other types of perturbations.

Changing variables, we have:

$$\begin{aligned}\mathcal{I}_1(\boldsymbol{x}) &= \int_{B_R} \operatorname{sinc}^2\big(|\boldsymbol{x}-\boldsymbol{x}'|/\eta\big)\delta c^{-2}(\boldsymbol{x}')\,\mathrm{d}\boldsymbol{x}' = \int_{B_\varepsilon} \operatorname{sinc}^2\big(|\boldsymbol{x}-\boldsymbol{x}'|/\eta\big)\,\mathrm{d}\boldsymbol{x}' \\ &= \varepsilon^3 \int_{B_1} \operatorname{sinc}^2\Big(\frac{\varepsilon}{\eta}|\boldsymbol{x}/\varepsilon-\boldsymbol{x}'|\Big)\,\mathrm{d}\boldsymbol{x}'.\end{aligned}$$

At the center of the perturbation, $\boldsymbol{x}=0$, we have

$$\mathcal{I}_1(0) = \varepsilon^3 \int_{B_1} \operatorname{sinc}^2\Big(\frac{\varepsilon}{\eta}|\boldsymbol{x}'|\Big)\,\mathrm{d}\boldsymbol{x}' = 4\pi\varepsilon^3 \int_0^1 \frac{\eta^2}{\varepsilon^2}\sin^2\Big(\frac{\varepsilon}{\eta}\rho\Big)\,\mathrm{d}\rho = 2\pi\varepsilon\eta^2\Big(1-\operatorname{sinc}(2\varepsilon/\eta)\Big).$$

For $\varepsilon \simeq \eta$ we have that $\mathcal{I}_1(0) = O(\varepsilon\eta^2)$. However, if $\varepsilon \ll \eta$ the order becomes $O(\varepsilon^3)$.

For $|\boldsymbol{x}| = O(1)$, what gives the order of amplitude of $\mathcal{I}_1(\boldsymbol{x})$ is the decay of the $sinc(x)$ function, which goes approximately as $1/x$. We have that

$$\mathcal{I}_1(\boldsymbol{x}) \le \varepsilon^3\eta^2 \int_{B_1} |\boldsymbol{x}-\varepsilon\boldsymbol{x}'|^{-2}\mathrm{d}\boldsymbol{x}' = O(\varepsilon^3\eta^2)\,.$$

Remark that the bound we have found is sharp, since there are $\boldsymbol{x}$ for which $\mathcal{I}_1$ is exactly of order $\varepsilon^3\eta^2$.

We see that the difference in amplitude between the centre of the perturbation and a point far from it is significant: it is of order η^{-2} when $\varepsilon \ll \eta$ and of order ε^{-2} if $\varepsilon \simeq \eta$.

Line singularities

We consider now line-type singularities, which is to say an almost one-dimensional perturbation of the velocity of propagation. We model it by a perturbation supported on a cylinder of radius ε:

$$\delta c^{-2}(\boldsymbol{x}) = \mathbb{1}_{\{C_\varepsilon\}}(\boldsymbol{x})\,, \qquad C_\varepsilon = B_\varepsilon \times [-1,1] \subset \mathbb{R}^2 \times \mathbb{R}\,. \tag{3.4.4}$$

We have

$$\begin{aligned}\mathcal{I}_1(\boldsymbol{x}) &= \int_{B_R} \operatorname{sinc}^2\big(|\boldsymbol{x}-\boldsymbol{x}'|/\eta\big)\delta c^{-2}(\boldsymbol{x}')\,\mathrm{d}\boldsymbol{x}' \\ &= \varepsilon^2 \int_{-1}^1 \int_{B_1} \operatorname{sinc}^2\Big(\frac{1}{\eta}\sqrt{(x-\varepsilon x')^2+(y-\varepsilon y')^2+(z-z')^2}\Big)\,\mathrm{d}\boldsymbol{x}'.\end{aligned}$$

At $\boldsymbol{x}=0$ this term reduces to

$$\mathcal{I}_1(0) = \varepsilon^2 \int_{-1}^1 \int_{B_1} \operatorname{sinc}^2\Big(\frac{1}{\eta}\sqrt{\varepsilon^2(x'^2+y'^2)+z'^2}\Big)\,\mathrm{d}x'\mathrm{d}y'\,\mathrm{d}z',$$

which is rapidly oscillating in z'. In the integral in z' we can therefore approximate sin^2 by its mean:

$$\begin{aligned}\mathcal{I}_1(0) &\simeq 2\pi\varepsilon^2 \int_0^1 \left(\frac{1}{2}\int_{-1}^1 \eta^2\Big(\varepsilon^2 r^2 + z'^2\Big)^{-1}\mathrm{d}z'\right) r\,\mathrm{d}r = 2\pi\varepsilon^2 \int_0^1 \frac{\eta^2}{\varepsilon r}\arctan\Big(\frac{1}{\varepsilon r}\Big)\, r\,\mathrm{d}r \\ &= 2\pi\,\varepsilon\eta^2 \int_0^1 \arctan\Big(\frac{1}{\varepsilon r}\Big)\,\mathrm{d}r \simeq \pi^2\varepsilon\eta^2 = O(\varepsilon\,\eta^2)\,.\end{aligned}$$

Far from the perturbation the integral is of order $\varepsilon^2\eta^2$. For example, for $x^2+y^2 = C = O(1)$ we have

$$\begin{aligned}\mathcal{I}_1(\boldsymbol{x}) &\lesssim \frac{1}{2}\varepsilon^2 \int_{-1}^1 \int_{B_1} \eta^2\Big((x-\varepsilon x')^2 + (y-\varepsilon y')^2 + (z-z')^2\Big)^{-1}\mathrm{d}\boldsymbol{x}' \\ &\simeq \frac{\pi}{2}\varepsilon^2\eta^2 \int_{-1}^1 \frac{1}{C+(z-z')^2}\,\mathrm{d}z' = O(\varepsilon^2\,\eta^2)\,. \end{aligned} \tag{3.4.5}$$

Therefore, the difference in amplitude seen between the centre of the line perturbation and a point far from it is of order ε^{-1}.

Plane singularities

Let us consider now singularities that are approximately two-dimensional: we call them surface-type singularities and model them by a perturbation of the velocity which is supported on a disc of thickness ε:

$$\delta c^{-2}(\boldsymbol{x}) = \mathbb{1}_{\{D_\varepsilon\}}(\boldsymbol{x})\,, \qquad\qquad D_\varepsilon = [-\varepsilon,\varepsilon]\times B_1 \subset \mathbb{R}\times\mathbb{R}^2\,. \tag{3.4.6}$$

With this notation we have

$$\mathcal{I}_1(\boldsymbol{x}) = \varepsilon \int_{-1}^1 \int_{B_1} \mathrm{sinc}^2\Big(\frac{1}{\eta}\sqrt{(x-\varepsilon x')^2 + (y-y')^2 + (z-z')^2}\Big)\,\mathrm{d}\boldsymbol{x}'.$$

At $\boldsymbol{x} = 0$

$$\begin{aligned}\mathcal{I}_1(0) &= 2\pi\varepsilon \int_{-1}^1 \int_0^1 \mathrm{sinc}^2\Big(\frac{1}{\eta}\sqrt{\varepsilon^2 x'^2 + r^2}\Big)\, r\,\mathrm{d}r\;\mathrm{d}x' \\ &\simeq \pi\varepsilon \int_{-1}^1 \int_0^1 \eta^2\Big(\varepsilon^2 x'^2 + r^2\Big)^{-1} r\,\mathrm{d}r\;\mathrm{d}x' = \pi\varepsilon\eta^2 \int_{-1}^1 \frac{1}{2}\ln\Big(1+\frac{1}{\varepsilon^2 x'^2}\Big)\,\mathrm{d}x' \\ &= O\Big(\varepsilon\,\eta^2\big|\ln(\varepsilon)\big|\Big)\end{aligned}$$

because the sin^2 in the first line is rapidly oscillating in r.

For $x = O(1)$ we have instead that

$$\begin{aligned}\mathcal{I}_1(\boldsymbol{x}) &\lesssim \varepsilon \int_{-1}^1 \int_{B_1} \eta^2\Big((x-\varepsilon x')^2 + (y-y')^2 + (z-z')^2\Big)^{-1}\mathrm{d}y'\mathrm{d}z'\;\mathrm{d}x' \\ &\simeq 2\pi\varepsilon\eta^2 \int_0^1 \frac{r}{x+r^2}\,\mathrm{d}r = O(\varepsilon\,\eta^2)\,.\end{aligned}$$

For this type of singularities, the difference in amplitude seen between the centre of the perturbation and a point far from it is very weak: it is only of order $|ln(\varepsilon)|$. This already hints to the fact that, with the imaging functional we consider, surface-type singularities are harder to locate than the other types. The analysis of fluctuations of the next subsection will confirm this result.

3.4.3 Fluctuations and typical contrast

We have obtained in the previous subsection the average contrast of the imaged perturbation. We want now to find confidence intervals for the typical contrast observed during the experiment. To do so, we must analyze the fluctuations in the result. They are given by the standard deviation of the estimated perturbation $\widetilde{\delta c}^{-2}$, which at a point $\boldsymbol{x}$ is given by

$$\mathcal{S}(\boldsymbol{x}) = \Big\langle \big|\widetilde{\delta c}^{-2}(\boldsymbol{x}) - \langle \widetilde{\delta c}^{-2}(\boldsymbol{x})\rangle\big|^2 \Big\rangle^{\frac{1}{2}} \ . \tag{3.4.7}$$

We need to compute the standard deviation at the location of the perturbation and at points far from it, and compare them with the expected amplitude of the estimated perturbation. Using (3.4.2) to write explicitly (3.4.7) we get

$$\begin{aligned}
\mathcal{S}(\boldsymbol{x}) &= \Big\langle \Big[\int_{B_R} \big(\mathcal{K}(\boldsymbol{x},\boldsymbol{x}') - \langle \mathcal{K}(\boldsymbol{x},\boldsymbol{x}')\rangle\big)\delta c^{-2}(\boldsymbol{x}')\mathrm{d}\boldsymbol{x}'\Big]^2 \Big\rangle^{\frac{1}{2}} \\
&= \Big[\iint_{B_R} \Big\langle \Big(\mathcal{K}(\boldsymbol{x},\boldsymbol{x}') - \langle \mathcal{K}(\boldsymbol{x},\boldsymbol{x}')\rangle\Big)\Big(\mathcal{K}(\boldsymbol{x},\boldsymbol{x}'') - \langle \mathcal{K}(\boldsymbol{x},\boldsymbol{x}'')\rangle\Big)\Big\rangle \delta c^{-2}(\boldsymbol{x}')\delta c^{-2}(\boldsymbol{x}'')\,\mathrm{d}\boldsymbol{x}'\mathrm{d}\boldsymbol{x}''\Big]^{\frac{1}{2}} \\
&= \Big[\iint_{B_R} \mathrm{Cov}\Big(\mathcal{K}(\boldsymbol{x},\boldsymbol{x}'),\mathcal{K}(\boldsymbol{x},\boldsymbol{x}'')\Big)\,\delta c^{-2}(\boldsymbol{x}')\delta c^{-2}(\boldsymbol{x}'')\mathrm{d}\boldsymbol{x}'\mathrm{d}\boldsymbol{x}''\Big]^{\frac{1}{2}},
\end{aligned}$$

where $\mathcal{K} = \mathcal{F}^*\mathcal{F}$. With the same computations used to obtain the variance of the kernel $\mathcal{F}^*\mathcal{F}$ in section 3.3 we obtain that the covariance is given by

$$\begin{aligned}
&2\pi\, T_\tau\, \mathrm{Cov}\Big(\mathcal{K}(\boldsymbol{x},\boldsymbol{x}'),\mathcal{K}(\boldsymbol{x},\boldsymbol{x}'')\Big) \\
&\simeq \int \mathrm{d}\omega\, \big|\widehat{f}(\omega)\big|^4\, \omega^8 \times \Big\{ \sum_{r=1}^{N_r} \overline{\widehat{G}}(\omega,\boldsymbol{x}_r,\boldsymbol{x})\widehat{G}(\omega,\boldsymbol{x}_r,\boldsymbol{x}')\ \sum_{r=1}^{N_r} \widehat{G}(\omega,\boldsymbol{x}_r,\boldsymbol{x})\overline{\widehat{G}}(\omega,\boldsymbol{x}_r,\boldsymbol{x}'') \\
&\qquad\qquad \times \Big\{ \sum_{s=1}^{N_s} \big|\widehat{G}(\omega,\boldsymbol{x},\boldsymbol{y}_s)\big|^2 \sum_{s=1}^{N_s} \widehat{G}(\omega,\boldsymbol{x}',\boldsymbol{y}_s)\overline{\widehat{G}}(\omega,\boldsymbol{x}'',\boldsymbol{y}_s) \\
&\qquad\qquad\qquad - \sum_{s=1}^{N_s} \big|\widehat{G}(\omega,\boldsymbol{x},\boldsymbol{y}_s)\big|^2 \widehat{G}(\omega,\boldsymbol{x}',\boldsymbol{y}_s)\overline{\widehat{G}}(\omega,\boldsymbol{x}'',\boldsymbol{y}_s)\Big\} \\
&\qquad + \sum_{r=1}^{N_r} \overline{\hat{G}}\big(\omega,\boldsymbol{x}_r,\boldsymbol{x}\big)\hat{G}\big(\omega,\boldsymbol{x}_r,\boldsymbol{x}'\big)\ \sum_{r=1}^{N_r} \overline{\hat{G}}\big(\omega,\boldsymbol{x}_r,\boldsymbol{x}\big)\hat{G}\big(\omega,\boldsymbol{x}_r,\boldsymbol{x}''\big) \\
&\qquad\qquad \times \Big\{ \sum_{s=1}^{N_s} \overline{\hat{G}}\big(\omega,\boldsymbol{x},\boldsymbol{y}_s\big)\hat{G}\big(\omega,\boldsymbol{x}',\boldsymbol{y}_s\big)\ \sum_{s=1}^{N_s} \overline{\hat{G}}\big(\omega,\boldsymbol{x},\boldsymbol{y}_s\big)\hat{G}\big(\omega,\boldsymbol{x}'',\boldsymbol{y}_s\big) \\
&\qquad\qquad\qquad - \sum_{s=1}^{N_s} \overline{\hat{G}}\big(\omega,\boldsymbol{x},\boldsymbol{y}_s\big)^2\hat{G}\big(\omega,\boldsymbol{x}',\boldsymbol{y}_s\big)\hat{G}\big(\omega,\boldsymbol{x}',\boldsymbol{y}_s\big)\Big\}\ \Big\}.
\end{aligned}$$

We recall that $T_\tau = \big(\int p_\tau^2(t)\,\mathrm{d}t\big)^{-1}$ and $p_\tau(t)$ is the probability density function of the random time delays. The quantity T_τ should be large so that the kernel $\mathcal{F}^*\mathcal{F}(\boldsymbol{x},\boldsymbol{x}')$ is statistically stable. For example, we have shown in section 3.3 that the maximal value of T_τ amongst all probability density functions p_τ compactly supported in $[-\tau_{max},\tau_{max}]$ is obtained for the uniform density over the interval and gives $T_\tau = 2\tau_{max}$. Since τ_{max} must be at most of the order of the recording time $\tau_{max} \simeq T/2$, to obtain a large value of T_τ one should take T large too (which is something we had already required in section 3.1).

Observe that in the above equation for the covariance, in each of the two terms on the right hand side we are summing N_s terms with a minus sign and N_s^2 with a plus sign, and they are all of the same order. The contribution of the terms with a minus sign is therefore small, and we can use the results of subsection 3.4.1 on the kernel of the imaging functional to simplify the above equation into

$$\begin{aligned}\mathrm{Cov}\Big(\mathcal{K}(\boldsymbol{x},\boldsymbol{x}'),\mathcal{K}(\boldsymbol{x},\boldsymbol{x}'')\Big) \simeq \frac{1}{2\pi\,T_\tau}\int \mathrm{d}\omega\,\big|\widehat{f}(\omega)\big|^4\,\omega^8 \\ \times\Big\{\mathrm{sinc}\Big(\frac{\omega}{c_0}|\boldsymbol{x}-\boldsymbol{x}'|\Big)\mathrm{sinc}\Big(\frac{\omega}{c_0}|\boldsymbol{x}-\boldsymbol{x}''|\Big)\mathrm{sinc}\Big(\frac{\omega}{c_0}|\boldsymbol{x}'-\boldsymbol{x}''|\Big) \\ +\mathrm{sinc}^2\Big(\frac{\omega}{c_0}|\boldsymbol{x}-\boldsymbol{x}'|\Big)\mathrm{sinc}^2\Big(\frac{\omega}{c_0}|\boldsymbol{x}-\boldsymbol{x}''|\Big)\Big\}.\end{aligned}$$

Similar computations for the case of stationary random sources, where the terms with a minus sign do not even appear, lead to

$$\begin{aligned}\mathrm{Cov}\Big(\mathcal{K}(\boldsymbol{x},\boldsymbol{x}'),\mathcal{K}(\boldsymbol{x},\boldsymbol{x}'')\Big) \simeq \frac{T}{2\pi}\int \mathrm{d}\omega\,\big|\widehat{F}(\omega)\big|^2\,\omega^8 \\ \times\Big\{\mathrm{sinc}\Big(\frac{\omega}{c_0}|\boldsymbol{x}-\boldsymbol{x}'|\Big)\mathrm{sinc}\Big(\frac{\omega}{c_0}|\boldsymbol{x}-\boldsymbol{x}''|\Big)\mathrm{sinc}\Big(\frac{\omega}{c_0}|\boldsymbol{x}'-\boldsymbol{x}''|\Big) \\ +\mathrm{sinc}^2\Big(\frac{\omega}{c_0}|\boldsymbol{x}-\boldsymbol{x}'|\Big)\mathrm{sinc}^2\Big(\frac{\omega}{c_0}|\boldsymbol{x}-\boldsymbol{x}''|\Big)\Big\}.\end{aligned}$$

Let us continue the computations in the case of noise blended sources. Putting everything together, we find that the standard deviation of the imaging functional at a point $\boldsymbol{x}$ is given by

$$\mathcal{S}(\boldsymbol{x}) = \left[\frac{1}{2\pi\,T_\tau}\int \big|\widehat{f}(\omega)\big|^4\,\omega^8\;\mathcal{I}_2(\boldsymbol{x},\omega)\,\mathrm{d}\omega\right]^{\frac{1}{2}}$$

with

$$\begin{aligned}\mathcal{I}_2(\boldsymbol{x},\omega) = \iint_{B_R}\Big[\mathrm{sinc}\Big(\frac{\omega}{c_0}|\boldsymbol{x}-\boldsymbol{x}'|\Big)\mathrm{sinc}\Big(\frac{\omega}{c_0}|\boldsymbol{x}-\boldsymbol{x}''|\Big)\mathrm{sinc}\Big(\frac{\omega}{c_0}|\boldsymbol{x}'-\boldsymbol{x}''|\Big) \\ +\mathrm{sinc}^2\Big(\frac{\omega}{c_0}|\boldsymbol{x}-\boldsymbol{x}'|\Big)\mathrm{sinc}^2\Big(\frac{\omega}{c_0}|\boldsymbol{x}-\boldsymbol{x}''|\Big)\Big]\delta c^{-2}(\boldsymbol{x}')\delta c^{-2}(\boldsymbol{x}'')\,\mathrm{d}\boldsymbol{x}'\mathrm{d}\boldsymbol{x}''.\end{aligned}$$

Again, we focus on the spatial integral $\mathcal{I}_2$ (and to simplify notations we drop the dependence on ω): the quantity we need to study is $\big[\mathcal{I}_2(\boldsymbol{x})/T_\tau\big]^{1/2}$ for the noise blended sources and $\big[T\cdot\mathcal{I}_2(\boldsymbol{x})\big]^{1/2}$ for the stationary random sources. The computations presented below are performed in the noise blended sources setting. To obtain the corresponding standard deviation for stationary random sources it suffices to substitute the factor $1/T_\tau$ (or $1/\sqrt{T_\tau}$)

by T (or $\sqrt{T}$). For comparison with the average amplitude, recall that for stationary random sources the results obtained in the previous subsection have to be multiplied by a factor T.

We can rewrite the integral $\mathcal{I}_2(\boldsymbol{x})$ as the sum of the two integrals

$$\mathcal{J}_1(\boldsymbol{x}) = \iint_{B_R} \mathcal{H}_1(\boldsymbol{x},\boldsymbol{x}',\boldsymbol{x}'')\,\delta c^{-2}(\boldsymbol{x}')\delta c^{-2}(\boldsymbol{x}'')\;\mathrm{d}\boldsymbol{x}'\mathrm{d}\boldsymbol{x}'' \;,$$
$$\mathcal{J}_2(\boldsymbol{x}) = \iint_{B_R} \mathcal{H}_2(\boldsymbol{x},\boldsymbol{x}',\boldsymbol{x}'')\,\delta c^{-2}(\boldsymbol{x}')\delta c^{-2}(\boldsymbol{x}'')\;\mathrm{d}\boldsymbol{x}'\mathrm{d}\boldsymbol{x}'' \;,$$

which is to say the double integral of the two kernels

$$\mathcal{H}_1(\boldsymbol{x},\boldsymbol{x}',\boldsymbol{x}'') = \mathrm{sinc}\Big(\frac{\omega}{c_0}|\boldsymbol{x}-\boldsymbol{x}'|\Big)\mathrm{sinc}\Big(\frac{\omega}{c_0}|\boldsymbol{x}-\boldsymbol{x}''|\Big)\mathrm{sinc}\Big(\frac{\omega}{c_0}|\boldsymbol{x}'-\boldsymbol{x}''|\Big)\,,$$
$$\mathcal{H}_2(\boldsymbol{x},\boldsymbol{x}',\boldsymbol{x}'') = \mathrm{sinc}^2\Big(\frac{\omega}{c_0}|\boldsymbol{x}-\boldsymbol{x}'|\Big)\mathrm{sinc}^2\Big(\frac{\omega}{c_0}|\boldsymbol{x}-\boldsymbol{x}''|\Big)$$

applied to the perturbation $\big(\delta c^{-2}(\boldsymbol{x}')\delta c^{-2}(\boldsymbol{x}'')\big)$, for every one of the three types of perturbation studied above. However, since

$$\mathcal{J}_2(\boldsymbol{x}) = \mathcal{I}_1^2(\boldsymbol{x})\,,$$

we will only need to analyze $\mathcal{J}_1$.

For the following estimates it is important to keep separated the scale of the dimension of the perturbation (ε) from the scale of the wavelength of the sources (η). Their relative amplitude will be specified, but to help the reader to keep track of the different orders, we stress that we will always have $\varepsilon \le \eta$.

Point singularities

We return to the case of point perturbations introduced in the previous subsection and modeled by (3.4.3). In this case, even a very rude estimation is sufficient to obtain a bound which guarantees that this perturbation can be imaged. Since $|sinc| \le 1$, changing variables we get

$$\begin{aligned}\big|\mathcal{J}_1(\boldsymbol{x})\big| &\le \varepsilon^6 \iint_{B_1} \big|\mathrm{sinc}\big(|\boldsymbol{x}-\varepsilon\boldsymbol{x}'|/\eta\big)\mathrm{sinc}\big(|\boldsymbol{x}-\varepsilon\boldsymbol{x}''|/\eta\big)\big|\,\mathrm{d}\boldsymbol{x}'\mathrm{d}\boldsymbol{x}'' \\ &\le K\varepsilon^6 \int_{B_1(\boldsymbol{x}/\varepsilon)} \mathrm{sinc}^2\big(|\boldsymbol{x}'|\varepsilon/\eta\big)\,\mathrm{d}\boldsymbol{x}'\,, \end{aligned} \tag{3.4.8}$$

where the constant $K = 4/3\pi$ comes from the use of the Cauchy-Schwarz inequality and $B_1(\boldsymbol{x}/\varepsilon)$ is the unitary ball in $\mathbb{R}^3$ centered in $\boldsymbol{x}/\varepsilon$. Since the *sinc* function is bounded, we obtain a bound for $\mathcal{J}_1(0)$ of order ε^6. This is only a rough upper bound, but it is not necessary to look for an improvement since it is already of the same order of the integral of the second kernel, for which we have $\mathcal{J}_2(0) = \mathcal{I}_1^2(0) = O(\varepsilon^6)$, for $\varepsilon \ll \eta$. Therefore,

$$\mathcal{I}_2(0) = O(\varepsilon^6)\,.$$

Using the decay of the *sinc* function, we can find near the center of the perturbation ($|\boldsymbol{x}| \simeq \varepsilon$) a bound for $\mathcal{I}_2$ of the same order. Oscillations are therefore of order $\varepsilon^3/\sqrt{T_\tau}$.

Recall that the average value observed on the peak is of order ε^3 for $\varepsilon \ll \eta$, so that the typical value observed remains of the same order due to the large factor T_τ. The same

results holds true also for $\varepsilon \sim \eta$, namely the typical value observed is of the same order of the average value.

Far from the perturbation the integrals of the two kernels decrease. Using the bound (3.4.8), the integral of the first kernel can be bounded for $|\boldsymbol{x}| = O(1)$ by

$$\big|\mathcal{J}_1(\boldsymbol{x})\big| \leq K\varepsilon^6 \int_{B_1} \eta^2 \big|\boldsymbol{x} - \varepsilon\boldsymbol{x}'\big|^{-2} \,\mathrm{d}\boldsymbol{x}' = K\,\varepsilon^6\eta^2\,.$$

With some more work, one can show that this bound is sharp, at least for $\varepsilon \ll \eta$. This can be done using the Fourier representation of the *sinc* function written in spherical coordinates $\boldsymbol{u} = \boldsymbol{u}(r,\theta,\phi) \in \mathbb{R}^3$:

$$\begin{aligned}\mathrm{sinc}(\lambda|\boldsymbol{x}|) &= \frac{1}{2}\int_{-1}^{1} e^{-i\lambda\zeta|\boldsymbol{x}|}\,\mathrm{d}\zeta = \frac{1}{2}\int_0^{\pi} e^{-i\lambda|\boldsymbol{x}|\cos(\theta)}\sin(\theta)\,\mathrm{d}\theta \\ &= \frac{1}{4\pi}\int_0^{2\pi}\int_0^{\pi} e^{-i\lambda\boldsymbol{x}\cdot\boldsymbol{u}(r,\theta,\phi)}\sin(\theta)\,\mathrm{d}\theta\,\mathrm{d}\phi = \frac{1}{4\pi}\int_{S^2} e^{i\lambda\boldsymbol{x}\cdot\boldsymbol{u}}\,\mathrm{d}\boldsymbol{u}\;, \end{aligned} \tag{3.4.9}$$

where $S^2 = \{\boldsymbol{x} \in \mathbb{R}^3 : |\boldsymbol{x}| = 1\}$ is the unitary sphere in $\mathbb{R}^3$. We can write

$$\begin{aligned}\mathcal{J}_1(\boldsymbol{x}) &= (4\pi)^{-3}\iint_{B_\varepsilon}\iiint_{S^2} e^{i\frac{1}{\eta}(\boldsymbol{x}-\boldsymbol{x}')\cdot\boldsymbol{u}}\, e^{i\frac{1}{\eta}(\boldsymbol{x}-\boldsymbol{x}'')\cdot\boldsymbol{v}}\, e^{i\frac{1}{\eta}(\boldsymbol{x}'-\boldsymbol{x}'')\cdot\boldsymbol{w}}\,\mathrm{d}\boldsymbol{u}\,\mathrm{d}\boldsymbol{v}\,\mathrm{d}\boldsymbol{w}\;\mathrm{d}\boldsymbol{x}'\mathrm{d}\boldsymbol{x}'' \\ &\simeq \frac{\varepsilon^6}{3^2 4\pi}\iiint_{S^2} e^{i\frac{1}{\eta}\boldsymbol{x}\cdot(\boldsymbol{u}+\boldsymbol{v})}\,\mathrm{d}\boldsymbol{u}\,\mathrm{d}\boldsymbol{v}\,\mathrm{d}\boldsymbol{w}\,,\end{aligned}$$

where we have used the assumption $\varepsilon \ll \eta$. Simplifying this equation and using again (3.4.9), we get for $|\boldsymbol{x}| = O(1)$

$$\mathcal{J}_1(\boldsymbol{x}) \simeq \frac{\varepsilon^6}{3^2}\Big[\int_{S^2} e^{i\frac{1}{\eta}\boldsymbol{x}\cdot\boldsymbol{u}}\mathrm{d}\boldsymbol{u}\Big]^2 = \frac{\varepsilon^6}{3^2}\Big[4\pi\,\mathrm{sinc}\big(|\boldsymbol{x}|/\eta\big)\Big]^2 = O(\varepsilon^6\eta^2)\,.$$

As for the integral of the second kernel, $\mathcal{J}_2(\boldsymbol{x})$, the bound we have is of order $\varepsilon^6\eta^4$. For $\varepsilon \ll \eta$ we have therefore

$$\mathcal{I}_2(\boldsymbol{x}) = O(\varepsilon^6\eta^2)\,.$$

In the general case $\varepsilon \leq \eta$, the above equation becomes an upper bound.

Recall that the statistical average of the imaging operator far from the perturbation is of order $\varepsilon^3\eta^2$. Assuming that T is large, but still $1 \ll T_\tau \leq 1/\eta^2$, the above result implies that the typical value observed is at most of order $\varepsilon^3\eta/\sqrt{T_\tau}$ (it is exactly of this order for $\varepsilon \ll \eta$). Therefore, the typical contrast is still at least of order $\sqrt{T_\tau}/\eta$, allowing for a precise localization of the perturbation (both when $\varepsilon \ll \eta$ and $\varepsilon \sim \eta$).

Line singularities

Consider the case of line singularities, modeled by (3.4.4). Using rude estimations similar to the ones presented above, we could only bound the integral of the (absolute value of the) first kernel near the origin with something of order $\varepsilon^4\eta^2\ln^2(\varepsilon)$. This means that, in order to be sure to able to image the perturbation, we would need to have $\varepsilon|\ln(\varepsilon)| \ll \eta$. But we can do better.

Assuming $\varepsilon \ll \eta$, we can use the approximation

$$\operatorname{sinc}\Big(\frac{1}{\eta}\sqrt{\varepsilon^2(x'^2+y'^2)+z'^2}\Big) \simeq \operatorname{sinc}\big(z'/\eta\big)\ . \tag{3.4.10}$$

It is then possible to use the Fourier representation of the *sinc* function

$$\operatorname{sinc}(\lambda z) = \frac{1}{2\lambda}\int_{-\lambda}^{\lambda} e^{-i\zeta z}\,\mathrm{d}\zeta = \frac{1}{2}\int_{-1}^{1} e^{-i\lambda\zeta z}\,\mathrm{d}\zeta$$

to obtain the amplitude of the fluctuations. At $\boldsymbol{x} = 0$ we can rewrite the integral of the first kernel as an integral over $C_1 = B_1 \times [-1,1] \subset \mathbb{R}^2 \times \mathbb{R}$, use (3.4.10) and integrate in x', y', x'', y'':

$$\begin{aligned}
\mathcal{J}_1(0) &= \iint_{C_\varepsilon} \operatorname{sinc}\big(|\boldsymbol{x}'|/\eta\big)\operatorname{sinc}\big(|\boldsymbol{x}''|/\eta\big)\operatorname{sinc}\big(|\boldsymbol{x}'-\boldsymbol{x}''|/\eta\big)\,\mathrm{d}\boldsymbol{x}'\mathrm{d}\boldsymbol{x}'' \\
&= \varepsilon^4 \iint_{C_1} \operatorname{sinc}\Big(\frac{1}{\eta}\sqrt{\varepsilon^2(x'^2+y'^2)+z'^2}\Big)\operatorname{sinc}\Big(\frac{1}{\eta}\sqrt{\varepsilon^2(x''^2+y''^2)+z''^2}\Big) \\
&\qquad\qquad \times \operatorname{sinc}\Big(\frac{1}{\eta}\sqrt{\varepsilon^2\big((x'-x'')^2+(y'-y'')^2\big)+(z'-z'')^2}\Big)\,\mathrm{d}\boldsymbol{x}'\mathrm{d}\boldsymbol{x}'' \\
&\simeq \pi^2\varepsilon^4 \iint_{z-1}^{z+1} \operatorname{sinc}\big(z'/\eta\big)\operatorname{sinc}\big(z''/\eta\big)\operatorname{sinc}\big((z'-z'')/\eta\big)\,\mathrm{d}z'\mathrm{d}z''\ ,
\end{aligned}$$

and using the Fourier representation introduced above we get

$$\begin{aligned}
\mathcal{J}_1(0) &= \frac{\pi^2}{2^3}\varepsilon^4 \iint_{z-1}^{z+1} \iiint_{-1}^{1} e^{-i\zeta' z'/\eta}\, e^{-i\zeta'' z''/\eta}\, e^{-i\zeta(z'-z'')/\eta}\,\mathrm{d}\zeta\,\mathrm{d}\zeta'\mathrm{d}\zeta''\ \mathrm{d}z'\mathrm{d}z'' \\
&= \frac{\pi^2}{2}\,\varepsilon^4 \iiint_{-1}^{1} \operatorname{sinc}\Big(\frac{1}{\eta}(\zeta'+\zeta)\Big)\operatorname{sinc}\Big(\frac{1}{\eta}(\zeta''-\zeta)\Big)\,\mathrm{d}\zeta\,\mathrm{d}\zeta'\mathrm{d}\zeta'' \\
&= \frac{\pi^2}{2}\,\varepsilon^4\eta^2 \int_{-1}^{1} \int_{(\zeta-1)/\eta}^{(\zeta+1)/\eta} \operatorname{sinc}(u_1)\,\mathrm{d}u_1 \int_{(-\zeta-1)/\eta}^{(-\zeta+1)/\eta} \operatorname{sinc}(u_2)\,\mathrm{d}u_2\ \mathrm{d}\zeta\,.
\end{aligned}$$

Since the function $s \mapsto \int_0^s \operatorname{sinc}(u)\,\mathrm{d}u$ is uniformly bounded in s, we get that

$$\mathcal{J}_1(0) = O(\varepsilon^4\eta^2)\,.$$

For the second kernel we have $\mathcal{J}_2(0) = \mathcal{I}_1^2(0) = O(\varepsilon^2\eta^4)$, and therefore

$$\mathcal{I}_2(0) = O(\varepsilon^2\eta^4)\,.$$

Remark that for $|\boldsymbol{x}| \simeq \varepsilon$ we can still bound fluctuations in the same way, because (3.4.10) still holds, and the integral

$$\int \Big((x-\varepsilon x')^2 + (y-\varepsilon y')^2 + (z-z')^2\Big)^{-1/2}\,\mathrm{d}\boldsymbol{x}'$$

is maximal when $\boldsymbol{x} = 0$.

We see that fluctuations near $\boldsymbol{x} = 0$ are of order $\varepsilon\eta^2/\sqrt{T_\tau}$. Since the average value observed at $\boldsymbol{x} = 0$ for the imaging functional is of order $\varepsilon\eta^2$, it is thanks to the large factor $T_\tau \gg 1$ that we get the statistical stability of the operator. This means that the typical

value observed on the perturbation remains of order $\varepsilon\eta^2$.

When $\boldsymbol{x}$ is far from the perturbation, oscillations are even smaller. Indeed, we can proceed as in (3.4.8) to find a bound for the integral of the absolute value of the first kernel. We get

$$\begin{aligned}\mathcal{J}_1(\boldsymbol{x}) &\leq \varepsilon^4 \Big[\int_{-1}^{1} \int_{B_1} \Big| \mathrm{sinc}\Big(\frac{1}{\eta} \sqrt{(x-\varepsilon x')^2 + (y-\varepsilon y')^2 + (z-z')^2} \Big) \Big| \, \mathrm{d}x' \mathrm{d}y' \, \mathrm{d}z' \Big]^2 \\ &\simeq \varepsilon^4 \eta^2 \Big[\int_{-1}^{1} \int_{B_1} \big((x-\varepsilon x')^2 + (y-\varepsilon y')^2 + (z-z)'^2 \big)^{-1/2} \, \mathrm{d}\boldsymbol{x}' \Big]^2 .\end{aligned}$$

Since the integrand is bounded, the bound we get is of order $\varepsilon^4\eta^2$. By (3.4.5), the second kernel is of a higher order, $\mathcal{J}_2(\boldsymbol{x}) \leq O(\varepsilon^4\eta^4)$, and therefore

$$\mathcal{I}_2(\boldsymbol{x}) \leq O(\varepsilon^4\eta^2) \, .$$

This bound implies that the typical value observed far from the perturbation is of order at most $\varepsilon^2\eta/\sqrt{T_\tau}$, so that the contrast is at least of order $\eta\sqrt{T_\tau}/\varepsilon$.

Plane singularities

We turn now to analyze fluctuations in the case of surface-type perturbations, modeled by (3.4.6). The difficult part is again to obtain good estimates on the integral of the first kernel, for which we use the Fourier representation of the *sinc* function obtained in (3.4.9). At $\boldsymbol{x} = 0$ we have

$$\begin{aligned}\mathcal{J}_1(0) &= \frac{1}{(4\pi)^3} \iint_{D_\varepsilon} \iiint_{S^2} e^{i\frac{1}{\eta}[\boldsymbol{x}'\cdot(\boldsymbol{u}+\boldsymbol{w}) + \boldsymbol{x}''\cdot(\boldsymbol{v}-\boldsymbol{w})]} \, \mathrm{d}\boldsymbol{u} \, \mathrm{d}\boldsymbol{v} \, \mathrm{d}\boldsymbol{w} \, \mathrm{d}\boldsymbol{x}' \mathrm{d}\boldsymbol{x}'' \\ &= \frac{1}{(4\pi)^3} \int_{S^2} \Big[\int_{S^2} \int_{D_\varepsilon} e^{i\frac{1}{\eta}\boldsymbol{x}'\cdot(\boldsymbol{u}+\boldsymbol{w})} \, \mathrm{d}\boldsymbol{x}' \, \mathrm{d}\boldsymbol{u} \Big]^2 \mathrm{d}\boldsymbol{w} \\ &\simeq \frac{4\varepsilon^2}{(4\pi)^3} \int_{S^2} \Big[\int_{S^2} \int_{B_1} e^{i\frac{1}{\eta}\boldsymbol{x}'_\perp\cdot(\boldsymbol{u}+\boldsymbol{w})} \, \mathrm{d}\boldsymbol{x}'_\perp \mathrm{d}\boldsymbol{u} \Big]^2 \mathrm{d}\boldsymbol{w} \, ,\end{aligned}$$

where the approximate equality holds for $\varepsilon \ll \eta$ and $\perp$ denotes the projection on the last two coordinates: $\boldsymbol{x}_\perp = (y,z) \in \mathbb{R}^2$. The integral in $\mathrm{d}\boldsymbol{x}'_\perp$ is computed on $(D_\varepsilon)_\perp = B_1 \in \mathbb{R}^2$. We can rewrite also the integrals on S^2 as (twice the) integrals on the projection $B_1 \in \mathbb{R}^2$, compute the integral in $\mathrm{d}\boldsymbol{x}'_\perp$ and change variables:

$$\begin{aligned}\mathcal{J}_1(0) &\simeq \frac{32\varepsilon^2}{(4\pi)^3} \int_{B_1} \Big[\iint_{B_1} e^{i\frac{1}{\eta}\boldsymbol{x}'_\perp\cdot(\boldsymbol{u}+\boldsymbol{w})_\perp} \sqrt{1-|\boldsymbol{u}_\perp|^2} \, \mathrm{d}\boldsymbol{x}'_\perp \, \mathrm{d}\boldsymbol{u}_\perp \Big]^2 \sqrt{1-|\boldsymbol{w}_\perp|^2} \, \mathrm{d}\boldsymbol{w}_\perp \\ &= \frac{2\varepsilon^2}{\pi} \int_{B_1} \Big[\int_{B_1} \frac{J_1\big(|\boldsymbol{u}_\perp + \boldsymbol{w}_\perp|\eta\big)}{|\boldsymbol{u}_\perp + \boldsymbol{w}_\perp|/\eta} \sqrt{1-|\boldsymbol{u}_\perp|^2} \, \mathrm{d}\boldsymbol{u}_\perp \Big]^2 \sqrt{1-|\boldsymbol{w}_\perp|^2} \, \mathrm{d}\boldsymbol{w}_\perp \\ &= \frac{2\,\varepsilon^2\eta^6}{\pi} \int_{B_{1/\eta}} \Big[\int_{B_{1/\eta}(\boldsymbol{w}_\perp)} \frac{J_1(|\boldsymbol{u}_\perp|)}{|\boldsymbol{u}_\perp|} \sqrt{1-|\boldsymbol{u}_\perp - \boldsymbol{w}_\perp|^2\,\eta^2} \, \mathrm{d}\boldsymbol{u}_\perp \Big]^2 \sqrt{1-|\boldsymbol{w}_\perp|^2\,\eta^2} \, \mathrm{d}\boldsymbol{w}_\perp \, .\end{aligned}$$

Here J_1 is the Bessel function of the first kind. Let us focus on the integral inside the square brackets. Observe that the origin of our system of coordinates is always inside $B_{1/\eta}(\boldsymbol{w}_\perp)$.

Changing to polar coordinates we have

$$\mathcal{Y} = \int_{B_{1/\eta}(\boldsymbol{w}_\perp)} \frac{J_1(|\boldsymbol{u}_\perp|)}{|\boldsymbol{u}_\perp|} \sqrt{1 - |\boldsymbol{u}_\perp - \boldsymbol{w}_\perp|^2\, \eta^2}\; \mathrm{d}\boldsymbol{u}_\perp = \int_0^{2\pi} \int_0^{\rho_{\boldsymbol{w}}(\theta)} J_1(r) \phi_{\boldsymbol{w}}(\theta, r)\, \mathrm{d}r\, \mathrm{d}\theta\,,$$

where we denote by $\phi_{\boldsymbol{w}}$ the square root term (written in polar coordinates), and the function $\rho_{\boldsymbol{w}}(\theta)$ takes values in $[\,1/\eta - |\boldsymbol{w}_\perp|\,,\, 1/\eta + |\boldsymbol{w}_\perp|\,] \subset [\,0\,, 2/\eta\,]$. We claim that the integral term $\mathcal{Y}$ is bounded. This can be proved by integrating by parts in r as follows. First, remark that the square root term is concave (as a function of $\boldsymbol{u}_\perp$), take its maximum over the domain of integration $B_{1/\eta}(\boldsymbol{w}_\perp)$ at the center of the ball and is zero at the boundary. Therefore, for every fixed $(\theta, \boldsymbol{w})$, the function $\phi_{\boldsymbol{w}}(\theta, \cdot)$ is still concave and bounded by 1. Then, one easily obtains that the integral of the absolute value of its derivative in r is bounded by 2. Also, the antiderivative of $J_1(r)$ is the Bessel function of order zero $-J_0(r)$, which is bounded (the maximum of its absolute value is obtained at $r = 0$, and $J_0(0) = 1$). Putting everything together, we finally get

$$\begin{aligned}
\mathcal{Y} &= \int_0^{2\pi} \left[- J_0(r) \phi_{\boldsymbol{w}}(\theta, r) \Big|_{r=0}^{r=\rho_{\boldsymbol{w}}(\theta)} + \int_0^{\rho_{\boldsymbol{w}}(\theta)} J_0(r)\, \partial_r \phi_{\boldsymbol{w}}(\theta, r)\, \mathrm{d}r \right] \mathrm{d}\theta \\
&\leq \int_0^{2\pi} \left[J_0(0) + J_0(0) \int_0^{\rho_{\boldsymbol{w}}(\theta)} \big|\partial_r \phi_{\boldsymbol{w}}(\theta, r)\big|\, \mathrm{d}r \right] \mathrm{d}\theta \;\leq\; 6\pi\,.
\end{aligned}$$

This proves the claim.

Using again the boundedness of the square root, we can bound the integral in $\mathrm{d}\boldsymbol{w}_\perp$ by π/η^2. We have therefore obtained a bound for $\mathcal{J}_1(0)$ of order $O(\varepsilon^2\eta^4)$. This is only an upper bound, but there is no need to look for an improvement, since it is already of a smaller order than the integral of the second kernel, for which we have

$$\mathcal{J}_2(0) = \mathcal{I}_1^2(0) = O\big(\varepsilon^2 \eta^4 \ln^2(\varepsilon)\big)\,.$$

Therefore,

$$\mathcal{I}_2(0) = O\big(\varepsilon^2 \eta^4 \ln^2(\varepsilon)\big)\,.$$

Far from the perturbation, fluctuations are even smaller. Recall the notation $\boldsymbol{x} = (x, \boldsymbol{x}_\perp) \in \mathbb{R} \times \mathbb{R}^2$ and $\boldsymbol{u} = (u_1, \boldsymbol{u}_\perp) \in \mathbb{R} \times \mathbb{R}^2$; the same notation is used for $\boldsymbol{v}$ and $\boldsymbol{w}$. Let us look at the integral of the first kernel; following the computations presented above we have

$$\begin{aligned}
\mathcal{J}_1(\boldsymbol{x}) &= \frac{1}{(4\pi)^3} \iint_{D_\varepsilon} \iiint_{S^2} e^{i\frac{1}{\eta}[(\boldsymbol{x}-\boldsymbol{x}')\cdot(\boldsymbol{u}+\boldsymbol{w}) + (\boldsymbol{x}-\boldsymbol{x}'')\cdot(\boldsymbol{v}-\boldsymbol{w})]}\, \mathrm{d}\boldsymbol{u}\, \mathrm{d}\boldsymbol{v}\, \mathrm{d}\boldsymbol{w}\; \mathrm{d}\boldsymbol{x}' \mathrm{d}\boldsymbol{x}'' \\
&\simeq \frac{4\varepsilon^2}{(4\pi)^3} \iiint_{S^2} \iint_{B_1} e^{i\frac{1}{\eta}[(\boldsymbol{x}-\boldsymbol{x}')_\perp\cdot(\boldsymbol{u}+\boldsymbol{w})_\perp + (\boldsymbol{x}-\boldsymbol{x}'')_\perp\cdot(\boldsymbol{v}-\boldsymbol{w})_\perp]}\, \mathrm{d}\boldsymbol{x}'_\perp \mathrm{d}\boldsymbol{x}''_\perp \\
&\qquad\qquad \times e^{i\frac{1}{\eta}[x(u+w)_1 + x(v-w)_1]}\, \mathrm{d}\boldsymbol{u}\, \mathrm{d}\boldsymbol{v}\, \mathrm{d}\boldsymbol{w} \\
&= \frac{32\varepsilon^2}{(4\pi)^3} \iiint_{B_1} \iint_{B_1} e^{-i\frac{1}{\eta}[\boldsymbol{x}'_\perp\cdot(\boldsymbol{u}+\boldsymbol{w})_\perp + \boldsymbol{x}''_\perp\cdot(\boldsymbol{v}-\boldsymbol{w})_\perp]}\, \mathrm{d}\boldsymbol{x}'_\perp \mathrm{d}\boldsymbol{x}''_\perp \;\times e^{i\frac{1}{\eta}[\boldsymbol{x}_\perp\cdot(\boldsymbol{u}+\boldsymbol{v})_\perp]} \\
&\qquad \times e^{i\frac{1}{\eta}x\left[\sqrt{1-|\boldsymbol{u}_\perp|^2} + \sqrt{1-|\boldsymbol{v}_\perp|^2}\right]} \times \sqrt{1-|\boldsymbol{u}_\perp|^2}\sqrt{1-|\boldsymbol{v}_\perp|^2}\sqrt{1-|\boldsymbol{w}_\perp|^2}\; \mathrm{d}\boldsymbol{u}_\perp \mathrm{d}\boldsymbol{v}_\perp \mathrm{d}\boldsymbol{w}_\perp
\end{aligned}$$

so that

$$\mathcal{J}_1(\boldsymbol{x}) \simeq \frac{2\varepsilon^2\eta^6}{\pi}\int_{B_{1/\eta}}\sqrt{1-|\boldsymbol{w}_\perp|^2\,\eta^2}\int_{B_{1/\eta}(\boldsymbol{w}_\perp)} e^{i\boldsymbol{x}_\perp\cdot\boldsymbol{u}_\perp}\,e^{ix\sqrt{\frac{1}{\eta^2}-\boldsymbol{u}_\perp^2}}\sqrt{1-|\boldsymbol{u}_\perp-\boldsymbol{w}_\perp|^2\,\eta^2}\,\frac{J_1(|\boldsymbol{u}_\perp|)}{|\boldsymbol{u}_\perp|}\,\mathrm{d}\boldsymbol{u}_\perp$$
$$\times\int_{B_{1/\eta}(-\boldsymbol{w}_\perp)} e^{i\boldsymbol{x}_\perp\cdot\boldsymbol{v}_\perp}\,e^{ix\sqrt{\frac{1}{\eta^2}-\boldsymbol{v}_\perp^2}}\sqrt{1-|\boldsymbol{v}_\perp+\boldsymbol{w}_\perp|^2\,\eta^2}\,\frac{J_1(|\boldsymbol{v}_\perp|)}{|\boldsymbol{v}_\perp|}\mathrm{d}\boldsymbol{v}_\perp\,\mathrm{d}\boldsymbol{w}_\perp.$$

For $|\boldsymbol{x}| \gg 1$, the last two integrals above are now much smaller than the corresponding ones for $\boldsymbol{x} = 0$. This is due to the fact that for $|\boldsymbol{x}|$ large, at least one of the two exponential terms, which have mean zero, is rapidly oscillating with respect to J_1. We therefore have that $\mathcal{J}_1(\boldsymbol{x})$ is at most of order $\varepsilon^2\eta^4$. Far from the perturbation, the (sharp) bound we have on the integral of the second kernel is of the same order: $\mathcal{J}_2(\boldsymbol{x}) \leq O(\varepsilon^2\eta^4)$. We have obtained that

$$\mathcal{I}_2(\boldsymbol{x}) \leq O(\varepsilon^2\eta^4)\,.$$

Thanks to the large factor T_τ, fluctuations are therefore smaller than the average value given by the imaging functional, both on the perturbation and far from it. The typical contrast remains therefore of the same order as the average contrast, namely of order $|\ln(\varepsilon)|$.

3.4.4 Comments

In this section we have analyzed the imaging functional given by (3.4.2) in the high frequency regime ($\eta \ll 1$) with respect to small perturbations ($\varepsilon \ll 1$) of the background velocity of propagation. Using a suitable geometry of the sources and receivers, we have been able to obtain quantitative estimates on the (average, with respect to the realization of the random time delays or the stationary random source signals) sensitivity of the imaging functional. The image presents a peak on the location of the perturbation, and the contrast is of order η^{-2} for point perturbations, of order ε^{-1} for line perturbations, and only of order $|\ln(\varepsilon)|$ for surface perturbations.

The most interesting result of this section concerns the quantitative analysis of the statistical stability of this functional, providing the typical contrast seen for the three perturbations considered.

An important fact is that the typical contrast found only depends on the type of perturbation one is trying to image, and not on the method used. All results are described below for noise blended sources, but the corresponding contrast for stationary random sources are obtained simply substituting T_τ with T.

We have shown that for point perturbations, both when $\varepsilon \ll \eta$ and $\varepsilon \sim \eta$, fluctuations due to the stochastic nature of the method are small, and the typical contrast is at least of order $\sqrt{T_\tau}/\eta$ ($\sqrt{T}/\eta$ for stationary random sources): point perturbations are easy to find.

For line perturbation the situation is different. We can image with a satisfactory accuracy and reasonable recording time only very thin line perturbations, $\varepsilon \ll \eta$. The typical contrast in this case is at least of order $\sqrt{T_\tau}\,\eta/\varepsilon$.

For plane perturbations the average contrast is quite poor, only of order $|\ln(\varepsilon)|$. However, for very thin perturbations ($\varepsilon \ll \eta$) also the typical contrast is of the same order.

These results are summarized in the tables 3.1 and 3.2, where we list for the three type of perturbations considered the order of the average value given by the imaging functional and of the standard deviation, both at the center of the perturbation and far from it.

	$\langle \widetilde{\delta c}^{-2}(\boldsymbol{x}) \rangle$		$\mathcal{S}(\boldsymbol{x})$	
	$\boldsymbol{x}=0$	$\lvert\boldsymbol{x}\rvert \gg 1$	$\boldsymbol{x}=0$	$\lvert\boldsymbol{x}\rvert \gg 1$
Points	$\simeq \varepsilon^3$	$\lesssim \varepsilon^3\eta^2$	$\simeq \varepsilon^3/\sqrt{T_\tau}$	$\lesssim \varepsilon^3\eta/\sqrt{T_\tau}$
Lines	$\simeq \varepsilon\eta^2$	$\lesssim \varepsilon^2\eta^2$	$\simeq \varepsilon\eta^2/\sqrt{T_\tau}$	$\lesssim \varepsilon^2\eta/\sqrt{T_\tau}$
Planes	$\simeq \varepsilon\eta^2 \lvert\ln(\varepsilon)\rvert$	$\lesssim \varepsilon\eta^2$	$\simeq \varepsilon\eta^2 \lvert\ln(\varepsilon)\rvert/\sqrt{T_\tau}$	$\lesssim \varepsilon\eta^2/\sqrt{T_\tau}$

Table 3.1: Noise blended sources: mean $\langle \widetilde{\delta c}^{-2}(\boldsymbol{x}) \rangle$ and standard deviation $\mathcal{S}(\boldsymbol{x})$ of the estimated velocity perturbation at the center of the perturbation ($\boldsymbol{x}=0$) and far from it ($|\boldsymbol{x}| \gg 1$), in the regime $\varepsilon \ll \eta \ll 1$. The cases of point, line and disc singularities are displayed.

	$\langle \widetilde{\delta c}^{-2}(\boldsymbol{x}) \rangle$		$\mathcal{S}(\boldsymbol{x})$	
	$\boldsymbol{x}=0$	$\lvert\boldsymbol{x}\rvert \gg 1$	$\boldsymbol{x}=0$	$\lvert\boldsymbol{x}\rvert \gg 1$
Points	$\simeq T\varepsilon^3$	$\lesssim T\varepsilon^3\eta^2$	$\simeq \sqrt{T}\varepsilon^3$	$\lesssim \sqrt{T}\varepsilon^3\eta$
Lines	$\simeq T\varepsilon\eta^2$	$\lesssim T\varepsilon^2\eta^2$	$\simeq \sqrt{T}\varepsilon\eta^2$	$\lesssim \sqrt{T}\varepsilon^2\eta$
Planes	$\simeq T\varepsilon\eta^2 \lvert\ln(\varepsilon)\rvert$	$\lesssim T\varepsilon\eta^2$	$\simeq \sqrt{T}\varepsilon\eta^2 \lvert\ln(\varepsilon)\rvert$	$\lesssim \sqrt{T}\varepsilon\eta^2$

Table 3.2: Stationary random sources: mean $\langle \widetilde{\delta c}^{-2}(\boldsymbol{x}) \rangle$ and standard deviation $\mathcal{S}(\boldsymbol{x})$ of the estimated velocity perturbation at the center of the perturbation ($\boldsymbol{x}=0$) and far from it ($|\boldsymbol{x}| \gg 1$), in the regime $\varepsilon \ll \eta \ll 1$. The cases of point, line and disc singularities are displayed.

3.5 Applications and simulations

3.5.1 Simultaneous source exploration

In this subsection we consider the formulation (3.1.1 - 3.3.1) as it describes a physical exploration problem. That is, the source term $n(t,\boldsymbol{x})$ results from the simultaneous emission of N_s point sources located at $(\boldsymbol{y}_s)_{s=1,\dots,N_s}$ and emitting randomly delayed pulses as in (3.3.1), and from the measurements at the N_r receiver points $(\boldsymbol{x}_r)_{r=1,\dots,N_r}$ we aim to recover the medium perturbations $\big(\delta c^{-2}(\boldsymbol{x})\big)_{\boldsymbol{x}\in\Omega}$. In this framework, only one experiment is performed to acquire the data set.

To put our approach in perspective we shall first consider the classic experimental configuration in which we can use the sources separately and obtains the full multi-static response matrix $\mathbf{d} = (d(t,\boldsymbol{x}_r,\boldsymbol{y}_s))_{r=1,\dots,N_r, s=1\dots,N_s, t\in[-T/2,T/2]}$. This requires us to perform N_s experiments. In the s^{th} experiment, $s=1,\dots,N_s$, we observe the signal $d(t,\boldsymbol{x}_r,\boldsymbol{y}_s)$ at the receiver point $\boldsymbol{x}_r$ when the point source at $\boldsymbol{y}_s$ emits a short pulse $f(t)$. The Reverse-Time imaging functional for the estimation of the medium perturbations δc^{-2} is based on the

application of the adjoint $\mathcal{F}_0^*$ on the data set [BCS]:

$$\mathcal{I}_{\rm RT}(\boldsymbol{x}) = \big(\mathcal{F}_0^*\mathbf{d}\big)(\boldsymbol{x}) = \sum_{s=1}^{N_s}\sum_{r=1}^{N_r}\int Q_0(t,\boldsymbol{x}_r,\boldsymbol{y}_s,\boldsymbol{x})\,d(t,\boldsymbol{x}_r,\boldsymbol{y}_s)\,\mathrm{d}t$$
$$= \frac{1}{2\pi}\sum_{s=1}^{N_s}\sum_{r=1}^{N_r}\int \omega^2\,\widehat{G}(\omega,\boldsymbol{x},\boldsymbol{x}_r)\widehat{G}(\omega,\boldsymbol{x},\boldsymbol{y}_s)\,\widehat{f}(\omega)\,\overline{\widehat{d}}(\omega,\boldsymbol{x}_r,\boldsymbol{y}_s)\,\mathrm{d}\omega\,. \qquad (3.5.1)$$

To evaluate the imaging functional, one needs a priori to solve $N_s + N_r$ times the wave equation in order to get $\widehat{G}(\omega,\boldsymbol{x},\boldsymbol{x}_r)$, for $r = 1,\ldots,N_r$, and $\widehat{G}(\omega,\boldsymbol{x},\boldsymbol{y}_s)$, for $s = 1,\ldots,N_s$. Usually the number of sources is smaller than the number of receivers $N_s < N_r$ and then the strategy that requires to call the numerical wave solver only $2N_s$ times is as follows:

1. for each $s = 1,\ldots,N_s$, compute the wave emitted by the source located at $\boldsymbol{y}_s$, that is to say evaluate $\widehat{v}^{(s)}(\omega,\boldsymbol{x})$ solution of the Helmholtz equation with the background velocity $c_0(\boldsymbol{x})$ and with the source term $\widehat{n}(\omega,\boldsymbol{x}) = \omega^2\,\widehat{f}(\omega)\,\delta(\boldsymbol{x}-\boldsymbol{y}_s)$.

2. for each $s = 1,\ldots,N_s$, time reverse the recorded data and propagate these time reversed signals from the receivers, that is to say evaluate $\widehat{u}^{(s)}(\omega,\boldsymbol{x})$ solution of the Helmholtz equation with the background velocity $c_0(\boldsymbol{x})$ and with the source term $\widehat{n}(\omega,\boldsymbol{x}) = \sum_{r=1}^{N_r}\overline{\widehat{d}}(\omega,\boldsymbol{x}_r,\boldsymbol{y}_s)\delta(\boldsymbol{x}-\boldsymbol{x}_r)$.

3. for each $s = 1,\ldots,N_s$, correlate the two pairs of signals, one of them being time-reversed first, and sum over the sources.

One gets

$$\mathcal{I}_{\rm RT}(\boldsymbol{x}) = \frac{1}{2\pi}\sum_{s=1}^{N_s}\int \widehat{v}^{(s)}(\omega,\boldsymbol{x})\,\widehat{u}^{(s)}(\omega,\boldsymbol{x})\,\mathrm{d}\omega\,,$$

which is equal to (3.5.1). In the Born approximation and for T large enough (i.e. larger than the typical travel time), we get

$$\mathcal{I}_{\rm RT}(\boldsymbol{x}) \approx \int_\Omega \mathcal{K}(\boldsymbol{x},\boldsymbol{x}')\,\delta c^{-2}(\boldsymbol{x}')\,\mathrm{d}\boldsymbol{x}'\,,$$
$$\mathcal{K}(\boldsymbol{x},\boldsymbol{x}') = \big(\mathcal{F}_0^*\mathcal{F}_0\big)(\boldsymbol{x},\boldsymbol{x}') = \frac{1}{2\pi}\int \omega^4\big|\widehat{f}(\omega)\big|^2\Big[\sum_{s=1}^{N_s}\overline{\widehat{G}}(\omega,\boldsymbol{x},\boldsymbol{y}_s)\widehat{G}(\omega,\boldsymbol{x}',\boldsymbol{y}_s)\Big]$$
$$\times\Big[\sum_{r=1}^{N_r}\overline{\hat{G}}\big(\omega,\boldsymbol{x}_r,\boldsymbol{x}\big)\hat{G}\big(\omega,\boldsymbol{x}_r,\boldsymbol{x}'\big)\Big]\,\mathrm{d}\omega\,. \qquad (3.5.2)$$

It is possible to equalize the spectrum and to divide the data by $\omega^4|\widehat{f}(\omega)|^2$ in the Fourier domain over the bandwidth in order to improve the accuracy of the estimation. We will see below that this functional gives an image of the velocity perturbations δc^{-2} with an accuracy of the order of the wavelength when the source and receiver array apertures are large enough.

We then return to the blended source configuration (3.1.1 - 3.3.1). In this case the data set consists of the vector $\boldsymbol{d} = \big(d(t,\boldsymbol{x}_r)\big)_{r=1,\ldots,N_r,t\in[-T/2,T/2]}$, where $d(t,\boldsymbol{x}_r)$ is the signal measured at $\boldsymbol{x}_r$ when the source term is (3.3.1). The imaging functional (for imaging the

medium perturbations) consists in applying the adjoint operator $\mathcal{F}^*$ to the data set:

$$\mathcal{I}_{\rm BS}(\boldsymbol{x}) = \big(\mathcal{F}^*\boldsymbol{d}\big)(\boldsymbol{x}) = \sum_{r=1}^{N_r} \int Q(t,\boldsymbol{x}_r,\boldsymbol{x}) d(t,\boldsymbol{x}_r)\,\mathrm{d}t$$
$$= \frac{1}{2\pi}\sum_{r=1}^{N_r} \iint \omega^2\, \widehat{G}(\omega,\boldsymbol{x},\boldsymbol{x}_r)\widehat{G}(\omega,\boldsymbol{x},\boldsymbol{y})\,\widehat{n}(\omega,\boldsymbol{y})\,\overline{\widehat{d}}(\omega,\boldsymbol{x}_r)\,\mathrm{d}\boldsymbol{y}\,\mathrm{d}\omega\,. \qquad (3.5.3)$$

To evaluate the imaging functional, one needs to solve the wave equation only two times. This is a considerable advantage compared to the standard technique described above that uses the full response matrix and that requires $2N_s$ calls to the numerical wave solver. More precisely the strategy to evaluate the imaging functional is as follows:

1. compute the wave emitted by the original source $n(t,\boldsymbol{x})$ given by (3.3.1), that is to say evaluate $\widehat{v}(\omega,\boldsymbol{x})$ solution of the Helmholtz equation with the background velocity $c_0(\boldsymbol{x})$ and with the source term $\widehat{n}(\omega,\boldsymbol{x})\,\omega^2$.

2. time reverse the recorded data and propagate these time reversed signals from the receivers, that is to say evaluate $\widehat{u}(\omega,\boldsymbol{x})$ solution of the Helmholtz equation with the background velocity $c_0(\boldsymbol{x})$ and with the source term $\widehat{n}(\omega,\boldsymbol{x}) = \sum_{r=1}^{N_r} \overline{\widehat{d}}(\omega,\boldsymbol{x}_r)\delta(\boldsymbol{x}-\boldsymbol{x}_r)$.

3. correlate the two pairs of signals, one of them being time-reversed first.

One gets

$$\mathcal{I}_{\rm BS}(\boldsymbol{x}) = \frac{1}{2\pi}\int \widehat{v}(\omega,\boldsymbol{x})\,\widehat{u}(\omega,\boldsymbol{x})\,\mathrm{d}\omega\,,$$

which is equal to (3.5.3). In the Born approximation and for T large enough (i.e. larger than the typical travel time and the typical time delay), we then find that

$$\mathcal{I}_{\rm BS}(\boldsymbol{x}) = \int_\Omega \mathcal{F}^*\mathcal{F}(\boldsymbol{x},\boldsymbol{x}')\delta c^{-2}(\boldsymbol{x}')\,\mathrm{d}\boldsymbol{x}' \approx \int_\Omega \big\langle \mathcal{F}^*\mathcal{F}(\boldsymbol{x},\boldsymbol{x}')\big\rangle\,\delta c^{-2}(\boldsymbol{x}')\,\mathrm{d}\boldsymbol{x}'$$
$$= \int_\Omega \mathcal{K}(\boldsymbol{x},\boldsymbol{x}')\delta c^{-2}(\boldsymbol{x}')\,\mathrm{d}\boldsymbol{x}'\,, \qquad (3.5.4)$$

where the kernel $\mathcal{K}(\boldsymbol{x},\boldsymbol{x}')$ is given by (3.5.2). Note that here we have used the crucial stabilization result $\mathcal{F}^*\mathcal{F} \simeq \big\langle \mathcal{F}^*\mathcal{F}\big\rangle$ that we derived in section 3.3.

The resolution in the perturbation estimate is given by the classic Kirchhoff resolution which characterizes the support of $\mathcal{K}$ [GP10]. We assume that the source and receiver arrays coincide and have a characteristic aperture or diameter a. Then:

- If the diameter a of the array is smaller than the distance L from the array to the target, the resolution is given by the standard Rayleigh resolution formulas: the cross range resolution is $\lambda_0 L/a$ and the range resolution is $\lambda_0(L/a)^2$ for narrowband sources and c_0/B for broadband sources with bandwidth $B > \omega_0(a/L)^2$. Here λ_0 is the central wavelength corresponding to the central frequency ω_0 of the pulse wave form f.

- If the diameter of the array is of the same order as or larger than the distance from the array to the target, then we find that the resolution is of the order of the central wavelength λ_0.

Note that we could also use the stationary random sources of the form (3.2.1, that in view of (3.3.3) gives the same resolution as the noise blended sources. Our analysis applies

directly to the important case when we do not have "controlled sources", rather "sources of opportunity". However the important assumption that we make here is that the (incoherent) traces of the sources and their locations are assumed to be known. Situations in which the sources are not assumed a priori known are discussed in [GS11].

3.5.2 Seismic forward simulations

We illustrate here how our results could be used in the context of forward simulations, which constitute an important ingredient in typical iterative imaging or inversion schemes.

Consider again first the situation when we in fact have measured the full multi-static response (MSR) matrix

$$\mathbf{d} = \big(d(t, \boldsymbol{x}_r, \boldsymbol{y}_s)\big)_{r=1,\dots,N_r,\, s=1,\dots,N_s,\, t\in[-T/2,T/2]}\,.$$

For each $s = 1, \dots, N_s$, denote by $u^{(s)}(t, \boldsymbol{x}; \hat{c})$ the numerical solution of (3.1.1) with the source term $n(t, \boldsymbol{x}) = \delta(\boldsymbol{x} - \boldsymbol{y}_s)f(t)$ when the medium perturbation is $\widetilde{\delta c}^{-2}$. Denote by $\mathbf{d}[\widetilde{c}]$ the corresponding computed MSR matrix, whose elements are defined by

$$d[\widetilde{c}](t, \boldsymbol{x}_r, \boldsymbol{y}_s) = u^{(s)}(t, \boldsymbol{x}_r; \widetilde{c}) = \big(\mathcal{F}_0\, \widetilde{\delta c}^{-2}\big)(t, \boldsymbol{x}_r, \boldsymbol{y}_s)\,.$$

An iterative imaging scheme can then be based on calculating and minimizing the quadratic misfit functional

$$\mathcal{J}[\widetilde{c}] = \sum_{s=1}^{N_s}\sum_{r=1}^{N_r}\int_{-\frac{T}{2}}^{\frac{T}{2}} \big|d(t, \boldsymbol{x}_r, \boldsymbol{y}_s) - d[\widetilde{c}](t, \boldsymbol{x}_r, \boldsymbol{y}_s)\big|^2\,\mathrm{d}t\,. \tag{3.5.5}$$

The implementation of a descent algorithm over $\widetilde{c}$ produces a sequence of estimates $\widetilde{c}_1, \widetilde{c}_2, \dots$ leading to an estimate, say $\widetilde{c}_N$, of c at termination. We find in the Born approximation that the residual in (3.5.5) is

$$\begin{aligned}\mathcal{J}[\widetilde{c}] &= \sum_{s=1}^{N_s}\sum_{r=1}^{N_r}\int_{-\frac{T}{2}}^{\frac{T}{2}} \big|\big(\mathcal{F}_0\, \delta c^{-2}\big)(t, \boldsymbol{x}_r, \boldsymbol{y}_s) - \big(\mathcal{F}_0\, \widetilde{\delta c}^{-2}\big)(t, \boldsymbol{x}_r, \boldsymbol{y}_s)\big|^2\,\mathrm{d}t \\ &= \iint_\Omega \mathcal{F}_0^*\mathcal{F}_0(\boldsymbol{x}, \boldsymbol{x}')\big[\delta c^{-2}(\boldsymbol{x}) - \widetilde{\delta c}^{-2}(\boldsymbol{x})\big]\big[\delta c^{-2}(\boldsymbol{x}') - \widetilde{\delta c}^{-2}(\boldsymbol{x}')\big]\,\mathrm{d}\boldsymbol{x}\,\mathrm{d}\boldsymbol{x}'\,,\end{aligned} \tag{3.5.6}$$

with $\mathcal{F}_0^*\mathcal{F}_0(\boldsymbol{x}, \boldsymbol{x}')$ defined by (3.1.18) when T is large enough (i.e. larger than the typical travel time). Note that this minimization approach requires the calculation of $\mathcal{J}[\widetilde{c}_j]$, $j = 1, \dots, N$ which is computationally very expensive because it requires computing the full multi-static response matrix with a new velocity function at each step, which amounts to solving the forward problem N_s times at each step.

Consider now the situation when the sources are defined as in (3.3.1), that is with simultaneous randomly delayed point sources. The data has the form of the vector

$$\boldsymbol{d} = \big(d(t, \boldsymbol{x}_r)\big)_{r=1,\dots,N_r,\, t\in[-T/2,T/2]}\,.$$

Denote by $u(t, \boldsymbol{x}; \widetilde{c})$ the solution of (3.1.1) when the medium perturbation is $\widetilde{\delta c}^{-2}$ and the source term is (3.3.1). Denote by $\boldsymbol{d}[\widetilde{c}]$ the corresponding computed data:

$$d[\widetilde{c}](t, \boldsymbol{x}_r) = u(t, \boldsymbol{x}_r; \widetilde{c}) = \big(\mathcal{F}\, \widetilde{\delta c}^{-2}\big)(t, \boldsymbol{x}_r)\,.$$

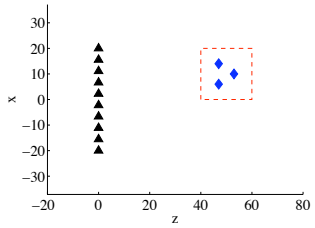

Figure 3.1: Numerical set-up: the triangles are the sensors of the array, the diamonds are the reflectors, the dashed lines determine the search window for the imaging functionals.

We can implement an iterative imaging scheme based on calculating and minimizing the least-square functional

$$\widetilde{\mathcal{J}}[\widetilde{c}] = \sum_{r=1}^{N_r} \int_{-\frac{T}{2}}^{\frac{T}{2}} \left| d(t, \boldsymbol{x}_r) - d[\widetilde{c}](t, \boldsymbol{x}_r) \right|^2 \mathrm{d}t \,.$$

We then find in the Born approximation and when T is large enough (i.e. larger than the typical travel time and the typical time delay for noise blended sources, or larger than the typical travel time and the decoherence time for stationary random sources) that

$$\begin{aligned}
\widetilde{\mathcal{J}}[\widetilde{c}] &= \sum_{r=1}^{N_r} \int_{-\frac{T}{2}}^{\frac{T}{2}} \left| \big(\mathcal{F}\,\delta c^{-2}\big)(t, \boldsymbol{x}_r) - \big(\mathcal{F}\,\widetilde{\delta c}^{-2}\big)(t, \boldsymbol{x}_r) \right|^2 \mathrm{d}t \\
&= \iint_{\Omega} \mathcal{F}^*\mathcal{F}(\boldsymbol{x}, \boldsymbol{x}') \big[\delta c^{-2}(\boldsymbol{x}) - \widetilde{\delta c}^{-2}(\boldsymbol{x})\big] \big[\delta c^{-2}(\boldsymbol{x}') - \widetilde{\delta c}^{-2}(\boldsymbol{x}')\big] \,\mathrm{d}\boldsymbol{x}\,\mathrm{d}\boldsymbol{x}' \\
&\approx \iint_{\Omega} \big\langle \mathcal{F}^*\mathcal{F}(\boldsymbol{x}, \boldsymbol{x}') \big\rangle \big[\delta c^{-2}(\boldsymbol{x}) - \widetilde{\delta c}^{-2}(\boldsymbol{x})\big] \big[\delta c^{-2}(\boldsymbol{x}') - \widetilde{\delta c}^{-2}(\boldsymbol{x}')\big] \,\mathrm{d}\boldsymbol{x}\,\mathrm{d}\boldsymbol{x}' \,, \qquad (3.5.7)
\end{aligned}$$

where we use the statistical stability property of the normal operator. Applying a descent algorithm on $\widetilde{\mathcal{J}}[\widetilde{c}]$ over $\widetilde{c}$ is much less computationally intensive than with the full MSR strategy, since it requires solving only one forward problem at each step of the algorithm. The essential observation here is that the residual in (3.5.6) corresponds to the residual in (3.5.7). Therefore, we can expect that the velocity model estimation based on the simultaneous sources will give estimates that are comparable to those obtained with (physical) measurements and successive numerical calculations based on simultaneous sources only, when in the scaling regime discussed in sections 3.2 and 3.3. We remark that the same random forcing should be used in each iteration, that is, the random forcing associated with the actual measured MSR matrix. Note, moreover, that if in fact the whole MSR matrix was measured in the physical experiment one could from this synthesize a "synthetic" simultaneous source experiment by convolution with simulated stationary random sources or randomly delayed sources.

3.5.3 Numerical illustrations

The numerical simulations presented in this section compare the image obtained with migration of the full MSR matrix and the one obtained with migration of a unique set of data

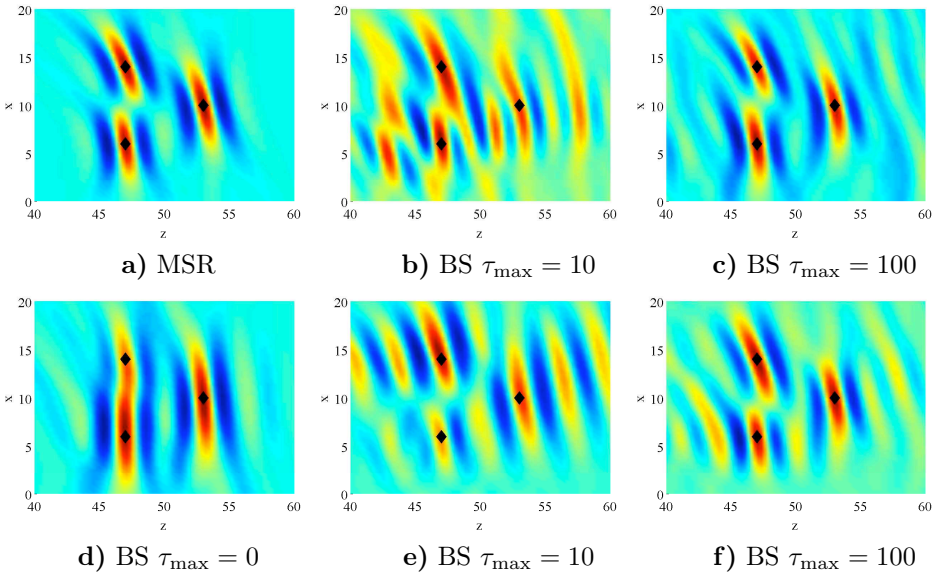

Figure 3.2: Images given by Kirchhoff migration of the full MSR matrix (a); migration of the data vector obtained with simultaneous sources without random time delays (d); migration of the data vector obtained with blended sources (BS) with random time delays uniformly distributed over $[-10, 10]$ for two realizations of the delays (b,e); migration of the data vector obtained with blended sources with random time delays uniformly distributed over $[-100, 100]$ for two realizations of the delays (c,f).

collected with blended (randomly time delayed) sources.

We consider a three-dimensional homogeneous background medium with velocity $c_0 = 1$. We compute the image in the plane (z, x) and use the homogeneous background Green's function (3.1.5) and the Born approximation for the three reflectors we want to image. The source and receiver arrays are coincident and the $N_s = 10$ sensors are uniformly spaced on the interval $\big(0, [-20, +20]\big)$, (Figure 3.1). The pulse signal is the second derivative of a Gaussian with Fourier transform $\widehat{f}(\omega) = \omega^2 \exp(-\omega^2)$. We consider three point reflectors at locations $(47, 14)$, $(53, 10)$, $(47, 6)$ with the same reflectivity. The search window in given by the square $[40, 60] \times [0, 20]$, and is marked with a dashed line in Figure 3.1. The random time delays of the sources are independent and identically distributed random variables with uniform distribution over $[-\tau_{\max}, \tau_{\max}]$ and we test three different values for $\tau_{\max}$ and two different realizations. The images obtained in the search window are shown in Figure 3.2. As expected by the theory, the image obtained with the data collected with blended sources is very similar to the one obtained with the full MSR matrix when $\tau_{\max}$ is large enough (here the time for a round trip from the array to the target is about 100). When $\tau_{\max}$ is small the image is unstable in that it depends on the particular realizations of the time delays.

3.6 Appendices

3.6.1 Appendix A: Statistical stability for a continuum of point sources

When the point sources are close to each other (closer than a wavelength apart), then it is possible to model the process $n(t, \boldsymbol{x})$ as a zero-mean stationary (in time) Gaussian process with autocorrelation function

$$\big\langle n(t_1, \boldsymbol{y}_1)\, n(t_2, \boldsymbol{y}_2)\big\rangle = F(t_2 - t_1)\, \delta(\boldsymbol{y}_2 - \boldsymbol{y}_1)\, \theta\Big(\frac{\boldsymbol{y}_1 + \boldsymbol{y}_2}{2}\Big)\,,$$

where the function θ describes the spatial support of the sources.

The product of second-order moments of the random process $n(t, \boldsymbol{x})$ is

$$\begin{aligned}\big\langle n(t-s, \boldsymbol{y}_1)\, n(t-u, \boldsymbol{y}_2)\big\rangle \big\langle n(t'-s', \boldsymbol{y}_1')\, n(t'-u', \boldsymbol{y}_2')\big\rangle \\ = F(s-u)F(s'-u')\, \theta(\boldsymbol{y}_1)\delta(\boldsymbol{y}_1 - \boldsymbol{y}_2)\, \theta(\boldsymbol{y}_1')\delta(\boldsymbol{y}_1' - \boldsymbol{y}_2')\,.\end{aligned}$$

The fourth-order moment of the Gaussian random process n is

$$\begin{aligned}&\big\langle n(t-s, \boldsymbol{y}_1)\, n(t-u, \boldsymbol{y}_2)\, n(t'-s', \boldsymbol{y}_1')\, n(t'-u', \boldsymbol{y}_2')\big\rangle \\ &\qquad = F(s-u)F(s'-u')\, \theta(\boldsymbol{y}_1)\delta(\boldsymbol{y}_1 - \boldsymbol{y}_2)\, \theta(\boldsymbol{y}_1')\delta(\boldsymbol{y}_1' - \boldsymbol{y}_2') \\ &\qquad\quad + F(t'-t-s'+s)F(t'-t-u'+u)\, \theta(\boldsymbol{y}_1)\delta(\boldsymbol{y}_1 - \boldsymbol{y}_1')\, \theta(\boldsymbol{y}_2)\delta(\boldsymbol{y}_2 - \boldsymbol{y}_2') \\ &\qquad\quad + F(t'-t-u'+s)F(t'-t-s'+u)\, \theta(\boldsymbol{y}_1)\delta(\boldsymbol{y}_1 - \boldsymbol{y}_2')\, \theta(\boldsymbol{y}_2)\delta(\boldsymbol{y}_1' - \boldsymbol{y}_2)\,.\end{aligned}$$

Consequently, we have that for any $T > 0$

$$\begin{aligned}&\iint_{-\frac{T}{2}}^{\frac{T}{2}} \Big(\big\langle n(t-s, \boldsymbol{y}_1)\, n(t-u, \boldsymbol{y}_2)\, n(t'-s', \boldsymbol{y}_1')\, n(t'-u', \boldsymbol{y}_2')\big\rangle \\ &\qquad - \big\langle n(t-s, \boldsymbol{y}_1)\, n(t-u, \boldsymbol{y}_2)\big\rangle\big\langle n(t'-s', \boldsymbol{y}_1')\, n(t'-u', \boldsymbol{y}_2')\big\rangle\Big)\, \mathrm{d}t\, \mathrm{d}t' \\ &\qquad\qquad = S_T(s-s', u-u')\, \theta(\boldsymbol{y}_1)\delta(\boldsymbol{y}_1 - \boldsymbol{y}_1')\, \theta(\boldsymbol{y}_2)\delta(\boldsymbol{y}_2 - \boldsymbol{y}_2') \\ &\qquad\qquad\quad + S_T(s-u', u-s')\, \theta(\boldsymbol{y}_1)\delta(\boldsymbol{y}_1 - \boldsymbol{y}_2')\, \theta(\boldsymbol{y}_2)\delta(\boldsymbol{y}_1' - \boldsymbol{y}_2)\,, \quad (3.6.1)\end{aligned}$$

with S_T defined by (3.2.11). We then get the same formulas as in the discrete model.

3.6.2 Appendix B: Resolution analysis

Consider the kernel

$$\mathcal{K}_\omega(\boldsymbol{x}, \boldsymbol{x}') = \sum_{r=1}^{N_r} \overline{\widehat{G}}(\omega, \boldsymbol{x}_r, \boldsymbol{x})\widehat{G}(\omega, \boldsymbol{x}_r, \boldsymbol{x}')\,. \quad (3.6.2)$$

We assume that the points $(\boldsymbol{x}_r)_{r=1}^{N_r}$ are at the surface $\Sigma = \{\boldsymbol{y} \in \mathbb{R}^3, y_3 = 0\}$ and are close to each other (closer than half-a-wavelength) so that a continuum approximation can be used:

$$\mathcal{K}_\omega(\boldsymbol{x}, \boldsymbol{x}') = \int_\Sigma \rho(\boldsymbol{x}_r)\overline{\widehat{G}}(\omega, \boldsymbol{x}_r, \boldsymbol{x})\widehat{G}(\omega, \boldsymbol{x}_r, \boldsymbol{x}')\, \mathrm{d}\sigma(\boldsymbol{x}_r)\,, \quad (3.6.3)$$

where ρ is the surface density of receivers. In the high-frequency asymptotics, for $\boldsymbol{x} = \boldsymbol{x}'$, we have

$$\mathcal{K}_\omega(\boldsymbol{x}, \boldsymbol{x}) = \int_\Sigma \rho(\boldsymbol{x}_r)\mathcal{A}(\boldsymbol{x}, \boldsymbol{x}_r)^2 \, \mathrm{d}\sigma(\boldsymbol{x}_r) \, .$$

For $|\boldsymbol{x} - \boldsymbol{x}'|$ of the order of the wavelength, we find

$$\mathcal{K}_\omega(\boldsymbol{x}, \boldsymbol{x}') \simeq \int_\Sigma \rho(\boldsymbol{x}_r)\mathcal{A}(\boldsymbol{x}', \boldsymbol{x}_r)^2 \exp\big(- i\omega\nabla_{\boldsymbol{x}'}\mathcal{T}(\boldsymbol{x}', \boldsymbol{x}_r) \cdot (\boldsymbol{x} - \boldsymbol{x}')\big) \, \mathrm{d}\sigma(\boldsymbol{x}_r) \, .$$

If, additionally, we assume that the background is homogeneous $c(\boldsymbol{x}) = c_0$, then $\mathcal{T}(\boldsymbol{x}', \boldsymbol{x}_r) = |\boldsymbol{x}' - \boldsymbol{x}_r|/c_0$ and $\mathcal{A}(\boldsymbol{x}', \boldsymbol{x}_r) = 1/\big(4\pi|\boldsymbol{x}' - \boldsymbol{x}_r|\big)$ and we have

$$\mathcal{K}_\omega(\boldsymbol{x}, \boldsymbol{x}') \simeq \frac{1}{(4\pi)^2} \int_\Sigma \rho(\boldsymbol{x}_r) \frac{1}{|\boldsymbol{x}' - \boldsymbol{x}_r|^2} \exp\Big(i\frac{\omega}{c_0} \frac{\boldsymbol{x}_r - \boldsymbol{x}'}{|\boldsymbol{x}_r - \boldsymbol{x}'|} \cdot (\boldsymbol{x} - \boldsymbol{x}')\Big) \, \mathrm{d}\sigma(\boldsymbol{x}_r) \, .$$

This expression gives the width and the form of the function $\mathcal{K}_\omega(\boldsymbol{x}, \boldsymbol{x}')$ along the diagonal band $\boldsymbol{x} \simeq \boldsymbol{x}'$. If the diameter a of the array (i.e. the support of ρ) is smaller than the distance from the array to $\boldsymbol{x}'$, then we find the standard Rayleigh resolution formulas. If the diameter of the array is of the same order as or larger than the distance from the array to $\boldsymbol{x}'$, then we find that the resolution is of the order of the wavelength.

Using stationary phase arguments, we obtain for $|\boldsymbol{x} - \boldsymbol{x}'|$ much larger than the typical wavelength:

$$\mathcal{K}_\omega(\boldsymbol{x}, \boldsymbol{x}') \simeq \frac{\rho(\boldsymbol{x}_0)}{(4\pi)^2} \, \frac{2\pi \, c_0 (x_3 - x_3')^2}{|\boldsymbol{x} - \boldsymbol{x}'|^3} \, \frac{i}{\omega} \, \mathrm{sgn}(x_3 - x_3') \exp\Big(- i\frac{\omega}{c_0}|\boldsymbol{x} - \boldsymbol{x}'|\Big) \, ,$$

where $\boldsymbol{x}_0$ is the intersection of the ray going through $\boldsymbol{x}$ and $\boldsymbol{x}'$ with the surface $y_3 = 0$:

$$\boldsymbol{x}_0 = \frac{x_3\boldsymbol{x}' - x_3'\boldsymbol{x}}{x_3 - x_3'} \, .$$

This expression gives the long-distance decay of the function $\mathcal{K}_\omega(\boldsymbol{x}, \boldsymbol{x}')$ for $\omega|\boldsymbol{x} - \boldsymbol{x}'|/c_0 \gg 1$.

Chapter 4

The stochastic transport equation

4.1 Introduction

Consider the stochastic linear transport (SLT) equation in Stratonovich form

$$\frac{\partial u}{\partial t} + b \cdot \nabla u + \sigma \nabla u \circ \frac{\mathrm{d}W}{\mathrm{d}t} = 0, \qquad u|_{t=0} = u_0 \,. \tag{4.1.1}$$

Here $W = (W_t)_{t \geq 0}$ is a d-dimensional Brownian motion defined on a filtered probability space $(\Omega, \mathscr{F}, \mathscr{F}_t, P)$, the drift $b : [0,T] \times \mathbb{R}^d \to \mathbb{R}^d$ is a given deterministic vector field, $\sigma \in \mathbb{R}$ and $u_0 : \mathbb{R}^d \to \mathbb{R}$ are given and the solution $u = u(x,t)$ will be a scalar random field on $(\Omega, \mathscr{F}, \mathscr{F}_t, P)$ defined for $(t,x) \in [0,T] \times \mathbb{R}^d$.

We deal with the problem of singularities of u starting from a regular initial condition u_0. When $\sigma = 0$ and b is not Lipschitz, singularities may appear, in the form of discontinuities (or blow-up of derivatives), as in the simple example $d = 1$, $b(x) = -sign(x)\sqrt{|x|}$: any non-symmetric smooth initial condition u_0 develops a discontinuity at $x = 0$ for any $t > 0$, because there are different, symmetric, initial conditions x_0 for the associated equation of characteristics

$$x'(t) = b(t, x(t)), \quad x(0) = x_0$$

which coalesce at $x = 0$ at any arbitrary positive time. Opposite to the question of uniqueness of weak L^∞ solutions, where positive results have been given under relatively weak assumptions on b, see for instance [DPL89, Am04], it seems that good results of no blow-up are not available in the deterministic case when b is not Lipschitz.

Our purpose is to show that, for $\sigma \neq 0$ and b of class

$$b \in L^q_p := L^q\left(0, T; L^p(\mathbb{R}^d, \mathbb{R}^d)\right),$$

$$p, q \geq 2\,, \qquad \frac{d}{p} + \frac{2}{q} < 1 \tag{4.1.2}$$

some regularity of the initial condition is maintained. In particular, discontinuities do not appear. We prove the following result.

Theorem 4.1. *If $\sigma \neq 0$, (4.1.2) holds and $u_0 \in \cap_{r \geq 1} W^{1,r}\left(\mathbb{R}^d\right)$ then there exists a unique solution u such that*

$$P\left(u(t,\cdot) \in \cap_{r \geq 1} W^{1,r}_{loc}\left(\mathbb{R}^d\right)\right) = 1$$

for every $t \in [0,T]$.

Moreover, the unique solution in this class is given by a representation formula, in terms of u_0, involving a weakly differentiable stochastic flow. By Sobolev embedding theorem, $u(t,\cdot)$ is α-Hölder continuous for every $\alpha \in (0,1)$, with probability one. Hence, from smooth initial conditions, discontinuities cannot arise.

The precise formulation of the concept of solution and other details are given in the sequel.

The intuitive idea is that, opposite to the deterministic case, when $\sigma \neq 0$ the characteristics cannot meet. They satisfy the stochastic differential equation (SDE)

$$\mathrm{d}X_t = b\left(X_t, t\right)\mathrm{d}t + \sigma\,\mathrm{d}W_t \tag{4.1.3}$$

which generates, under assumptions (4.1.2), a stochastic flow of Hölder continuous homeomorphisms, with some weak form of differentiability. The existence of an Hölder continuous stochastic flow has been proved in [FF11], [FF12a], [Zh11]. A differentiability property in terms of finite increments has been given in [FF12a]. Here we establish Sobolev type differentiability. A similar Sobolev regularity of the flow is investigated in [MNP12] by different tools (Malliavin calculus). See also [MP10].

The assumption (4.1.2) has been introduced in the framework of stochastic differential equations by Krylov and Röckner in [KR05], where they prove strong uniqueness for equation (4.1.3). In the fluid dynamic literature, with $\leq$ in place of $<$, this condition is known as the Ladyzhenskaya-Prodi-Serrin condition [Fl, Pr59]. One of its main consequences is that it gives uniform bounds on gradients of solutions to an auxiliary parabolic problem (see theorem 4.2 below) essential for our approach, along with good properties of the second derivatives.

The possibility that noise may prevent the emergence of singularities is an intriguing phenomenon that is under investigation for several systems. For linear transport equations with $b \in L^\infty\left([0,T]\,; C_b^\alpha\left(\mathbb{R}^d, \mathbb{R}^d\right)\right)$ it may be deduced from [FGP10] (the result presented here is more general). For nonlinear systems there are negative results, like the fact that noise does not prevent shocks in Burgers equation, see [Fl], and positive results for special kind of singularities (collapse of measure valued solutions) for the vorticity field of 2-dimensional Euler equations, see [FGP11], and for the 1-dimensional Vlasov-Poisson equation, see [DFV12]. Moreover, for Schrödinger equations, there are several theoretical and numerical results of great interest, see [dBD02a, dBD10, DdM02a, DdM02b, DT11]. For a list of results concerning the restored uniqueness due to noise and address to the lecture note [Fl] on this subject.

After the result of theorem 4.1, it remains open the question whether the solution is Lipschitz continuous (or more) when $u_0 \in W^{1,\infty}\left(\mathbb{R}^d\right)$ (or more). In dimension d we think that this is a difficult question under assumption (4.1.2). The answer is positive when $b \in L^\infty\left([0,T]\,; C_b^\alpha\left(\mathbb{R}^d, \mathbb{R}^d\right)\right)$ because the stochastic flow is made of diffeomorphisms, see [FGP10] and it is also positive in dimension $d = 1$ for certain discontinuous drift b, including for instance $b\left(x\right) = sign\left(x\right)$, see [At10].

It must be emphasized that, although this "regularization by noise" may look related to the regularization produced by the addition of a Laplacian to the equation, in fact it preserves the hyperbolic structure of the equation. The equations remain reversible and the solution at time t is, in the problem treated in this paper, just given by the initial condition composed with a flow. If the initial condition has a discontinuity, the solution also has a discontinuity; no smoothing effect is introduced. However, the emergence of singularities (shocks in our case) is prevented.

This chapter is organized as follows. In section 4.2 we present some results on regularity and approximation properties of the flow associated to the SDE (4.1.3). They are obtained via the study of an associated SDE and the regularity of its solutions. The main results are contained in lemmas 4.3 and 4.5, while more technical results are collected in appendix A. In section 4.3 we define weakly differentiable solutions of the SLT equation and prove their existence in theorem 4.10. A technical result on convergence of random fields in Sobolev spaces is left to the last appendix. Finally, uniqueness of weakly differentiable solutions of the SLT equation is proved in section 4.4.

4.2 Convergence results

In this section we present some technical results on an associated SDE that we will study as an intermediate step to obtain some regularity and approximation properties of the stochastic flow generated by the SDE (4.1.3). The main results are contained in lemmas 4.3 and 4.5. In order not to overload this section, many technical results are left to appendix A.

Let us start by setting the notation used and recalling some results. We will use the following auxiliary SDE, introduced in [FF12a]:

$$\mathrm{d}Y_t = \lambda U(t, \gamma_0^{-1}(x))\mathrm{d}t + \big(\nabla U(t, \gamma_0^{-1}(x)) + Id\big)\mathrm{d}W_t \ , \qquad Y_0 = x \ . \tag{4.2.1}$$

The link between this SDE and the one presented in the introduction is given by the $\mathcal{C}^1$-diffeomorphism γ_t: $Y_t = \gamma_t \circ X_t \circ \gamma_0^{-1}$, where $\gamma_t(x) = x + U(t,x)$ and $U : \mathbb{R}^{d+1} \to \mathbb{R}^d$ is the solution of the partial differential equation (PDE)

$$\begin{cases} \partial_t U + \frac{1}{2}\Delta U + b \cdot \nabla U - \lambda U + b = 0 \\ U(T,x) = 0 \end{cases} .$$

This PDE is well posed in the space

$$H^q_{2,p}(T) := L^q\left(0,T\,;\, W^{2,p}(R^d)\right) \cap W^{1,q}\left(0,T\,;\, L^p(R^d)\right).$$

Further details on the regularity properties of function in this space are given by lemma 4.12 in appendix A. We refer the reader to [KR05], where a proof of this lemma as well as of the theorem below (in a similar setting) are given. In this paper it is also shown that the classical Itô formula extends to functions in $H^q_{2,p}$.

We report here the precise result on the well-posedness of the PDE shown above, which is taken from [FF12a, Theorem 3.3]. The proof is recalled in Appendix A.

Theorem 4.2. *Take p, q such that (4.1.2) holds, $\lambda > 0$ and two vector fields $b, f\,(t,x) : \mathbb{R}^{d+1} \to \mathbb{R}^d$ belonging to $L^q_p(T)$. Then in $H^q_{2,p}(T)$ there exists a unique solution of the backward parabolic system*

$$\begin{cases} \partial_t u + \frac{1}{2}\Delta u + b \cdot \nabla u - \lambda u + f = 0 \\ u(T,x) = 0 \end{cases} . \tag{4.2.2}$$

For this solution there exists a finite constant N depending only on d, p, q, T, λ and $\|b\|_{L^q_p(T)}$

such that

$$\|u\|_{H^q_{2,p}(T)} \leq N\|f\|_{L^q_p(T)}\,. \tag{4.2.3}$$

We will use the result of this theorem with $f = b$.

Let b^n be a sequence of smooth vector fields converging to b in L^q_p. Let U be the unique solution to the PDE (4.2.2) provided by the above theorem and U^n the solutions obtained using the approximating vector fields b^n. Lemma 4.14 in appendix A shows that the vector fields U^n converge in $H^q_{2,p}$ to U.

In [FF12a] is also proved the existence of Hölder flows of homeomorphisms for the two SDEs above, which we denote by $\phi_t(\cdot)$ for the SDE (4.1.3), and $\psi_t(\cdot)$ for (4.2.1). We will use $\phi^n_t(\cdot)$ to denote the flows obtained for the approximating vector fields b^n, and $\psi^n_t(\cdot)$ for the flows corresponding to the auxiliaries SDEs obtained via the diffeomorphisms $\gamma^n_t = Id + U^n(t,\cdot)$. We will use $\phi^t_0(\cdot)$, $\phi^{t,n}_0(\cdot)$, and $\psi^{t,n}_0(\cdot)$ for the inverse flows. Remark that the inverse flows ϕ^t_0 and $\phi^{t,n}_0$ are solutions of the same SDEs as the direct flows, but driven by the drifts $-b$ and $-b^n$.

We can now state and prove the two main regularity results on the flows $\phi^{t,n}_0$.

Lemma 4.3. *For every $R > 0$, $p \geq 1$ and $x, y \in B_R$,*

$$\lim_{n\to\infty} \sup_{t\in[0,T]} \sup_{x\in B_R} E\Big[\big|\phi^{t,n}_0(x) - \phi^t_0(y)\big|^p\Big] \leq C_{p,T}\,|x-y|^p\,.$$

In particular,

$$\lim_{n\to\infty} \sup_{t\in[0,T]} \sup_{x\in B_R} E\left[\left|\phi^{t,n}_0(x) - \phi^t_0(x)\right|^p\right] = 0\,. \tag{4.2.4}$$

Proof. **Step 1** (preliminary estimates). By lemma 4.14 of appendix A we have that for every $r > 0$ there exist a function f such that $\lim_{n\to\infty} f(n) = 0$ and

$$\begin{aligned}
\sup_{x\in\mathbb{R}^d} \sup_{t\in[0,T]} \big|\nabla U(t,x)\big| &\leq \frac{1}{2}\,,\\
\sup_{x\in B_r} \sup_{t\in[0,T]} \big|U^n(t,x) - U(t,x)\big| &\leq f(n)\,,\\
\sup_{x\in B_r} \sup_{t\in[0,T]} \big|\nabla U^n(t,x) - \nabla U(t,x)\big| &\leq f(n)\,.
\end{aligned}$$

Since $\phi_t(x)$ is jointly continuous in space and time, there exist an $r < \infty$ such that the image of $B_R \times [0,T]$ will be contained in B_r for all $t \leq T$. In the following we will always take $x, y \in B_R$. It follows that

$$\begin{aligned}
\big|U^n(t,\phi^n_t(x)) - U(t,\phi_t(y))\big| &\leq f(n) + \frac{1}{2}\big|\phi^n_t(x) - \phi_t(y)\big|\,,\\
\big|\nabla U^n(t,\phi^n_t(x)) - \nabla U(t,\phi_t(y))\big| &\leq f(n) + \big|\nabla U^n(t,\phi^n_t(x)) - \nabla U^n(t,\phi_t(y))\big|\,.
\end{aligned}$$

To shorten notation, we will write ϕ^n and ϕ to denote $\phi^n_t(x)$ and $\phi_t(y)$, $U^n(\phi^n)$ and $U^n(x)$ to denote $U^n(t,\phi^n)$ e $U^n(0,x)$, etc. The same holds for the flows of the SDE (4.2.1). From the definition $\psi^n_t = \gamma_t \circ \phi^n_t \circ (\gamma^n_0)^{-1}$ and the properties of the diffeomorphisms γ^n_t obtained

from lemma 4.14 and remark 4.15, we immediately have

$$\begin{aligned} |\psi^n - \psi| &\geq |\phi^n - \phi + U^n(\phi^n) - U^n(\phi)| - f(n) \\ &\geq \frac{1}{2}|\phi^n - \phi| - f(n)\,, \\ 2\Big(|\psi^n - \psi| + f(n)\Big) &\geq |\phi^n - \phi| \end{aligned} \tag{4.2.5}$$

and

$$|\psi^n - \psi| \leq \frac{3}{2}|\phi^n - \phi| + f(n)\,. \tag{4.2.6}$$

Step 2 (computations). We start by proving the convergence of the flows of the auxiliary SDE (4.2.1). By Itô formula, for any $a \geq 2$

$$\begin{aligned} \frac{1}{a}\,\mathrm{d}\big|\psi^n - \psi\big|^a &= \big|\psi^n - \psi\big|^{a-2}\Big\{\lambda\big\langle(\psi^n - \psi), U^n(\phi^n) - U(\phi)\big\rangle_{\mathbb{R}^d}\,\mathrm{d}t \\ &\quad + \big\langle(\psi^n - \psi), \big(\nabla U^n(\phi^n) - \nabla U(\phi)\big)\cdot \mathrm{d}W_t\big\rangle_{\mathbb{R}^d} \\ &\quad + \frac{a-1}{2}\,\mathrm{Tr}\Big(\big[\nabla U^n(\phi^n) - \nabla U(\phi)\big]\big[\nabla U^n(\phi^n) - \nabla U(\phi)\big]^T\Big)\,\mathrm{d}t\Big\} \\ &= \big|\psi^n - \psi\big|^{a-2}\Big\{A_1 + A_2 + A_3\Big\}\,, \end{aligned}$$

where $\langle\,\cdot,\cdot\,\rangle_{\mathbb{R}^d}$ denotes the standard scalar product on $\mathbb{R}^d$. Let us analyze the three terms A_1, A_2, A_3. Using (4.2.5) we have

$$\begin{aligned} A_1 &\leq \lambda\big|\psi^n - \psi\big|\Big(f(n) + \frac{1}{2}\big|\phi^n - \phi\big|\Big)\,\mathrm{d}t \\ &\leq \lambda\big|\psi^n - \psi\big|^2\,\mathrm{d}t + 2\lambda f(n)\big|\psi^n - \psi\big|\,\mathrm{d}t\,. \end{aligned}$$

Since ∇U^n is bounded (uniformly in n, see lemma 4.14) and since by equation (4.5.16) of remark 4.15 $|\psi^n|^a$ belongs to $L^2(\Omega\times[0,T])$ for any $a \geq 1$, we can write $A_2 = \mathrm{d}M_t^n$, where for every n, $\mathrm{d}M_t^n$ is the differential of a zero mean martingale.

As for the third term, using twice the inequality $(\alpha+\beta)^2 \leq 2(\alpha^2+\beta^2)$ and the estimates of the first step, we get

$$\begin{aligned} \frac{2}{d^2(a-1)}\,A_3 &\leq \Big\{2\big|\nabla U^n(\phi^n) - \nabla U^n(\phi)\big|^2 + 2f^2(n)\Big\}\,\mathrm{d}t \\ &\leq \big|\phi^n - \phi\big|^2\mathrm{d}A_t^n + 2f^2(n)\,\mathrm{d}t \\ &\leq 8\big|\psi^n - \psi\big|^2\mathrm{d}A_t^n + 8f^2(n)\,\mathrm{d}A_t^n + 2f^2(n)\,\mathrm{d}t\,, \end{aligned}$$

where for every n

$$A_t^n := 2\int_0^t \frac{\big|\nabla U^n(\phi_s^n) - \nabla U^n(\phi_s)\big|^2}{\big|\phi_s^n - \phi_s\big|^2}\mathbb{1}_{\{\phi_s^n \neq \phi_s\}}\,\mathrm{d}s \tag{4.2.7}$$

is a nondecreasing adapted stochastic process, with $A_0^n = 0$, and uniformly in n $\mathbb{E}[A_T^n] \leq$

$C < \infty$, see lemma 4.16. Set $B_t^n := \big[4\,d^2 a(a-1)\big] A_t^n$. From the above estimates and after renaming M_t (which remains a zero mean martingale), we get

$$\begin{aligned}\mathrm{d}\Big(e^{-B_t^n}\big|\psi^n-\psi\big|^a\Big) \le e^{-B_t^n}\Big[a\lambda|\psi^n-\psi|^a + 2a\lambda f(n)|\psi^n-\psi|^{a-1}\Big]\,\mathrm{d}t \\ + \mathrm{d}M_t + f^2(n)e^{-B_t^n}\big|\psi^n-\psi\big|^{a-2}\,\mathrm{d}B_t^n \\ + d^2a(a-1)\,e^{-B_t^n}f^2(n)\big|\psi^n-\psi\big|^{a-2}\,\mathrm{d}t\,.\end{aligned}$$

Integrating in time, taking the expected value, and finally the supremum over $t\in[0,T]$, we get

$$\begin{aligned}\sup_{t\in[0,T]}\mathbb{E}\Big[e^{-B_t^n}\big|\psi_t^n-\psi_t\big|^a\Big] \le \big|\psi_0^n-\psi_0\big|^a + a\lambda\mathbb{E}\Big[\int_0^T e^{-B_s^n}\big|\psi_s^n-\psi_s\big|^a\,\mathrm{d}s\Big] \\ + C_{a,d,\lambda}f(n)\,\mathbb{E}\Big[\int_0^T e^{-B_s^n}\Big(\big|\psi_s^n-\psi_s\big|^{a-1} + f(n)\big|\psi_s^n-\psi_s\big|^{a-2}\Big)\,\mathrm{d}s\Big] \\ + f^2(n)\,\mathbb{E}\Big[\int_0^T e^{-B_s^n}\big|\psi_s^n-\psi_s\big|^{a-2}\,\mathrm{d}B_s^n\Big]\,. \qquad (4.2.8)\end{aligned}$$

The expected value in the second line above is bounded uniformly in n. This fact is easily seen using for each term the Hölder inequality together with the integrability properties of the flows ψ^n and of the exponential of the processes B_s^n. These two integrability properties are provided by equation (4.5.16) of remark 4.15 and lemma 4.16, respectively. We claim that also the expected value of the last line is bounded.

Claim 4.4. *There exists a constant C such that for every n and $p\ge 0$*

$$\mathbb{E}\Big[\int_0^T e^{-B_s^n}\big|\psi_s^n-\psi_s\big|^p\,\mathrm{d}B_s^n\Big] \le C\,.$$

Proof of the Claim. Using the definition of B_t^n we can rewrite the term on the left hand side as

$$\mathbb{E}\Big[\int_0^T e^{-B_s^n}\big|\psi_s^n-\psi_s\big|^p\frac{\big|\nabla U(s,\phi_s^n)-\nabla U(s,\phi_s)\big|^2}{\big|\phi_s^n-\phi_s\big|^2}\,\mathrm{d}s\Big]\,.$$

Using Hölder inequality, for some $\varepsilon > 1$ small (to be fixed later) and k the conjugate exponent, we obtain the two terms

$$\mathbb{E}\Big[\int_0^T e^{-kB_s^n}\big|\psi_s^n-\psi_s\big|^{kp}\,\mathrm{d}s\Big]\,,$$

for which we have already explained how to obtain a uniform bound, and

$$\mathbb{E}\Big[\int_0^T \frac{\big|\nabla U^n(s,\phi_s^n)-\nabla U^n(s,\phi_s)\big|^{2\varepsilon}}{\big|\phi_s^n-\phi_s\big|^{2\varepsilon}}\mathrm{d}s\Big]\,. \qquad (4.2.9)$$

For this term, we proceed as in the proof of lemma 4.16. The key point is the estimate of the term

$$\int_0^1\mathbb{E}\Big[\int_0^T\big|\nabla^2U^n(s,\phi_s^{n,r})\big|^{2\varepsilon}\,\mathrm{d}s\Big]\,\mathrm{d}r\,,$$

where

$$\phi_t^{n,r} = rx + (1-r)y + \int_0^t rb^n(s,\phi_s^n) + (1-r)b(s,\phi_s)\,\mathrm{d}s + W_t\ .$$

We can conclude as in the proof of lemma 4.16 if we use the result of lemma 4.17. In particular, we obtain that (4.2.9) is controlled by $\|b\|_{L_p^q}$. □

We return to the proof of lemma 4.3. Thanks to the uniform bounds obtained for the expectations in the second and third lines of (4.2.8), we can pass to the limit in n to obtain

$$\begin{aligned}
\limsup_n \sup_{t\in[0,T]} \mathbb{E}\Big[e^{-B_t^n}\big|\psi_t^n - \psi_t\big|^a\Big] &\\
&\le \limsup_n C_a\big(|\phi_0(x)-\phi_0(y)|^a + f(n)^a\big)\\
&\quad + C_{a,\lambda}\limsup_n \mathbb{E}\Big[\int_0^T e^{-B_s^n}\big|\psi_s^n-\psi_s\big|^a\,\mathrm{d}s\Big]\\
&\le C_a|x-y|^a + C_{a,\lambda}\int_0^T \limsup_n \sup_{t\in[0,s]} \mathbb{E}\Big[e^{-B_t^n}\big|\psi_t^n-\psi_t\big|^a\Big]\,\mathrm{d}s\,.
\end{aligned}$$

Using Gronwall lemma we get

$$\limsup_n \sup_{t\in[0,T]} \mathbb{E}\Big[e^{-B_t^n}\big|\psi_t^n-\psi_t\big|^a\Big] \le C_{a,\lambda,T}\,|x-y|^a\ . \tag{4.2.10}$$

We can now get rid of the exponential factor using again Hölder inequality

$$\begin{aligned}
\limsup_n \sup_{t\in[0,T]} \mathbb{E}\Big[|\psi^n-\psi|^a\Big] &\le \limsup_n \Big\{\mathbb{E}\Big[e^{2B_T^n}\Big]^{1/2}\sup_{t\in[0,T]}\mathbb{E}\Big[e^{-2B_t^n}\big|\psi_t^n-\psi_t\big|^{2a}\Big]^{1/2}\Big\}\\
&\le C_{p,\lambda,T}\,|x-y|^a.
\end{aligned}$$

With $a = 2p$, redefining B_t^n as $1/2$ of the process defined above and using the relation (4.2.5), we can finally transport this bound to the flows ϕ^n:

$$\begin{aligned}
\limsup_n \sup_{t\in[0,T]} \mathbb{E}\Big[|\phi_t^n-\phi_t|^p\Big] &\le C_p \limsup_n \Big(\sup_{t\in[0,T]}\mathbb{E}\Big[|\psi_t^n-\psi_t|^p\Big] + f^p(n)\Big)\\
&\le C_{p,\lambda,T}|x-y|^p\,.
\end{aligned}$$

Remark that all the estimates found are uniform in $x, y \in B(0,R)$, so that we have obtained the desired result for the forward flows. But since the backward flows $\phi_0^{t,n}(\cdot)$ and $\phi_0^t(\cdot)$ are solution of the same SDE driven by the drifts $-b^n$ and $-b$, the same result holds for them too. □

Lemma 4.5. *For every $p \ge 1$, there exists a constant $C_{d,p,T} > 0$ such that*

$$\sup_{t\in[0,T]}\sup_{x\in\mathbb{R}^d} E\left[\left|\nabla\phi_0^{t,n}(x)\right|^p\right] \le C_{d,p,T} \tag{4.2.11}$$

uniformly in n.

Proof. Since the backward flow satisfies the same SDE of the forward flow with a drift of opposite sign, it is enough to show that the uniform bound (4.2.11) holds for the forward

flows. Let θ^n and ξ^n be the derivatives of ϕ^n and ψ^n, respectively. Since $\phi^n_t = (\gamma^n_t)^{-1} \circ \psi_t \circ \gamma^n_0$, from equation (4.5.15) of remark 4.15 we have $|\theta^n_i|^p \leq C_{d,p}|\xi^n|^p$. Therefore, we only need to show that the estimate (4.2.11) holds for the flow ψ^n, which solves

$$\mathrm{d}\xi^n_t(x) = \lambda \nabla U^n\big(t, \phi^n_t(x)\big)\, \xi^n_t(x)\, \mathrm{d}t + \nabla^2 U^n\big(t, \phi^n_t(x)\big)\, \xi^n_t(x)\, \mathrm{d}W_t$$

with initial condition $\xi^n_0(x) = Id$. For the rest of the proof we take any fixed $x \in \mathbb{R}^d$. ∇U^n is bounded uniformly in n and the function $\nabla^2 U$ is at least of class L^q_p, so that the last term is the differential of a martingale ($\mathrm{d}M^n_t$) due to lemma 4.17. By Itô formula we have therefore

$$\mathrm{d}|\xi^n|^p \leq C|\xi^n_t|^p\, \mathrm{d}t + \mathrm{d}M^n_t + |\xi^n_t|^{p-2}\, \mathrm{Tr}\Big(\big[\nabla^2 U^n\left(t, \phi^n_t(x)\right) \xi^n_t\big]\big[\nabla^2 U^n\left(t, \phi^n_t(x)\right) \xi^n_t\big]^T\Big)\, \mathrm{d}t\,.$$

The constant C can be chosen independently of n, and the trace of the matrix in the last term above is controlled by a constant $C_{p,d}$, depending on p and the dimension d of the space, times $|\xi^n_t|^2 |\nabla^2 U^n(t, \phi^n_t)|^2$. Introduce the process

$$A^n_t := C_{p,d} \int_0^t \big|\nabla^2 U^n\big(s, \phi^n_s\big)\big|^2\, \mathrm{d}s\,. \tag{4.2.12}$$

This is a continuous, adapted, non decreasing process, with $A^n_0 = 0$ and, due to lemma 4.17, $\mathbb{E}[A^n_T] \leq C$ uniformly in n. Lemma 4.16 even provides the bound $\mathbb{E}\big[e^{kA^n_t}\big] \leq C_{\|U^n\|}$ for any real constant k. We can therefore find a bound uniform in n reasoning as in lemma 4.14. We find that

$$\mathrm{d}e^{-A^n_t}|\xi^n_t|^p \leq Ce^{-A^n_t}|\xi^n_t|^p\, \mathrm{d}t + e^{-A^n_t}\, \mathrm{d}M^n_t$$

and after integrating and taking the expected value one obtains

$$\mathbb{E}\big[e^{-A^n_t}|\xi^n_t|^p\big] \leq |\xi_0|^p + C\int_0^t \mathbb{E}\big[e^{-A^n_s}|\xi^n_s|^p\big]\, \mathrm{d}s\,.$$

Take the supremum over all $t \in [0,T]$ and apply Gronwall inequality to get

$$\sup_{t\in[0,T]} \mathbb{E}\big[e^{-A^n_t}|\xi^n_t|^p\big] \leq C_T|\xi^n_0|^p = C_{d,p,T}\,,$$

uniformly in n and $x \in \mathbb{R}^d$. Using Hölder inequality as in the proof of the previous lemma, we finally obtain estimate (4.2.11) for the derivative of the flow ψ^n, which concludes the proof. □

4.3 Existence of weakly differentiable solutions

In this section we introduce the definition of weakly differentiable solution of the SLT equation and prove the main theorem on existence of such weakly differentiable solutions when b only satisfies some integrability conditions. This is done considering the solutions u_n of approximating regular problems and proving their convergence to a function u which is sufficiently regular and is a solution in the weak sense of the SLT equation.

Consider the SLT equation in Stratonovich form (4.1.1). The Itô formulation (as explained in detail also in [FGP10]) is

$$\mathrm{d}u + b\cdot\nabla u\,\mathrm{d}t + \sigma\nabla u\,\mathrm{d}W = \frac{\sigma^2}{2}\Delta u\,\mathrm{d}t\,, \qquad u|_{t=0} = u_0\,.$$

In this section we assume $b \in L^q_p$, with p, q as in (4.1.2).

Definition 4.6. Assume that $b \in L^q_p$, with p, q satisfying condition (4.1.2). We say that u is a weakly differentiable solution of the stochastic partial differential equation (SPDE) (4.1.1) if

1. $u : \Omega \times [0,T] \times \mathbb{R}^d \to \mathbb{R}$ is measurable and $\int u\,(t,x)\,\varphi\,(x)\,\mathrm{d}x$ (well defined by property 2 below) is progressively measurable for each $\varphi \in C_0^\infty\left(\mathbb{R}^d\right)$;

2. $P\left(u\,(t,\cdot) \in \cap_{r\geq 1} W^{1,r}_{loc}\left(\mathbb{R}^d\right)\right) = 1$ for every $t \in [0,T]$ and both u and ∇u are in $\mathcal{C}^0\big([0,T]; \cap_{r\geq 1} L^r(\Omega\times\mathbb{R}^d)\big)$;

3. u is a weak solution of (4.1.1), which is to say that for every $\varphi \in C_0^\infty\left(\mathbb{R}^d\right)$ and $t \in [0,T]$, with probability one

$$\begin{aligned}\int u(t,x)\varphi(x)\,\mathrm{d}x + \int_0^t\int b(s,x)\cdot\nabla u(s,x)\varphi(x)\,\mathrm{d}x\,\mathrm{d}s \\ = \int u_0(x)\varphi(x)\,\mathrm{d}x + \sigma\sum_{i=1}^d \int_0^t \left(\int u\,(s,x)\,\partial_{x_i}\varphi\,(x)\;\mathrm{d}x\right)\mathrm{d}W^i_s \\ + \frac{\sigma^2}{2}\int_0^t\int u(s,x)\Delta\varphi(x)\,\mathrm{d}x\,\mathrm{d}s\,.\end{aligned}$$

We shall make a few remarks on the above definition.

Remark 4.7. The process $s \mapsto Y^i_s := \int u\,(s,x)\,\partial_{x_i}\varphi\,(x)\,\mathrm{d}x$ is progressively measurable by property 1 and satisfies $\int_0^T \left|Y^i_s\right|^2 \mathrm{d}s < \infty$ by property 2, hence the Itô integral of Y^i_s is well defined.

Remark 4.8. The term $\int_0^t\int b\,(s,x)\cdot\nabla u\,(s,x)\,\varphi\,(x)\,\mathrm{d}x\,\mathrm{d}s$ is well defined with probability one because of the integrability properties in (t,x) of b (assumptions) and ∇u (property 2).

Remark 4.9. From 3 it follows that $\int u\,(t,x)\,\varphi\,(x)\,\mathrm{d}x$ has a continuous adapted modification, for every $\varphi \in C_0^\infty(\mathbb{R}^d)$.

Let $\phi_t\,(\omega) : \mathbb{R}^d \to \mathbb{R}^d$ be the α-Hölder continuous stochastic flow of homeomorphisms, for every $\alpha \in (0,1)$, associated to the SDE

$$\mathrm{d}X^x_t = b\,(t, X^x_t)\,\mathrm{d}t + \mathrm{d}W_t\,, \qquad X^x_0 = x\,.$$

The existence and regularity properties of this flow is shown in [FF12a]. Recall that the inverse of ϕ_t is denoted by ϕ^t_0.

We can finally state and prove the main theorem on the existence of weakly differentiable solutions of the SLT equation.

Theorem 4.10. *Assume $b \in L^q_p$ with p, q as in (4.1.2). If $u_0 \in \cap_{r\geq 1} W^{1,r}(\mathbb{R}^d)$ then $u\,(t,x) := u_0\,(\phi^t_0(x))$ is a weakly differentiable solution of the SPDE (4.1.1).*

Proof. Even though we shall use some technical results from appendices A and B, the proof is quite long. We divide it in five steps. To help the reader follow the ideas of the proof we present its general scheme in step 1, leaving the more technical points on the convergence of approximating solutions and the regularity of the limit function for the following steps.

Step 1 (preparation). Observe that the random field $(\omega, t, x) \mapsto u_0\big(\phi_0^t(x)\big)$ is jointly measurable and $(\omega, t) \mapsto \int u_0\big(\phi_0^t(x)\big)\varphi(x)\,\mathrm{d}x$ is progressively measurable for each $\varphi \in C_0^\infty(\mathbb{R}^d)$. Hence part 1 of Definition 4.6 is true. We could prove part 2 by chain rule and Sobolev properties of $\phi_0^t(x)$. However, a direct verification of part 3 from the formula $u(t,x) := u_0(\phi_0^t(x))$ is difficult because of lack of calculus. Hence we choose to approximate $u(t,x)$ by a smooth field $u_n(t,x)$; doing this, we prove both 2 and 3 by means of this approximation.

Let u_0^n be a sequence of smooth functions which converges to u_0 in $W^{1,r}(\mathbb{R}^d)$ and uniformly on $\mathbb{R}^d$. It is easy to check that these properties are satisfied for instance by $u_0^n(x) = \int \theta_n(x-y)\,u_0(y)\,\mathrm{d}y$ when θ_n are usual mollifiers; for instance, the uniform convergence property can be obtained from

$$\begin{aligned}|u_0^n(x) - u_0(x)| &\le \int \theta_n(x-y)\,|u_0(y) - u_0(x)|\,\mathrm{d}y \\ &\le C\int \theta_n(x-y)\,|y-x|^\alpha\,\mathrm{d}y = C\int \theta_n(y)\,|y|^\alpha\,\mathrm{d}y\end{aligned}$$

because $u_0 \in \mathcal{C}^{0,\alpha}$.

Let $\phi_t^n(\omega) : \mathbb{R}^d \to \mathbb{R}^d$ be the stochastic flow of smooth diffeomorphisms associated to the equation

$$\mathrm{d}X_t^{x,n} = b_n(t, X_t^{x,n})\,\mathrm{d}t + \mathrm{d}W_t\,, \qquad X_0^{x,n} = x\,,$$

where b_n are smooth approximations of b as considered in the previous section, and let $\phi_0^{t,n}$ be the inverse of ϕ_t^n. Then $u_n(t,x) := u_0^n\big(\phi_0^{t,n}(x)\big)$ is a smooth solution of

$$\mathrm{d}u_n + b_n\cdot\nabla u_n\,\mathrm{d}t + \sigma\nabla u_n\,\mathrm{d}W = \frac{\sigma^2}{2}\Delta u_n\,\mathrm{d}t\,, \qquad u_n\big|_{t=0} = u_0^n\,,$$

see [Ku, Theorem 6.1.5], and thus it satisfies

$$\begin{aligned}\int u_n(t,x)\,\varphi(x)\,\mathrm{d}x &+ \int_0^t\int b_n(s,x)\cdot\nabla u_n(s,x)\,\varphi(x)\,\mathrm{d}x\,\mathrm{d}s \\ &= \int u_0^n(x)\,\varphi(x)\,\mathrm{d}x + \sigma\sum_{i=1}^d\int_0^t\left(\int u_n(s,x)\,\partial_{x_i}\varphi(x)\,\mathrm{d}x\right)\mathrm{d}W_s^i \\ &\quad + \frac{\sigma^2}{2}\int_0^t\int u_n(s,x)\,\Delta\varphi(x)\,\mathrm{d}x\,\mathrm{d}s\end{aligned}$$

for every $\varphi \in C_0^\infty(\mathbb{R}^d)$ and $t \in [0,T]$, with probability one. We need to establish suitable bounds on $u_n(t,x)$ and suitable convergence properties of $u_n(t,x)$ to $u(t,x)$ in order to apply lemma 4.18 of appendix B - which is the first step to obtain the regularity properties of u of point 2 of Definition 4.6 - and pass to the limit in the equation. More precisely, for

every $\varphi \in C_0^\infty(\mathbb{R}^d)$, $t \in [0,T]$ and bounded random variable Z we have

$$\begin{aligned}\mathbb{E}\left[Z\int u_n(t,x)\,\varphi(x)\,\mathrm{d}x\right] + \mathbb{E}\left[Z\int_0^t\int b_n(s,x)\cdot\nabla u_n(s,x)\,\varphi(x)\,\mathrm{d}x\,\mathrm{d}s\right]\\ = \int u_0^n(x)\,\varphi(x)\,\mathrm{d}x + \sigma\sum_{i=1}^d \mathbb{E}\left[Z\int_0^t\left(\int u_n(s,x)\,\partial_{x_i}\varphi(x)\,\mathrm{d}x\right)\mathrm{d}W_s^i\right]\\ + \frac{\sigma^2}{2}\mathbb{E}\left[Z\int_0^t\int u_n(s,x)\,\Delta\varphi(x)\,\mathrm{d}x\,\mathrm{d}s\right]. \qquad (4.3.1)\end{aligned}$$

We shall pass to the limit in each one of these terms. We are forced to use this very weak convergence due to the term

$$\mathbb{E}\left[Z\int_0^t\int b_n(s,x)\cdot\nabla u_n(s,x)\,\varphi(x)\,\mathrm{d}x\,\mathrm{d}s\right]$$

where we may only use weak convergence of ∇u_n.

Step 2 (convergence of u_n to u). We claim that, uniformly in n and for every $r \geq 1$,

$$\sup_{t\in[0,T]}\int_{\mathbb{R}^d}\mathbb{E}\Big[|u_n(t,x)|^r\Big]\mathrm{d}x \leq C_r\,, \qquad (4.3.2)$$

$$\sup_{t\in[0,T]}\int_{\mathbb{R}^d}\mathbb{E}\Big[|\nabla u_n(t,x)|^r\Big]\mathrm{d}x \leq C_r\,. \qquad (4.3.3)$$

Let us show how to prove the second bound; the first one can be obtained in the same way. We use the representation formula for u_n and Hölder inequality to obtain

$$\left(\int_{\mathbb{R}^d}\mathbb{E}\Big[|\nabla u_n(t,x)|^r\Big]\,\mathrm{d}x\right)^2 \leq \int_{\mathbb{R}^d}\mathbb{E}\Big[\big|\nabla u_0^n\big(\phi_0^{t,n}(x)\big)\big|^{2r}\Big]\,\mathrm{d}x\int_{\mathbb{R}^d}\mathbb{E}\Big[\big|\nabla\phi_0^{t,n}(x)\big|^{2r}\Big]\,\mathrm{d}x\,.$$

The last integral on the right hand side is uniformly bounded by (4.2.11). Also the other integral term can be bounded uniformly: changing variables (recall that all functions involved are regular) we get

$$\int_{\mathbb{R}^d}\mathbb{E}\Big[\big|\nabla u_0^n\big(\phi_0^{t,n}(x)\big)\big|^{2r}\Big]\,\mathrm{d}x \leq \int_{\mathbb{R}^d}\big|\nabla u_0^n(y)\big|^{2r}\,\mathbb{E}\big[J_{\phi_t^n(y)}\big]\,\mathrm{d}y\,,$$

where $J_{\phi_t^n(y)}$ is the Jacobian of $\phi_t^n(y)$; this last term can be controlled using again Hölder inequality, (4.2.11) and the convergence of u_0^n in $W^{1,r}$ (for every $r \geq 1$). Remark that all the bounds obtained are uniform in n and t.

We consider now the problem of the convergence of u_n to u. Let us first prove that, given $t \in [0,T]$ and $\varphi \in C_0^\infty(\mathbb{R}^d)$,

$$P - \lim_{n\to\infty}\int_{\mathbb{R}^d} u_n(t,x)\,\varphi(x)\,\mathrm{d}x = \int_{\mathbb{R}^d} u(t,x)\,\varphi(x)\,\mathrm{d}x \qquad (4.3.4)$$

(convergence in probability). This is the first assumption of lemma 4.18 and allows also to pass to the limit in the first term of equation (4.3.1) using the uniform bound (4.3.2) and

Vitali convergence theorem (we are on the compact support of the test function φ). Since

$$\begin{aligned}\int_{\mathbb{R}^d} u_n(t,x)\,\varphi(x)\,\mathrm{d}x &= \int_{\mathbb{R}^d} u_0^n\left(\phi_0^{t,n}(x)\right)\varphi(x)\,\mathrm{d}x \\ &= \int_{\mathbb{R}^d}\left(u_0^n-u_0\right)\left(\phi_0^{t,n}(x)\right)\varphi(x)\,\mathrm{d}x + \int_{\mathbb{R}^d} u_0\left(\phi_0^{t,n}(x)\right)\varphi(x)\,\mathrm{d}x\,,\end{aligned}$$

using the Sobolev embedding $W^{1,2d}\hookrightarrow \mathcal{C}^{0,1/2}$ we find that

$$\begin{aligned}\left|\int_{\mathbb{R}^d}\left(u_n(t,x)-u(t,x)\right)\varphi(x)\,\mathrm{d}x\right| &\le \|u_0^n-u_0\|_{L^\infty}\,\|\varphi\|_{L^1} \\ &\quad + C\,\|\varphi\|_{L^\infty}\int_{B_R}\left|\phi_0^{t,n}(x)-\phi_0^t(x)\right|^{1/2}\mathrm{d}x\,.\end{aligned}$$

The first term converges to zero by the uniform convergence of u_0^n to u_0. To treat the second one, recall we have proved property (4.2.4). Hence

$$\lim_{n\to\infty}\mathbb{E}\left[\int_{B_R}\left|\phi_0^{t,n}(x)-\phi_0^t(x)\right|\,\mathrm{d}x\right]=0$$

and thus

$$P-\lim_{n\to\infty}\int_{B_R}\left|\phi_0^{t,n}(x)-\phi_0^t(x)\right|\,\mathrm{d}x=0\,.$$

Property (4.3.4) is proved.

Similarly, we can show that, given $\varphi\in C_0^\infty\left(\mathbb{R}^d\right)$,

$$P-\lim_{n\to\infty}\int_0^T\left|\int_{\mathbb{R}^d}\left(u_n(t,x)-u(t,x)\right)\varphi(x)\,\mathrm{d}x\right|^2\mathrm{d}t=0\,. \tag{4.3.5}$$

This implies that we can pass to the limit in the last two terms of equation (4.3.1). Indeed, property (4.3.5) implies that

$$P-\lim_{n\to\infty}\int_0^t\left(\int u_n(s,x)\,\partial_{x_i}\varphi(x)\,\mathrm{d}x\right)\mathrm{d}W_s^i=\int_0^t\left(\int u(s,x)\,\partial_{x_i}\varphi(x)\,\mathrm{d}x\right)\mathrm{d}W_s^i$$

for each $i=1,...,d$. Moreover,

$$\mathbb{E}\left[\left|\int_0^t\left(\int u_n(s,x)\,\partial_{x_i}\varphi(x)\,\mathrm{d}x\right)\mathrm{d}W_s^i\right|^2\right]=\mathbb{E}\left[\int_0^t\left|\int u_n(s,x)\,\partial_{x_i}\varphi(x)\,\mathrm{d}x\right|^2\mathrm{d}s\right],$$

which is uniformly bounded in n due to (4.3.2). By Vitali convergence theorem we obtain that

$$\lim_{n\to\infty}\mathbb{E}\left[Z\int_0^t\left(\int u_n(s,x)\,\partial_{x_i}\varphi(x)\,\mathrm{d}x\right)\mathrm{d}W_s^i\right]=\mathbb{E}\left[Z\int_0^t\left(\int u(s,x)\,\partial_{x_i}\varphi(x)\,\mathrm{d}x\right)\mathrm{d}W_s^i\right].$$

The proof of convergence for the last term of equation (4.3.1) is similar.

Step 3 (regularity of u). Let us prove property 2 of definition 4.6. The key estimate is provided by property (4.2.11).

Given $r\ge 1$ and $t\in[0,T]$, we shall prove that $P\left(u(t,\cdot)\in W^{1,r}_{loc}(\mathbb{R}^d)\right)=1$. We want to

use lemma 4.18 of appendix B with $F = u$, $F_n = u_n$. Condition 1 of lemma 4.18 is provided by (4.3.4). It is clear that $u_n(t,\cdot) \in W^{1,r}_{loc}(\mathbb{R}^d)$ for P-almost every ω, so that condition 2 follows from the uniform bound on ∇u_n obtained in (4.3.3). We can then apply lemma 4.18 and get $u(t,\cdot) \in W^{1,r}_{loc}(\mathbb{R}^d)$ for P-almost every ω.

Let us prove the second part of property 2 of definition 4.6. We have, from lemma 4.18 and equation (4.3.3),

$$\mathbb{E}\left[\int_{B_R} |\nabla u(t,x)|^r \,\mathrm{d}x\right] \le \limsup_{n\to\infty} \mathbb{E}\left[\int_{B_R} |\nabla u_n(t,x)|^r \,\mathrm{d}x\right] \le C_r$$

for every $R > 0$ and $t \in [0,T]$. Hence, by monotone convergence we have

$$\sup_{t\in[0,T]} \mathbb{E}\left[\int_{\mathbb{R}^d} |\nabla u(t,x)|^r \,\mathrm{d}x\right] \le C_r\,. \tag{4.3.6}$$

A similar bound can be proved for u itself: using (4.3.2), the convergence in probability proved in the previous step and Vitali convergence theorem we get that for any $r' < r$, $R > 0$ and uniformly in time,

$$\int_{B_R} \mathbb{E}\Big[|u(t,x)|^{r'}\Big]\,\mathrm{d}x = \lim_{n\to\infty} \int_{B_R} \mathbb{E}\Big[|u_n(t,x)|^{r'}\Big]\,\mathrm{d}x \le C_r\,;$$

by monotone convergence it follows that

$$\sup_{t\in[0,T]} \int_{\mathbb{R}^d} \mathbb{E}\Big[|u(t,x)|^{r'}\Big]\,\mathrm{d}x \le C_r\,.$$

Step 4 (passage to the limit). Finally, we have to prove that we can pass to the limit in equation (4.3.1) and deduce that u satisfies property 3 of Definition 4.6. We have already proved that all terms converge to the corresponding ones except for the term $\mathbb{E}\left[Z\int_0^t\int b_n(s,x)\cdot\nabla u_n(s,x)\,\varphi(x)\,\mathrm{d}x\,\mathrm{d}s\right]$. We do not want to integrate by parts, for otherwise we would have to assume something on $\operatorname{div} b$. Since $b_n \to b$ in $L^q_p = L^q\left([0,T]\,;L^p(\mathbb{R}^d)\right)$, it is sufficient to use a suitable weak convergence of ∇u_n to ∇u. Precisely, if we set

$$\mathbb{E}\left[Z\int_0^t\int b_n(s,x)\cdot\nabla u_n(s,x)\,\varphi(x)\,\mathrm{d}x\,\mathrm{d}s\right] - \mathbb{E}\left[Z\int_0^t\int b(s,x)\cdot\nabla u(s,x)\,\varphi(x)\,\mathrm{d}x\,\mathrm{d}s\right] = I_n^{(1)}(t) + I_n^{(2)}(t)\,,$$

where

$$I_n^{(1)}(t) = \mathbb{E}\left[Z\int_0^t\int \big(b_n(s,x) - b(s,x)\big)\cdot\nabla u_n(s,x)\,\varphi(x)\,\mathrm{d}x\,\mathrm{d}s\right]$$
$$I_n^{(2)}(t) = \mathbb{E}\left[Z\int_0^t\int \varphi(x)\,b(s,x)\cdot\big(\nabla u_n(s,x) - \nabla u(s,x)\big)\,\mathrm{d}x\,\mathrm{d}s\right],$$

we have to prove that both $I_n^{(1)}(t)$ and $I_n^{(2)}(t)$ converge to zero as $n\to\infty$. By Hölder inequality,

$$I_n^{(1)}(t) \le C\,\|b_n - b\|_{L^q\left([0,T];L^p(\mathbb{R}^d)\right)}\,\mathbb{E}\left[\|\nabla u_n\|_{L^{q'}\left([0,T];L^{p'}(\mathbb{R}^d)\right)}\right]$$

where $1/p+1/p'=1$ and $1/q+1/q'=1$. Thus, from (4.3.3) it follows that $I_n^{(1)}(t)$ converges to zero.

Let us treat $I_n^{(2)}(t)$. Using the integrability properties shown above we have

$$\mathbb{E}\left[Z\int_0^t\int\varphi(x)\,b(s,x)\cdot\big(\nabla u_n(s,x)-\nabla u(s,x)\big)\,\mathrm{d}x\,\mathrm{d}s\right]$$
$$=\int_0^t\mathbb{E}\left[\int Z\varphi(x)\,b(s,x)\cdot\big(\nabla u_n(s,x)-\nabla u(s,x)\big)\,\mathrm{d}x\right]\mathrm{d}s\,.$$

The function

$$h_n(s):=\mathbb{E}\left[\int Z\varphi(x)\,b(s,x)\cdot\big(\nabla u_n(s,x)-\nabla u(s,x)\big)\,\mathrm{d}x\right]$$

converges to zero as $n\to\infty$ for almost every s and satisfies the assumptions of Vitali convergence theorem (we shall prove these two claims in step 5 below). Hence $I_n^{(2)}(t)$ converges to zero.

Now we may pass to the limit in equation (4.3.1) and get

$$\mathbb{E}\left[Z\int u(t,x)\,\varphi(x)\,\mathrm{d}x\right]+\mathbb{E}\left[Z\int_0^t\int b(s,x)\cdot\nabla u(s,x)\,\varphi(x)\,\mathrm{d}x\,\mathrm{d}s\right]$$
$$=\int u_0(x)\,\varphi(x)\,\mathrm{d}x+\sigma\sum_{i=1}^d\mathbb{E}\left[Z\int_0^t\left(\int u(s,x)\,\partial_{x_i}\varphi(x)\,\mathrm{d}x\right)\mathrm{d}W_s^i\right]$$
$$+\frac{\sigma^2}{2}\mathbb{E}\left[Z\int_0^t\int u(s,x)\,\Delta\varphi(x)\,\mathrm{d}x\,\mathrm{d}s\right]$$

The arbitrariness of Z implies property 3 of definition 4.6.

Step 5 (auxiliary facts). We have to prove the two properties of $h_n(s)$ claimed in step 4. Recall we may use lemma 4.18 at each value of time, which gives us

$$\mathbb{E}\left[\int_{\mathbb{R}^d}\partial_{x_i}u(s,x)\,\varphi(x)\,Z\,\mathrm{d}x\right]=\lim_{n\to\infty}\mathbb{E}\left[\int_{\mathbb{R}^d}\partial_{x_i}u_n(s,x)\,\varphi(x)\,Z\,\mathrm{d}x\right]\tag{4.3.7}$$

for every $\varphi\in C_0^\infty(\mathbb{R}^d)$ and bounded random variable Z, at each $s\in[0,T]$. We have $b\in L^q\big([0,T];L^p(\mathbb{R}^d)\big)$, hence $b(s,\cdot)\in L^p(\mathbb{R}^d)$ for almost every $s\in[0,T]$. The space $C_0^\infty(\mathbb{R}^d)$ is dense in $L^p(\mathbb{R}^d)$, so that we may extend the convergence property (4.3.7) to all $\varphi\in L^p(\mathbb{R}^d)$ by means of the bounds (4.3.3) and (4.3.6). Hence $h_n(s)\to0$ as $n\to\infty$, for almost every $s\in[0,T]$.

Moreover, for every $\varepsilon>0$ there is a constant $C_{Z,\varphi,\varepsilon}$ such that

$$\int_0^T h_n^{1+\varepsilon}(s)\,\mathrm{d}s\le C_{Z,\varphi,\varepsilon}\int_0^T\mathbb{E}\Big[\int_{B_R}\big|b(s,x)\big|^{1+\varepsilon}\cdot\Big(\big|\nabla u_n(s,x)\big|^{1+\varepsilon}+\big|\nabla u(s,x)\big|^{1+\varepsilon}\Big)\,\mathrm{d}x\Big]\,\mathrm{d}s$$
$$\le C_{Z,\varphi,\varepsilon}\,\|b\|_{L_p^q}^{1+\varepsilon}\left(\mathbb{E}\int_0^T\int_{B_R}\big|\nabla u_n(s,x)\big|^r\mathrm{d}x\,\mathrm{d}s\right)^{\frac{1+\varepsilon}{r}}$$
$$+C_{Z,\varphi,\varepsilon}\,\|b\|_{L_p^q}^{1+\varepsilon}\left(\mathbb{E}\int_0^T\int_{B_R}\big|\nabla u(s,x)\big|^r\mathrm{d}x\,\mathrm{d}s\right)^{\frac{1+\varepsilon}{r}}$$

for a suitable r depending on ε (we have used Hölder inequality). The bounds (4.3.3) and (4.3.6) imply that $\int_0^T h_n^{1+\varepsilon}(s)\,\mathrm{d}s$ is uniformly bounded. Hence Vitali theorem can be applied to prove that $I_n^{(2)}(t) = \int_0^t h_n(s)\,\mathrm{d}s \to 0$ as $n \to \infty$. The proof is complete. □

4.4 Uniqueness of weakly differentiable solutions

Theorem 4.10 of the previous section provides a weak differentiable solution of the SLT equation as from definition 4.6. For this special solution we also have a representation formula in terms of the initial condition u_0 and the (inverse) stochastic flow of an associated SDE, which governs the evolution of characteristics of the SLT equation. This representation formula guarantees also some regularity properties of the solution, and in particular forbids the emergence of singularities. This section is devoted to the proof that this fairly regular solution is actually the unique weakly differentiable solution of the SLT equation.

Theorem 4.11. *The weakly differentiable solutions of definition 4.6 are unique.*

Proof. Let u^i, $i = 1, 2$, be two weakly differentiable solutions of the SLT equation (4.1.1). Then $u := u^1 - u^2$ is a weakly differentiable solution of

$$\frac{\partial u}{\partial t} + b \cdot \nabla u + \sigma \nabla u \circ \frac{\mathrm{d}W}{\mathrm{d}t} = 0\,, \qquad u|_{t=0} = 0\,. \tag{4.4.1}$$

We want to prove that u is identically zero. We divide the proof in three steps. In the first step we shall prove that u^2 solves the SPDE (4.4.2) with zero initial conditions. This is done using a sequence of regularized functions $u_\varepsilon \to u$ obtained by mollification and passing to the limit the equation for u_ε^2. In the second step we use this result to obtain an equation for $v(t,x) = \mathbb{E}\left[u^2(t,x)\right]$. With a long series of estimates, in the last step will rewrite the equation for v so as to be able to apply the Gronwall lemma and obtain that $v = 0$.

Step 1 (Equation for u^2) The first step consists in proving that u^2 is also a weakly differentiable solution of

$$\frac{\partial u^2}{\partial t} + b \cdot \nabla u^2 + \sigma \nabla u^2 \circ \frac{\mathrm{d}W}{\mathrm{d}t} = 0\,, \qquad u|_{t=0} = 0 \tag{4.4.2}$$

namely that

$$\begin{aligned}\int u^2(t,x)\,\varphi(x)\,\mathrm{d}x + \int_0^t \int b(s,x) \cdot \nabla u^2(s,x)\,\varphi(x)\,\mathrm{d}x\,\mathrm{d}s \\ = \sigma \sum_{i=1}^d \int_0^t \left(\int u^2(s,x)\,\partial_{x_i}\varphi(x)\,\mathrm{d}x \right) \mathrm{d}W_s^i + \frac{\sigma^2}{2} \int_0^t \int u^2(s,x)\,\Delta\varphi(x)\,\mathrm{d}x\,\mathrm{d}s\end{aligned}$$

for any $\varphi \in \mathcal{C}_0^\infty(\mathbb{R}^d)$. Let $\theta^\varepsilon(x)$ be a sequence of standard mollifiers. We will denote u_ε the convolution (in space only) $\big(u(t,\cdot) \star \theta^\varepsilon(\cdot)\big)(x)$. From the definition of weak solution, using $\varphi_y^\varepsilon(x) = \theta^\varepsilon(y - x)$, we have

$$u_\varepsilon(t,y) + \int_0^t b(s,y) \cdot \nabla u_\varepsilon(s,y)\,\mathrm{d}s + \sigma \sum_{i=1}^d \int_0^t \partial_{y_i} u(s,y) \circ \mathrm{d}W_s^i = \int_0^t R_\varepsilon(s,y)\,\mathrm{d}s\,,$$

where the commutator R_ε is given by

$$R_\varepsilon(s,y) = \Big[\int \Big(b(s,y) - b(s,x) \Big) \nabla u(s,x) \theta^\varepsilon(x-y)\,\mathrm{d}x \Big] .$$

The function u_ε is smooth in space. For any fixed y, by Itô formula we have

$$\begin{aligned} \mathrm{d}u_\varepsilon^2(t,y) &= 2u_\varepsilon(t,y)\,\mathrm{d}u_\varepsilon(t,y) \\ &= -2u_\varepsilon(t,y)\,b(t,y)\nabla u_\varepsilon(t,y)\,\mathrm{d}t - 2\sigma\, u_\varepsilon(t,y) \sum_{i=1}^d \partial_{y_i} u_\varepsilon(s,y) \circ \mathrm{d}W_s^i \\ &\quad + 2u_\varepsilon(t,y) R_\varepsilon(t,y)\,\mathrm{d}t \end{aligned}$$

which, rewritten in the week formulation using a generic test function φ, reads

$$\begin{aligned} &\int u_\varepsilon^2(t,y)\varphi(y)\,\mathrm{d}y + \int_0^t \int b(s,y)\nabla u_\varepsilon^2(s,y)\varphi(y)\,\mathrm{d}y\,\mathrm{d}s \\ &\qquad + \sigma \sum_{i=1}^d \int_0^t \Big(\int \partial_{y_i} u_\varepsilon^2(s,y)\varphi(y)\,\mathrm{d}y \Big) \circ \mathrm{d}W_s^i = \int_0^t \int 2u_\varepsilon(s,y) R_\varepsilon(s,y)\varphi(y)\,\mathrm{d}y\,\mathrm{d}s\,. \end{aligned}$$

We want now to pass to the limit for $\varepsilon \to 0$ in the different terms. Since for every t, $u_\varepsilon \to u$ uniformly on compact sets, by dominated convergence the first term tends to

$$\int u^2(t,y)\varphi(y)\,\mathrm{d}y\,.$$

For the following terms, we consider s fixed. Using Hölder inequality and the convergence of $\|\nabla u_\varepsilon\|_{L^p} \to \|\nabla u\|_{L^p}$ on compact sets (recall that φ is of compact support) for any $p \geq 1$, we have

$$\begin{aligned} \int b(s,y)\varphi(y)\Big(\nabla u_\varepsilon^2(s,y) - \nabla u^2(s,y) \Big)\,\mathrm{d}y &\leq \big\| b(s,y)\varphi(y) \big\|_{L^{r'}} \big\| \nabla u_\varepsilon^2(s,y) - \nabla u^2(s,y) \big\|_{L^r} \\ &\leq C_{r,\|b\|_{L^p}} \big\| \nabla u_\varepsilon^2(s,y) - \nabla u^2(s,y) \big\|_{L^r} \longrightarrow 0\,, \end{aligned}$$

which is enough to obtain the convergence of the second term. In the same way one obtains also the convergence of the third term. As for the term containing the commutator R_ε, we can use again Hölder inequality and the uniform convergence of u_ε to reduce the problem to the convergence of R_ε to zero in L^r for some $r \geq 1$. This can be achieved using again Hölder inequality, the equi-boundedness of ∇u_ε in L^p for every $p \geq 1$, and the continuity in mean (for almost every y) of the function $b \in L^p(\mathbb{R}^d)$. This proves (4.4.2).

Step 2 (equation for v^2) We know that u is almost surely continuous in space and time (and therefore locally bounded) and by definition of weak solution $\nabla u \in L^r([0,T]\times\mathbb{R}^d)$ for every $r \geq 1$ almost surely. It follows that $f(s) = \int \nabla u^2(s,y)\varphi(y)\,\mathrm{d}y$ is still almost surely a function in $L^r(0,T)$. This means that, writing (4.4.2) in Itô form, the stochastic integral is

a martingale and

$$\int \mathbb{E}\left[u^2(t,x)\right]\varphi(x)\,\mathrm{d}x + \int_0^t \int b(s,x)\cdot\nabla\,\mathbb{E}\left[u^2(s,x)\right]\varphi(x)\,\mathrm{d}x\,\mathrm{d}s \\ = \frac{\sigma^2}{2}\int_0^t \int \mathbb{E}\left[u^2(s,x)\right]\Delta\varphi(x)\,\mathrm{d}x\,\mathrm{d}s\,.$$

Hence $v(t,x) = \mathbb{E}\left[u^2(t,x)\right]$ satisfies

$$\int v(t,x)\varphi(x)\,\mathrm{d}x + \int_0^t \int b(s,x)\cdot\nabla v(t,x)\varphi(x)\,\mathrm{d}x\,\mathrm{d}s = \frac{\sigma^2}{2}\int_0^t \int v(t,x)\Delta\varphi(x)\,\mathrm{d}x\,\mathrm{d}s$$

and is fairly regular: $v \in \mathcal{C}^0\big([0,T];W^{1,r}(\mathbb{R}^d)\big)$ for every $r \geq 1$. This follows by Hölder inequality because

$$\int |\nabla v(t,x)|^r \mathrm{d}x = \int \big|\mathbb{E}\big[u\nabla u\big]\big|^r \mathrm{d}x \leq \int \Big(\mathbb{E}\big[|u|^2\big]\mathbb{E}\big[|\nabla u|^2\big]\Big)^{r/2}\mathrm{d}x \\ \leq \Big(\int \mathbb{E}\big[|u|^{2r}\big]^2\mathrm{d}x\Big)^{1/2}\Big(\int \mathbb{E}\big[|\nabla u|^{2r}\big]^2\mathrm{d}x\Big)^{1/2} \leq C\,,$$

holds uniformly in t by the second point of definition 4.6. Similar computations provide the same result for the function v.

Thanks to its global integrability properties, using approximating functions as in the first step, one can prove that v solves

$$\int v^2(t,x)\,\mathrm{d}x + \sigma^2\int_0^t \int |\nabla v(t,x)|^2\,\mathrm{d}x\,\mathrm{d}s \\ = -2\int_0^t \int b(s,x)\cdot\nabla v(t,x)\,v(t,x)\,\mathrm{d}x\,\mathrm{d}s\,. \tag{4.4.3}$$

Step 3 (final estimates) We want to find suitable bounds on the last term of (4.4.3) allowing to apply Gronwall inequality. This, combined with the initial condition $v(0,x) = 0$, will complete the proof.

To ease notation for the different estimates obtained in the step, we shall drop the dependence on (t,x) for the function involved, b and v.

For every $t \in [0,T]$, we have

$$\left|\int v\,b\cdot\nabla v\,\mathrm{d}x\right| \leq \left(\int |\nabla v|^2\,\mathrm{d}x\right)^{1/2}\left(\int v^2\,|b|^2\,\mathrm{d}x\right)^{1/2}$$

and

$$\int v^2\,|b|^2\,\mathrm{d}x \leq \left(\int v^{2r}\,\mathrm{d}x\right)^{1/r}\left(\int |b|^p\,\mathrm{d}x\right)^{2/p}, \tag{4.4.4}$$

where $1/r + 2/p = 1$, which is to say $1/r = 1 - 2/p = (p-2)/p$, or

$$r = \frac{p}{p-2}\,.$$

One also has the interpolation inequality

$$\left(\int v^\alpha \mathrm{d}x\right)^{1/\alpha} \leq \left(\int v^2 \mathrm{d}x\right)^{(1-s)/2} \left(\int |\nabla v|^2 \,\mathrm{d}x\right)^{s/2}, \qquad s = \frac{\alpha-2}{2\alpha} d\,.$$

The idea of the result comes from the Sobolev imbedding $W^{s,2} \subset L^\alpha$ for $1/\alpha = 1/2 - s/d$, namely $\frac{s}{d} = \frac{1}{2} - \frac{1}{\alpha} = \frac{\alpha-2}{2\alpha}$, or $s = \frac{\alpha-2}{2\alpha} d$; and then

$$\left(\int v^\alpha \,\mathrm{d}x\right)^{1/\alpha} \leq \|v\|_{W^{s,2}} \leq \|v\|_{L^2}^{1-s} \|v\|_{W^{1,2}}^{s}\,.$$

Using this interpolation inequality we get

$$\left(\int v^{2r} \,\mathrm{d}x\right)^{1/r} = \left(\int v^\alpha \,\mathrm{d}x\right)^{2/\alpha} \leq \left(\int v^2 \,\mathrm{d}x\right)^{1-s} \left(\int |\nabla v|^2 \,\mathrm{d}x\right)^{s}$$

for

$$r = \frac{p}{p-2}\,, \quad \alpha = 2r\,, \quad s = \frac{\alpha-2}{2\alpha} d\,.$$

We are lucky enough to find that s has a very easy and convenient expression:

$$s = \frac{2r-2}{4r}\, d = \frac{2\frac{p}{p-2} - 2}{4\frac{p}{p-2}}\, d = \frac{d}{p}\,.$$

Thus the bound (4.4.4) becomes

$$\int v^2 \,|b|^2 \,\mathrm{d}x \leq \left(\int v^2 \,\mathrm{d}x\right)^{1-\frac{d}{p}} \left(\int |\nabla v|^2 \,\mathrm{d}x\right)^{\frac{d}{p}} \left(\int |b|^p \,\mathrm{d}x\right)^{2/p}$$

and we find a first bound for the last term in (4.4.3):

$$\left|\int v\, b \cdot \nabla v \,\mathrm{d}x\right| \leq \left(\int |\nabla v|^2 \,\mathrm{d}x\right)^{\frac{p+d}{2p}} \left(\int v^2 \mathrm{d}x\right)^{\frac{p-d}{2p}} \left(\int |b|^p \,\mathrm{d}x\right)^{1/p}.$$

Recall that if $\frac{1}{s} + \frac{1}{r} = 1$, then $ab \leq a^s/s + b^r/r$. Using this inequality with $s = \frac{2p}{p+d}$ and $r = \frac{2p}{p-d}$ we can rewrite the above bound in a more useful form, in view of the application of the Gronwall lemma. We have

$$\left|\int v\, b \cdot \nabla v \,\mathrm{d}x\right| \leq \frac{\sigma^2}{2} \left(\int |\nabla v|^2 \,\mathrm{d}x\right) + C \left(\int v^2 \mathrm{d}x\right) \left(\int |b|^p \,\mathrm{d}x\right)^{\frac{2}{p-d}},$$

and we can transform equation (4.4.3) into the following inequality:

$$\int v^2\,(t,x)\,\mathrm{d}x \leq C \int_0^t \left(\int v^2 \mathrm{d}x\right) \left(\int |b|^p \,\mathrm{d}x\right)^{\frac{2}{p-d}} \mathrm{d}s\,.$$

Hence, if

$$\int_0^T \left(\int |b|^p \,\mathrm{d}x\right)^{\frac{2}{p-d}} \mathrm{d}s < \infty \tag{4.4.5}$$

we may apply Gronwall lemma and deduce that

$$\int v^2\,(t,x)\,\mathrm{d}x = 0\,.$$

This implies that $v = 0$, so that also $u = 0$, which completes the proof of the theorem.

We are left with only (4.4.5) to prove. But this is not difficult to achieve, since we already know that

$$\int_0^T \left(\int |b|^p\,\mathrm{d}x\right)^{\frac{q}{p}} \mathrm{d}s < \infty$$

for certain $p, q \geq 2$ such that $\frac{d}{p} + \frac{2}{q} < 1$: it is hypothesis (4.1.2). And manipulating the exponents we immediately find

$$\frac{2}{p-d} < \frac{q}{p}\,,$$

because $2p < qp - qd$, and $\frac{2}{q} < 1 - \frac{d}{p}$. □

4.5 Appendix A: technical results

For completeness, we collect here some modifications of known results, mostly from [FF11, FF12a, KR05], used in sections 4.2 and 4.3. We will use the notation introduced in there.

The following lemma provides the regularity properties of functions in the space $H^q_{2,p}$. It is proven in [KR05].

Lemma 4.12. *Let $p, q \in (1,\infty)$, $T \in (0,\infty)$ and $u \in H^q_{2,p}(T)$. Then we have:*

1. *If $\frac{d}{p} + \frac{2}{q} < 2$ then $u(t,x)$ is a bounded Hölder continuous function on $[0,T]\times R^d$. More precisely, for any $\varepsilon,\ \delta \in (0,1]$ satisfying*

$$\varepsilon + \frac{d}{p} + \frac{2}{q} < 2, \qquad 2\delta + \frac{d}{p} + \frac{2}{q} < 2$$

there exists a constant N, depending only on $p, q, \varepsilon, \delta$, such that for all $s,t \in [0,T]$ and $x, y \in R^d$, $x \neq y$ we have

$$|u(t,x) - u(s,x)| \leq N|t-s|^{\delta}\,\|u\|^{1-1/q-\delta}_{\mathbb{H}^q_{2,p}(T)}\,\|D_t\,u\|^{1/q+\delta}_{L^q_p(T)}\,; \tag{4.5.1}$$

$$|u(t,x)| + \frac{|u(t,x)-u(t,y)|}{|x-y|^{\varepsilon}} \leq NT^{-1/q}\Big(\|u\|_{\mathbb{H}^q_{2,p}(T)} + T\|D_t\,u\|_{L^q_p(T)}\Big)\,. \tag{4.5.2}$$

2. *If $\frac{d}{p} + \frac{2}{q} < 1$ then $\nabla u(t,x)$ is Hölder continuous in $[0,T]\times R^d$, namely for any $\varepsilon \in (0,1)$ satisfying*

$$\varepsilon + \frac{d}{p} + \frac{2}{q} < 1$$

there exists a constant N, depending only on p, q, ε, such that for all $s,t \in [0,T]$ and $x, y \in R^d$, $x \neq y$, equations (4.5.1) and (4.5.2) holds with ∇u in place of u and $\delta = \varepsilon/2$.

We now report and prove theorem 4.2. This theorem was proved in a similar setting in [KR05], and the adaptation to this setting can also be found in [FF12a].

Theorem 4.13. *Take p, q such that (4.1.2) holds, $\lambda > 0$ and two vector fields $b, f\,(t,x) : \mathbb{R}^{d+1} \to \mathbb{R}^d$ belonging to $L^q_p(T)$. Then in $H^q_{2,p}(T)$ there exists a unique solution of the backward parabolic system*

$$\begin{cases} \partial_t u + \frac{1}{2}\Delta u + b\cdot\nabla u - \lambda u + f = 0 \\ u(T,x) = 0 \end{cases} . \tag{4.5.3}$$

For this solution there exists a finite constant N depending only on d, p, q, T, λ and $\|b\|_{L^q_p(T)}$ such that

$$\|u\|_{H^q_{2,p}(T)} \le N\|f\|_{L^q_p(T)} . \tag{4.5.4}$$

Proof. Since we are working in $\mathbb{R}^d$, we emphasize that (4.5.3) is actually a collection of d independent equations. In other words, (4.5.3) has to be interpreted componentwise.

We divide the proof in three steps. First, we consider the easier case of $b = 0$, $\lambda = 0$. Then, to prove the general case, we obtain the *a-priori* estimate (4.5.4) and we finally get the existence and uniqueness of solutions applying the *method of continuity*.

Step 1 The existence and uniqueness of a solution when $b = 0$ and $\lambda = 0$ is proved in [Kr01, Theorem 1.2], together with the estimate for the second spatial derivatives of u: $\|\nabla^2 u\|_{L^q_p(T)} \le N\|f\|_{L^q_p(T)}$. The equation itself then provides the estimate for $\|D_t u\|_{L^q_p(T)}$, and to complete the Schauder estimate (4.5.4) the only missing norm is $\|u\|_{L^q_p(T)}$, which can be estimated by means of

$$\big\|u(t)\big\|^q_{L_p(\mathbb{R}^d)} \le \int_t^T \big\|D_s\, u(s)\big\|^q_{L_p(\mathbb{R}^d)}\,\mathrm{d}s\,.$$

Step 2 We turn now to prove the *a-priori* Schauder estimate in the general case. In the following, K will indicate different constants depending only on d, p, q, T.

Assume that the solution u exists and is unique. Set $\tilde f := f + b\cdot\nabla u - \lambda u$ and, just as above, the result of [Kr01] gives for $S \in [0,T]$

$$I(S) := \big\|D_t u\big\|^q_{L^q_p(S,T)} + \|u\|^q_{\mathbb{H}^q_{2,p}(S,T)} \le K\Big(\|f\|^q_{L^q_p(S,T)} + \|b\cdot\nabla u\|^q_{L^q_p(S,T)} + \lambda^q\|u\|^q_{L^q_p(S,T)}\Big)\,.$$

By lemma 4.12, for $t \in (S,T)$ and p, q such that $\frac{d}{p} + \frac{2}{q} < 1$ (we use that ∇u is Hölder continuous in time)

$$\big|\nabla u(t,x)\big| = \big|\nabla u(t,x) - \nabla u(T,x)\big| \le K I^{\frac{1}{q}}(t)\,. \tag{4.5.5}$$

Furthermore

$$\big\|b\cdot\nabla u\big\|^q_{L^q_p(S,T)} \le \int_S^T \sup_x |\nabla u(t,x)|^q \|b(t,\cdot)\|^q_{L^p(\mathbb{R}^d)}\,\mathrm{d}t \le K\int_S^T I(t)\|b(t,\cdot)\|^q_{L^p(\mathbb{R}^d)}\,\mathrm{d}t \tag{4.5.6}$$

and

$$\|u\|^q_{L^q_p(S,T)} \le K\int_S^T \Big(\int_t^T \|D_s u(s)\|_{L^p(\mathbb{R}^d)}\,\mathrm{d}s\Big)^q \mathrm{d}t \le K\int_S^T\int_t^T \|D_s u(s)\|^q_{L^p(\mathbb{R}^d)}\,\mathrm{d}s\,\mathrm{d}t$$
$$\le K\int_S^T I(t)\,\mathrm{d}t\,.$$

Combining the above equations we get

$$I(S) \le K\|f\|^q_{L^q_p(S,T)} + K\int_S^T I(t)\Big(\|b(t,\cdot)\|^q_{L^p(\mathbb{R}^d)} + \lambda^q\Big)\,\mathrm{d}t\,.$$

Finally, we estimate $I(0)$ by means of Grönwall's inequality

$$I(0) \le K\,\|f\|^q_{L^q_p(0,T)} + K\int_0^T \|f\|^q_{L^q_p(t,T)}\big(\|b(t,\cdot)\|^q_{L^p(\mathbb{R}^d)} + \lambda^q\big)\,e^{\int_t^T \left(\|b(r,\cdot)\|^q_{L^p(\mathbb{R}^d)}+\lambda^q\right)\mathrm{d}r}\,\mathrm{d}t$$

to obtain

$$\|D_t u\|_{L^q_p(T)} \le \frac{N}{2}\|f\|_{L^q_p(T)}\,, \qquad \|u\|_{\mathbb{H}^q_{2,p}(T)} \le \frac{N}{2}\|f\|_{L^q_p(T)}\,.$$

The Schauder estimates (4.5.4) immediately follows.

Step 3 It is now possible to apply the *method of continuity*. For $\mu \in [0,1]$ set $L^\mu := \frac{1}{2}\triangle + \mu(b^i u_{x^i} - \lambda u)$. Let Λ be the set of values of $\mu \in [0,1]$ such that

$$D_t u + L^\mu u + f = 0 \tag{4.5.7}$$

has a unique solution. We already know from step 1 that $0 \in \Lambda$, so that Λ is not empty, and to prove the theorem we only need to show that $1 \in \Lambda$ too. In fact, we will show that $\Lambda = [0,1]$.

Fix any $\mu_0 \in \Lambda$ and define the linear operator $\mathcal{R} : L^q_p(T) \to H^q_{2,p}(T)$ that maps f into the (unique) solution of (4.5.7) with $\mu = \mu_0$. By assumption $\mathcal{R}$ is well defined and by the estimate (4.5.4), which we have already proved in step 2, it is also bounded. In order to show that for $\mu \in [0,1]$ near to μ_0 equation (4.5.7) is solvable, we rewrite it as

$$D_t\,u + L^{\mu_0}u + f + (L^\mu - L^{\mu_0})\,u = 0, \qquad u = \mathcal{R}f + \mathcal{R}(L^\mu - L^{\mu_0})\,u$$

and define the linear operator $\mathcal{T}^\mu : H^q_{2,p}(T) \to H^q_{2,p}(T)$ as $\mathcal{T}^\mu u := \mathcal{R}f + \mathcal{R}(L^\mu - L^{\mu_0})\,u$. Now, the solution we are looking for is a fix point of $\mathcal{T}^\mu$; therefore, if $\mathcal{T}^\mu$ is a contraction, we obtain that the problem is solvable for μ near μ_0, and also μ is in Λ.

We will denote by C various constants independent of μ_0, μ, u, v. Define, for any $u, v \in H^q_{2,p}(T)$, the function J in a way similar to the definition of I above:

$$J(t) := \|D_t\,(u-v)\|^q_{L^q_p(t,T)} + \|u-v\|^q_{\mathbb{H}^q_{2,p}(t,T)}$$

Observe that

$$J(t) \le \big(\|D_t(u-v)\|_{L^q_p(t,T)} + \|u-v\|_{\mathbb{H}^q_{2,p}(t,T)}\big)^q = \|u-v\|^q_{H^q_{2,p}(t,T)}\,.$$

We use the definition of $\mathcal{T}^\mu$, the boundedness of $\mathcal{R}$, the estimate (4.5.6) and the estimate

for J we have just obtained to write

$$\begin{aligned}\left\|\mathcal{T}^\mu u - \mathcal{T}^\mu v\right\|_{H^q_{2,p}(T)} &= \left\|\mathcal{R}(L^\mu - L^{\mu_0})(u-v)\right\|_{H^q_{2,p}(T)} \le C\left\|(L^\mu - L^{\mu_0})(u-v)\right\|_{L^q_p(T)} \\ &= C|\mu-\mu_0|\,\left\|b\cdot\nabla(u-v) + \lambda(u-v)\right\|_{L^q_p(T)} \\ &\le C|\mu-\mu_0|\left[\left(K\int_0^T J(t)\,\|b(t,\cdot)\|^q_{L^p}\,\mathrm{d}t\right)^{\frac{1}{q}} + \lambda\|(u-v)\|_{L^q_p(T)}\right] \\ &\le C|\mu-\mu_0|\left[K^{\frac{1}{q}}\|b\|_{L^q_p(T)}J(0)^{\frac{1}{q}} + \lambda\|(u-v)\|_{L^q_p(T)}\right] \\ &\le C|\mu-\mu_0|\,\|(u-v)\|_{H^q_{2,p}(T)}\,.\end{aligned}$$

This implies that for any $\mu \in [0,1]$ such that $|\mu-\mu_0| \le \frac{1}{2C} = \delta$, the operator $\mathcal{T}^\mu$ is indeed a contraction. Therefore $\mathcal{T}^\mu$ has a fixed point u, which is the (unique) solution of (4.5.7).

Since we have proved that, if $\mu_0 \in \Lambda$ then

$$\big[\mu_0-\delta, \mu_0+\delta\big] \cap [0,1] \subset \Lambda\,,$$

in a finite number of steps we get that $1 \in \Lambda$. The theorem is proved. □

Lemma 4.14. *Let U_n be the solution of the PDE (4.2.2) for $f = b = b^n$, as defined in section 4.2. Then*

i) $U^n(t,x)$ and $\nabla U^n(t,x)$ converge pointwise in (t,x) to $U(t,x)$ and $\nabla U(t,x)$ respectively, and the convergence is uniform on compact sets;

ii) there exists a λ for which $\sup_{t,x}\left|\nabla U^n(t,x)\right| \le 1/2$;

iii) $\left\|\nabla^2 U^n(t,x)\right\|_{L^q_p(T)} \le C$.

Proof. The proof of the second point follows from a result contained in [FF12a], where it was proved that, for a fixed n,

$$\sup_{t\in[0,T]} \|\nabla u_\lambda(t)\|_{\mathcal{C}^0(\mathbb{R}^d)} \to 0 \qquad \text{as } \lambda \to +\infty\,. \tag{4.5.8}$$

However, inspecting the proof we see that all the bounds obtained depend on $\|b\|_{L^q_p}$, but never on b itself. Since $\|b^n\|_{L^q_p} \to \|b\|_{L^q_p}$, the uniformity in n follows. We report here for self-containedness the proof of (4.5.8).

Rewrite the PDE (4.2.2) as

$$D_t\,u_\lambda + \frac{1}{2}\triangle u_\lambda - \lambda\,u_\lambda = -(f + b\cdot\nabla u_\lambda) = g\,, \tag{4.5.9}$$

where we use the subscript to underline the dependence of the solution on the parameter λ present in the PDE. Denoting by P_t the heat semigroup, we have the well-known estimate

$$\left\|\nabla^\alpha P_t\,g\right\|_{L^p(\mathbb{R}^d)} \le Ct^{-\frac{\alpha}{2}}\,\left\|g\right\|_{L^p(\mathbb{R}^d)}\,. \tag{4.5.10}$$

Extend the functions b and f to $[0,\infty)\times\mathbb{R}^d$ defining them as zero for $t > T$ (this does not change their L^q_p-norm) and keep the same notation for the extended functions. The solution

u_λ can then be written as a convolution (the integrand is zero after time T):

$$u_\lambda(t,x) = \int_t^T e^{-\lambda(r-t)}\, P_{r-t}\, g(r,\cdot)(x)\,\mathrm{d}r\,.$$

Differentiating in the above formula we get

$$\big\|\nabla u_\lambda(t)\big\|_{L^\infty(\mathbb{R}^d)} \le \int_t^T e^{-\lambda(r-t)}\, \big\|\nabla P_{r-t}\, g(r)\big\|_{L^\infty(\mathbb{R}^d)}\,\mathrm{d}r\,. \tag{4.5.11}$$

We can obtain an L^p estimate by Sobolev embedding theorem $\big(W^{s,p}(\mathbb{R}^d) \hookrightarrow L^\infty(\mathbb{R}^d)$ for $s \ge d/p\big)$ and (4.5.10):

$$\begin{aligned}\big\|\nabla P_{r-t}\, g(r)\big\|_{L^\infty(\mathbb{R}^d)} &\le C\Big(\big\|\nabla P_{r-t}\, g(r)\big\|_{L^p(\mathbb{R}^d)} + \big\|\nabla^s \nabla P_{r-t}\, g(r)\big\|_{L^p(\mathbb{R}^d)}\Big)\\ &\le \frac{C\|g(r)\|_{L^p(\mathbb{R}^d)}}{(r-t)^{1/2}} + \frac{C\|g(r)\|_{L^p(\mathbb{R}^d)}}{(r-t)^{(1+s)/2}}\\ &\le K_{p,d,T}\; t^{-(1+s)/2}\|g(r)\|_{L^p(\mathbb{R}^d)}\,.\end{aligned}$$

For $d/p < s < 1 - 2/q$ we have that $(1+s)/2 < 1 - 1/q = 1/q'$, implying that the positive function $\theta(t) := K_{p,d,T}\; t^{-(1+s)/2}$ belongs to $L^{q'}(\mathbb{R}_+)$. Equation (4.5.9) itself gives $\|g(t)\|_{L^p(\mathbb{R}^d)} \in L^q(\mathbb{R}_+)$, so that by (4.5.11) and Hölder inequality we get

$$\begin{aligned}\big\|\nabla u_\lambda(t)\big\|_{L^\infty(\mathbb{R}^d)} \le{}& \int_t^T e^{-\lambda(r-t)}\,\theta(r-t)\,\|f(r)\|_{L^p(\mathbb{R}^d)}\,\mathrm{d}r \\ &+ \int_t^T e^{-\lambda(r-t)}\,\theta(r-t)\,\|b(r)\|_{L^p(\mathbb{R}^d)}\,\|\nabla u_\lambda(r)\|_{L^\infty(\mathbb{R}^d)}\,\mathrm{d}r\,.\end{aligned} \tag{4.5.12}$$

Since by lemma 4.12 u_λ is bounded, for any $t \in [0,T]$ the functions $\theta(r-t)\|b(r)\|_{L^p(\mathbb{R}^d)}$ and $u(r)\ theta(r-t)\|b(r)\|_{L^p(\mathbb{R}^d)}$, seen as functions of r, belong to $L^1(t,T)$. The classical Gronwall lemma can be easily adapted to our situation where the free extreme of integration domain is the lower one. Then, using the Gronwall lemma we obtain from (4.5.12) that

$$\big\|\nabla u_\lambda(t)\big\|_{L^\infty(\mathbb{R}^d)} \le \alpha(t) + \int_t^T \alpha(s)\,\theta(s-t)\|b(s)\|_{L^p(\mathbb{R}^d)}\,\exp\Big(\int_t^s \theta(r-t)\|b(r)\|_{L^p(\mathbb{R}^d)}\,\mathrm{d}r\Big)\,\mathrm{d}s\,, \tag{4.5.13}$$

where

$$\alpha(t) = \int_t^T e^{-\lambda(r-t)}\,\theta(r-t)\,\|f(r)\|_{L^p(\mathbb{R}^d)}\,\mathrm{d}r \ge 0\,.$$

We can easily control the function α: keeping in mind the definition of θ, for any given $\varepsilon > 0$ it is possible to find a $\delta \in (0, T-t)$ such that $\|\theta\|_{L^{q'}(0,\delta)} < \varepsilon$. We can then split the integral defining α on the interval $[t, t+\delta]$ and the complement of it, where the exponential term $e^{-\lambda\delta}$ is arbitrarily small (say, less than ε) for λ large enough:

$$\begin{aligned}\alpha(t) &\le \Big(\int_0^\delta \theta(r)^{q'}\,\mathrm{d}r\Big)^{1/q'}\|f\|_{L^q_p(T)} + \Big(\int_\delta^{T-t} e^{-q'\lambda r}\,\theta(r)^{q'}\,\mathrm{d}r\Big)^{1/q'}\|f(r)\|_{L^q_p(T)}\\ &\le \varepsilon\Big(1 + \|\theta\|_{L^{q'}(0,T)}\Big)\|f\|_{L^q_p(T)}.\end{aligned} \tag{4.5.14}$$

Note that the bound on α we have obtained is uniform in t. Set

$$K_{T,d,p,q,s,\|b\|_{L^q_p(T)}} := \|\theta\|_{L^{q'}(T)} \|b\|_{L^q_p(T)} \geq \int_t^s \theta(r-t) \|b(r)\|_{L^p(\mathbb{R}^d)} \, \mathrm{d}r$$

and obtain from (4.5.13) and (4.5.14)

$$\big\|\nabla u_\lambda(t)\big\|_{L^\infty(\mathbb{R}^d)} \leq \varepsilon \|f\|_{L^q_p(T)} \Big(1 + \|\theta\|_{L^{q'}(0,T)}\Big)\Big(1 + Ke^K\Big).$$

Since by lemma 4.12 ∇u_λ is a continuous function and since $\varepsilon \to 0$ for $\lambda \to \infty$, we obtain (4.5.8). This completes the proof of the second point of the lemma.

To prove the other two points, set $V^n := U^n - U$; then

$$\partial_t V^n + \frac{1}{2}\Delta V^n + b \cdot \nabla V^n - \lambda V^n = -\big(b^n - b\big) \cdot \big(Id + \nabla U^n\big), \quad V^n(T,x) = 0\,.$$

From the bound (4.2.3) on the solution provided by theorem 4.2, we obtain

$$\big\|V^n\big\|_{H^q_{2,p}} \leq N \|b^n - b\|_{L^q_p} \to 0\,.$$

It follows that $U^n \to U$ in $H^q_{2,p}$, which proves the last point. Since by lemma 4.12 $U, U^n, \nabla U$ and ∇U^n are all Hölder continuous functions, there exists a subsequence (that we still call U^n) such that $U^n \to U$ and $\nabla U^n \to \nabla U$ for every (t,x) and uniformly on compact sets. □

Remark 4.15. The following results hold uniformly in n because, as remarked in the previous proof, all the bounds obtained depend on the norm of b.

i) Using the solution u_λ of the PDE (4.2.2) with a value of λ obtained from the second point of the above lemma 4.14 we have that

$$\sup_n \sup_{t\in[0,T]} \big\|\nabla(\gamma^n_t)^{-1}(\cdot)\big\|_{\mathcal{C}(\mathbb{R}^d)} \leq 2\,. \tag{4.5.15}$$

This can be obtained as follows. We know now that $(\gamma^n_t)^{-1}(\cdot)$ is of class $\mathcal{C}^1(\mathbb{R}^d)$, so that for all $y \in \mathbb{R}^d$

$$\begin{aligned}\nabla(\gamma^n_t)^{-1}(y) &= \Big[\nabla\gamma^n_t\big((\gamma^n_t)^{-1}(y)\big)\Big]^{-1} = \Big[I + \nabla u\big(t,(\gamma^n_t)^{-1}(y)\big)\Big]^{-1} \\ &= \sum_{k\geq 0}\Big[-\nabla u\big(t,(\gamma^n_t)^{-1}(y)\big)\Big]^k.\end{aligned}$$

It follows that

$$\sup_n \sup_{t\in[0,T]} \big\|\nabla(\gamma^n_t)^{-1}(\cdot)\big\|_{\mathcal{C}(\mathbb{R}^d)} \leq \sum_{k\geq 0}\Big[\sup_{t\geq 0}\big\|\nabla u_\lambda(t,\cdot)\big\|_{\mathcal{C}^0(\mathbb{R}^d)}\Big]^k \leq 2\,.$$

ii) From the uniform boundedness of the coefficients (U^n and ∇U^n) of the SDE (4.2.1), we get

$$\sup_{t\in[0,T]} \mathbb{E}\Big[\big|\psi^n_t(x)\big|^a\Big] \leq C\Big(1 + |x|^a\Big)\,. \tag{4.5.16}$$

Lemma 4.16. *For every n, both the process*

$$A_t^n = 2\int_0^t \frac{\left|\nabla U^n(\phi_s^n) - \nabla U^n(\phi_s)\right|^2}{\left|\phi_s^n - \phi_s\right|^2} \mathbb{1}_{\{\phi_s^n \neq \phi_s\}}\, \mathrm{d}s$$

defined by (4.2.7) and

$$A_t^n = C_{p,d}\int_0^t \left|\nabla^2 U^n\big(s, \phi_s^n\big)\right|^2 \mathrm{d}s$$

defined by (4.2.12) are continuous, adapted, nondecreasing, with $A_0^n = 0$, $\mathbb{E}[A_T^n] \leq C$ and for every $k \in \mathbb{R}$,

$$\mathbb{E}\big[e^{kA_T^n}\big] \leq C\,.$$

The constant C can be chosen independently of n.

Proof. For the process defined by (4.2.7) the proof follows the same steps of the proof of [FF11, Lemma 7]. We only remark that the function U is the solution of a different PDE, but it has the same properties in terms of regularity. Moreover, the flows ϕ and ϕ^n solve two SDEs with different drifts b and b^n, which means that in the proof one has to use twice the result of [FF11, Corollary 13], once for every drift.

For the process defined by (4.2.12), the result is already contained in [FF11, Corollary 13]. □

Lemma 4.17. *Let f^n be a sequence of vector fields belonging to L_p^q, convergent to $f \in L_p^q$. Then, there exists $\varepsilon > 1$ such that*

$$\mathbb{E}\Big[\int_0^T \left|f^n(s, \phi_s^n)\right|^{2\varepsilon} \mathrm{d}s\Big] \leq C < \infty\,. \tag{4.5.17}$$

Proof. To prove the result for a fixed n one can use [FF11, Corollary 13] and follow the proof of [FF11, Lemma 8 and Corollary 9], which still works due to the strict inequality in the conditions imposed on p, q. Then, since all the bounds only depend on the norm of f but never on the function itself, one obtains that (4.5.17) is uniform in n. □

4.6 Appendix B: Sobolev regularity of random fields

Let $r \geq 1$ be given. We recall that $f \in W_{loc}^{1,r}\left(\mathbb{R}^d\right)$ if $f \in L_{loc}^r\left(\mathbb{R}^d\right)$ and there exist $g_i \in L_{loc}^r\left(\mathbb{R}^d\right)$, $i = 1, ..., d$, such that

$$\int_{\mathbb{R}^d} f(x)\, \partial_{x_i}\varphi(x)\, dx = -\int_{\mathbb{R}^d} g_i(x)\, \varphi(x)\, dx$$

for all $\varphi \in C_0^\infty\left(\mathbb{R}^d\right)$. When this happens, we set $\partial_{x_i} f(x) = g_i(x)$. From the definition and easy arguments one has the following criterion: if $f \in L_{loc}^r\left(\mathbb{R}^d\right)$ and there exist a sequence $\{f_n\} \subset W_{loc}^{1,r}\left(\mathbb{R}^d\right)$ such that $f_n \to f$ in $L_{loc}^1\left(\mathbb{R}^d\right)$ (or even in distributions) and for all $R > 0$ one has a constant $C_R > 0$ such that $\int_{B_R} |\nabla f_n(x)|^r\, dx \leq C_R$ uniformly in n, then $f \in W_{loc}^{1,r}\left(\mathbb{R}^d\right)$. This criterion will not be used below; it is only stated for comparison with the next result.

Let now $F : \Omega \times \mathbb{R}^d \to \mathbb{R}$ be a random field. When we use below this name we always assume that it is jointly measurable.

Lemma 4.18. *Assume that $F(\omega,\cdot) \in L^r_{loc}\left(\mathbb{R}^d\right)$ for P-almost every ω and there exist a sequence $\{F_n\}_{n\in\mathbb{N}}$ of random fields such that*

1. *$F_n(\omega,\cdot) \to F(\omega,\cdot)$ in distributions in probability, namely*

$$P-\lim_{n\to\infty}\int_{\mathbb{R}^d} F_n(\omega,x)\,\varphi(x)\,\mathrm{d}x = \int_{\mathbb{R}^d} F(\omega,x)\,\varphi(x)\,\mathrm{d}x$$

   for every $\varphi \in C_0^\infty\left(\mathbb{R}^d\right)$;

2. *$F_n(\omega,\cdot) \in W^{1,r}_{loc}\left(\mathbb{R}^d\right)$ for P-almost every ω, and for every $R>0$ there exists a constant $C_R>0$ such that*

$$\mathbb{E}\left[\int_{B_R} |\nabla F_n(x)|^r\,\mathrm{d}x\right] \le C_R$$

   uniformly in n.

Then $F(\omega,\cdot) \in W^{1,r}_{loc}\left(\mathbb{R}^d\right)$ for P-almost every ω,

$$\mathbb{E}\left[\int_{\mathbb{R}^d} \partial_{x_i} F(\cdot,x)\,\varphi(x)\,Z\,\mathrm{d}x\right] = \lim_{n\to\infty}\mathbb{E}\left[\int_{\mathbb{R}^d} \partial_{x_i} F_n(\cdot,x)\,\varphi(x)\,Z\,\mathrm{d}x\right] \tag{4.6.1}$$

for all $\varphi \in C_0^\infty\left(\mathbb{R}^d\right)$ and bounded random variable Z,

$$P-\lim_{n\to\infty}\int_{\mathbb{R}^d} \partial_{x_i} F_n(\omega,x)\,\varphi(x)\,\mathrm{d}x = -\int_{\mathbb{R}^d} F(\omega,x)\,\partial_{x_i}\varphi(x)\,\mathrm{d}x \tag{4.6.2}$$

for all $\varphi \in C_0^\infty\left(\mathbb{R}^d\right)$, and for every $R>0$

$$\mathbb{E}\left[\int_{B_R} |\nabla F(x)|^r\,\mathrm{d}x\right] \le \limsup_{n\to\infty}\mathbb{E}\left[\int_{B_R} |\nabla F_n(x)|^r\,\mathrm{d}x\right]. \tag{4.6.3}$$

Proof. Given $R>0$, there is a subsequence $\{n_k\}$ and a vector valued random field G such that ∇F_{n_k} converges weakly to G in $L^r\left(\Omega\times\mathbb{R}^d\right)$, as $k\to\infty$. Taking $R\in\mathbb{N}$, we may apply a diagonal procedure and find a single subsequence $\{n_k\}$ and vector valued random fields G^R, $R\in\mathbb{N}$, such that ∇F_{n_k} converges weakly to G^R in $L^r(\Omega\times B_R)$, as $k\to\infty$, for each $R\in\mathbb{N}$. Using suitable test functions, one can see that $G^{R'}=G^R$ on $\Omega\times B_R$ if $R'>R$. Hence we have found a single vector valued random field G, such that ∇F_{n_k} converges weakly to G in $L^r(\Omega\times B_R)$, as $k\to\infty$, for each $R\in\mathbb{N}$ and thus for each real $R>0$. At the end of the proof, G will be identified by ∇F, independently of the subsequence $\{n_k\}$. Thus, a fortiori, the full sequence ∇F_n converges weakly to G in $L^r\left(\Omega\times\mathbb{R}^d\right)$, as $n\to\infty$. For this reason, to simplify notations, we omit the notation of the subsequence.

For each $\varphi\in C_0^\infty(\mathbb{R}^d)$, by assumptions 1 and 2

$$\begin{aligned}\int_{\mathbb{R}^d} F(\omega,x)\,\partial_{x_i}\varphi(x)\,\mathrm{d}x &= \lim_{n\to\infty}\int_{\mathbb{R}^d} F_n(\omega,x)\,\partial_{x_i}\varphi(x)\,\mathrm{d}x\\ &= -\lim_{n\to\infty}\int_{\mathbb{R}^d} \partial_{x_i} F_n(\omega,x)\,\varphi(x)\,\mathrm{d}x,\end{aligned}$$

the limits being understood in probability. For each bounded random variable Z, this implies that

$$\lim_{n\to\infty}\int_{\mathbb{R}^d} \partial_{x_i} F_n(\omega,x)\,\varphi(x)\,Z(\omega)\,\mathrm{d}x = -\int_{\mathbb{R}^d} F(\omega,x)\,\partial_{x_i}\varphi(x)\,Z(\omega)\,\mathrm{d}x$$

in probability. This limit holds also in $L^1(\Omega)$ by Vitali convergence criterion because, by Hölder inequality,

$$\mathbb{E}\left[\left|\int_{\mathbb{R}^d}\partial_{x_i}F_n(\omega,x)\,\varphi(x)\,Z(\omega)\,\mathrm{d}x\right|^p\right]\leq C_{R,p}\,\|\varphi\|_{L^\infty}\,\|Z\|_{L^\infty}\mathbb{E}\left[\int_{B_R}|\partial_{x_i}F_n(\omega,x)|^p\,\mathrm{d}x\right]$$
$$\leq C_{R,p}\,\|\varphi\|_{L^\infty}\,\|Z\|_{L^\infty}C_R$$

uniformly in n, for some $p>1$, and with R such that B_R contains the support of φ.

From the weak convergence above, we also get that

$$\lim_{n\to\infty}\mathbb{E}\left[\int_{\mathbb{R}^d}\partial_{x_i}F_n(\cdot,x)\,\varphi(x)\,Z\mathrm{d}x\right]=\mathbb{E}\left[\int_{\mathbb{R}^d}G_i(\cdot,x)\,\varphi(x)\,Z\mathrm{d}x\right].$$

Hence

$$\mathbb{E}\left[\int_{\mathbb{R}^d}G_i(\cdot,x)\,\varphi(x)\,Z\mathrm{d}x\right]=-\mathbb{E}\left[\int_{\mathbb{R}^d}F(\cdot,x)\,\partial_{x_i}\varphi(x)\,Z\mathrm{d}x\right].$$

By the arbitrariness of Z this gives us

$$\int_{\mathbb{R}^d}F(\omega,x)\,\partial_{x_i}\varphi(x)\,\mathrm{d}x=-\int_{\mathbb{R}^d}G_i(\omega,x)\,\varphi(x)\,\mathrm{d}x \tag{4.6.4}$$

for P-almost every ω. This is the identification of G mentioned above, which implies the weak convergence of the full sequence ∇F_n.

Identity (4.6.4) holds P-almost surely for every $\varphi\in C_0^\infty(\mathbb{R}^d)$ a priori given. Thus it holds P-almost surely, uniformly on a dense countable set $\mathcal{D}$ of test functions φ, dense for instance in $W^{1,r'}_{loc}(\mathbb{R}^d)$, $1/r+1/r'=1$. Using the integrability properties of $F(\omega,\cdot)$ and $G_i(\omega,\cdot)$ we may extend identity (4.6.4) to all $\varphi\in W^{1,r'}_{loc}(\mathbb{R}^d)$ and thus all $\varphi\in C_0^\infty(\mathbb{R}^d)$, uniformly with respect to the good set of ω for which it holds on $\mathcal{D}$.

Thus, from identity (4.6.4) in the stronger form just explained, we deduce - by definition - that $F(\omega,\cdot)\in W^{1,r}_{loc}(\mathbb{R}^d)$ for P-almost every ω. And $\nabla F(\omega,x)=G(\omega,x)$. We immediately have (4.6.1) and (4.6.2).

We have shown that, for every function $\xi(\omega,x)$ of the form

$$\xi(\omega,x)=\sum_{k=1}^m\varphi_k(x)Z_k(\omega),$$

with φ and Z as above, we have

$$\left|\mathbb{E}\left[\int_{B_R}\nabla F(\cdot,x)\,\xi(\cdot,x)\,\mathrm{d}x\right]\right|\leq\lim_{n\to\infty}\left|\mathbb{E}\left[\int_{B_R}\nabla F_n(\cdot,x)\,\xi(\cdot,x)\,\mathrm{d}x\right]\right|$$
$$\leq\mathbb{E}\left[\int_{B_R}|\xi(\cdot,x)|^{r'}\,\mathrm{d}x\right]^{1/r'}\limsup_{n\to\infty}\mathbb{E}\left[\int_{B_R}|\nabla F_n(\cdot,x)|^r\,\mathrm{d}x\right]^{1/r}$$

(in the last passage we have used Hölder inequality). The set of functions ξ introduced is

dense in $L^{r'}(\Omega \times B_R)$, so that

$$\mathbb{E}\bigg[\int_{B_R} \big|\nabla F(\cdot,x)\big|^r \mathrm{d}x\bigg]^{1/r} = \big\|\nabla F\big\|_{L^r(\Omega\times B_R)} \leq \sup_{\|\xi\|_{L^{r'}}\leq 1} \bigg|\mathbb{E}\left[\int_{B_R} \nabla F\left(\cdot,x\right)\xi(\cdot,x)\,\mathrm{d}x\right]\bigg|$$
$$\leq \limsup_{n\to\infty} \mathbb{E}\left[\int_{B_R} \left|\nabla F_n\left(\cdot,x\right)\right|^r \mathrm{d}x\right]^{1/r}.$$

This completes the proof. □

Bibliography

[AC] M.J. Ablowitz and P.A. Clarkson, *Solitons, Nonlinear Evolution Equations and Inverse Scattering*. LMS Lecture Note Series **149**, Cambridge University Press (1992).

[APT] M.J. Ablowitz, B. Prinari and A.D. Trubatch, *Discrete and Continuous Nonlinear Schrödinger Systems*. LMS Lecture Note Series **302**, Cambridge University Press (2004).

[AS] M.J. Ablowitz and H. Segur, *Solitons and the Inverse Scattering Transform*. Cambridge University Press (2006).

[Al78] D. Aldous, *Stopping times and tightness.* Annals of Probability, **6**, 335–340 (1978).

[Am04] L. Ambrosio, *Transport equation and Cauchy problem for BV vector fields*. Inventiones Mathematicae, **158**, 227–260 (2004).

[ABGW12] H. Ammari, E. Bretin, J. Garnier and A. Wahab, *Noise source localization in an attenuating medium*. SIAM Journal on Applied Mathematics, **72**, 317–336 (2012).

[AKO] L. Arnold, W. Kliemann and E. Oeljeklaus, *Lyapunov exponents of linear stochastic systems*. Lecture Notes in Mathematics, **1186**, 85–125 (1986).

[APW86] L. Arnold, G. Papanicolau and V. Wihstutz, *Asymptotic analysis of the Lyapunov exponent and rotation number of the random oscillator and applications*. SIAM Journal on Applied Mathematics, **46**, 427–450 (1986).

[At10] S. Attanasio, *Stochastic flows of diffeomorphisms for one-dimensional SDE with discontinuous drift*. Electronic Communications in Probability, **15**, 213–226 (2010).

[Ba10] C. Bagaini, *Acquisition and processing of simultaneous vibroseis data*. Geophysical Prospecting, **58**, 81–99 (2010).

[Be09a] A.J. Berkhout, *Changing the mindset in seismic data acquisition*. The Leading Edge, **27**, 924–938 (2009).

[Be09b] A.J. Berkhout, G. Blacquiere, and D.J. Verschuur, *The concept of double blending: Combining incoherent shooting with incoherent sensing*. Geophysics, **74**, A59–A62 (2009).

[BCS] N. Bleistein, J.K. Cohen, and J.W. Stockwell Jr, *Mathematics of Multidimensional Seismic Imaging, Migration, and Inversion*. Springer Verlag, New York (2001).

[BW] M. Born and E. Wolf, *Principles of Optics*. Cambridge University Press (1999).

[BSC08] F. Brenguier, N.M. Shapiro, M. Campillo, V. Ferrazzini, Z. Duputel, O. Coutant and A. Nercessian, *Towards forecasting volcanic eruptions using seismic noise*. Nature Geoscience, **1**, 126–130 (2008).

[BSC07] F. Brenguier, N.M. Shapiro, M. Campillo, A. Nercessian and V. Ferrazzini, *3-D surface wave tomography of the Piton de la Fournaise volcano using seismic noise correlations*. Geophysical Research Letters, **34**, L02305 (2007).

[Bu88] J. Burzlaff, *The soliton number of optical soliton bound states for two special families of input pulses*. Journal of Physics A: Mathematical and General **21**, 561–566 (1988).

[CGS06] A. Curtis, P. Gerstoft, H. Sato, R. Snieder and K. Wapenaar, *Seismic interferometry - turning noise into signal*. The Leading Edge, **25**, 1082–1092 (2006).

[DaS09] W. Dai and J. Schuster, *Least-squares migration of simultaneous sources data with a deblurring filter*. SEG Houston 2009 International exposition and Annual Meeting.

[dBD02a] A. de Bouard and A. Debussche, *On the effect of the noise on the solutions of supercritical Schrödinger equation*. Probability Theory Related Fields, **123**, 76–96 (2002).

[dBD02b] A. de Bouard and A. Debussche, *Finite time blow-up in the additive supercritical stochastic nonlinear Schrödinger equation: the real noise case*, Contemporary Mathematics, **301**, 183–194 (2002).

[dBD05] A. de Bouard and A. Debussche, *Blow-up for the stochastic nonlinear Schrödinger equation with multiplicative noise*. Annals of Probability, **33**, 1078–1110 (2005).

[dBD07] A. de Bouard and A. Debussche, *Random modulation of solitons for the stochastic Korteweg - de Vries equation*. Annales de l'Institut Henri Poincaré (C), Analyse Non Linéaire, **24**, 251–278 (2007).

[dBD09] A. de Bouard and A. Debussche, *Soliton dynamics for the Korteweg-de Vries equation with multiplicative homogeneous noise*. Electronic Journal of Probability, **14**, 1727–1744 (2009).

[dBD10] A. de Bouard and A. Debussche, emphThe nonlinear Schrödinger equation with white noise dispersion. Journal of Functional Analysis, **259**, 1300–1321 (2010).

[DdM02a] A. Debussche and L. di Menza, *Numerical simulation of focusing stochastic nonlinear Schrödinger equations*. Physica D, **162**, 131–154 (2002).

[DdM02b] A. Debussche and L. di Menza, *Numerical resolution of stochastic focusing NLS equations*. Applied Mathematics Letters, **15**, 661–669 (2002).

[DP99] A. Debussche and J. Printems, *Numerical simulation of the stochastic Korteweg - de Vries equation*. Physica D, **134**, 200–226 (1999).

[DT11] A. Debussche and Y. Tsutsumi, *1D quintic nonlinear Schrödinger equation with white noise dispersion*. Journal de Mathématiques Pures et Appliquées, **96**, 363–376 (2011).

[DFGS12] M. de Hoop, E. Fedrizzi, J. Garnier and K. Sølna, *Imaging with noise blending*. Contemporary Mathematics, **577** (2012).

[DeS09] M. de Hoop and K. Sølna, *Estimating a Green's function from field-field correlations in a random medium*. SIAM Journal on Applied Mathematics, **69**, 909–932 (2009).

[DFV12] F. Delarue, F. Flandoli and D. Vincenzi, *Noise prevents collaps of Vlasov-Poisson point charges*. preprint.

[DP08] S.A. Derevyanko and J.E. Prilepsky, *Random input problem for the nonlinear Schrödinger equation*. Physical Review E, **78**, 016603 (2008).

[DPL89] R.J. DiPerna and P.L. Lions, *Ordinary differential equations, transport theory and Sobolev spaces*. Inventiones Mathematicae, **98**, 511–547 (1989).

[EK] S.N. Ethier and T.G. Kurtz, *Markov Processes – Characterization and Convergence*. Wiley Series in Probability and Statistics, **623**. Wiley Intescience, Hoboken, New Jersey (2005).

[FKLT01] G.E. Falkovich, I. Kolokolov, V. Lebedev and S.K. Turitsyn, *Statistics of soliton-bearing systems with additive noise*. Physical Review E, **63**, 025601(R) (2001).

[Fe12a] E. Fedrizzi, *Stability of solitons under rapidly oscillating random perturbations of the initial conditions*. Preprint (2012), available on ArXiv:1201.3753.

[Fe12b] E. Fedrizzi, *High frequency analysis of imaging with noise blending*. Preprint, available on arXiv:1210.2382 (2012).

[FF11] E. Fedrizzi and F. Flandoli, *Pathwise uniqueness and continuous dependence for SDEs with nonregular drift*. Stochastics **83** 241–257 (2011).

[FF12a] E. Fedrizzi and F. Flandoli, *Hölder flow and differentiability for SDEs with nonregular drift*. To appear in Stochastic Analysis and Applications.

[FF12b] E. Fedrizzi and F. Flandoli, *Noise prevents singularities in linear transport equations*. Preprint, available on arXiv: 1205.5505 (2012).

[Fl] F. Flandoli, *Random Perturbation of PDEs and Fluid Dynamic Models*. Saint Flour Summer School Lectures 2010, Lecture Notes in Mathematics, **2015**, Springer, Berlin (2011).

[FGP10] F. Flandoli, M. Gubinelli and E. Priola, *Well-posedness of the transport equation by stochastic perturbation*. Inventiones Mathematicae, **180**, 1–53 (2010).

[FGP11] F. Flandoli, M. Gubinelli and E. Priola, *Full well-posedness of point vortex dynamics corresponding to stochastic 2D Euler equations*. Stochastic Processes and their Applications, **121** 1445–1463 (2011).

[FCD00] M. Fink, D. Cassereau, A. Derode, C. Prada, P. Roux, M. Tanter, J.-L. Thomas and F. Wu, *Time-reversed acoustics*. Reports on Progress in Physics, **63**, 1933–1995 (2000).

[FGPS] J.-P. Fouque, J. Garnier, G. Papanicolaou and K. Sølna, *Wave Propagation and Time Reversal in Randomly Layered Media*. Stochastic Modelling and Applied Probability, **56**. Springer, New York (2007).

[GG67] C.S. Gardner, J.M. Greene, M.D. Kruskal and R.M. Miura, *Method for solving the Korteweg - de Vries equation*, Physical Review Letters, **19**, 1095–1097 (1967).

[Ga01] J. Garnier, *Long-Time Dynamics of KortewegÐde Vries Solitons Driven by Random Perturbations*. Journal of Statistical Physics, **105**, 789–833 (2001).

[GP09] J. Garnier and G. Papanicolaou, *Passive sensor imaging using cross correlations of noisy signals in a scattering medium*. SIAM Journal on Imaging Sciences, **2**, 396–437 (2009).

[GP10] J. Garnier and G. Papanicolaou, *Resolution analysis for imaging with noise*. Inverse Problems, **26**, 074001 (2010).

[GP11] J. Garnier and G. Papanicolaou, *Fluctuation theory of ambient noise imaging*. CRAS Geoscience **343**, 502–511 (2011).

[GS11] J. Garnier and K. Sølna, *Filtered Kirchhoff migration of cross correlations of ambient noise signals*. Inverse Problems and Imaging, **5**, 371–390 (2011).

[GSB08] P. Gouédard, L. Stehly, F. Brenguier, M. Campillo, Y. Colin de Verdière, E. Larose, L. Margerin, P. Roux, F.J. Sanchez-Sesma, N.M. Shapiro and R.L. Weaver, *Cross-correlation of random fields: mathematical approach and applications*. Geophysical Prospecting, **56**, 375–393 (2008).

[HSH08] G. Hampson, J. Stefani and F. Herkenhoff, *Acquisition using simultaneous sources*. The Leading Edge, **27**, 918–923 (2008).

[Ka79] V.I. Karpman *Soliton evolution in the presence of perturbation*. Physica Scripta, **20**, 462–478 (1979).

[KM08] P. Kazakopoulos and A.L. Moustakas, *Nonlinear Schrödinger equation with random Gaussian input: distribution of inverse scattering data and eigenvalues*. Physical Review E, **78** (2008).

[Ki89] Y.S. Kivshar, *On the soliton generation in optical fibres*. J. Phys. A: Math. Gen., **22**, 337–340 (1989).

[KA83] W. Kliemann and L. Arnold, *Lyapunov exponents of linear stochastic systems*. Forschungsschwerpunkt Dynamische Systeme, Report **93**, Universität Bremen (1983).

[KV1] D.J. Korteweg and G. de Vries, *On the change of form of long waves advancing in a rectangular canal and on a new type of long stationary waves*. Philosophical Magazine, Series 5, **39**, 422–443 (1895).

[Kr01] N.V. Krylov, *The heat equation in $L_q((0,T),L_p)$- spaces with weights*. Siam Journal on Mathematical Analysis, **32**, 1117–1141 (2001).

[KR05] N.V. Krylov and M. Röckner, *Strong solutions to stochastic equations with singular time dependent drift*. Probability Theory and Related Fields, **131**, 154–196 (2005).

[Ku84] H. Kunita, *Stochastic differential equations and stochastic flows of diffeomorphisms*. XII École d'été de probabilités de Saint-Flour – 1982. Lecture Notes in Mathematics, **1097**, 143–303. Springer, Berlin (1984).

[Ku] H. Kunita, *Stochastic Flows and Stochastic Differential Equations*, Cambridge Studies in Advanced Mathematics, **24**, Cambridge University Press (1990).

[LMD06] E. Larose, L. Margerin, A. Derode, B. Van Tiggelen, M. Campillo, N. Shapiro, A. Paul, L. Stehly and M. Tanter, *Correlation of random wave fields: an interdisciplinary review*. Geophysics, **71**, SI11–SI21 (2006).

[La68] P. Lax, *Integrals of nonlinear equations of evolution and solitary waves*. Communications on Pure and Applied Mathematics, **21**, 467–490 (1968).

[MDB11] A. Mahdad, P. Doulgeris and G. Blacquiere, *Separation of blended data by iterative estimation and subtraction of blending interference noise*. Geophysics, **76**, Q9–Q17 (2011).

[Ma73] S.V. Manakov, *On the theory of two-dimensional stationary self-focusing of electromagnetic waves*. Journal of Experimental and Theoretical Physics, **65**, 505–516 (1973).

[MNPZ] S.V. Manakov, S. Novikov, L.P. Pitaevskii and V.E. Zakharov, *Theory of Solitons: The Inverse Scattering Method*. Consultants Bureau, New York (1984).

[Me] M. Metivier, *Stochastic Partial Differential Equations in Infinite Dimensional Spaces*, Quaderni, Scuola Normale Superiore, Pisa (1988).

[Me84] M. Metivier, *Convergence faible et principe d'invariance pour des martingales à valeurs dans des espaces de Sobolev*. Rapport interne CMAP-Ecole Polytechnique **106**, Paris (1984).

[MP10] T. Meyer-Brandis and F. Proske, *Construction of strong solutions of SDE's via Malliavin calculus*, Journal of Functional Analysis, **258**, 3922–3953 (2010).

[Mi79] J.W. Miler *On internal solitary waves*. Tellus B, **31**, 456–462 (1979).

[MNP12] S.E.A. Mohammed, T.K. Nilssen and F.N. Proske, *Sobolev Differentiable Stochastic Flows of SDE's with Measurable Drift and Applications*, preprint, arXiv:1204.3867.

[MN] J.V. Moloney and A.C. Newell, *Nonlinear Optics*. Westview Press, Boulder (2004).

[Mu78] A.C. Murray, *Solutions of the Korteweg - De Vries equation from irregular data*. Duke Mathematical Journal, **45**, 149–181 (1978).

[PS] L. Pitaevskii and S. Stringari, *Bose-Einstein Condensation*. Oxford University Press, (2003).

[Pr59] G. Prodi, *Un teorema di unicità per le equazioni di Navier-Stokes*. Annali di Matematica Pura ed Applicata, **4**, 173–182 (1959).

[RY] D. Revuz and M. Yor, *Continuous martingales and Brownian motion*. Third edition, Springer, Berlin (1999).

[Ri] D.W. Ricker, *Echo Signal Processing*. Springer, (2003).

[Ru1] J.S. Russell *Report of the committee on waves*. Report of the 7^{th} Meeting of the British Association for the Advancement of Science, 417–469, Liverpool (1838).

[Ru2] J.S. Russel *Report on waves*. Report of the 14^{th} Meeting of the British Association for the Advancement of Science, London (1845).

[SRG06] K.G. Sabra, P. Roux, P. Gerstoft, W.A. Kuperman and M. C . Fehler, *Extracting coherent coda arrivals from cross correlations of long period seismic waves during the Mount St. Helens 2004 eruption*. Geophysical Research Letters, **33**, L06313 (2006).

[SRC98] M. Scalerandi, A. Romano and C.A. Condat, *Korteweg - de Vries solitons under additive stochastic perturbations*. Physical Review E, **58**, 4166–4173 (1998).

[SWH11] G.T. Schuster, X. Wang, Y. Huang, W. Dai and C. Boonyasiriwat, *Theory of multisource crosstalk reduction by phase-encoded statics*. Geophysical Journal International, **184**, 1289–1303 (2011).

[SCSR05] N.M. Shapiro, M. Campillo, L. Stehly and M. H. Ritzwoller, *High-resolution surface-wave tomography from ambient seismic noise*. Science, **307**, 1615–1618 (2005).

[SCS06] L. Stehly, M. Campillo and N. M. Shapiro, *A study of the seismic noise from its long-range correlation properties*. Journal of Geophysical Research **111**, B10306 (2006).

[VB11] D.J.E. Verschuur and A.J.G. Berkhout, *Seismic migration of blended shot records with surface-related multiple scattering*. Geophysics, **76**, A7–A13, (2011).

[WNT12] K. Wapenaar, J. van der Neut and J. Thorbecke, *On the relation between seismic interferometry and the simultaneous-source method*. Geophysical Prospecting, **60**, 802–823 (2012).

[Wh] G.B. Whitham, *Linear and nonlinear waves*. Pure and Applied Mathematics, Wiley-Interscience, New York (1999).

[YVD06] H. Yao, R.D. van der Hilst, and M. de Hoop, *Surface-wave array tomography in SE Tibet from ambient seismic noise and two-station analysis Ð I. Phase velocity maps*. Geophysical Journal International, **166**, 732–744, (2006).

[Za68] V. Zakharov, *Stability of periodic waves of finite amplitude on the surface of a deep fluid*. Journal of Applied Mechanics and Technical Physics, **9**, 86–94 (1968).

[ZK65] N.J. Zabusky and M.D. Kruskal, *Interaction of "solitons" in a collisionless plasma and the recurrence of initial states*. Physical review letters, **15**, 240–243 (1965).

[Zh11] X. Zhang, *Stochastic Homeomorphism Flows of SDEs with Singular Drifts and Sobolev Diffusion Coefficients*, Electronic Journal of Probability, **16**, 1096–1116 (2011).